Ditopic ligands for the extraction of divalent metal salts

Kate Jennifer Smith

A thesis submitted towards the degree of Doctor of Philosophy

The University of Edinburgh

2004

Dedication

This work is dedicated to my family and Struan for encouraging me all the way.

Abstract

This thesis extends earlier work at the University of Edinburgh aimed at opening up new flowsheets for the hydrometallurgical recovery of base metals using tetradentate ligands which are capable of transporting metal salts {both a metal cation and its attendant anion(s)}. Prototypes were based on salicylaldimine derivatives of diamines, "salen" ligands in which coordination of a metal dication releases the two phenolic protons which are captured by pendant secondary amine groups generating a preorganised dicationic binding site for the anion(s).

The thesis initially deals with the design, synthesis and evaluation of ligands to improve the strength, selectivity and speed of binding of nickel(II) sulfate by incorporating two additional donors in the salen unit to generate $N_2X_2O_2^{2-}$ binding sites for the nickel yielding *pseudo* octahedral complexes. The ligands N,N´ or O,O´ or S,S´ *o*-aminophenyl-substituted 1,2-diaminoethane, 1,2-dioxaethane, 1,3-dioxapropane or 1,2-dithioethane were also used in a screening study with some other divalent metal salts (calcium, cobalt, copper, magnesium, manganese and zinc) commonly found in the feed solutions in commercial processes.

Chapter two deals with the nickel(II) coordination chemistry of a series of sexadentate ($N_2X_2O_2^{2-}$) ligands. Nickel-ligand-anion complexes have been synthesised for sulfate, nitrate and chloride salts and neutral nickel-ligand complexes have been made. Crystal structures of complexes all contain the same isomer which has a planar *mer* arrangement of the salicylaldimato XNO^- units. A "nickel only" complex of an $X_2N_2O_2^{2-}$ ligand with pendant piperidine groups shows that these could provide a cavity to encapsulate a single sulfate anion. All the ligands were found to be very weak extractants and showed slow complexation kinetics and phase transfer of nickel sulfate.

The synthesis and characterisation of a series of tridentate ligands related to the sexadentate ligands, with NXO^- binding sites, are reported in chapter three. In theory these could form complexes with a ligand: nickel ratio of 2:1, with a more nearly "ideal" octahedral donor set. Solid state structures of the ligands show them to be

pre-organised with an approximately 90° X···N···O angle. Nickel complexes have been synthesised for sulfate, chloride and acetate salts. Analysis indicates that complexes with ligand: nickel: dianion ratios of 2:1:1 were formed. The tridentate ligands were found to be very weak extractants for nickel sulfate.

Chapter four describes the screening of the potentially sexadentate $N_2X_2O_2^{2-}$, tridentate NXO^- and the tetradentate "salen" ligands $N_2O_2^{2-}$ in which the complexation and phase transfer of calcium(II), cobalt(II), copper(II), magnesium(II), manganese(II), nickel(II) and zinc(II) sulfates and chlorides were studied. Calcium(II) and magnesium(II) as expected were not extracted. For the remaining metals the anion has a major affect upon metal uptake and for the chlorides of cobalt(II), copper(II) and zinc(II) loadings of the organic phase exceeded those expected for 1:1 (ligand: metal) complex formation with the sexadentate $N_2X_2O_2^{2-}$ and tetradentate $N_2O_2^{2-}$ or 2:1 complex formation with the NXO^- ligands.

Preliminary investigations into the characterisation of complexes formed in the screening study are discussed in chapter five. Chloride analyses of the loaded ligands show metal: chloride ratios of 1:2 for the copper and zinc complexes. A series of cobalt, copper and zinc solid state complexes have been synthesised for sulfate nitrate and acetate salts. A crystal structure of a copper complex shows the copper coordinated to four donor atoms ($N_2O_2^{2-}$) of a sexadentate $N_2X_2O_2^{2-}$ ligand.

Preface and Declaration

Since graduation from University of Edinburgh in 2000 with a BSc. (Hons) degree in Chemistry, the author has been engaged in a full time research under the supervision of Professor P.A. Tasker at the University of Edinburgh.

I declare that this has been entirely composed by myself and that the work described herein is my own work except where clearly mentioned either in acknowledgement, reference or text. No part of the work referred to in this thesis has been submitted in support of an application for another degree or qualification from this or any other university or other institute of learning.

Kate Jennifer Smith

Acknowledgements

I would like to thank my supervisor, Prof, Peter Tasker, for all his help and support. I also wish to thank the University of Edinburgh for funding this project.

I would like to say a big thank you to Dr. Timothy Higgs, Dr. Lee West, Dr. David Henderson and Dr. Paul Plieger for their help and guidance and all those many questions which they answered, and also all the past and present Tasker group members for an enjoyable three years.

I thank Mr John Miller for all his NMR work. I am very grateful to Mr Alan Taylor for the many mass spectroscopy he has done for me and to the C/H/N analysis service. I am very grateful to Dr. Simon Parsons and his group, past and present especially to Dr. Andrew Parkin and Mr James Davidson for X-ray structure analysis of my compounds.

Finally I would like to thank all the good friends I have made during my PhD. A special thanks goes to Kerry Bunyan, Sarah Resouly and Jenny Wood for heaps of support and many laughs. Last but definitely not least, many thanks go to my Mum, Dad, Allison and Douglas and of most of all Struan.

Table of contents

Chapter 2: Sexadentate ligands

Chapter 3: Tridentate ligands

Chapter 4: Screening study

Chapter 5: Preliminary investigations into the complexes formed through extraction

Abbreviations

δ	Chemical shift
λ	Wavelength
ν	Wavenumber
γ	Activity coefficient
ε	Extinction coefficient
°	Degree
θ	Circle diffraction angle
°C	Degree centigrade
χ_M	Molar susceptibility
μm	Micrometer
%	Percentage
$\bar{L}$	Substance in the organic phase
Å	Angstrom
ΔG	Free energy
Δ_o	Octahedral crystal field splitting parameter
Δ_t	Tetrahedral crystal field splitting parameter
A	Chloride ion activity
acac	2, 4-pentanedione
Alk	Alkyl
Ar	Aryl
atm	Atmosphere
BOC	Di-*tert*-butyldicarbonate
Bp	Boiling point
Br	Broad
ca	*Circa*
$CDCl_3$	deuterated chloroform
Calc.	Calculated
cis	*Cisoid*
cm^{-1}	Wavenumber
CSD	Cambridge Structural Database
CFSE	Crystal field stabilisation energy
c.f.	Compared with
d (NMR)	Doublet
D_2O	Deuterated water
dd (NMR)	Doublet of doublets
E	Electrode potential
E^o	Standard electrode potential
EBD	1,2-Ethanediamine,N,N'-bis(2-aminoethyl)-N,N'dimethyl
Ed.	Editor
Edn.	Edition
EIMS	Electron impact mass spectroscopy
EPR	Electron paramagnetic resonance
ESA	2,2'-ethane-1,2-diylbissulfanyl-bis-ethylamine
Et. al.	*Et alli* (and others)
Et	Ethyl

EtOH	Ethanol
F	Faraday constant
FABMS	Fast atom bombardment mass spectroscopy
g	Gram
gl^{-1}	Grams per litre
HDTB	2-Hydroxy-3-(dihexylaminomethyl)-5-*tert*-butylbenzaldehyde
HPTB	2-Hydroxy-3-(piperidinyl-4-ylmethyl)-5-*tert*-butylbenzaldehyde
Hr	Hour
ICP-AES	Inductively coupled plasma absorption emission spectroscopy
IR	Infra-red
K	Kelvin
K	Equilibrium constant
LIX	Liquid Ion Exchange
m	*Meta*
m (IR)	Medium
m (NMR)	Multiplet
Me	Methyl
m.p.	Melting point
M/z	mass per unit charge
MeCN	Acetonitrile
MeOH	Methanol
MHz	mega hertz
M^3/h	Meters cubed per hour
min	Minute
ml	Millilitre
mmHg	Millimetres of mercury
mmol	Millimoles
mol	Moles
Mt	Megatonne
mV	Millivolt
NMR	Nuclear magnetic resonance
o	*Ortho*
OH^-	Hydroxide anion
p	*Para*
p.a.	Per annum
pH	Negative logarithm (base ten) of the hydrogen ion concentration
$pH_{½}$	pH at which half the metal is extracted into the organic phase
Ph	Phenyl
Pip	Piperidine
Pipa	Piperazine
pK_a	Negative logarithm (base ten) of the acid dissociation constant
ppm	Parts per million

ppb	Parts per million
q (NMR)	Quartet
R	Ideal gas constant
r.p.m	revolutions per minute
s (IR)	Strong
s (NMR)	Singlet
T	Temperature
t	Tonne
t (NMR)	Triplet
trans	*Transoid*
Tren	Tris(2-aminoethyl)amine
Trine	Triethylenetetramine
UV/vis	Ultra violet/visible
Vol	Volume
w (IR)	Weak
Z	Number of asymmetric units per unit cell

Thesis format

Each Chapter in this thesis is written as a separate entity, such that the numbering of compounds, figures, tables and references is individual to each chapter. All X-ray data may be found on the compact disk at the back of the thesis. The compounds numbering for chapter 2-4 is summarised in the following section.

Index of compounds

Chapter 2:

Sexadentate ligands

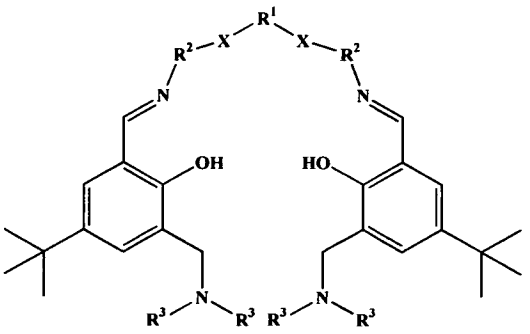

Ligand	X	R^1	R^2	NR^3_2
1	NH	$-(CH_2)_2-$	$-(CH_2)_2-$	piperidine
2[c]	NCH_3	$-(CH_2)_2-$	$-(CH_2)_2-$	piperidine
3	NH	$-(CH_2)_4-$ [a]	$-(CH_2)_2-$	piperidine
4	NH	$-(CH_2)_4-$ [a]	$-(CH_2)_2-$	$N(C_6H_{13})_2$
5	O	$-(CH_2)_2-$	*o*-C_6H_4-	piperidine
6	O	$-(CH_2)_2-$	*o*-C_6H_4-	$N(C_6H_{13})_2$
7	O	$-(CH_2)_3-$	*o*-C_6H_4-	piperidine
8	O	$-(CH_2)_3-$	*o*-C_6H_4-	$N(C_6H_{13})_2$
9	S	$-(CH_2)_2-$	$-(CH_2)_2-$	piperidine
10	S	$-(CH_2)_2-$	$-(CH_2)_2-$	$N(C_6H_{13})_2$
11	S	$-(CH_2)_2-$	*o*-C_6H_4-	piperidine
12	S	$-(CH_2)_2-$	*o*-C_6H_4-	$N(C_6H_{13})_2$

[a] **As part of a piperazine**

Nickel complexes of sexadentate ligands

13	[Ni(**1**)$(C_2H_3O_2)_2$]
14	[Ni(**5**)(SO_4)]
15	[Ni(**5**)$(NO_3)_2$]
16	[Ni(**5**)$(Cl)_2$]
17	[Ni(**5**-2H)]
18	[Ni(**7**)(SO_4)]
19	[Ni(**7**)$(NO_3)_2$]
20	[Ni(**7**)$(Cl)_2$]
21	[Ni(**7**-2H)]
22	[Ni(**9**)(SO_4)]
23	[Ni(**9**)$(NO_3)_2$]
24	[Ni(**9**)$(Cl)_2$]
25	[Ni(**9**-2H)]
26	[Ni(**11**)(SO_4)]
27	[Ni(**11**)$(NO_3)_2$]
28	[Ni(**11**)$(Cl)_2$]
29	[Ni(**11**-2H)]

Chapter 3:

Tridentate ligands

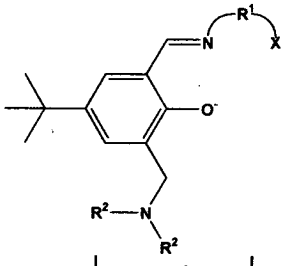

	X	R^1	NR^2_2
30	$N(CH_3)_2$	$-(CH_2)_2-$	piperidine
31	$N(CH_3)_2$	$-(CH_2)_2-$	$N(C_6H_{13})_2$
32	OCH_3	$-(CH_2)_2-$	piperidine
33	OCH_3	$-(CH_2)_2-$	$N(C_6H_{13})_2$
34	OCH_3	*o*-C_6H_4-	piperidine
35	OCH_3	*o*-C_6H_4-	$N(C_6H_{13})_2$
36	SCH_3	*o*-C_6H_4-	piperidine
37	SCH_3	*o*-C_6H_4-	$N(C_6H_{13})_2$

Nickel complexes of tridentate ligands

38	[Ni(**30**)(SO_4)]
39	[Ni(**30**)Cl_2]
40	[Ni(**30**)$_2$($C_2H_3O_2$)$_2$]
41	[Ni(**32**)(SO_4)]
42	[Ni(**32**)Cl_2]
43	[Ni(**32**)$_2$($C_2H_3O_2$)$_2$]
44	[Ni(**34**)(SO_4)]
45	[Ni(**34**)Cl_2]
46	[Ni(**34**)$_2$($C_2H_3O_2$)$_2$]
47	[Ni(**36**)(SO_4)]
48	[Ni(**36**)Cl_2]
49	[Ni(**36**)$_2$($C_2H_3O_2$)$_2$]

Chapter 4:

Tetradentate ligands

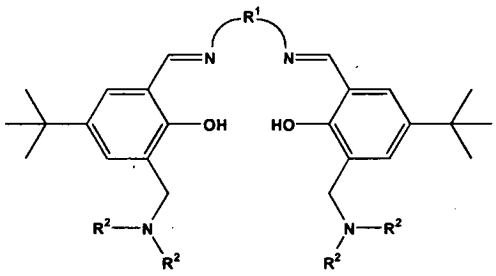

	R^1	NR^2_2
50	-C_6H_{10}-	N(C_6H_{13})$_2$
51	-C_6H_4-	N(C_6H_{13})$_2$
52	-biphenyl-	N(C_6H_{13})$_2$
53	-(CH_2)$_2$-	N(C_6H_{13})$_2$

Chapter 5:

Copper Complexes

54	[Cu(**5**-H)($C_2H_3O_2$)]

Chapter One

Introduction

Contents Page

1.1 Aim

The work described in this thesis aims to develop and design ditopic ligands to function as extractants of divalent transition metal salts containing metal ions which show a preference for octahedral coordination geometry. The initial aim was to identify new systems to extract and transport nickel(II) cations and sulfate dianions in hydrometallurgical circuits derived from the leaching of sulfidic or lateritic ores.

This chapter provides a background to the research, outlining the history of pyrometallurgical and hydrometallurgical recovery of base metals (sections 1.2 and 1.3), the use of solvent extraction in the recovery and separation of cobalt and nickel, which occur jointly in most natural deposits,[1] (sections 1.5 and 1.6) and the developments of a novel class of complexing agent for metal salts including the work at The University of Edinburgh in section 1.7. The last section 1.8 outlines the specific objectives of the research in this thesis targeted at the extraction of metal salts containing a metal which show a preference for octahedral coordination geometry.

1.2 Pyrometallurgy

The primordial atmosphere was predominantly composed of SO_2 and CO_2. Consequently, during this time the metal ores formed consisted principally of metal sulfides. Around 10^9 years ago photosynthesis became a dominant process and oxygen became a significant component of the Earth's atmosphere resulting in the upper layers of sulfidic ore deposits undergoing aerial oxidation.[2] As a result of these changes to the composition of the Earth's atmosphere, a metal deposit typically consists of a lower sulfide layer, a middle mixed sulfide/oxide layer and a top metal oxide layer.[2]

The smelting of copper ores was first performed around 4000 BC, by heating[2] the ore in a primitive hearth/furnace with a reducing agent such as carbon. Such ores often

contain metal sulfides as well as oxides and smelting is often preceded by the conversion of the sulfide to an oxide by roasting in air, (Equation 1.1).

Equation 1.1 $2Cu_2S(s) + 3O_2(g) \longrightarrow 2Cu_2O(s) + 2SO_2(g)$

The recovery of a metal by heating is commonly known as pyrometallurgy and is generally practised for the recovery of base metals such as copper, iron, nickel and zinc.[3] The principal disadvantages[3] of pyrometallurgical methods can be the resultant emission of gases, high-energy consumption, excessive dust formation and its inability to be used to purify complex or low grade ores.

As shown in Equation 1.1, if pyrometallurgical methods are used to recover metals from sulfidic ores, SO_2 production results. If the amount of SO_2 formed is high enough in concentration then it can be recovered[3] by conversion to sulfuric acid. When the concentration of SO_2 is low then alternative disposal methods can be used, but these are expensive. Emission of SO_2 also occurs[3] during the transport of the molten slags and matte that are usually saturated with SO_2. Consequently, SO_2 is often released into the atmosphere, during and even following pyrometallurgical treatment of ores, contributing to acid rain.[3]

Pyrometallurgical recovery is an energy-intensive process typically performed at a temperature of around 1,200 °C. Also, capital costs are high due to the expensive equipment needed for heat recovery and the large refinement plants.

The fossil fuels consumed during metal recovery via pyrometallurgy produces large volumes of gaseous pollutants. These gases often contain a fine dust from the ore which is itself often a valuable material.[3] This dust has to be recovered to reduce pollution.

Pyrometallurgical processes are unsuitable for the treatment of complex ores and low-grade ores due to separation being difficult and the large amount of energy required to melt the ores.[3]

1.3 Hydrometallurgy

1.3.1 Background

The declining availability of high grade ores and the consequent need to process low grade or complex ores along with the imposition of stricter environmental laws have led to the development of new technologies for the recovery of base metals. These include hydrometallurgy, which is a branch of metallurgy that utilises aqueous media to extract metals from their ores. Hydrometallurgy began to be practised at the end of the 19th Century,[3] when two major processes were developed: the cyanidation process for gold and silver recovery and the Bayer process for the recovery of aluminium from bauxite. In the cyanidation process a powder mineral slurry, which typically contains approximately 10 ppm of gold, is treated with a sodium cyanide solution, (Equation 1.2). The resulting filtrate is then treated by a cementation process, (Equation 1.3), which involves the displacement/precipitation of gold from the leach solution using zinc chips. Roasting of the impure gold followed by melting produces gold of 80-90% purity.

The technologies now account for considerable percentages of the world's production of metals, over 90% for instance in the case of gold, around 80% for zinc and 100% for alumina.[4]

Equation 1.2 $4Au + 8NaCN + 2H_2O + O_2 \longrightarrow 4Na[Au(CN)_2] + 4NaOH$

Equation 1.3 $2Na[Au(CN)_2] + 2Zn \longrightarrow 2Na[Zn(CN)_2] + 2Au$

The Bayer process[5, 6] is outlined in Figure 1.1 and involves the leaching of crushed bauxite ($AlO_x(OH)_{3-2x}$, $0<x<1$) with caustic aluminate solutions containing NaOH (100-300 gl^{-1}). The reaction is carried out above its boiling point at 140-280 °C in a pressure reactor (≤ 35 atm) (Equation 1.4). The caustic solution only reacts with the alumina, leaving the impurities to be separated by filtration, giving a clear solution. The dissolved aluminium hydroxide is recovered by dilution and cooling to

50-70 °C. The pure solution is then seeded by addition of gibbsite and agitation in large crystallisers for three days to precipitate aluminium tri-hydroxide. This is filtered washed, dried and calcined to yield pure aluminium oxide, (Equation 1.5). Molten cryolite (Al_2O_3) can then be electrolysed to yield pure aluminium metal by the Herault Hall reaction.

Equation 1.4 $AlO(OH) + NaOH \longrightarrow NaAlO_2 + H_2O$

Equation 1.5 $2Al(OH)_3 \longrightarrow Al_2O_3 + 3H_2O$

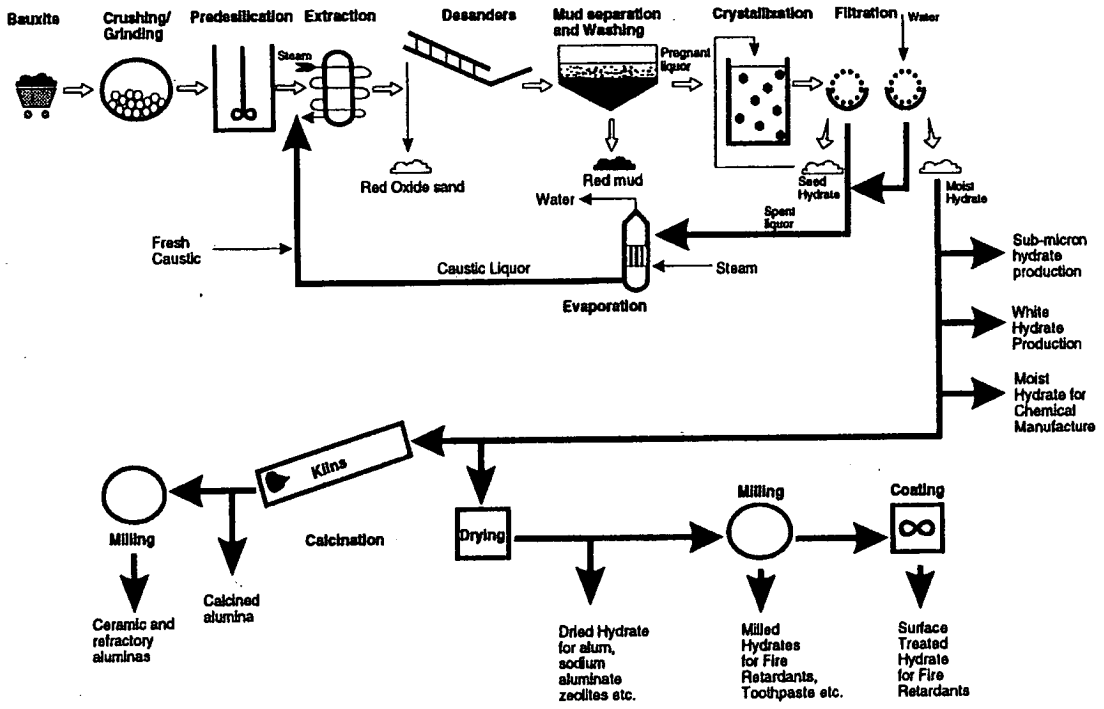

Figure 1.1 The Bayer process[6]

Worldwide production of aluminium hydroxide exceeds 55 million tonnes per year and approximately 90% is calcined to aluminium oxide, most of which is used in the production of aluminium metal.[6]

The advantages of hydrometallurgy are that it is suitable for processing mixed metal ores, mixed oxide-sulfide ores, dump stocks, residues and intermediate products.[3] This is important as the world's resources of high-grade ores are dwindling or are

often found in politically unstable areas. It can be used to treat sulfides without generating SO_2 e.g. by oxidative pressure or biological leaching (Equation 1.6) or by ferric chloride leaching (Equation 1.7). Material handling is easier as the solutions and slurries can be transported in pipes. The energy consumption and costs are a lot less due to the lower temperatures involved,[3] usually below 100 °C, and hence less fuel is needed. Also the hydrometallurgical plants can be located close to the ore bodies and therefore lower transport costs are needed.

Equation 1.6 $MS + 2O_2 \longrightarrow MSO_4$

Equation 1.7 $MS + 2FeCl_3 \longrightarrow MCl_2 + 2FeCl_2 + S$

The main drawback of hydrometallurgy is the finely divided hydrated solids or "sludges" that are produced. If they are left to dry they create dust problems and if wet they gradually release[3] metal ions. However, the disposal of waste solutions and sludges is less troublesome than the disposal of the gases produced by pyrometallurgical processes, and consequently in the past 60 years[3] the development of hydrometallurgy has been advancing and competing with pyrometallurgy, and even replacing some pyrometallurgical processes.

1.3.2 Solvent extraction

Solvent extraction is applied in hydrometallurgical metal recovery where a specific metal ion in the aqueous phase is transferred into and concentrated in an organic phase via complexation with a hydrophobic ligand. The metal can be subsequently stripped from the organic phase to give a pure aqueous metal solution. It was used[3] for the first time on a preparative scale in the 1940's in connection with the Manhattan Project in the USA, when high-grade uranium concentrate was dissolved in HNO_3, and uranium was selectively extracted by ether, then stripped using water to give a concentrated solution of pure uranium nitrate used for the production of an atomic bomb. This was followed by the gradual development[3] of hydrometallurgical methods for other high-value metals such as plutonium, thorium, niobium, tantalum,

zirconium, hafnium, boron, beryllium and finally molybdenum. In the 1960's solvent extraction technology was used for the first time in copper mining (see section 1.5.1). Today solvent extraction is widely used for the separation, purification and recovery of many metals including copper, cobalt, nickel, zinc, tantalum, niobium, zirconium, uranium, chromium, precious metals and the rare earths.

1.4 Nickel and cobalt ores

Most of the world's nickel is produced from sulfidic deposits and to some extent from nickel laterites.[7, 8]

Sulfidic ores bearing copper and nickel (~30% of the world's land based nickel resources)[9] also contain minor quantities of cobalt (accounting for 30% of world cobalt "known" resources)[10] plus trace amounts of precious metals. They occur mainly within Canada and Russia. In Canada, large established sulfide ore bodies are in active operation within the Sudbury Basin, where both Inco Ltd and Falconbridge Ltd operate many underground mines and some open pits.[10] The ore bodies extend to considerable depths (e.g. Creighton Mine, Inco mined at depths of up to 2,295 m below the surface).[11]

Laterite ores are located close to the earth's surface, therefore they can be mined at lower costs than the underground sulfide ores.[9] Nickel ferrous lateritic ores contain close to 70% of the world's known land-based nickel resources [1] and 70% of global cobalt reserves.[10] These oxide ores essentially may be classified as either limonite or serpentine ore types, which require slightly different processing techniques to remove impurities such as magnesium, iron, manganese, aluminium, chromium, and other metals. Large laterite ore reserves have been identified in the Southern Hemisphere in locations such as Australia, New Caledonia, Indonesia and New Guinea and in the Northern Hemisphere, the Philippines and Cuba.[10] The Goro laterite deposit in New Caledonian comprises of 20% of the world's laterite nickel reserves.[1]

Sea nodules were discovered on the ocean bed in the late 1800's.[10] They contain metals such as copper, nickel and cobalt as oxides and oxyhydroxides of iron and manganese.[10] It is estimated that there is 600 Mt of cobalt contained in deep-sea nodules and the oceanic crusts compared with land based resources which contain about 10 Mt giving us a 500 year resource at present rates of consumption.[10] Over the years numerous studies have been undertaken to develop practical and cost effective means of treating this source of valuable base metals but so far no viable processes have been developed.

The emphasis on preserving the ecology has resulted in environmental measures to recycle metal bearing materials. This has led to a steady growth in the production of nickel and cobalt from secondary sources such as scrap and intermediates such as mill tailing and metallurgical slags.[7, 10]

In general the untreated or pre-treated materials are leached in ammoniacal or acidic media.[7, 9] The leach solutions chiefly contain nickel and cobalt along with other impurities such as iron, copper, chromium, aluminium, silica.[7] From such solutions impurities such as iron, chromium, aluminium, silica etc can be removed by lime precipitation.[7]

For solvent extraction to occur on a molecular level the metal ion and the extractant molecule(s) must diffuse together and react in either the organic or aqueous phase or at the interface and then the resulting metal complex must diffuse into the bulk of the organic liquor.[12] (Substances in the organic phase are represented below a horizontal bar e.g. $\overline{L}$)

1.5 Extractants

Solvent extractants can be broadly classified into 3 categories:[12]

1) *Acidic extractants and cation extractants*, form neutral complexes with metal centres using an anionic form of the ligand which is often generated by loss of one or more protons from the ligands.

Equation 1.8 $\overline{nLH} + M^{n+} \longrightarrow \overline{L_nM} + nH^+$

2) *Basic or anion exchangers*, generally quaternary ammonium compounds and alkylamines. Extraction is dependent on the ability of the metal ion to form an anionic species in the aqueous phase and then be extracted as an ion pair.

Equation 1.9 $\overline{n[R_3NH]X} + MY^{n-} \longrightarrow \overline{[R_3NH]MY} + nX^-$

3) *Solvating extractants,* which compete with water for a position in the first or second coordinating sphere of the metal ion. The replacement of the water of hydration by these reagents facilitates the transfer of the metal ion complex into an organic phase. Neutrality of the extractant complex is often achieved by an anion entering the first coordination sphere (as in Equation 1.10) or formation of an ion pair.

Equation 1.10 $[M(H_2O)_x]^{n+} + xL + \overline{Y^{n-}} \longrightarrow \overline{[M(L)_xY]} + xH_2O$

1.5.1 Acidic extractants used in copper recovery

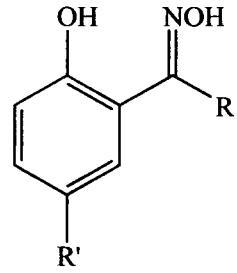

Type	R	R'	Trade name
Ketoxime	C_6H_5	$C_{12}H_{25}$	LIX 64
Ketoxime	C_6H_5	C_9H_{19}	LIX 65
Ketoxime	CH_3	C_9H_{19}	LIX 84
Aldoxime	H	C_9H_{19}	Acorgap50
Aldoxime	H	$C_{12}H_{25}$	LIX 860

Figure 1.2 Phenolic oxime extractants

One relevant example of a solvent extraction process using an acidic extractant is the industrial process for the recovery of copper. In the mid-1960's the first commercial copper-selective extractants based on hydroxyoxime reagents were developed[9, 11] (Figure 1.3).

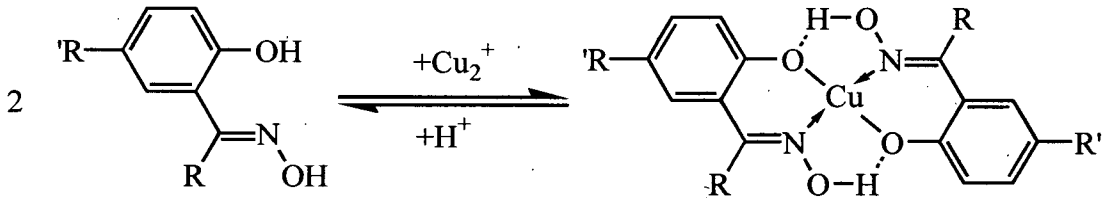

Figure 1.3 Extractant of copper(II) using phenolic oxime extractant

The flowsheet (Figure 1.4) outlines the process for the extraction of copper from oxide ores to pure copper metal in four stages: leaching, extracting, stripping and electrowinning. Sulfuric acid leaching of the oxidic ore makes an impure copper sulfate solution. The pregnant leach solution typically contains a higher concentration of iron(III) than copper(II). It is contacted with a hydrocarbon solvent containing a hydrophobic phenolic oxime ligand (pH 1.5-2.0)[11] of the type shown in

Figure 1.2. The ligand [for example LIX 63, LIX 64 and LIX 65 (Figure 1.2)] is able to selectively extract the copper(II) ion from aqueous solutions (typically 1-3 g of copper per litre)[11] into the hydrocarbon phase and by doing so releases two protons into the aqueous phase (Figure 1.5). The copper(II) is stripped from the ligand by contacting the organic phase with stronger sulfuric acid than that present in the pregnant leach solution generating a pure solution of copper sulfate (50 g l^{-1} copper and 150-180 gl^{-1} H_2SO_4)[9, 11] for electrolytic reduction, regenerating the hydroxyoxime which can be recycled (Figure 1.5).

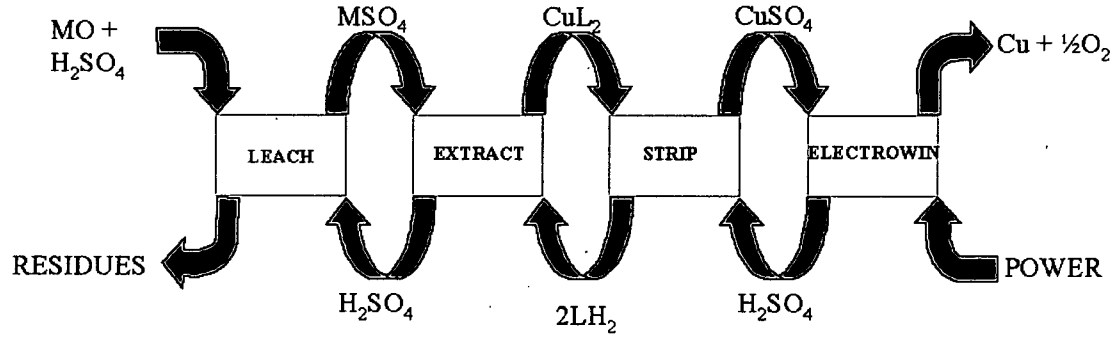

Figure 1.4 A flowsheet for the recovery of copper from oxidic ores using sulfuric leaching, solvent extraction with phenolic oxime reagents and electrowinning

As the loading and stripping of the copper in this circuit is controlled by maintaining a pH gradient across the circuit it is often referred to as a "pH-swing" process. The electrowinning step regenerates the acid consumed in stripping. Effectively the electrical power applied in electrolysis maintains the pH gradient across the circuit to drive the transport of copper(II) from left to right and $2H^+$ from right to left.

$CuO + H_2SO_4$	$\rightleftharpoons$	$CuSO_4 + H_2O$	Leach
$CuSO_4 + \overline{2LH}$	$\rightleftharpoons$	$\overline{CuL_2} + H_2SO_4$	Extract
$\overline{CuL_2} + H_2SO_4$	$\rightleftharpoons$	$CuSO_4 + \overline{2LH}$	Strip
$CuSO_4 + H_2O$	$\rightleftharpoons$	$Cu + ½O_2 + H_2SO_4$	Electrowin
CuO	$\rightleftharpoons$	$Cu + ½O_2$	Overall

Figure 1.5 The materials balance for recovery of copper from oxidic ores using sulfuric acid leaching, solvent extraction with phenolic oxime reagents, acid stripping and electrowinning

The use of solvent extraction in copper mining resulted in significant reduced operating costs (by some estimates, about 50% lower than by previous cementation with iron route).[9] Today there are about 50 such plants with a total production capacity of close to 2 million tonnes of copper p.a.. The individual solvent extraction capacity of these plants ranges from ~200-3,000 m^3h^{-1} of pregnant leach solution (PLS).[9]

The hydrometallurgical extraction of copper from its oxide ores using phenolic oxime extractants (Figure 1.2) is now a commercially successful industrial process. [13] Their high selectivity for copper(II) over iron(III) is one reason for their commercial success.[11] The reason for this selectivity is that they form a square planar complex with copper(II) containing two 6 membered and two 5 membered rings (Figure 1.6).[11]

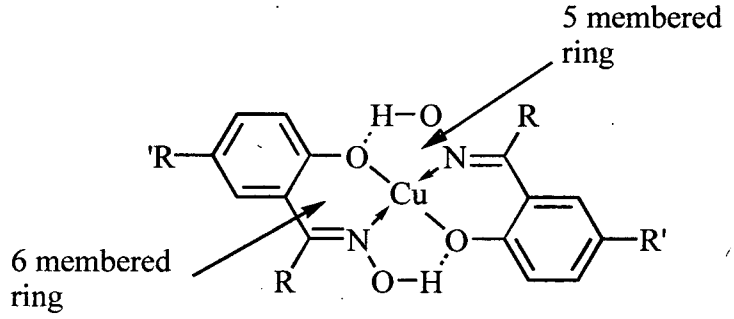

Figure 1.6 The commercially used phenolic oxime extractants

Due to the formation of the five membered rings and their high stabilisation via intermolecular hydrogen bonding, the formation constant of the 1:2 complex greatly exceeds that of the 1:1. The iron(III) complex on other hand is an octahedral complex with no extended planar ring formation. Therefore, the stability of the iron(III) complex is less than the copper(II) complex and hence the extraction of copper can be carried out at pH values lower than those required for iron, see Figure 1.7. Also the copper(II) extraction is enhanced and the iron(III) loading suppressed by short phase-contact times.

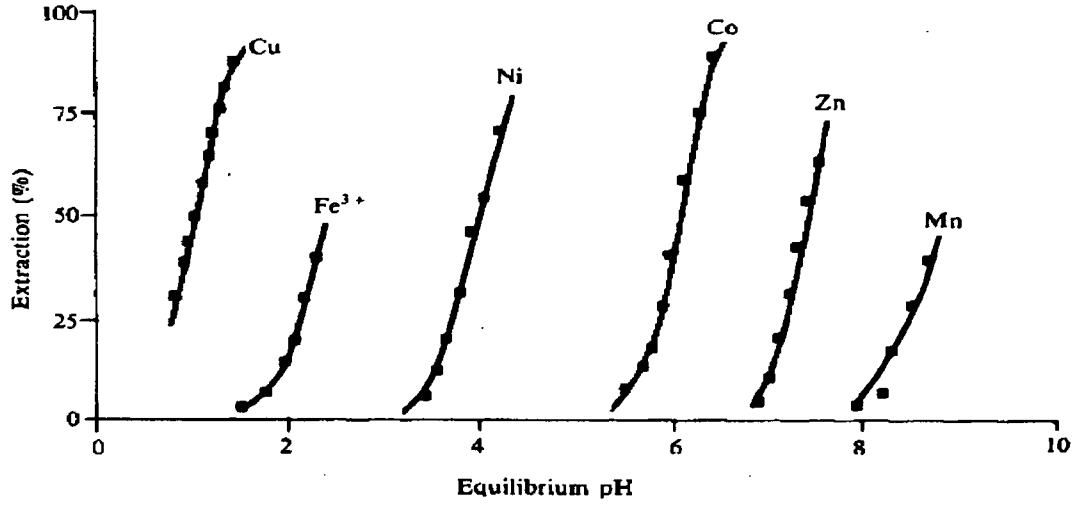

Figure 1.7 Extraction of some divalent metals and iron(III) (0.01 M as nitrates) from 0.2 M ammonium nitrate by 0.10 M solutions of *anti*-1-(2-hydroxy-5-methylphenyl)octane-1-one oxime in xylene at 30°C. For the divalent metals, the order is largely as expected from the Irving Williams Series of stability constants[11]

Secondly the excellent overall materials balance for this circuit contributes to its economical viability and this is the reason for the growth in the hydrometallurgical recovery of copper in the last decade. Currently, *ca.* 25% of the primary copper production world-wide involves[14] hydrometallurgical recovery based on solvent extraction. The world-wide production of copper by solvent extraction in 1999 exceeded 2 x 10^6 t. At present several plants producing up to 200 t of copper per day by an integrated leach, solvent extraction, electrowinning route are in operation throughout the world.[11] The disadvantages of the process are the slow kinetics of the leaching process,[11] the large volume of solution required per unit mass of copper and the complicated processes required for extraction of precious metals that remain in the leaching residues.

The ortho-hydroxyoxime extractants used in the commercially successful extraction of copper from sulfate solutions can also be used as extractants for a variety of other metals. The extractants such as LIX (Liquid Ion Exchange)[15, 16] are becoming increasingly popular for the extraction of nickel from ammoniacal solutions because of the low energy requirements and generation of small volumes of waste solutions for disposal.[15]

For LIX there are two basic process alternatives for metal separation in a multi-component system.[15, 16]

1. Selective Extraction
2. Selective Stripping

Selective stripping is more economical (in most cases) and requires fewer stages. For example copper and nickel bearing ammoniacal solution can be either selectively extracted which requires ammonia removal from both the copper and nickel organic circuits, whereas for co-extraction only one organic stream would require ammonia stripping.

When ammoniacal solutions are used to leach nickel bearing ores nickel amine complexes are formed. Such complexes are also generated by acid leaching followed by treatment with ammonia.[17] (Copper(II), nickel(II) and cobalt(II) are found in the aqueous solution as stable amine complexes where as iron(II) forms very weak complexes and complexes with iron(III) with ammonia have not been observed hence iron is rejected from the process as the oxide at the leaching stage.[11])

One of the earliest copper and nickel plants was in El Paso, Texas and was operated by SEC in the 1970's.[9, 11, 18, 19] It was on a very small scale (2 t of copper and 0.5 t of Ni/day) with the aqueous feed solution consisting of a crystalliser discharge stream from a local copper refinery and containing ~70 gl^{-1} copper and 20 gl^{-1} nickel.[11] It used a 9% solution of the extractant LIX 64N[11] (LIX 65N containing ~1 vol% LIX 63) (order of extraction of LIX 64N copper(II) > iron(III) > nickel(II) > zinc(II) > cobalt(II)[11]). Copper was initially extracted at pH 1.6-2.2, the pH of the solution was then raised with ammonia gas to ~8.5[19] to extract nickel into the organic giving a NiL_2 (L = LIX64N) complex.[9, 11] As ammonia was co-extracted by the ligand, before stripping could be accomplished the ammonia was removed by neutralisation with water or a dilute acid solution (~1 gl^{-1} H_2SO_4). The nickel could then be stripped from the organic extractant with dilute H_2SO_4 at pH~2 producing $NiSO_4$ electrolyte for nickel electrowinning.[9]

There are several problems associated with LIX type reagents in the solvent extraction of nickel/cobalt containing solutions. Firstly during solvent extraction cobalt(II) is extracted by the hydroxyoxime where it is oxidised and accumulates in the organic as very stable non-labile cobalt(III) complexes.[9, 20] The cobaltic compound can be reduced by a variety of agents after which the cobalt is easily stripped.[20] Or the nickel(II) and cobalt(II) solution can be aerated to oxidise the cobalt(II) to cobalt(III).[11] Therefore the nickel can be selectively extracted by the ortho-hydroxyoxime due to much faster reaction kinetics of nickel and slow cobalite kinetics[20] and low extraction of cobalt(III) by the extractant.[11]

Secondly[9] LIX 64N loses its oxime group (C=NOH) by conversion to a ketone (C=O) through cobalt catalysed oxidation, hence losing its extractive capacity. But the ketone can be re-oximated by contact with hydroxylamine salts in alkaline solutions to give the original oxime.

Despite these difficulties LIX 64N is used commercially to extract nickel from ammoniacal solution in a number of operations, for example in the Nippon Mining's Hitachi refinery and the El Paso refinery described previously. The feed consists of a solution of cobalt, nickel and other metal sulfates obtained by the high-pressure oxidative leaching of a mixed metal sulfide ore.[11] Iron and copper are removed by chemical precipitation methods, followed by sequential zinc and cobalt removal by an organophosphorus acid extractant under weakly acidic conditions (see section1.5.3.2).[11] The pH is adjusted (pH 9-9.5)[11] with ammonia and nickel is extracted into a 25% solution of LIX 64N in an alkane.[11] The process produced ~3,300 t of nickel and 1,300 t of cobalt p.a. in the early 1980's..

In more recent years LIX 87QN (LIX 84 with an added ingredient)[17, 21] a ketoxime-based reagent has been specially developed by the technical staff of Queensland Nickel and the Minerals Industry of Henkel corporation, Tucson, Arizona for use in the Queensland Nickel Yabult Plant.[17]

LIX 87QN is used to extract nickel from ammoniacal carbonate solutions[17, 19] (cobalt is subsequently recovered by a second solvent extraction circuit). Followed by a stripping at higher concentrations of ammonium carbonate with concentrated solution of ammonia and CO_2. The operation results in a high purity nickel carbonate solution suitable for the preparation of basic nickel carbonate/nickel oxide.

The Centauris Cawse project (Australia) uses LIX 84 [1, 19, 22] to extract nickel and cobalt from ammoniacal solution containing nickel and cobalt. LIX 84 from Henkel (also known as Acorga M5640 from Avecia)[1] is a hydroxyoxime chelating extractant used in copper solvent extraction operations. LIX 84 is selective for cobalt and nickel over zinc, calcium, magnesium and manganese but its downsides are slow nickel loading kinetics and the difficulty in stripping the cobalt due to it being oxidised to cobalt(III).

1.5.2 ß-Diketones

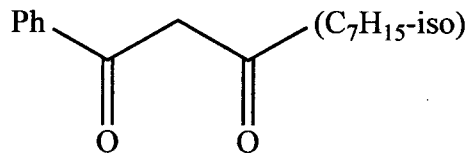

Figure 1.8 LIX 54 extractant

LIX 54 is a commercially available extractant from Henkel[21, 23, 24] containing a ß-diketone moiety (Figure 1.8). It has been reported that its composition is based on 6 isomeric 1-phenyldecane-1,3-diones, heptane-8,10-dione,1,3-diphenylpropane-1,3-dione and an unknown compound.[21, 24, 25] The available extractant also contains some hydrocarbons. ß-diketones are used extensively in radiochemical laboratories for various separations.[23] The main advantage of ß-diketones is that they do not extract ammonia from aqueous solutions[21] and therefore have been commercially recommended for copper extraction from ammoniacal leach solutions.[23]

The order of extraction by LIX 54 as defined by $pH_{½}$ values is as follows:

Lead(II) < copper(II) < iron(II) < zinc(II) < cobalt(II) < nickel(II) < manganese(II) < cadmium(II)[23]

Small differences between $pH_{½}$ values for cobalt(II) and nickel(II) suggest that the separation of these metals is difficult. However nickel(II) can be easily separated with LIX 54 after oxidation of the cobalt in an aqueous ammoniacal solution by hydrogen peroxide. The nickel can be then stripped from LIX 54 with H_2SO_4.[23]

Equation 1.11 $\overline{Ni^{2+}} + 2HL \rightleftharpoons \overline{NiL_2} + 2H^+$

For each mole of nickel extracted two protons are liberated into the aqueous phase, Equation 1.11, hence the pH of the aqueous solution control the equilibria and the reaction.

As the pH is increased the "% nickel extracted" increases and peaks at about pH 8.5[21] (Figure 1.9). At this point the equilibrium favours the formation of the NH_4^+ species as shown in Equation 1.12.

Equation 1.12 $NH_3 + H^+ \rightleftharpoons NH_4^+$

As the pH is increased above 8.5 the equilibrium is pushed to the left which favours the formation of NH_3 which reacts with the nickel(II) ions to form a non-extractable nickel amine complex.[21, 24]

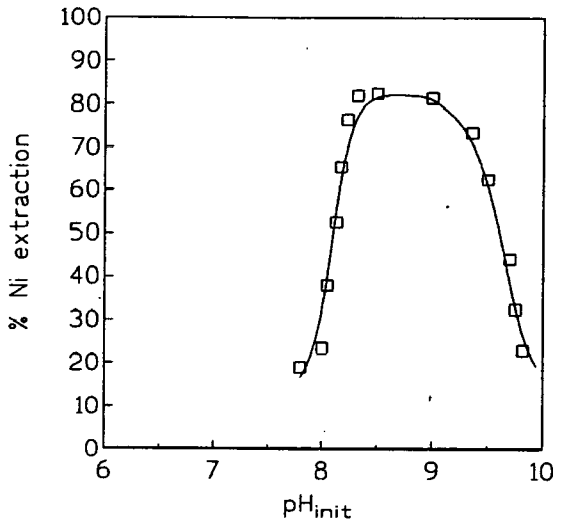

Figure 1.9 Effect of initial pH nickel extraction. Organic phase 10% v/v LIX 54 in iberfluid. aqueous phase: 0.5 gl^{-1} nickel and 0.3 $moll^{-1}$ $(NH_4)_2SO_4$. Temperature: 20 °C. Equilibrium time: 20 mins[21]

1.5.3 Acidic extractants and sulfate solutions

Sulfate solutions result from oxidative pressure leaching and/or H_2SO_4 leaching of sulfide concentrates and precipitates, matte and lateritic ores. They are a common matrix in hydrometallurgy and have received a lot of attention in recent years. Several commercial extractants have been used to date including Versatic 10, D2EHPA, PC-88A/Ionquest 801, Cyanex 272 and recently Cyanex 301.

1.5.3.1 Carboxylic acids

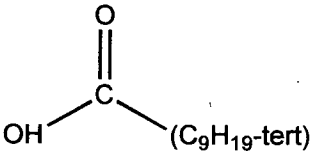

Figure 1.10 Versatic 10

Carboxylic acids are readily available, inexpensive extractants.[9, 11] However they have limited applications in commercial processes probably due to their generally low selectivity and poor pH functionality.[11]

Versatic 10 (Figure 1.10) is a commercial extractant consisting mainly of 2-ethyl-2-methylheptanoic acid and similar highly branched C_{10} isomers.[11] It is partially selective for nickel over cobalt, calcium and magnesium[9] giving it an advantage over the organophosphorus acid extractants described in section 1.5.3.2.

For the divalent metals of the first transition series, the order of extraction follows that expected on the basis of the Irving-Williams series for the stability constants of the octahedral complexes (Figure 1.11).[11]

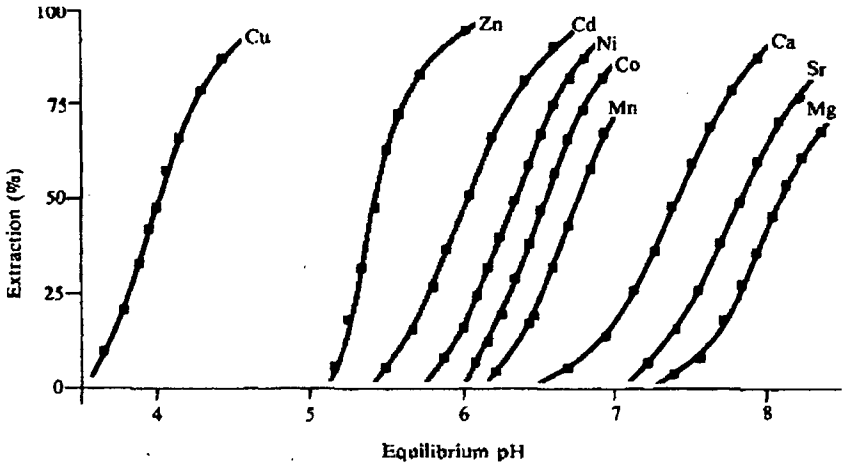

Figure 1.11 Extraction of some divalent metals (0.05 M as nitrates) from 1.0 M sodium nitrate solutions by 0.05 M solutions of Versatic 10 acid in xylene at 20 °C[10]

As it is a weak extractant it requires a high feed pH of 7 which causes high aqueous solubility (3-5 gl^{-1})[9] and hence poor phase separation and requires a ligand recovery step to be built into systems employing this reagent. However, because it is very cheap to produce considerable efforts have been made to increase its affinity for nickel by introducing various modifiers.[9]

Recent interest in Versatic 10 centres around its use at the Bulong laterite plant[1] for nickel solvent extraction. The Bulong laterite contains on average 1.1% nickel and 0.09% cobalt.[26] Out of the three new processes in Western Australia it is the only one to use solvent extraction directly on the partially neutralised nickel-cobalt leach solution.

The Bulong process has a similar flowsheet to those used for uranium extraction,[22] which involves solvent extraction with minimal intermediate products which lowers the capital and operational costs. Iron, aluminium and chromium are precipitated at relatively low pH to give a mixed metal sulfate solution containing gl^1 3.5 nickel, 0.3 cobalt, 1.0 manganese, 15 magnesium and 0.5 calcium.[9] Two solvent extraction circuits are used on the stream. The first circuit[9] uses a phosphoric acid type extractant, Cyanex 272 (see section 1.5.3.2.3) to extract cobalt and manganese. Unfortunately, even though Cyanex is selective for cobalt over magnesium, due to a large excess of magnesium being present it is also transferred and hence the loaded reagent contains mainly manganese and magnesium with only about 10% cobalt. The second extraction stage[9] uses Versatic 10 to separate nickel from calcium and magnesium. If there is incomplete cobalt extraction by the Cyanex 272 the cobalt is co-extracted with the nickel by the Versatic 10 and hence trace amounts can be found in the electrowon nickel metal.

1.5.3.2 Phosphorus acid based extractants

Organophosphorus compounds containing the phosphorus group P=O, such as, D2EHPA, PC-88A, Cyanex 272, have been widely used as analytical extractants since the 1940's.[27] In general such extractants, extract both cobalt and nickel, but have selectivity for cobalt over nickel.

The organophosphorus acid extractants fall into three main types[1] as shown in Figure 1.12:

1. Phosphoric acid (e.g. D2EHPA)
2. Phosphonic acids (e.g. lonquest-801 and PC-88A)
3. Phosphinic acids (e.g. Cyanex 272)

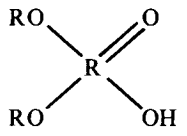

Phosphoric acid

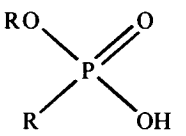

Phosphonic acid

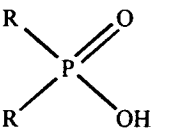

Phosphinic acid

Figure 1.12 Common phosphoric, phosphonic and phosphinic acid extractants

When organophosphorus acids are dissolved in organic aliphatic and aromatic solvents, such as those used in commercial extraction processes, they exist in a dimeric form having an eight membered ring hydrogen bonded ring Figure 1.13.[11]

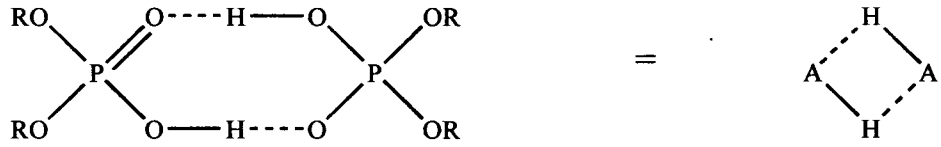

Figure 1.13 Phosphoric acids

When they extract metals the complexes often contain both deprotonated and protonated (solvating) reagents in which the H-bonding between two ligands is preserved forming 8-membered *pseudo* chelate rings. There is little evidence for reagents acting in a simple bidentate manor forming 4-membered chelate rings.

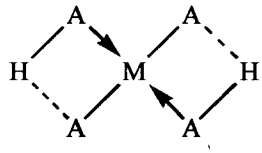

Divalent metal ions that show a preference for tetrahedral coordination are extracted with a ligand: metal (L:M) ratio of 4:1 [e.g. zinc(II)].

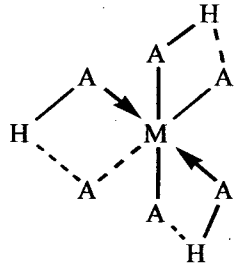

Trivalent metal ions that show a preference for octahedral coordination are extracted with a L:M ratio of 6:1 [e.g. iron(III)].

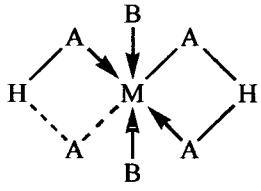

Divalent metals that show a preference for octahedral coordination are extracted with a L:M ratio of 4:1 with two additional ligands (B) bound to the metal ion to retain the preferred geometry. B can = HA or H_2A_2 or water or other solvent.

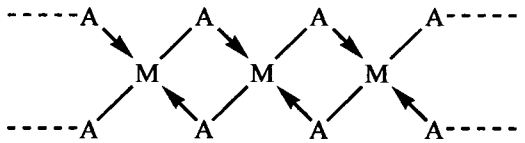

When large amounts of metal are loaded into organic phase then the limiting ratio of L:M, 2:1, is approached and polymerised complexes are formed in which PO_2^- groups acts as a bridging ligand between adjacent metal ions. This causes viscosity problems.

Evidence from spectral, thermogravimetric, magnetic and ESR studies[11] suggest that zinc and manganese form tetrahedral complexes, copper forms square planar or distorted octahedral complexes, nickel forms octahedral complexes and cobalt forms a mixture of tetrahedral and octahedral complexes (the tetrahedral form being favoured at elevated temperatures due to entropy of the reaction).

Phosphorus based reagents show increased selectivity for cobalt over nickel in the order: [11, 28] phosphinic > phosphonic > phosphoric. This order is explained by the fact that as the alkyl groups are brought closer to the metal-coordinating site by removal of the linking oxygen atom causing steric crowding.[11] This brings about considerable destabilisation of the octahedral nickel complex relative to the tetrahedral cobalt complex. This is enhanced when the alkyl group is branched at the alpha-carbon atom. So for example, when R = 2-ethylhexyl, the separation between the curves for cobalt and nickel extraction for a 0.2 M solution of extractant in toluene at 20 °C increases from 0.53 pH units for the phosphoric acid to 1.42 for the phosphinic, and 1.93 pH units for the phosphinic.[11]

1.5.3.2.1 D2EHPA-Phosphoric acid extractant

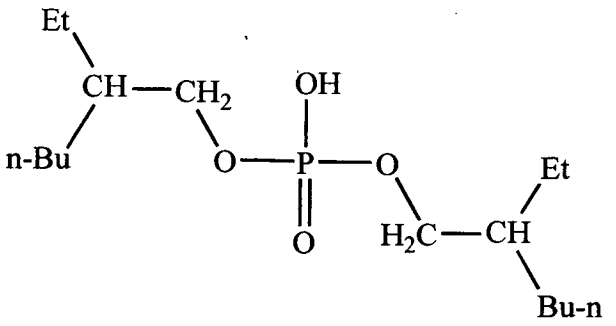

Figure 1.14 D2EHPA

D2EHPA (di-2-ethylhexylphosphoric acid) developed by Ritcey *et. al.*[29] in the 60's, was the first extractant used for cobalt separation from nickel (Figure 1.14). It was developed for the Eldorado Nuclear refinery in Canada for ammoniacal leach solutions. Prior to extraction the leach solution was aerated to oxidise cobalt(II) to cobalt(III) which is extracted by D2EHPA in preference to nickel.

The extraction of metals with di(2-ethylhexyl)phosphoric acid as shown in Figure 1.15 shows no correlation to the Irving Williams series for the stability constant of octahedral complexes. Instead it reflects the ease with which the respective metal ions adopt the tetrahedral configuration (or for copper(II) and chromium(II) a tetragonal distorted octahedral geometry) that is favoured by bulky dimeric ligands.

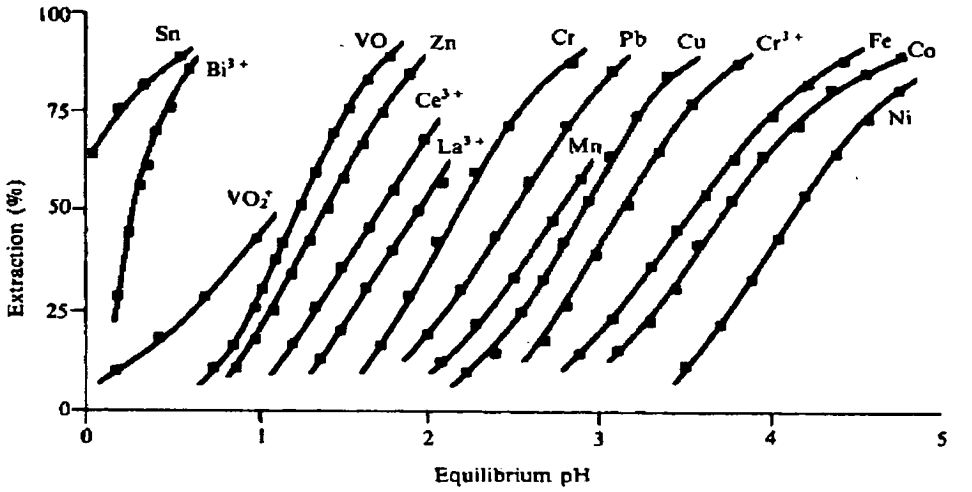

Figure 1.15 Extraction of some metal ions (divalent unless shown otherwise) by 0.50 M solutions of di(2-ethylhexyl)phosphoric acid in xylene at 20 °C[10]

In the 1970's at CANMET Ottawa, D2EHPA was first used to extract cobalt(II) from sulfate solutions. The extractant was preloaded with ammonia which avoided the further addition of base to produce a solution of pH 5-6 which is needed for cobalt(II) extraction. The cobalt was stripped from D2EHPA with H_2SO_4 to produce an electrolyte for electrowinning.

The disadvantages of D2EHPA are that it strongly extracts iron(III) which requires either reductive or HCl stripping, its low degree of cobalt/nickel selectivity and its preferential extraction of calcium,[26] magnesium and manganese over cobalt and nickel. Nevertheless D2EHPA's development as a cobalt extractant has led to advances in refining from sulfate solutions and caused attention to be pushed on to other organophosphorus reagents. It is now a well established reagent in the recovery of base metals and is used commercially in the separation of cobalt from nickel, the separation of zinc from impurities such as copper and cadmium, the

recovery of uranium, beryllium and vanadium and in separation involving yttrium and the rare earth metals.[11]

D2EHPA is used commercially to extract zinc, for example at the Nippon Mining Company.[11] D2EHPA extracts zinc in a single contact at pH 2-3 from a cobalt nickel stream. The cobalt and nickel are then extracted by phosphonic acid extractants. For more information on zinc extraction see chapter 4 (section 4.1.1).

1.5.3.2.2 PC-88A-Phosphonic extractant

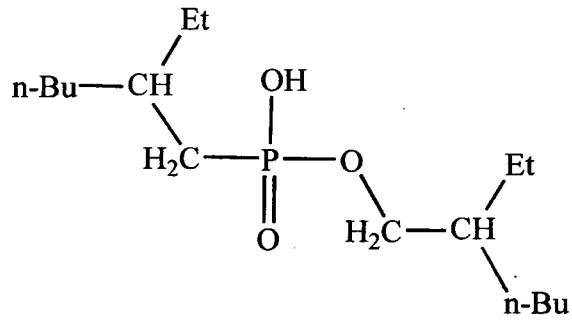

Figure 1.16 PC-88A

2-Ethylhexyl phosphonic acid mono-2-ethylhexyl ester developed and marketed as PC-88A by the Daihachi Chemical Industry and as SME by Shell is being used by the Nippon Mining Company.

In 1978 the Nippon Mining company changed their extractant from D2EHPA to the organophosphonic acid extractant PC-88A (Figure 1.16), to extract cobalt at their Hitachi refinery.[30] PC-88A has a similar extraction operation as D2EHPA but is a poorer nickel extractant and is therefore more selective for cobalt. This was confirmed at Nippon where it was found that PC-88A was ~200 times better at cobalt/nickel separation than D2EHPA.[30] Therefore, even though it is more expensive it was adopted as the new extractant. The new circuit initially involved D2EHPA for the removal of zinc impurities followed by the removal of iron by precipitation. PC-88A was then used to extract cobalt at about pH 5.5.[19] The pH was then increased to 8.5 and the nickel was extracted with LIX 65N.

1.5.3.2.3 Cyanex 272-Phosphinic acid extractant

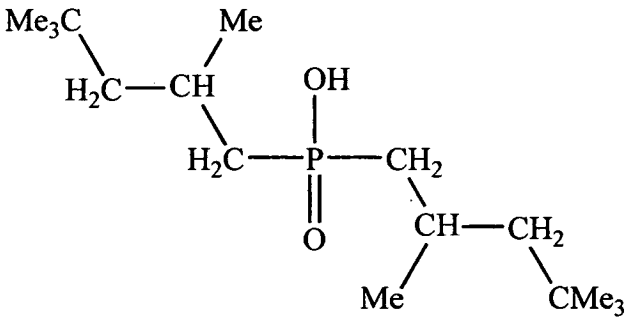

Figure 1.17 Cyanex 272

In 1980 American Cyanamid (now Cytec) produced a new extractant Cyanex CNX in Welland, Ontario. Independent work by Inco's research laboratory in Mississauga, Ontario reported it had a higher selectivity for cobalt over nickel but was "not perfect" (being solid). In 1982 after further research Cyanamid produced an improved version, Cyanex 272 ("27" signified cobalt and the "2" the second generation) (Figure 1.17). As it is an even poorer nickel extractant it is therefore easier to achieve (through fewer extraction and scrubbing stages) the required high percentage of cobalt (> 99.8%) in the electrolyte. As a consequence Cyanex 272 has been adopted by a number of nickel-cobalt commercial operations. The first plant to use Cyanex 272 was in 1985; by 1990 three more plants (including two in Europe) were in operation, by 1995 the number of plants had doubled. Cyanex 272 is presently being used for cobalt/nickel separation in numerous plants around the world including Australia, Belgium, Brazil, Canada and Finland. The latest plant to use Cyanex 272 is the newly upgraded and expanded Outokumpu's Harjavalte nickel-cobalt refinery. The development of Cyanex 272 has therefore caused the expansion of the cobalt/nickel extraction industry and hence has led to the replacement of some of the costly environmentally harmful and operator unfriendly operations.

1.5.3.2.4 Cyanex 301-Dithiophosphinic acid extractant

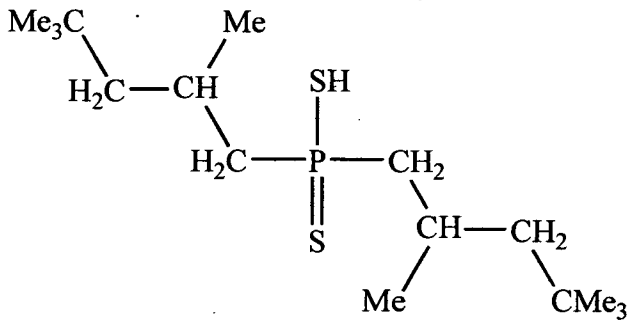

Figure 1.18 Cyanex 301

In the 1960's studies on the corresponding sulfur analogues (organothiophosphorus) were initiated.[27] The substitution from oxygen to sulfur increases the acidity of the extractant as predicted by the hard-soft acid-base (HSAB) principle.[31] Therefore reagents containing sulfur donor atoms are expected to be strong extractants for soft Lewis acid (class b type) metal ions such as silver(I), nickel(II), zinc(II), copper(I), gold(I) and platinum groups metals.[27] In the late 1980's Cytec developed[32] Cyanex 301 (Figure 1.18) and Cyanex 302 (monothiophosphinic acid) for the selective recovery of zinc from effluent streams containing calcium. It was found that both extractants were capable of extracting a number of metal and metalloid species over a large acidity range. Development of the extractant Cyanex 301 by Inco found[9] it to quickly and efficiently remove nickel and cobalt from sulfate solution with fast extraction kinetics (>99.9%).

Cyanex 301 is a dithiophosphinic acid which has an analogous structure to Cyanex 272 with the two oxygens being replaced with sulfur. This slight change greatly effects the chemical properties of the extractant because the affinity of a metal cation to form a chemical bond with hard oxygens is very different from that with soft sulfurs.[32] As nickel prefers to coordinate with softer ligands, Cyanex 301 complexes nickel[1] as well as cobalt at pH <2 and in preference to manganese, calcium and magnesium. As the temperature is increased the amount of metal extracted is also increased. Cyanex 301 has a similar function to H_2S but without the safety concerns associated with the use of H_2S. Copper is also extracted by Cyanex 301 but cannot

be easily stripped, however this is not a problem as it can be easily removed first by ion-exchange ahead of solvent extraction with Cyanex 301.[1, 9] Zinc and ferric iron are co-extracted by the extractant whereas ferrous iron is only extracted at high pH.

Cyanex 301 has the lowest aqueous stability out of D2EHPA, Versatic 10, PC-88A and Cyanex 272[9] and it is even lower under the acidic conditions of the raffinite ($pH \leq 1.5$). Therefore the phase separation is fast for both extraction and stripping and hence there is low soluble and entrapment losses.[1] At this low pH Cyanex 301 does not extract manganese[1] which results in major simplifications of the Cyanex 301 recovery circuit compared to Cyanex 272, which is a key advantage of Cyanex 301 over other extractants which require expensive base addition.

As nickel and cobalt are strongly extracted and their stripping kinetics are very slow they need to be stripped at high acid concentrations over relatively long residence times at elevated temperatures.[1] Normally H_2SO_4 is used but with Cyanex 301 the free acid would need to be neutralised to allow the separation of cobalt from the nickel and for nickel electrowinning. Therefore HCl is used to produce a concentrated nickel-cobalt strip solution (~80-100 gl^{-1} nickel) with about 20 fold reduction in volume,[9] significantly reducing the size of the downstream refining circuit. By using a tertiary amine solvent extractant (see section1.5.4) the $CoCl_4^{2-}$ species is easily extracted leaving the pure nickel amine solution from which the nickel can be recovered by using pyrohydrolysis yielding the nickel oxide product and HCl, which is used in the strip.

The downside[1, 9] of Cyanex 301 is its stability. It is degraded to organophosphorus disulfide by metal-catalysed [e.g. iron(III)] oxidation in air. There are several processes to regenerate it, for example by reduction of the disulfide by contacting the degraded organic with acid and an active zinc powder. However to cut out the regeneration step, the entire solvent extraction process is operated under an oxygen-free atmosphere.

Cyanex 301 is being used in the Goro process for the recovery of nickel and cobalt from laterite ores.[1] The process differs from other PAL (pressure acid leach) processes currently being used for laterites as it involves the recovery of nickel and cobalt by direct solvent extraction with Cyanex 301 from a partially neutralised leach solution to produce a marketable nickel oxide product. Its simple metal recovery scheme, which involves a one step process for the extraction of nickel and cobalt directly from the dilute leach solution, is a major advantage over other commercial cobalt/nickel operations. At present the Goro nickel plant is at detailed engineering stage but is expected to have an annual capacity of 54,000 t of nickel and 5,400 t of cobalt.

1.5.4 Base anion exchange extractants

Amine salts are the only commercially important anion exchange type extractants[11] (Figure 1.19). They are used in the solvent extraction of base metals from chloride media. The formation of chloride solutions can result from Cl_2/HCl leaching of nickel matte, intermediates or secondary nickel sources (see chapter 4 for more examples). Chloride streams are generated at Falconbridge's Kristianland,[11] SLN's Le Havre[11, 19] and SMM's Nihama Metallurgy Hoboken refineries.

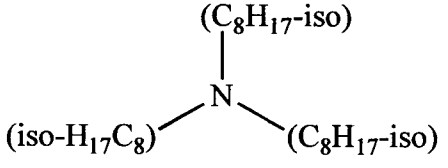

tri-iso-octylamine

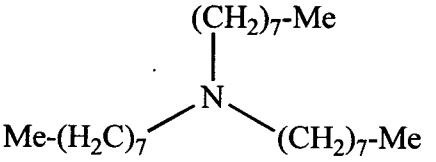

tri-n-octylamine

Figure 1.19 Commercial amine extractants

Amine extractants are most widely used in the extraction of uranium from sulfate leach liquors.[33] They were used in the first commercial application of solvent extraction in the nickel industry and are still in use today. They work because cobalt forms anionic chloro complexes such as $CoCl_3^-$ and $CoCl_4^{2-}$ more readily than nickel. Major developments from the late 60's through to the mid 70's produced the tertiary

amines tri-iso-octylamine (TIOA) and tri-n-octylamine (TnOA). The tertiary alkyl amines in their salt form ($R_3NH^+X^-$) can be used as anion exchange extractants to selectively extract $CoCl_4^{2-}$ into the organic phase (Equation 1.13).

Equation 1.13 $\overline{\qquad\qquad}$ $2[R_3NH]X + CoCl_4^{2-} \longrightarrow \overline{\qquad\qquad\qquad}$ $[R_3NH]_2[CoCl_4] + 2X^-$

Cobalt can be stripped from the organic phase with an aqueous solution low in chloride such as water (Equation 1.14). The equilibrium concentration of chloride ion in the strip liquor therefore lies on the lower portion of the extraction curve, where substantial aquation of the extracted chlorometallate occurs and the cobalt cation returns to the aqueous phase to give $CoCl_2$ ($\geq$60 gl^{-1} cobalt) which can then be purified and electrowon to give cobalt metal.

Equation 1.14 $\overline{[R_3NH]_2CoCl_4} + 6H_2O \longrightarrow Co(H_2O)_6^{2+} + 2Cl^- + \overline{2[R_3NH]Cl}$

The nickel is recovered in these circuits by purifying the raffinates from the cobalt(II) solvent extraction, by removal of lead and manganese and electrowinning to give nickel metal and Cl_2 which is reused in the leaching step.

Equation 1.15 $NiCl_2 \longrightarrow Ni + Cl_2$

The order of extractability of different metals from chloride solution by a given amine usually follows the order of stability of the chlorometallate complex MCl_4^{2-} (Figure 1.20).[11] Thus one disadvantage of the amine reagent is that metals such as iron(III), copper(II) and zinc(II) which also form stable chloro-complexes are co extracted with the cobalt. However, these can be separated from the cobalt by a selective strip followed by a purification circuit for cobalt.

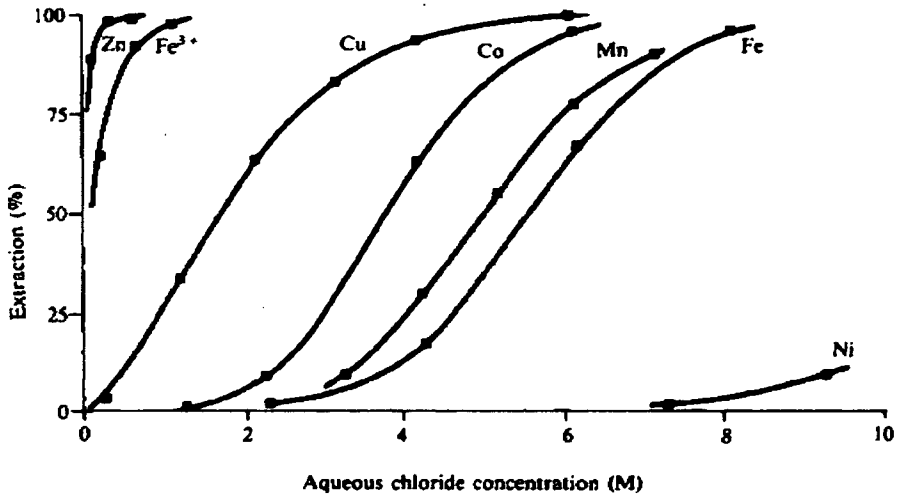

Figure 1.20 Extraction of some divalent metals and iron(III) (0.10 M as chloride) from solutions of lithium chloride containing 0.01 M hydrochloric acid by 0.50 M solutions of Alamine 336 (commercial tri-n-octylamine hydrochloride) in xylene at 20 °C[11]

Another disadvantage of the amine reagent is that if the concentration of nickel is much higher than cobalt in the feed solution, then nickel is co-extracted as it can be easily entrapped within the organic phase.

Falconbridge's Nikkelvertin Kristiansand circuit involves the leaching of nickel-cobalt matte in 8M HCL to give a solution containing nickel(II) 120 gl^{-1} and iron(III), cobalt(II) and copper(II). The iron is removed with the extractant tri-butyl-phosphate followed by the co-extraction of cobalt and copper into a 10% solution of tri-iso-octylamine over three contacts. The cobalt and the copper are then selectively stripped with water. Using an organic: aqueous ratio of 30:1 the cobalt is firstly stripped, followed by copper stripping with a 20:1 ratio. The nickel is also recovered from the nickel chloride raffinate by electrowinning.

Tri-n-octylamine is also used by the Sumitomo Metal in Japan as a 40% solution in xylene to separate cobalt and nickel in a chloride media.

1.6 Problems associated with the use of existing extractants in nickel and cobalt recovery

All of the commercially available extractants described above have technical limitations when used in cobalt/ nickel recovery circuits. The carboxylic acids, amines, oximes, ß-diketones and aromatic hydroxyoximes have the problem of solvent loss which requires strict control of aqueous phase parameters for achieving the separation of the desired metals. The amines have a high molecular weight which leads to a low weight extraction ratio. The alkyl phosphorus reagents also have disadvantages, D2EHPA forms emulsions at high pH and is hydrolytically unstable.[34] Cyanex 272 is highly selective for cobalt over nickel but still extracts some nickel and Cyanex 301 has to be operated under an oxygen excluded atmosphere which is not ideal.

1.7 Extractants to transport metal salts

The initial aims of this thesis involve the design and synthesis of extractants that aim to achieve the selective extraction of nickel(II) from a crude sulfate solution formed from the oxidative leach of sulfide ores. As the oxidative leaching step does not consume sulfuric acid if an anionic extractant is used in the extraction step, then a build-up of acid occurs at the front end of the circuit (Figure 1.21). This acid build up must be recovered from the raffinate, incurring additional costs, or neutralised by base to maintain a pH balance, which in turn would cause further problems as the salt waste generated would need to be removed from the solution and disposed of.[35]

$MS + 2O_2$	$\rightleftharpoons$	MSO_4	Leach
$MSO_4 + \overline{2LH}$	$\rightleftharpoons$	$\overline{ML_2} + H_2SO_4$	Extract
$\overline{ML_2} + H_2SO_4$	$\rightleftharpoons$	$MSO_4 + \overline{2LH}$	Strip
$MSO_4 + H_2O$	$\rightleftharpoons$	$M + \frac{1}{2}O_2 + H_2SO_4$	Electrowin
$MS + 1\frac{1}{2}O_2 + H_2O$	$\rightleftharpoons$	$M + H_2SO_4$	Overall

Figure 1.21 Equations illustrating potential build up of H_2SO_4 in leachate for extraction circuit of metal sulfide ores

These problems could be removed by avoiding the production of sulfuric acid by using ligands which extract both the metal cation and the sulfate anion from the pregnant leach solution. The resulting metal-ligand-anion complex would then be stripped to generate a pure metal sulfate solution from which the pure metal can be electrowon by conventional processes (Figure 1.22 and Figure 1.23).

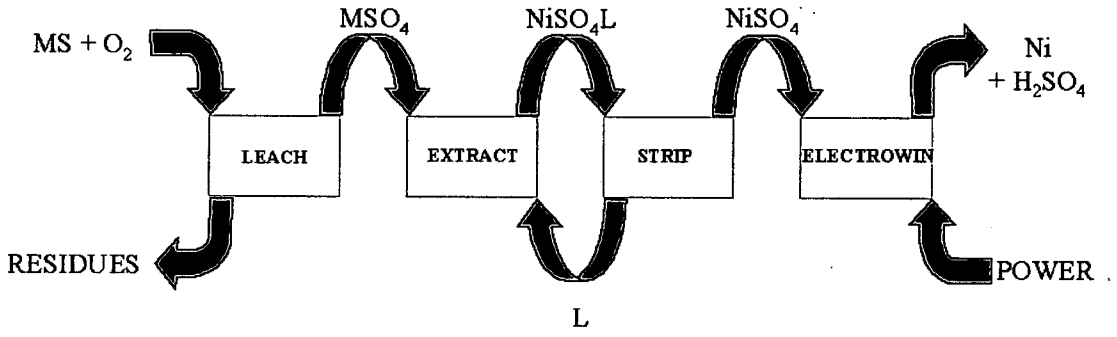

Figure 1.22 A proposed flowsheet for recovery of metals from sulfidic ores using oxidative leaching, solvent extraction with metal salt transportation and electrowinning

The overall equations for the two flowsheets are the same (Figure 1.21 and Figure 1.22) but in Figure 1.22 the sulfuric acid is produced in the final step which is less problematic.

$MS + 2O_2$	$\rightleftharpoons$	MSO_4	Leach
$MSO_4 + \overline{L}$	$\rightleftharpoons$	$\overline{MLSO_4}$	Extract
$\overline{MLSO_4}$	$\rightleftharpoons$	$MSO_4 + \overline{L}$	Strip
$MSO_4 + H_2O$	$\rightleftharpoons$	$M + \frac{1}{2}O_2 + H_2SO_4$	Electrowin
$MS + H_2O + 1\frac{1}{2}O_2$	$\rightleftharpoons$	$M + H_2SO_4$	Overall

Figure 1.23 A proposed material balance for recovery of metals from sulfidic ores using oxidative leaching, solvent extraction with metal salt transportation and electrowinning

1.7.1 Anion binding

Compared to cation receptors, the chemistry of anion binding has been rather slow to develop.[36-38] The coordination of chemical species by virtue of their anionic nature, plays a central role in both inorganic and biological processes[38, 39] for instance a large majority of substrates and cofactors engaged in biological processes are anions. In 1968 the first synthetic receptor for inorganic anions was reported.[40] In 1976 Graf and Lehn reported[41] that a protonated cryptand encapsulates F^-, Br^- and Cl^- anions. Since then several other positively charged anion receptors have been developed. In the past few years it has been recognised as a new area of coordination chemistry stimulating the interest of many researchers.[42-50]

Anion-binding sites containing strong hydrogen bond donors,[36, 51] are able to efficiently bind anions. Examples[36, 38, 44, 48, 52-54] include amides, sulphonamides, thio-ureas and ureas which can be either neutral or cationic. Positively charged anion receptors usually contain protonated nitrogen atoms or metal ions e.g. systems reported by Lehn *et al.*[55, 56]

1.7.2 Ditopic ligands

Since the 1970's a large number of articles have been published[27, 37, 45, 50, 51, 53, 57-67] describing systems which can simultaneously bind both a cation and anion, either by separate cation or anion binding sites[27, 36, 37, 39, 45, 53, 57-67] or by arranging for the anion to interact directly with the metal centre via a vacant coordination site[36, 51] (Figure 1.24). Such systems have potential as new selective extraction and

transportation reagents for a metal salt[42, 66] or can be used to mimic important biological functions and coordinate biologically significant species such as zwitterionic amino acids and peptides.[42]

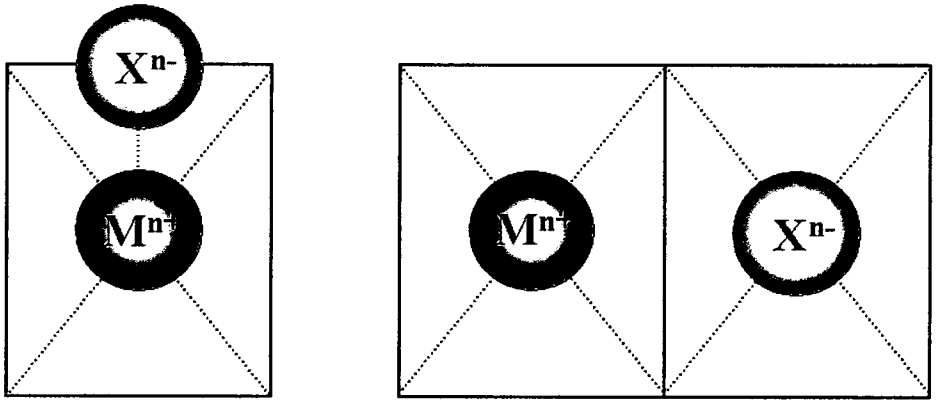

Organic receptors for anions that bind through hydrogen bonding or an ion-dipole interaction.

Inorganic receptors that coordinate anions at the lewis acid.

Figure 1.24 Schematic diagram to illustrate the two different classes of anion binding receptors

In theory the extraction of a metal salt into a water immiscible solvent can be achieved via four contrasting reagent designs (Figure 1.25). Dissociated monotopic ligands utilize two separate reagents,[37] a cation-binding and an anion-binding ligand, (type I) where as with associated monotopic ligands (type II) the two different types of ligands self assemble when they extract the metal salt. Preorganised ditopic ligands (type III) contain both binding sites separated in the same molecular entity, where as in their monotopic analogue (type IV) the metal cation and anion interact and are present in the same site.

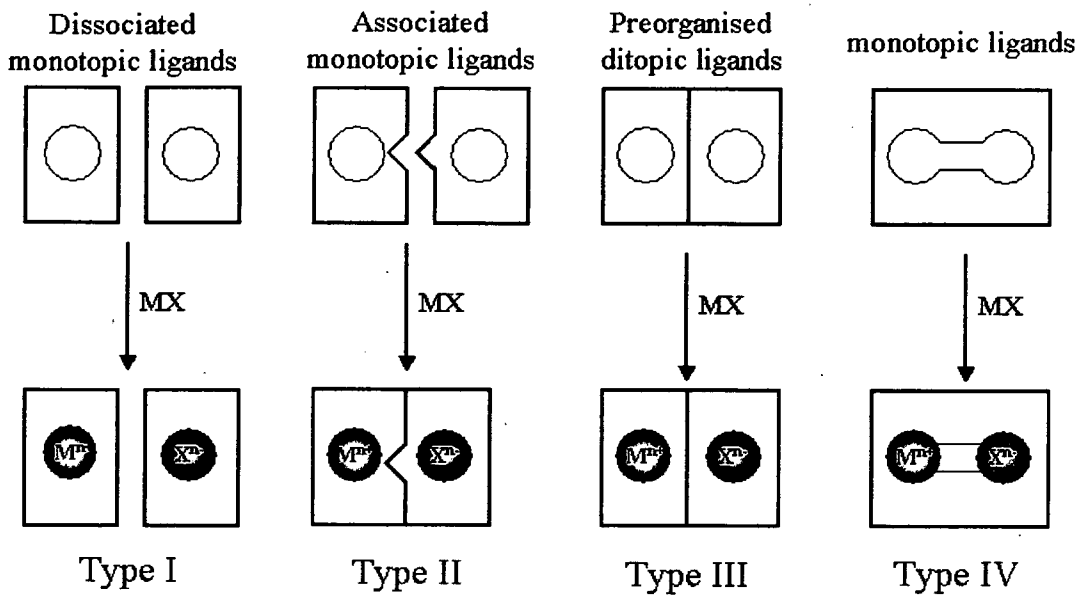

Figure 1.25 Schematic diagram to illustrate four contrasting designs of reagents to extract metal salts

In all cases (types I-IV) it is possible that the metal salt complex is formed by interaction of M^{n+} and X^{n-} with binding sites which carry charges associated with transfer of protons from one site to another shown schematically for type I in Figure 1.26. In the cases of type III and IV ligands this involves the "active" form of the reagent existing in a zwitterionic form.

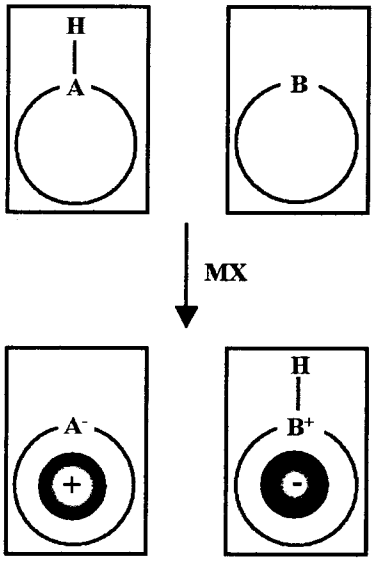

Figure 1.26 Schematic diagram to illustrate the formation of cation and anion binding sites by the transfer of protons from one site to another

Kavallieratos *et. al.* describe a type I system (Figure 1.25) to transport $CsNO_3$.[37] Tetrabenzo-24-crown-8, a well-known caesium (Cs^+) cation receptor, in conjunction with various nitrate host molecules, such as benzene-1,3,5-tricarboxamide or tripodal systems derived from tris(2-aminoethyl)amine (Tren) (Figure 1.27).

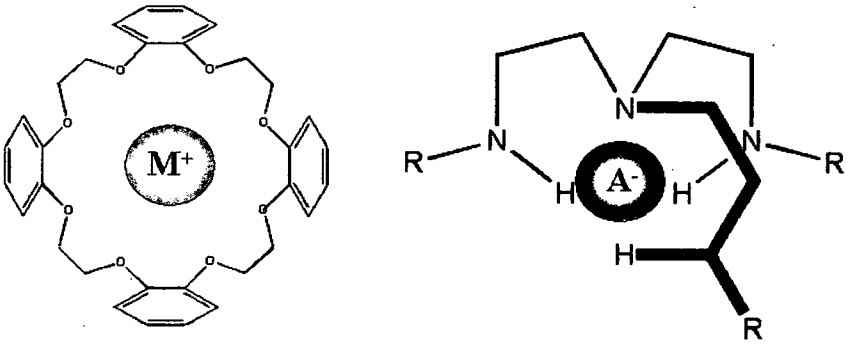

Figure 1.27 Transport of $CsNO_3$ by two host receptors (type I in Figure 1.25)[37]

There are several ditopic ligand systems of type III reported for main group metal salts,[37, 48, 49, 68] but only recently have systems for transition metal salts been developed.[35, 49, 69-74] In general the ion-pair receptors for main group metal salts are based on modified cation receptors[66, 68, 75, 76] such as crown ether or calixarenes combined with hydrogen bonding positively charged or Lewis acidic groups to coordinate the anion for example schiff-base supported uranyls amides, boryls.

An example of a calixarene type ligand is shown by Reinhoudt *et. al.*[65] Calixarenes have been widely reported to act as receptors for cations and neutral molecules.[66] Reinhoudt obtained a calix[4]arene derivative with cation binding ester groups on the lower rim and anion binding ureas on the upper rim which can effectively bind Cl^- only in the presence of Na^+.

Beer *et. al.* have synthesised a number of calixarene and crown ether-based ion-pair receptors and sensors.[42, 43, 45-48, 51, 64, 67, 75, 77-80] Examples are shown in Figure 1.28, Figure 1.29 and Figure 1.31.

The heteroditopic rhenium(I) and ruthenium(II) bipyridyl calix[4]arene, (Figure 1.28)[64] simultaneously complex alkali metal cation-anion pairs at the calixarene lower rim.

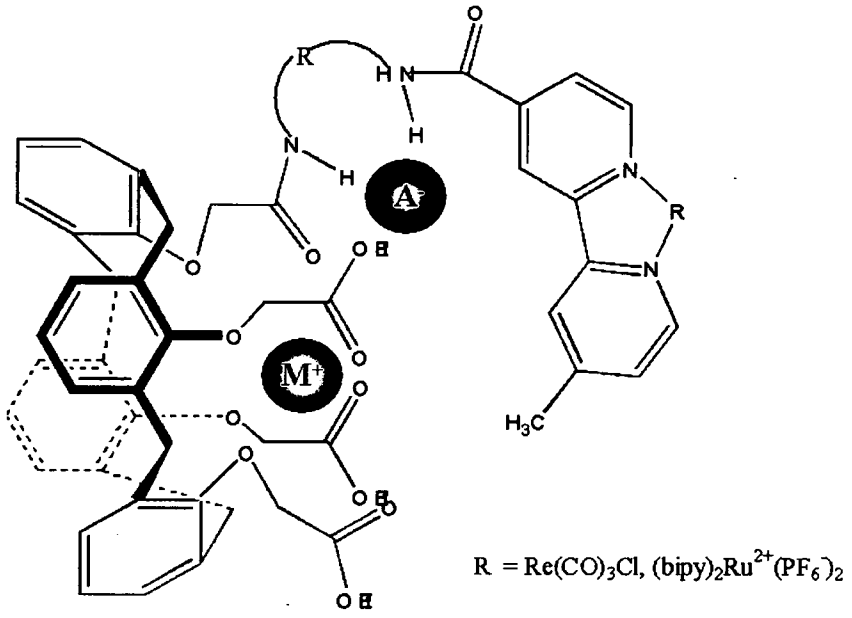

Figure 1.28 Complexation of an alkali metal cation-anion pair by a rhenium(I)/ruthenium(II) bipyridyl calix[4]arene[64]

Figure 1.29 shows an example of a type III reagent where the metal is coordinated in an anionic form. Three crown ether units are linked by tris(2-aminoethyl)amine Tren to form a tripodal tris(aminobenzo-15-crown-5) ditopic ligand, (Figure 1.29),[67] which extracts technetium as the $[NH_4][TcO_4]$ ion pair.

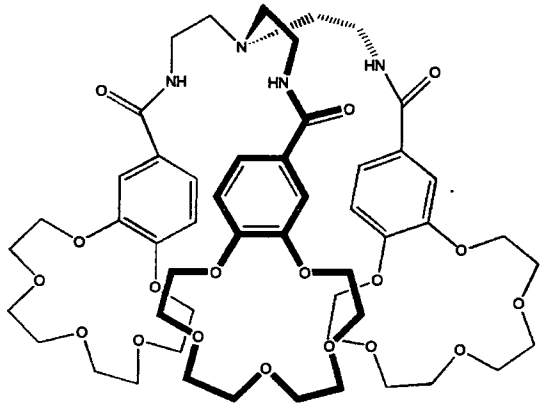

Figure 1.29 A tripodal ligand for the extraction of $[NH_4][TcO_4]$[67]

Ditopic ligands often exhibit cooperative and allosteric effects[42, 43, 68, 78] whereby the incorporation of one ion influences the binding affinity of the counter ion through electrostatic and conformational effects. The cooperativity can be positive or negative depending on whether the binding affinity is enhanced or reduced.

An example of the anion effecting the cation binding is shown by Pochini *et. al.*[81] (Figure 1.30) who have reported a positive allosteric effect during ion-pair binding by extended cavity calix[4]arene in the cone formation. The sulfonate anion hydrogen-bonds to the phenolic units in the upper rim of the calixarene, preorganising the ether unit for binding a tetramethylammonium cation.

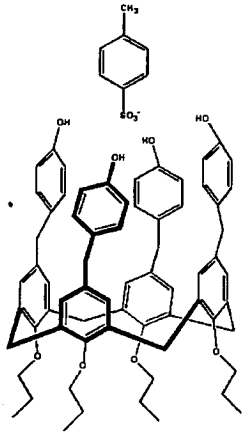

Figure 1.30 Ion pair bind by an extended calix[4]arene[81]

An example of a receptor where the binding of a metal cation enhances anion-affinity is shown in Figure 1.31. The receptor binds an alkali metal cation at the lower rim of the calix[4]arene units and an anion in the amide cleft of the bipyridyl unit. The affinity of the receptor for iodide increases from 40 to 350 M^{-1} upon addition of lithium cations in deuterated acetonitrile.[64]

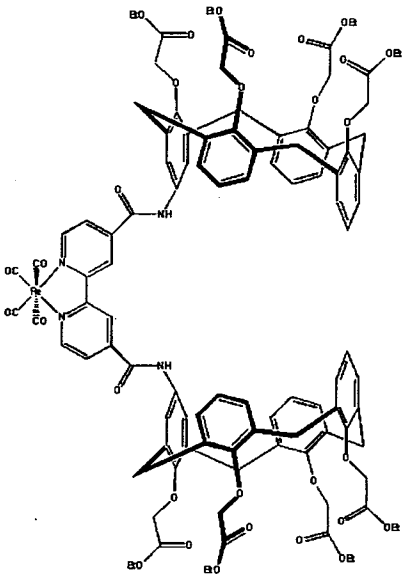

Figure 1.31 Ion pair where metal binding enhances anion binding[64]

1.7.3 Previous work at The University of Edinburgh

Previous work at Edinburgh[35, 69-73, 82, 83] involving the extraction of nickel sulfate has been based on the design and synthesis of ligands with separate cation and anion binding sites (type III in Figure 1.25). In most cases these systems have a diacidic site and a dibasic site, (Figure 1.32) and when the metal is bound, two protons released from the diacidic site are captured by the basic sites. This forms a dipositive cavity for the sulfate anion. The metal can then be stripped by contacting the loaded organic solution with strong sulfuric acid which reprotonates the acidic binding sites and generates an aqueous metal sulfate solution. The sulfate anion can be removed by deprotonation of the basic sites with a base, *e.g.* ammonia and the ligand recycled. Electrowinning the metal sulfate solution produces the metal and regenerates the acid needed for stripping. The ammonium sulfate from ligand regeneration will be a saleable by-product.

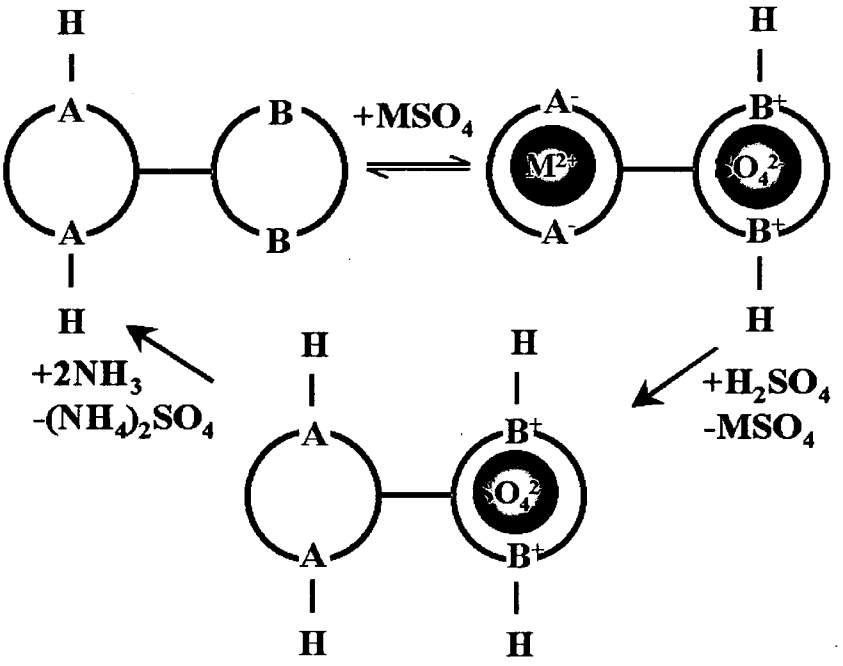

Figure 1.32 Schematic representation of ditopic ligands for metal salts with diacidic/ dibasic sites to enable the hydrometallurgical unit operations of concentration and separation

The prototype zwitterionic ligands (Figure 1.33), investigated by Miller *et al.* contained the H_2salen moiety which produces an $N_2O_2^{2-}$ donor set showing a preference for metal ions with a square planar coordination geometry.[35, 69, 72, 83]

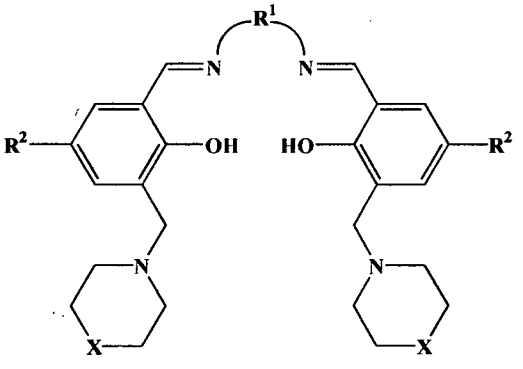

R^1 = -$(CH_2)_2$-, -C_6H_{10}-, -C_6H_4-, $C_{12}H_8$ (as part as a piphenyl unit)

R^2 = *t*-C_4H_9, C_9H_{19}

X = CH_2, O

Figure 1.33 Tetradentate N_2O_2 ditopic ligands[20] containing the bis(salicylaldimine) or "salen-type" unit

Coordination of a metal dication is accompanied by deprotonation of the phenol groups. The released protons are captured by the pendant amine groups, which have been aligned by metal binding to form a dicationic cavity for the anion (Figure 1.34). An example of this templating effect is produced by the X-ray crystal structure [35, 69] shown in Figure 1.35.

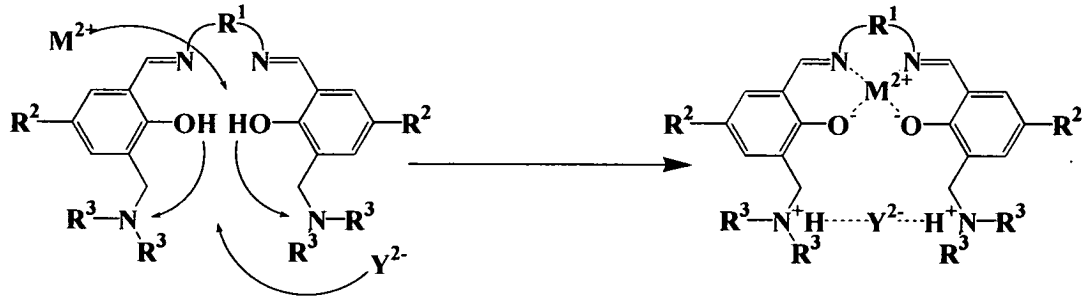

$M^{2+} = Ni^{2+}, Cu^{2+}, Zn^{2+}$

$Y^{2-} = SO_4^{2-}, (NO^-_3)_2$

Figure 1.34 A schematic representation of the formation of the metal-ligand-anion assembly

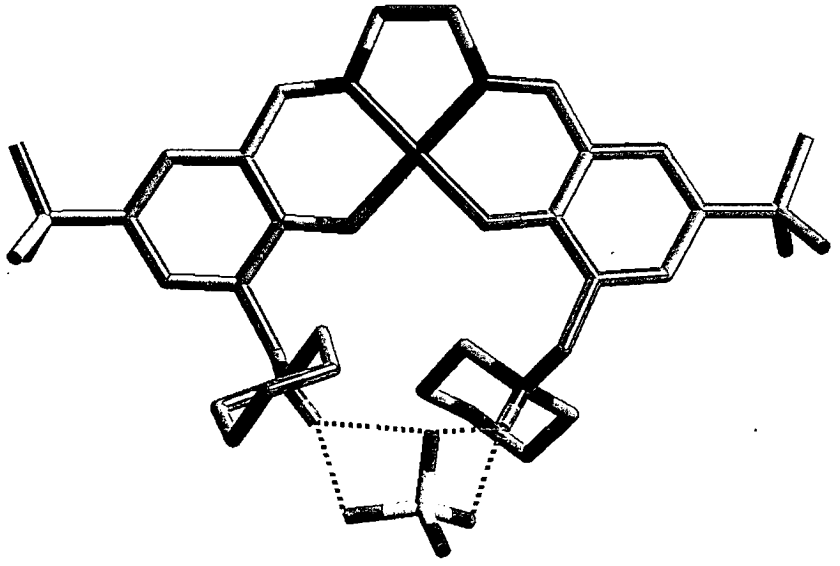

Figure 1.35 The X-ray crystal structure of a $NiSO_4$ complex of "salen –type" ligand carrying pendant morpholine and tertiary butyl sudstituents showing the alignment of the morphiline nitrogen atoms which allow strong electrostatic and H-bonding to a sulfate ion[35, 69]

Variations in the bridging group (R^1) were made to alter the strength and selectivity of the ligand to extract the metal dications. The solvent extraction experiments

showed incomplete loading for nickel(II) sulfate suggesting the ligands are not "strong" enough. It was also found that the kinetics of phase transfer were very slow and long equilibration times are necessary. [35, 69]

1.8 Overview

As the nickel sulfate extraction results proved to be very low for the formation of low spin complexes with the tetradentate ligands, the design of ditopic ligands which contain sexadentate or bis-tridentate binding sites for octahedral metal ions is initially considered in this thesis. In chapters 2 and 3 the synthesis of sexadentate and tridentate ligands and their nickel salt complexes are discussed and their ability to extract nickel sulfate is investigated.

The second theme of the thesis involves the ability of the ligands to extract other divalent metal salts (sulfates and chlorides) typically found in an industrial leach stream. Chapter 4 involves a screening study, which reports on the success of the ligands with each metal. Preliminary studies to explain the types of complexes formed during extraction are then discussed in chapter 5.

1.9 References

1 I. Mihaylov, E. Krause, D. F. Colton, Y. Okita, J. P. Duterque and J. L. Perraud, *CIM Bull.*, 2000, **93**, 124.

2 D. F. Shriver, P. W. Atkins and C. H. Langford, 'Inorganic Chemistry', Oxford University Press, Oxford, 1994, chapter 7, 274-312.

3 F. Habashi, 'A Textbook of Hydrometallurgical', Imprimerie d'Edition Marqueis Limite, Quebec, 1993, chapter 2, 13-26.

4 M. T. Anthony and D. S. Flett, 'Hydrometallurgy - An environmentally sustainable technology?' Chapman and Hall, London, 1994, 13-26.

5 K. A. Evans and N. Brown, 'Speciality Inorganic Chemicals', ed. R. Thompson, published by The Royal Society of Chemistry, 1981.

6 R. Thompson, 'Industrial Inorganic Chemicals: Production and Uses', published by The Royal Sociely of Chemistry, 1995.

7 B. R. Reddy, C. Parija and P. Sarma, *Hydrometallurgy*, 1999, **53**, 11.

8 K. S. Rao, P. C. Rath and T. Subbaiah, *Miner. Metall. Process.*, 1997, **14**, 8.

9 G. Bacon and I. Mihaylov, International Solvent Extraction Conference, Cape Town, South Africa, 2002, 1-13.

10 R. R. Moskalyk and A. M. Alfantazi, *Miner. Metall. Process.*, 2000, **17**, 205.

11 M. J. Nicol, C. A. Fleming and J. S. Preston, in 'Application to Extractive Metallurgy', ed. S. G. Wilkinson, Oxford, 1987, 779-842.

12 G. W. Stevens, J. M. Perera and F. Grieser, *Curr. Opin. Colloid Interface Sci.*, 1997, **2**, 629.

13 T. W. Swaddle, 'Inorganic of Chemistry An Industrial and Environmental Perspective', Academic Press, London, 1997, chapter 17, 357-386.

14 R. M. Swart, 'Personal communication', 1999.

15 A. Sandhibigraha and P. V. R. Bhaskara Sarma, *Hydrometallurgy*, 1997, **45**, 211.

16 C. Parija and P. V. R. Bhaskara Sarma, *Hydrometallurgy*, 2000, **54**, 195.

17 P. V. R. Bhaskara Sarma and K. C. Nathsarma, *Hydrometallurgy*, 1996, **42**, 83.

18 B. K. Tait, K. E. Mdlalose and I. Taljaard, *Hydrometallurgy*, 1995, **38**, 1.

19 G. M. Ritcey, *Pub. Aust. Inst. Min. Metall.*, 1996, **6/96**, 251.

20 G. L. Hubred, Nickel Metall., Symp., Proc., 25th Annu. Conf. Metall., 1986, 598-611.

21 F. J. Alguacil and A. Cobo, *Hydrometallurgy*, 1998, **48**, 291.

22 V. H. Ness and N. L. Hayward, SME Annual Meeting 2001, Denver, Colorado, 2001.

23 V. Ramesh and G. N. Rao, *Indian J. Technol.*, 1987, **25**, 418.

24 F. J. Alguacil, M. Alonso and F. A. Lopez, *J. Chem. Eng. Jpn.*, 2001, **34**, 83.

25 E. Dziwinski and J. Szymanowski, *Solvent Extr. Ion Exch.*, 1996, **14**, 219.

26 K. Soldenhoff, N. Hayward and D. Wilkins, EPD Congress 1998, Proceedings of Sessions and Symposia held at the TMS Annual Meeting, San Antonio, Feb. 16-19, 1998, 1998, 153-165.

27 K. C. Sole and J. B. Hiskey, *Hydrometallurgy*, 1995, **37**, 129.

28 Z. Hubicki, A. Jakowicz and M. Rudas, *Chemical & Environmental Research*, 1999, **8**, 319.

[29] G. M. Ritcey and A. W. Ashbrook, 1968, Separation of cobalt and nickel by liquid-liquid extraction from acid solutions, US Patent No 3 399055

[30] T. Zhu, *Miner. Process. Extr. Metall. Rev.*, 2000, **21**, 1.

[31] G. Cote and D. Bauer, *Rev. Inorg. Chem.*, 1989, **10**, 121.

[32] G. Cote, J.-V. Martin, D. Bauer and Y. Mottot, International Solvent Extraction Conference, Cape Town, South Africa, 2002, 291-298.

[33] J. D. Miller and M. B. Mooiman, *Sep. Sci. Technol.*, 1984, **19**, 895.

[34] B. Gupta, S. N. Tandon and A. Deep, International Solvent Extraction Conference, Cape Town, South Africa, 2002, 793-797.

[35] H. A. Miller, N. Laing, S. Parsons, A. Parkin, P. A. Tasker and D. J. White, *J. Chem. Soc.-Dalton Trans.*, 2000, 3773.

[36] M. M. G. Antonisse and D. N. Reinhoudt, *Chem. Commun.*, 1998, 443.

[37] K. Kavallieratos, R. A. Sachleben, G. J. Van Berkel and B. A. Moyer, *Chem. Commun.*, 2000, 187.

[38] C. Bazzicalupi, A. Bencini, A. Bianchi, M. Cecchi, B. Escuder, V. Fusi, E. Garcia-Espana, C. Giorgi, S. V. Luis, G. Maccagni, V. Marcelino, P. Paoletti and B. Valtancoli, *J.Am.Chem.Soc.*, 1999, **121**, 6807.

[39] A. Bianchi, K. Bowman-James and E. Garcia-España, 'Supramolecular Chemistry of Anions', Wiley-VCH, New York, 1997, 1-480.

[40] C. H. Park and H. E. Simmons, *J.Am.Chem.Soc.*, 1968, **90**, 2431.

[41] E. Graf and J.-M. Lehn, *J.Am.Chem.Soc.*, 1976, **98**, 6403.

[42] P. R. A. Webber and P. D. Beer, *J. Chem. Soc.-Dalton Trans.*, 2003, 2249.

[43] J. E. Redman, P. D. Beer, S. W. Dent and M. G. B. Drew, *Chem. Commun.*, 1998, 231.

[44] S. Nishizawa, P. Buehlmann, M. Iwao and Y. Umezawa, *Tetrahedron*, 1995, **36**, 6483.

[45] P. D. Beer and J. B. Cooper, *Chem. Commun.*, 1998, 129.

[46] J. B. Cooper, M. G. B. Drew and P. D. Beer, *J. Chem. Soc.-Dalton Trans.*, 2000, 2721.

[47] P. D. Beer and P. A. Gale, *Angew.Chem.,Int.Ed.Engl.*, 2001, **40**, 486.

[48] N. G. Berry, T. W. Shimell and P. D. Beer, *Journal of Supramolecular Chemistry*, 2003, **2**, 89.

[49] S. L. Renard, C. A. Kilner, J. Fisher and M. A. Halcrow, *J. Chem. Soc.-Dalton Trans.*, 2002, 4206.

[50] P. A. Gale, *Coordination Chemistry Reviews*, 2001, **213**, 79.

[51] P. D. Beer and D. K. Smith, in 'Anion binding and recognition by inorganic based receptors', ed. K. D. Karlin, London, 1997, 1-96.

[52] B. C. Hamann, N. R. Branda and J. J. Rebek, *Tetrahedron Letters*, 1993, **34**, 6837.

[53] C. Seel and J. de-Mendoza, in 'From chloride katapinates to trinucleotide complexes. Development in molecular recognition in molecular recognition anionic species', ed. F. Vogle, Oxford, 1996, 519-552.

[54] T. R. Kelly and M. H. Kim, *J.Am.Chem.Soc.*, 1994, **116**, 7072.

[55] M. W. Hosseini and J.-M. Lehn, *Helv. Chim. Acta*, 1986, **69**, 587.

[56] M. W. Hosseini and J.-M. Lehn, *J.Am.Chem.Soc.*, 1982, **104**, 3525.

[57] F. P. Schmidtchen and M. Berger, *Chem. Rev.*, 1997, **97**, 1609.

[58] U. Olsher, F. Frolow, N. K. Dalley, W. Jiang, Z. Y. Yu, J. M. Knobeloch and R. A. Bartsch, *J.Am.Chem.Soc.*, 1991, **113**, 6570.

[59] E. A. Arafa, K. I. Kinnear and J. C. Lockhart, *Chem. Commun.*, 1992, 61.

[60] P. J. Smith, M. V. Reddington and C. S. Wilcox, *Tetrahedron*, 1992, **33**, 6085.

[61] S. S. Flack, J. L. Chaumette, J. D. Kilburn, G. J. Langley and M. Webster, *Chem. Commun.*, 1993, 399.

[62] P. B. Savage, S. K. Holmgren and S. H. Gellman, *J.Am.Chem.Soc.*, 1994, **116**, 4069.

[63] M. T. Reetz, in 'Simultaneous binding of cations and anions', ed. F. Vogle, Oxford, 1996, 553-562.

[64] J. B. Cooper, M. G. B. Drew and P. D. Beer, *J. Chem. Soc.-Dalton Trans.*, 2001, 392.

[65] L. A. J. Chrisstoffels, F. de Jong, D. N. Reinhoudt, S. Sivelli, L. Gazzola, A. Casnati and R. Ungaro, *J.Am.Chem.Soc.*, 1999, **121**, 10142.

[66] N. Pelizzi, A. Casnati, A. Friggeri and R. Ungaro, *J. Chem. Soc. Perkin. Trans. II*, 1998, 1307.

[67] P. D. Beer, P. K. Hopkins and J. D. McKinney, *Chem. Commun.*, 1999, 1253.

[68] M. W. Glenny, A. J. Blake, C. Wilson and M. Schroeder, *J. Chem. Soc.-Dalton Trans.*, 2003, 1941.

[69] D. J. White, N. Laing, H. Miller, S. Parsons, S. Coles and P. A. Tasker, *Chem. Commun.*, 1999, 2077.

[70] S. G. Galbraith, P. G. Plieger and P. A. Tasker, *Chem. Commun.*, 2002, 2662.

[71] P. G. Plieger, S. Parsons, A. Parkin and P. A. Tasker, *J. Chem. Soc.-Dalton Trans.*, 2002, 3928.

[72] D. M. Gunn, H. A. Miller, R. M. Swart, P. A. Tasker, L. C. West and D. J. White, International Solvent Extraction Conference, Cape Town, South Africa, 2002, 280-290.

[73] R. A. Coxall, L. F. Lindoy, H. A. Miller, A. Parkin, S. Parsons, P. A. Tasker and D. J. White, *J. Chem. Soc.-Dalton Trans.*, 2003, 55.

[74] S. Memon and M. Yilmaz, *J. Mol. Struct.*, 2001, **595**, 101.

[75] L. H. Uppadine, J. E. Redman, S. W. Dent, M. G. B. Drew and P. D. Beer, *Inorg. Chem.*, 2001, **40**, 2860.

[76] T. Tuntulani, S. Poompradub, P. Thavornyutikarn, N. Jaiboon, V. Ruangpornvisuti, N. Chaichit, Z. Asfari and J. Vicens, *Tetrahedron*, 2001, **42**, 5541.

[77] P. D. Beer, M. G. B. Drew, R. J. Knubley and M. I. Ogden, *J. Chem. Soc.-Dalton Trans.*, 1995, 3117.

[78] P. D. Beer and S. W. Dent, *Chem. Commun.*, 1998, 825.

[79] P. D. Beer and D. Gao, *Chem. Commun.*, 2000, 443.

[80] L. H. Uppadine, M. G. B. Drew and P. D. Beer, *Chem. Commun.*, 2001, 291.

[81] A. Arduini, G. Giorgi, A. Pochini, A. Secchi and J. Ugozzoli, *J. Org. Chem.*, 2001, **66**, 8302.

[82] N. Akkus, J. C. Campbell, J. Davidson, D. K. Henderson, H. A. Miller, A. Parkin, S. Parsons, P. G. Plieger, R. M. Swart, P. A. Tasker and L. C. West, *J. Chem. Soc.-Dalton Trans.*, 2003, 1932.

[83] P. A. Tasker and D. J. White, 1999, Br.Pat., 9907485.8,

Chapter Two

Sexadentate ligands

Contents

2.1 The coordinate chemistry of nickel(II) and cobalt(II)

The flowsheets outlined in chapter 1 (Figure 1.22 and 1.23) require the design of highly selective complexing agents to transport both the desired metal cation and its attendant anion. Criteria for a good solvent extractant are shown in Figure 2.1.

To meet ideal best practice criteria, a hydrometallurgical process should:[1]

1. Utilise non toxic reagents.
2. Take into solution from the ore or concentrate metal values to leave an inert leach residue.
3. Purify the value metal liquor streams to the requirements of the refining stage.
4. Remove all other metals into saleable by-products and failing that into inert and disposable residues.

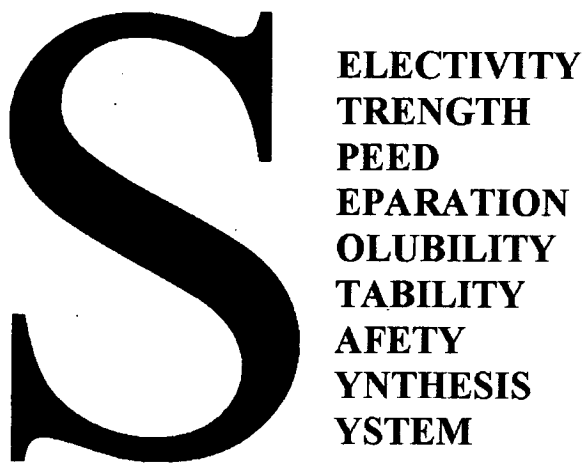

Figure 2.1 Criteria for a good solvent extractant

Nickel(II) is the most common oxidation state for nickel, but nickel(III) and Nickel(IV) are also known.[2] Nickel(II) ions with a d^8 electron configuration show coordination numbers in the range three-six[3] but four and six coordination are more common. The tetrahedral form has two paired and two unpaired electrons in e orbitals and four paired electrons in the lower t_2 orbitals and has a crystal field stabilisation energy (CFSE) of $4/5\Delta_{tet}$. However for the vast majority of four coordinate nickel(II) complexes, a planar geometry is preferred due to the d^8

configuration.[3] The eight electrons occupy the other four d orbitals, leaving the strongly antibonding one $d_{(x^2-y^2)}$ empty. Planar complexes of nickel(II) are therefore diamagnetic. They are frequently red, yellow or brown having an absorption band of medium intensity [ε~60(1000 cm^2mol^{-1})] in the range 450 to 600 nm.[3]

Nickel(II) forms a larger number of octahedral complexes compared to its other geometries.[4] This is due to a high CFSE ($6/5\Delta_{oct}$) with two unpaired electrons in the higher energy e_g orbitals and six paired electrons in the lower energy t_{2g} set. Octahedral complexes are characteristically blue or purple.[3]

Nickel and cobalt are usually found together in nature and hence defining any differences in their coordination chemistry is important in devising methods for separation. For cobalt(II) there are more tetrahedral complexes than any other first row transition metal ions[5] because the CFSE is favourable ($6/5\Delta_{tet}$) relative to octahedral complexes ($4/5\Delta_{oct}$).

This preference for different coordination geometries can be exploited in the separation of cobalt(II) from nickel(II) for example in using the phosphoric acid extractant D2EHPA (section 1.5.2.2.1).[6] When D2EHPA is mixed with an aqueous solution of cobalt(II) and nickel(II) salts, both the metals retain their six coordination sphere, forming [M(D2EHPA-H)$_2$(H_2O)] complexes which are water soluble and nonextractable. By raising the temperature to about 50 °C two water molecules are lost from the octahedral cobalt complex, forming a bright blue neutral tetrahedral complex [Co(D2EHPA-H)$_2$] which is easily extracted into kerosene. Nickel remains octahedral in the aqueous phase because for nickel(II) the CFSE of the octahedral field is higher.

Based on crystal field arguments preferential extraction of nickel(II) from cobalt(II) should be based on reagents which present a square planar or octahedral donor set.

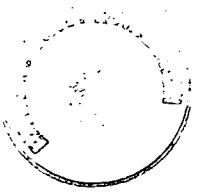

2.2 Six coordinate ligands for the transport of nickel(II) salts

Previous work at Edinburgh University (section 1.8.3) involved evaluation of tetradentate/square planar ligands containing salen units.[7, 8] These were shown to form various nickel salt complexes, but when used in extraction the nickel loading was poor due to the kinetics of complexation/ decomplexation and phase transfer of nickel sulfate proved to be very slow. This chapter considers ditopic ligands which provide an octahedral $X_2N_2O_2^{2-}$ donor set and a site for bonding the attendant anion(s). The salen structure has been altered to accommodate two extra donor atoms into the backbone as shown in Figure 2.2.

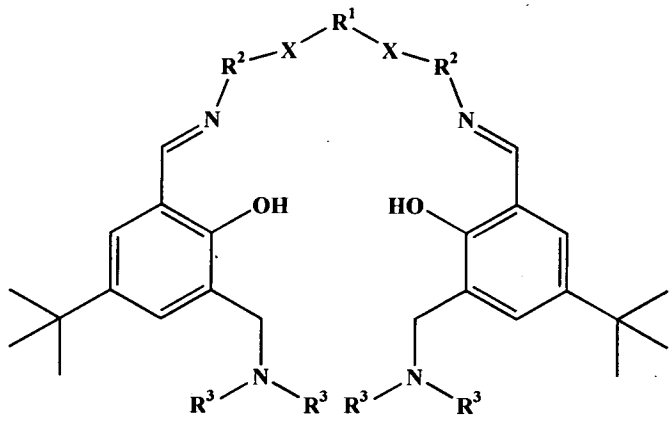

X = O, S, NH, NCH_3

R^1 = $-(CH_2)_2-$, $-(CH_2)_3-$, C_4H_8 (as a piperazine ring)

R^2 = $-(CH_2)_2-$, *o*-C_6H_4-

NR^3_2 = piperidine, $N(C_6H_{13})_2$

Figure 2.2 Sexadentate ligands which provide octahedral $X_2N_2O_2^{2-}$ donor sets and pendant dialkylamine groups

Various permutations have been synthesised.

1. Variations in the backbone X group between nitrogen, oxygen and sulfur allow the difference between hard (oxygen) and soft (sulfur) donors on extraction to be assessed. As nickel(II) is a borderline metal it should theoretically coordinate to all the above ligands.[9]

1. The size of the donor set cavity was altered by varying the R^1 bridge between an ethyl and propyl chain.

2. Changing saturation levels in the backbone of the extractant was investigated by altering the R^2 group between an aromatic *o*-C_6H_4 and an ethane bridge. The introduction of the aromatic rings should reduce the σ-donor power of the bridging donor atoms and increase the rigidity of the donor set.

3. Variations in R^3 were made to alter the solubility of the ligand for use in extraction experiments.

2.3 Synthesis of sexadentate ligands

The sexadentate ligands in Figure 2.3 were prepared by adaptations of routes to the tetradentate "salen" analogues[10, 11] by a four-step convergent synthesis (Scheme 2.1) from a substituted salicylaldehyde, paraformaldehyde, piperidine or N-dihexylamine and a diamine which defines the central bridge.

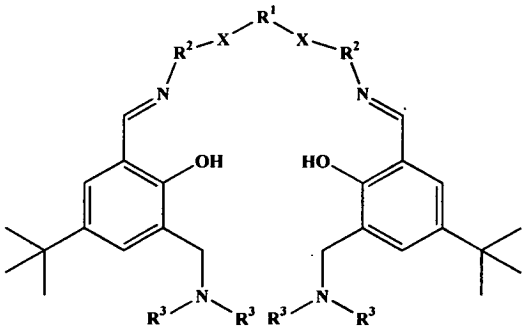

Ligand	X	R^1	R^2	NR^3_2
1	NH	$-(CH_2)_2-$	$-(CH_2)_2-$	piperidine
2[b]	NCH_3	$-(CH_2)_2-$	$-(CH_2)_2-$	piperidine
3	NH	$-(CH_2)_4-$ [a]	$-(CH_2)_2-$	piperidine
4	NH	$-(CH_2)_4-$ [a]	$-(CH_2)_2-$	$N(C_6H_{13})_2$
5	O	$-(CH_2)_2-$	*o*-C_6H_4-	piperidine
6	O	$-(CH_2)_2-$	*o*-C_6H_4-	$N(C_6H_{13})_2$
7	O	$-(CH_2)_3-$	*o*-C_6H_4-	piperidine
8	O	$-(CH_2)_3-$	*o*-C_6H_4-	$N(C_6H_{13})_2$
9	S	$-(CH_2)_2-$	$-(CH_2)_2-$	piperidine
10	S	$-(CH_2)_2-$	$-(CH_2)_2-$	$N(C_6H_{13})_2$
11	S	$-(CH_2)_2-$	*o*-C_6H_4-	piperidine
12	S	$-(CH_2)_2-$	*o*-C_6H_4-	$N(C_6H_{13})_2$

Figure 2.3 Generic form of the sexadentate

[a] As part of a piperazine, [b] Unable to purify

The final step of the convergent synthesis involves a Schiff base condensation between the appropriate diamines and two parts equivalent of the substituted salicylaldehydes (Scheme 2.1). The preparation of the substituted salicylaldehyde and diamine precursors for the central bridge are described in sections 2.3.1 and 2.3.2 respectively.

Initial preparation of the ligands **5**, **7** and **11** were during my undergraduate project.

2.3.1 5-Alkyl-3-dialkylaminomethyl-2hydroxybenzaldehydes

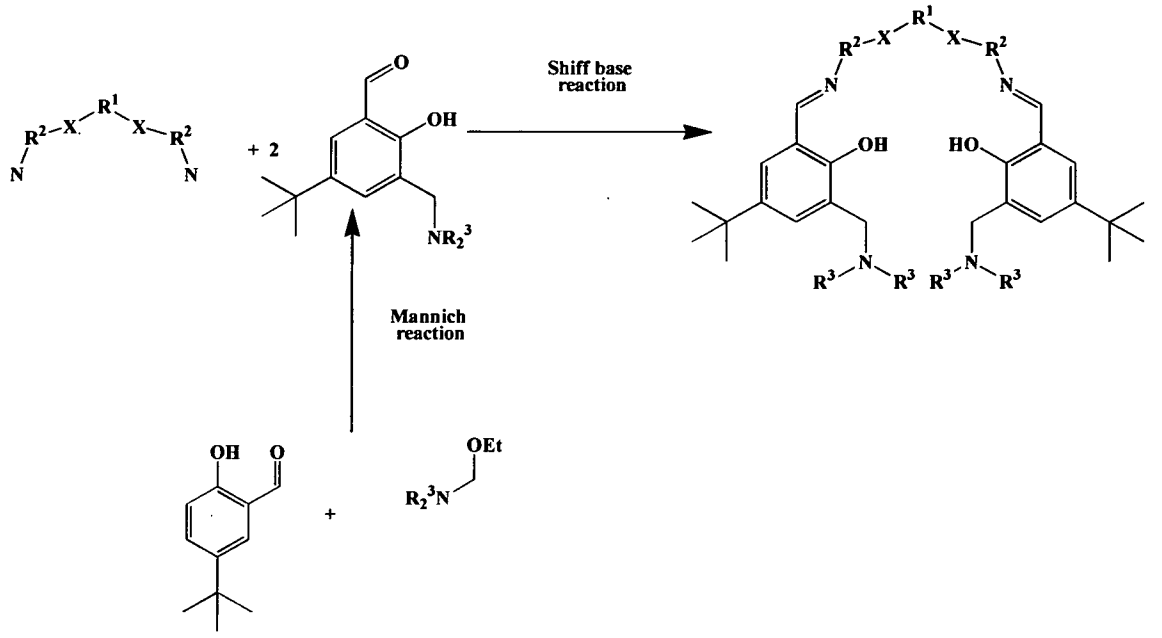

Scheme 2.1 Synthesis of ligands (**3-12**) via the Mannich reaction and a Schiff base condensation

The first step involved the substitution of the *ortho* position of the 2-hydroxy-5-alkylbenzaldehyde with ethoxy-N-piperidinylmethane or ethoxy-N-dihexylamine *via* a Mannich reaction (Scheme 2.1).

2.3.2 Ligands with $N_2O_4^{2-}$ donor sets

The method described by Uppal[12] (Scheme 2.2) was adapted for the synthesis of 1,2-bis(2-aminophenyloxy)ethane and 1,3-bis(2-aminophenyloxy)propane. To increase reduction of the nitro groups, hydrazine hydrate was substituted for hydrazine monohydrate and the reaction time was increased. For the synthesis of 1,3-bis(2-aminophenyloxy)propane the amount of palladium on activated carbon was increased (1.5 increase) to allow full reduction of both the nitro groups. The overall yields for 1,2-bis(2-aminophenyloxy)propane and 1,3-bis(2-aminophenyloxy)propane were 39% and 50% respectively.

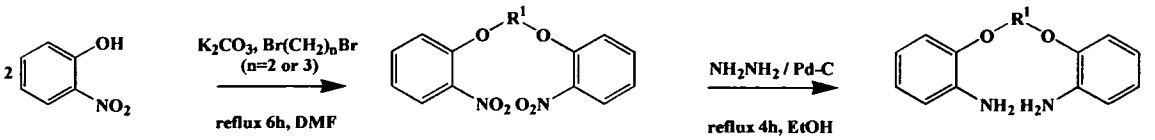

Scheme 2.2 Synthesis of 1,2-bis(2-aminophenyloxy)ethane and 1,3-bis(2-aminophenyloxy)propane

2.3.3 Ligands with $N_2S_2O_2^{2-}$ donor sets

1,2-Bis-(2-aminophenylthio)ethane was prepared by an adaptation of the method of Kumar *et. al.*[13] see Scheme 2.3, with a 42% yield and good purity.

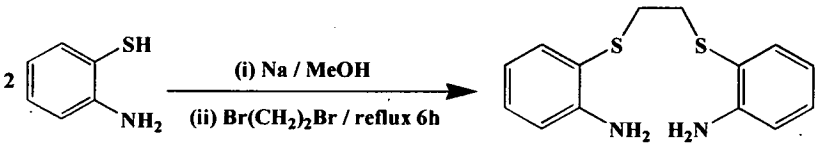

Scheme 2.3 Synthesis of 1,2-bis(2-aminophenylthio)ethane

2,2'-ethane-1,2-diylbissulfanyl-bis-ethylamine, **ESA**, was more difficult to synthesise. Several approaches were tried with varying degrees of success.

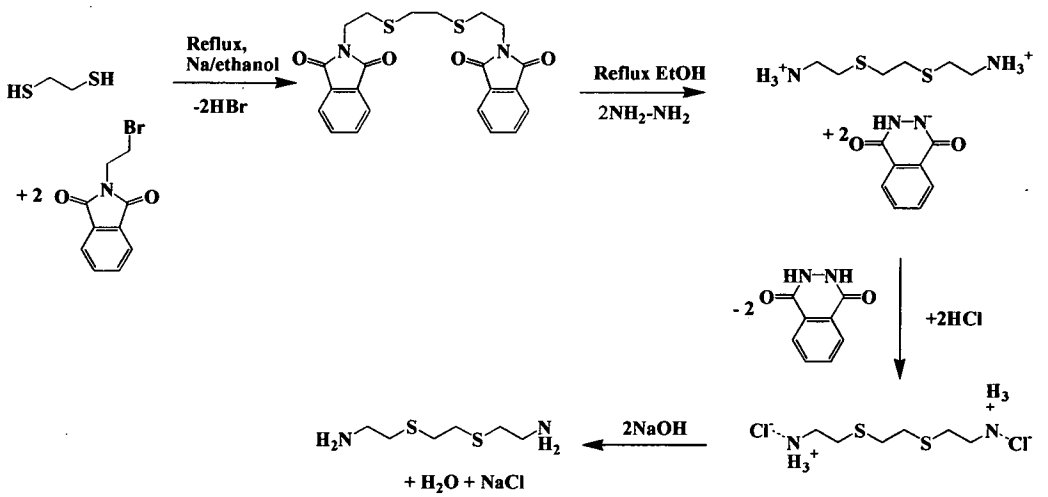

Scheme 2.4 Synthesis of **ESA** by N-2-bromoethylphthalimide protecting group

A method described by Dwyer *et.al.*[14] involved a two-step process (Scheme 2.4). The starting materials N-2-bromoethylphthalimide and ethane-1,2-dithiol are commercially available and with the addition of sodium ethoxide form a phthalimide-protected form of **ESA**. After removal of the phthalimide groups **ESA** (Scheme 2.5) was stored as the dihydrochloride salt, due to the diamine's deliquescent nature and its rapid absorption of CO_2.[15] The product obtained by this route was pure but could not be obtained in a sufficient yield (9% overall).

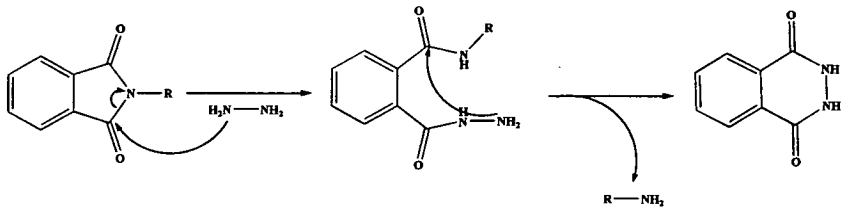

Scheme 2.5 Removal of the protection group by the Gabriel synthesis of primary amines

In an adaptation of the Dwyer method[14] 2-chloroethylamine hydrochloride was deprotonated by reaction with triethylamine and the amine functionality protected by reaction with di-*tert*-butyldicarbonate, (BOC) as shown in Scheme 2.6. Reaction with ethane-1,2-dithiolate gave the BOC-protected **ESA** intermediate which was deprotected by reaction with trifluoroacetic acid, and **ESA** was extracted into dichloromethane. A problem in forming the BOC-protected **ESA** intermediate caused the final **ESA** product to be hard to purify. The attempted synthesis of the target molecule was stopped at this point.

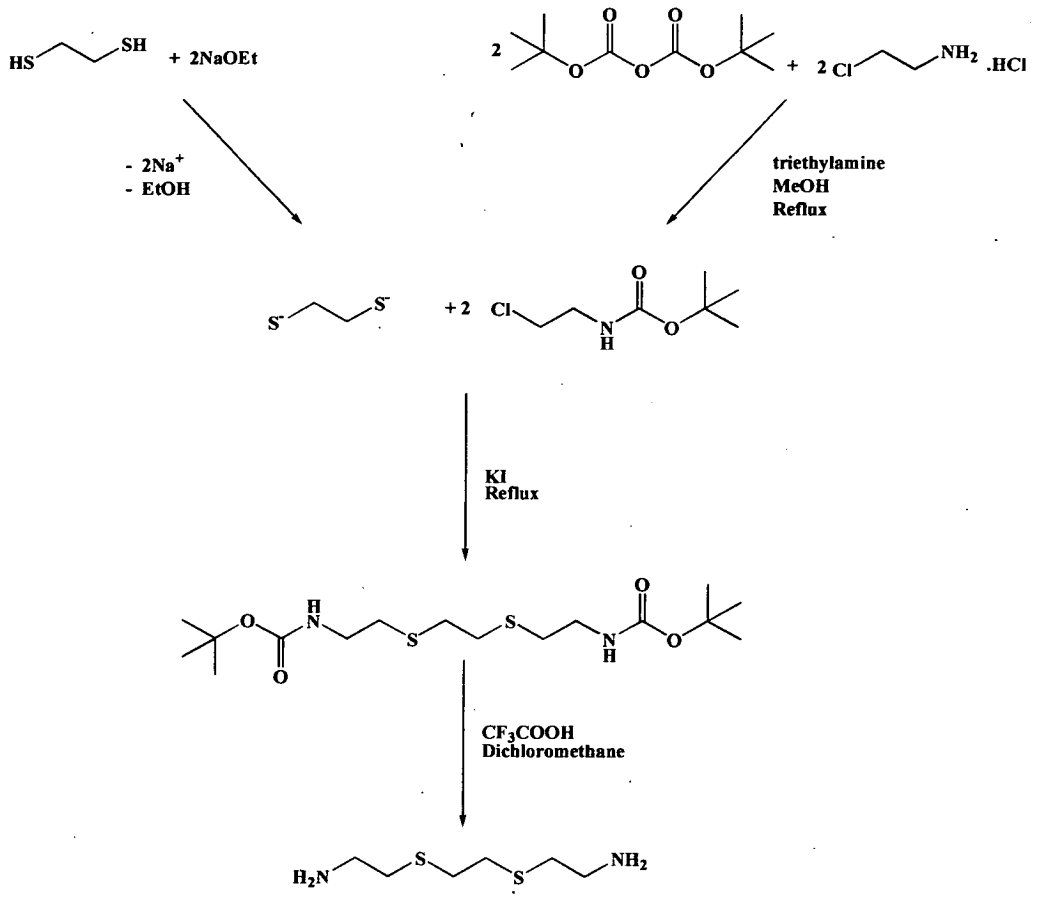

Scheme 2.6 Synthesis of ESA using BOC protecting group

The third attempted protocol involved the preparation of **ESA** by adaptation of the method of Zheng *et. al.*[15] As the precursor 2-aminoethanethiol hydrochloride was air sensitive the reaction was carried out in a nitrogen atmosphere with degassed reagents and solvents. The reaction (Scheme 2.7) involved addition of enough $NaHCO_3$ to neutralise the hydrogen bromide liberated and to generate the free base from the precursor hydrochloride, allowing extraction of the product into acetonitrile as the free amine.

This proved to be the best method giving a high purity product and a higher yield (48%) and was used to generate the **ESA** for Schiff base reaction to form ligands **9** and **10**.

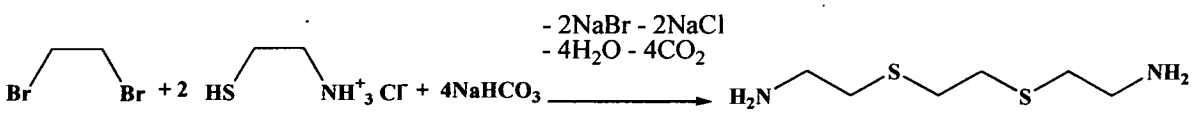

Scheme 2.7 A single step synthesis of **ESA**

2.3.4 Ligands with $N_4O_2^{2-}$ donor sets

The donor atoms X in the sexadentate ligands (Figure 2.3) were varied to nitrogen to generate a ligand with four nitrogen and two oxygen donor atoms.

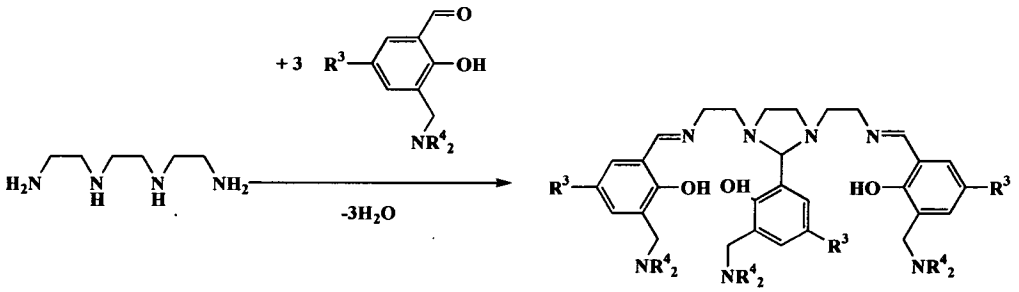

Scheme 2.8 Condensation reaction with **trine** and 5-alkyl-3-dialkylaminomethyl-2-hydroxybenzaldehydes

Triethylenetetramine (**trine**) is available commercially but previous work has shown that when reacted with salicylaldehyde a 1:3 condensation product is obtained (Scheme 2.8).[16] Several approaches to overcome this problem were considered:

1. Conversion of the 3:1 condensed product to the derived 2:1 compound by a metal-assisted hydrolysis of the central imidazoline ring (section 2.3.4.1) as previously done with iron(II).[16]
2. Using an alternative tetra-amine containing tertiary amine atoms X in the backbone [these would not condense with aldehyde groups (section 2.3.4.2)].
3. Attempt using a metal ion template directed synthesis of a complex of ligand **1** (section 2.3.4.3).

2.3.4.1 Attempted metal ion promoted hydrolysis of the imidazoline derivative

One equivalent of triethylenetetramine was reacted with three equivalents of the substituted salicylaldehydes to form the product shown in Scheme 2.8. Recrystallisation of the product from hexane and cooling using a propan-2-ol ice bath produced a creamy coloured product. Analysis of the product through mass spectrometry showed that the 1:3 (tri-amine: salicylaldehyde) product had been formed but NMR spectroscopy showed that the product was not pure. Hence, the product was recrystallised by slow diffusion from hexane to produce white crystals. X-ray crystallography showed that the starting material, the substituted salicylaldehydes had been isolated. (See Figure 2.4 for the crystal structure of 2-hydroxy-3-(piperidinyl)-4-ylmethyl)-5-tert-butylbenzaldehyde.)

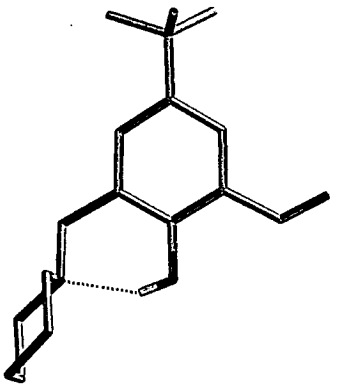

Figure 2.4 Crystal structure of 2-hydroxy-3-(piperidinyl)-4-ylmethyl)-5-tert-butylbenzaldehyde

After crystallisation the crystals were removed and the filtrate was re-analysed by NMR to show an increase in purity. It is presumed that as some of the starting material had not reacted, various substitution reactions had occurred, hence giving a mixture of 1:1, 1:2 and 1:3 (tetra-amine: salicyaldehyde) products. Attempts to recrystallise the desired product were unsuccessful due to the similar properties of the various side products. Therefore the attempted synthesis of the target molecule was stopped at this point, as a relatively pure "greasy" dihexyl ligand is needed to study its ability as a commercial extractant.

2.3.4.2 1,2-Ethanediamine,N,N'-bis(2-aminoethyl)-N,N'dimethyl, EBD

Two papers describe the synthesis of 1,2-ethanediamine,N,N'-bis(2-aminoethyl)-N,N'dimethyl, **EBD**, from N,N'-dimethyl-1,2-diaminoethane by reaction with N-2-bromoethylphthalimide to give the intermediate, 4,7-dimethyl-1,4,7,10-tetra-azadecomediphthalimide as in Scheme 2.9.[17, 18]

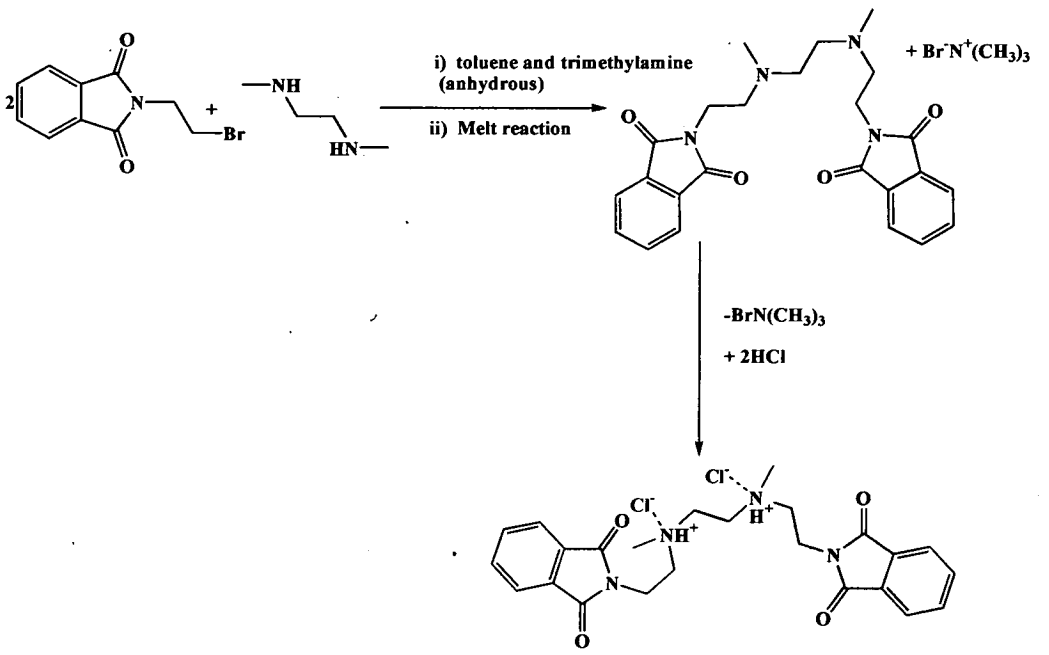

Scheme 2.9 Reported syntheses of 4,7-dimethyl-1,4,7,10-tetra-azadecomediphthalimide i) in anhydrous toluene in the presence of trimethylamine[17], ii) as a melt[18]

The reaction in toluene[17] gave a white solid which was found to be the unreacted phthalimide.

An adaptation of the melt reaction[18] where one equivalent of N,N'-dimethyl-1,2-diaminoethane was added to two equivalents of N-(2-bromoethyl)phthalimide and heated produce an impure solid which proved to be very problematic to purify due to being very hydroscopic.

The crude material was used as obtained for the next step as it was believed that purification after the Gabriel synthesis would be simpler. The method as described in section 2.3.3 was used to form a dark orange solid which on analysis suggested the

formation of the desired tetra-amine product and also a tri-amine formed due to only half of the starting N,N'-dimethyl-1,2-diaminoethane reacting with the N-(2-bromoethyl)phthalimide. Various techniques to separate the two diamines were tried but their properties were too similar.

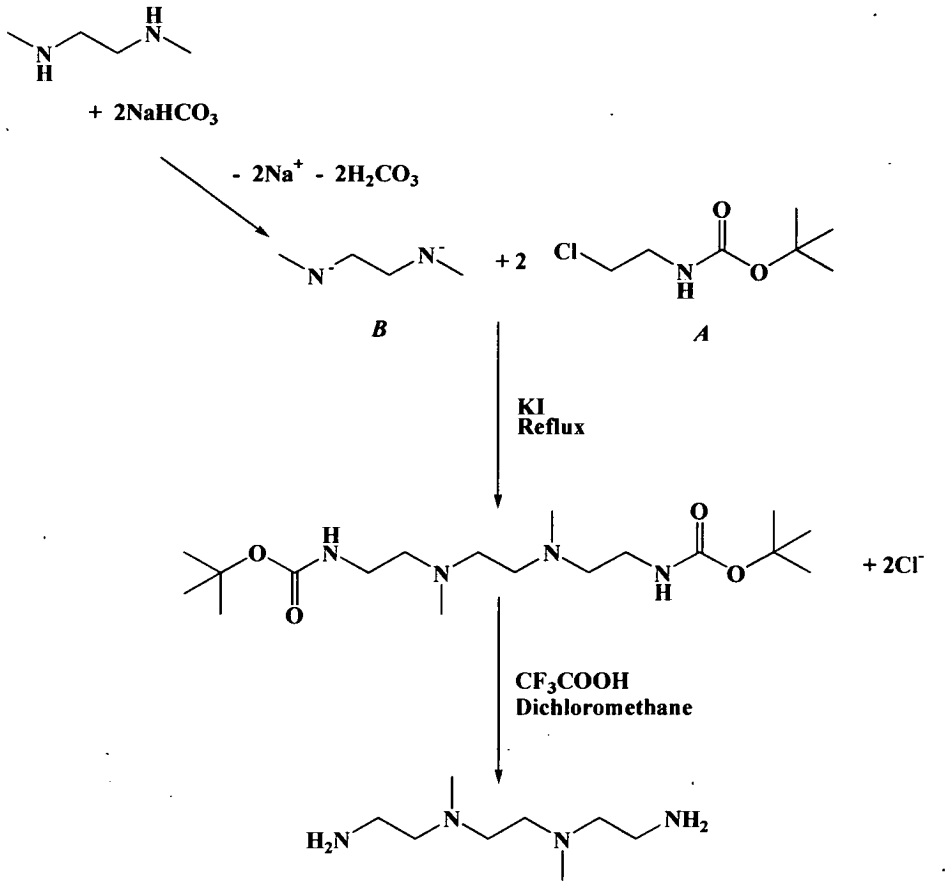

Scheme 2.10 Attempted synthesis of 1,2-ethanediamine,N,N'-bis(2-aminoethyl)-N,N'dimethyl using di-*tert*-butyldicarbonate protecting groups

An alternative to the use of phthalimido-groups for protection involved an adaptation of a method used to make ESA, see section 2.3.3, was tried in which *A* was reacted with *B* as in Scheme 2.10 to give the BOC-protected 1,2-ethanediamine,N,N'-bis(2-aminoethyl)-N,N'dimethyl intermediate. Unfortunately this could not be synthesised in a high enough yield (2%) to make the route viable. Attempts to purify the intermediate after deprotection were unsuccessful.

2.3.4.3 Template syntheses from triethylenetetramine

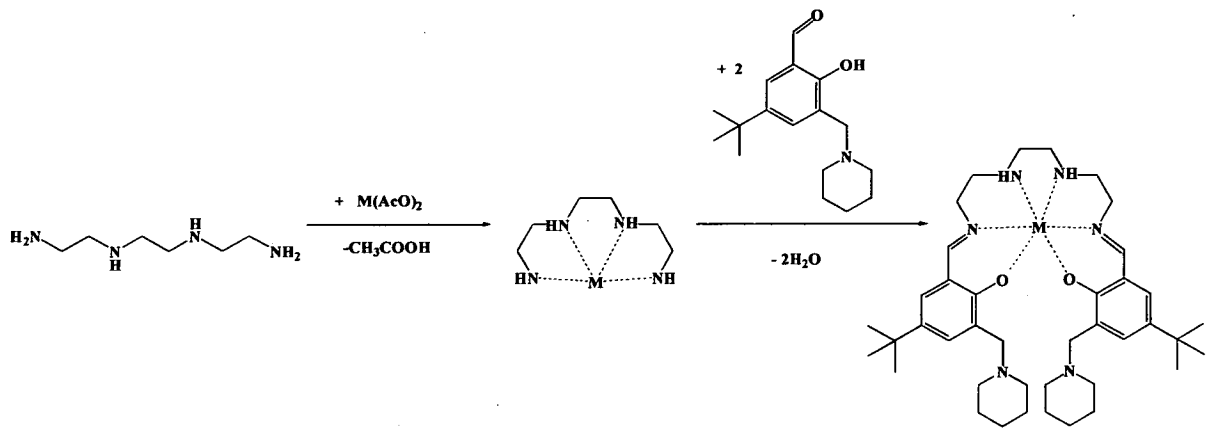

Scheme 2.11 Template synthesis of "metal-only complexes" of ligand **1**

The template synthesis outlined in Scheme 2.11 exploits the formation of a metal-**Trien** complex which would protect the two secondary amines in the following Schiff base condensation. In theory the metal template ion could be stripped from the complex by reprotonation of the phenolic oxygens to give the free ligand or the "metal-only complex" could be used in anion loading experiments.[19]

The template synthesis could be attempted in the presence of cobalt(II), copper(II), nickel(II) or zinc(II). Cobalt(II) can be oxidised to the very inert[2] cobalt(III) form, which could be problematic to remove. Copper(II) shows a strong preference for the formation of tetrahedral complexes[9] and thus will be a very poor template ion favouring formation of other amine/salicylaldehyde combinations. Therefore in practice the template synthesis was only attempted with nickel and zinc acetate.

On complexation with **Trien** the nickel and zinc complexes were found to be very hydroscopic due to the four amines and hence the complex could not be purified. As a pure ligand is needed to study it's ability as a nickel extractant the method to form a "greasy" dihexyl ligand was stopped.

For proof of concept one equivalent of the impure nickel-**Triene** complexe was reacted with two equivalents of 2-hydroxy-3-(piperidinyl)-4-ylmethyl)-5-tert-butylbenzaldehyde and purified to form a nickel acetate complex with ligand **1**.

Somewhat surprisingly the nickel-only complex was not isolated but instead the complex was found to have both the acetate anions hydrogen bonded to the pendant tertiary amines. This is the only nickel complex synthesised with a sexadentate ligand to have the acetates coordinated. (See section 2.6.1.7 for crystal structure of the complex.)

2.3.4.4 Piperazine-bridged ligands 3 and 4

1,4, Piperazinediethanamine can be obtained in mg quantities, but the experiment was attempted to explore the melt method described by Searle *et. al.*[18] (section 2.3.4.2). One equivalence of piperazine was directly heated and melted with two equivalents of N,N-dimethylenediamine. The solid was purified to give the piperazine 1,4-diphthalimido-3,6-diazoctane product.

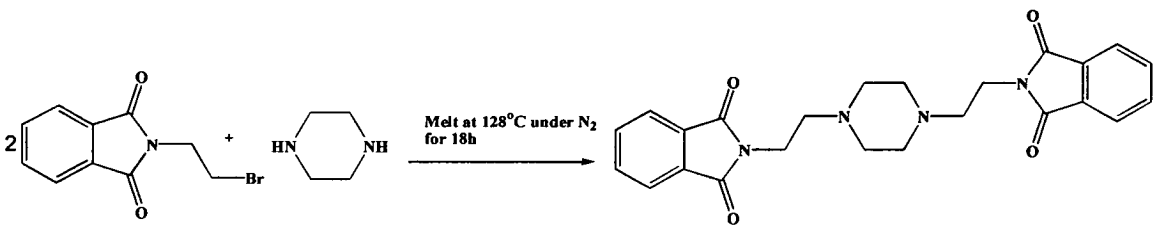

Scheme 2.12 Synthesis of piperazine 1,4-diphthalimido-3,6-diazoctane

The protecting group was removed by the Gabriel synthesis of amines,[20] see Scheme 2.5. 1,4, Piperazinediethanamine was then reacted with the appropriate salicyaldehyde to give ligands **3** and **4**.

If a similar nickel binding site (to the ethane and propane bridged ligands) were to be formed, with ligands **3** and **4**, then this would involve the piperazine ring adopting a boat conformation to allow both lone pairs (from the two nitrogens) to be directed towards the nickel cation. In doing so this would cause all six donors to lie in the

same plane due to the conjugation through the phenol ring. If the lone pairs of the imine nitrognes were also to be directed towards a central nickel binding site this would result in the unfeasible arrangement shown in Figure 2.5.

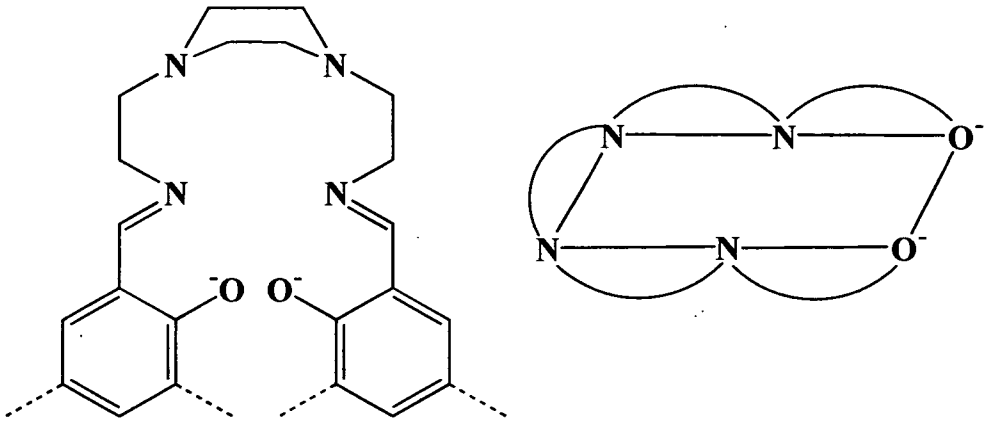

Figure 2.5 Diagram showing all six donor atoms lying in the same plane for ligands **3** and **4**

Therefore, ligand **3** was not used in any complexation reactions as it could not form the wanted zwitterionic structure with independent dibasic and diacidic binding sites (see chapter 1, section 1.7). Ligand **4** was used in the solvent extraction experiment (section 2.7) as a comparative ligand type.

2.4 Characterisation of ligands

All the ligands were characterised by ^{1}H and ^{13}C NMR spectroscopy, FAB mass spectrometry and elemental analysis.

2.4.1 ^{1}H NMR Spectroscopy

The ^{1}H NMR spectrum of ligand **9** (Figure 2.6) is typical. Eleven proton resonances were observed corresponding to atoms types *A, B, C, D, E, F, G, H, I, J* and *K* protons (Figure 2.6)- consistent with the two halves of the ligand or each side of the central ethane bridge being equivalent.

The strong signal at 1.28 ppm can be assigned to the 18 methyl protons of the *t*-butyl groups, *G*. The three type of piperidine protons give broad peaks with some fine

structure, at 1.55 ppm (*K*), at 1.57 ppm (*J*) and at 2.44 ppm (*I*). The upfield position of the 1.55 ppm signal and its integral (4H) being half that of *I* and *J* can be used to assign it as arising from the four piperidine methylene groups *K*. The remaining piperidine protons are expected to resonate somewhat downfield, as the adjacent nitrogen atom is electron withdrawing. This is consistent with the signal at 2.44 ppm arising from the protons *I* and that at 1.57 ppm from the protons *J*.

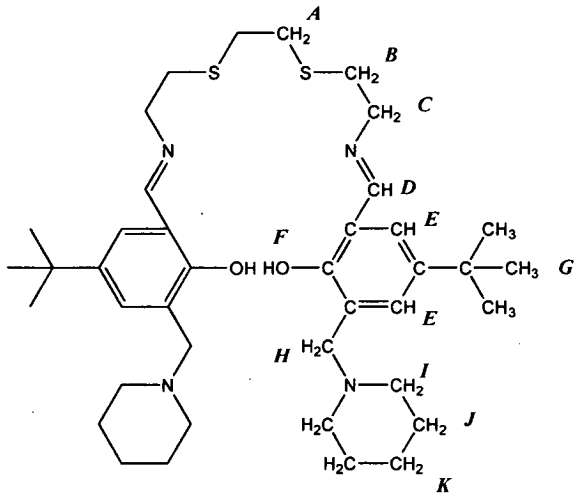

Figure 2.6 Labelling of H-atoms used for assignment of peaks in the ^{1}H spectra of ligand **9**

The two singlets at 2.73 ppm and 3.57 ppm represent protons *A* and *H* respectively. The two triplets at 2.82 ppm and 3.73 ppm both have an integral corresponding to four protons relative to the 18 methyl protons of *G* and could be assigned to positions *B* or *C*. The lower field signal (3.73) is assigned to the more electronegative imino nitrogen atom (*C*). The resonances from the two aromatic protons *E* appear as two singlets at 7.35 and 7.34 ppm. The remaining two singlets arise from the imine-carbon protons *D* (8.36) or the phenol protons *F* (10.35).

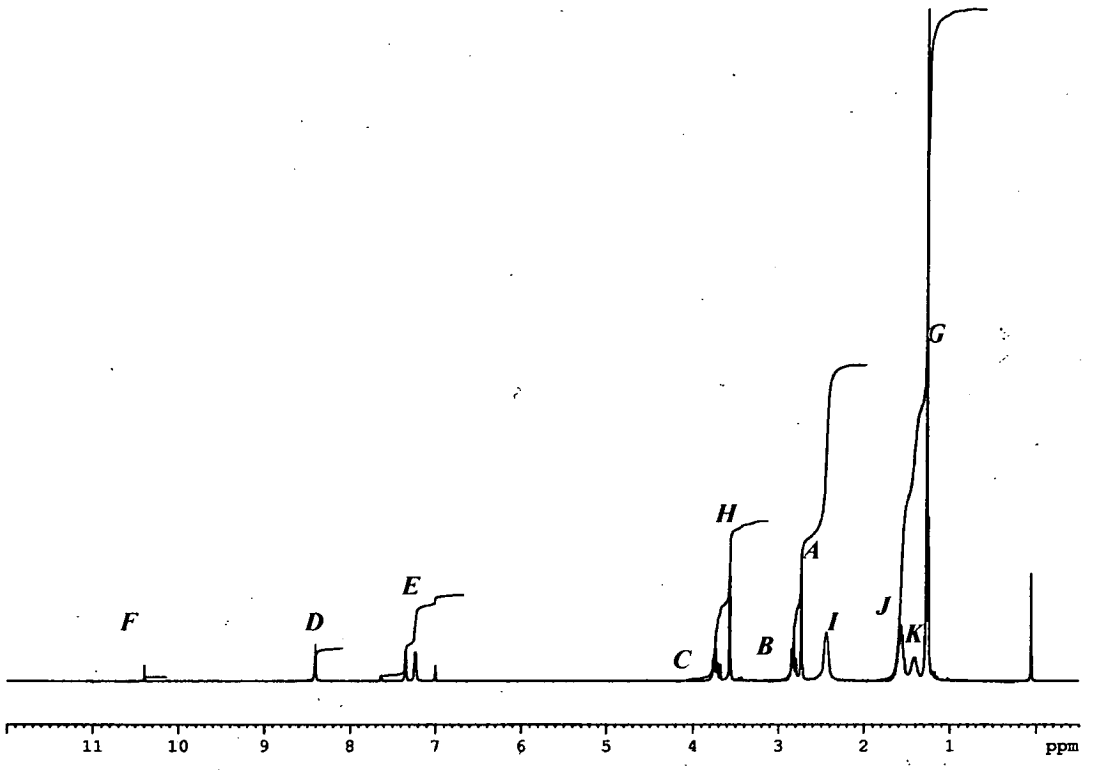

Figure 2.7 250 MHz ^{1}H Spectrum of ligand **9** in $CDCl_3$

2.4.2 ^{13}C NMR Spectroscopy

Standard ^{13}C spectra in the range 0-220 ppm and DEPT spectra to distinguish between the methyl, methylene, methyne and quarternary carbons (Figure 2.8) were recorded for each ligand. The results for ligand **9** (Figure 2.8) are typical.

The intense resonance at 31.9 ppm was assigned to the methyl carbons *H* and the small resonance at 34.4 ppm to the fulcrum quaternary carbon *G* atoms of the *t*-butyl groups. The methylene carbons *L*, *K* and *J* of the piperidine rings gave the signals at 24.7, 26.4 and 54.8 ppm respectively. The two signals at 32.9 and 33.5 ppm arise from the CH_2-S, carbons, *A* and *B* and those at 58.0 and 60.2 ppm from the methylene groups adjacent to the amino (*I*) and imino (*C*) nitrogen atoms respectively.

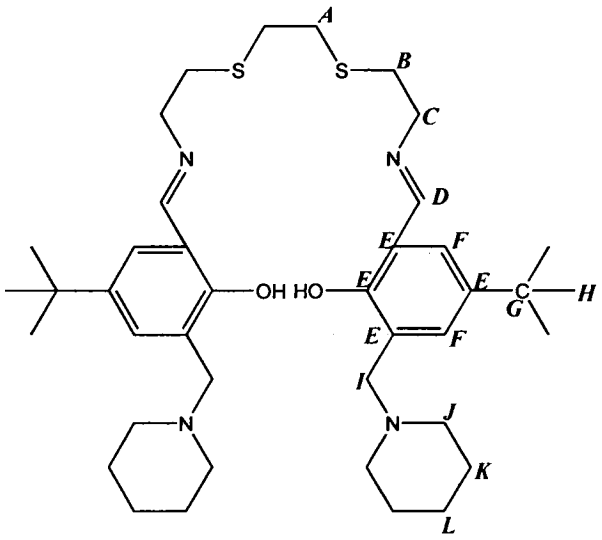

Figure 2.8 Labelling of C-atoms used for assignment of peaks in the ^{13}C spectra of ligand **9**

The aromatic carbons appear in the region 118.6-165.7, the different resonances from methyne *F* and quarternary *E*, can be assigned using the DEPT experiment. The resonances arising from the *F* carbons correspond to the resonances at 126.3 and 131.1 ppm. The resonance of carbons *E* correspond to the resonances 118.6, 125.0, 141.1 and 157.6 ppm. The lower field resonance at 191.5 ppm is due to the imine carbon, *D*.

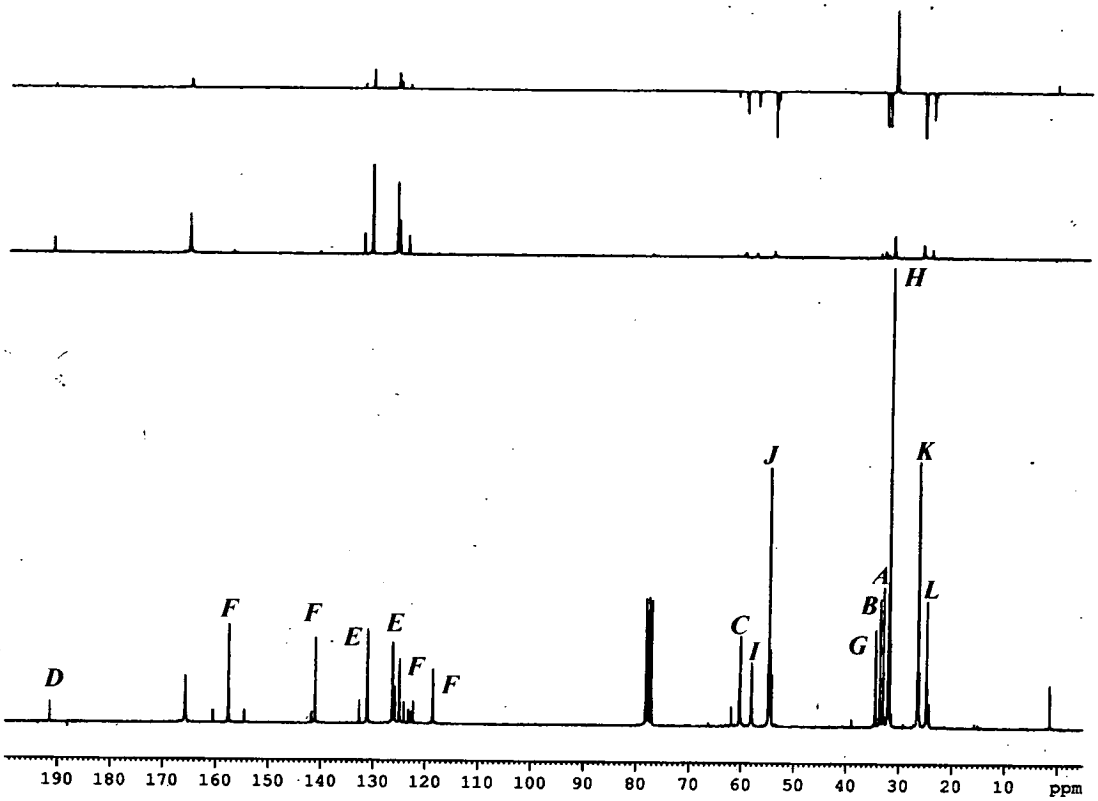

Figure 2.9 The 65 MHz ^{13}C and 65 MHz DEPT spectra of ligand **9** in $CDCl_3$

2.4.3 Crystal structure of ligand 5

Single crystals of ligand **5** suitable for X-ray structure determination were grown by evaporation of a hexane solution. There are two molecules (AB and CD) in the asymmetric unit each with chemically equivalent halves "A" and "B", and "C" and "D" (Figure 2.10).

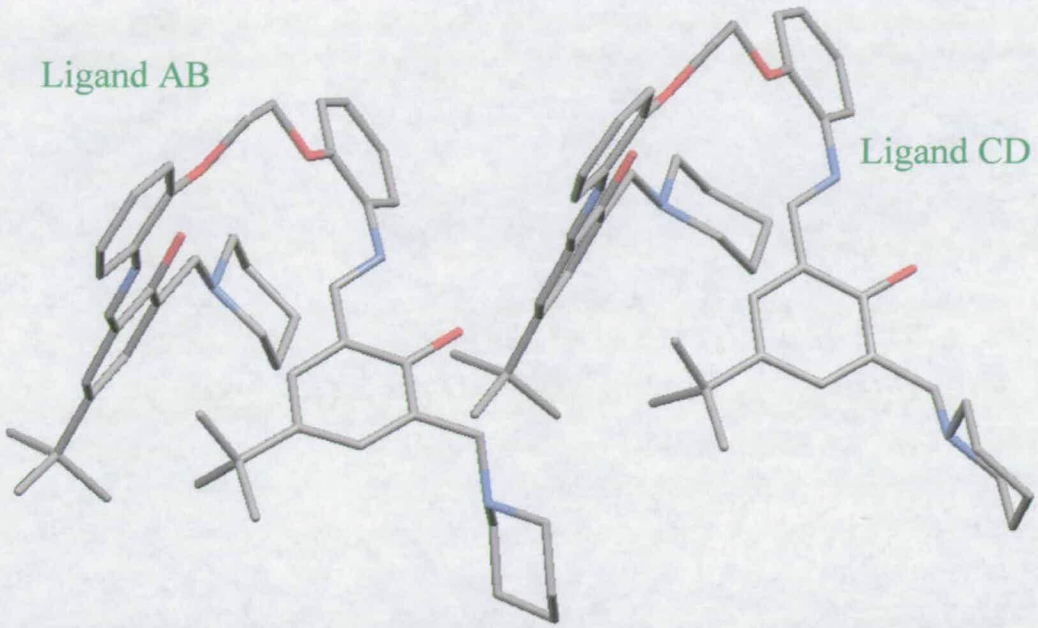

Figure 2.10 The two crystallographically independent molecules in the X-ray structure of ligand **5**

Ligand CD has one *t*-butyl group which is disordered but otherwise the two molecules have very similar configurations as shown in Figure 2.10. Whilst the two molecules have very similar configurations overall, the two halves of each adopt significantly different configurations. These will be compared for sides "A" and "B" using atom labelling shown in Figure 2.11.

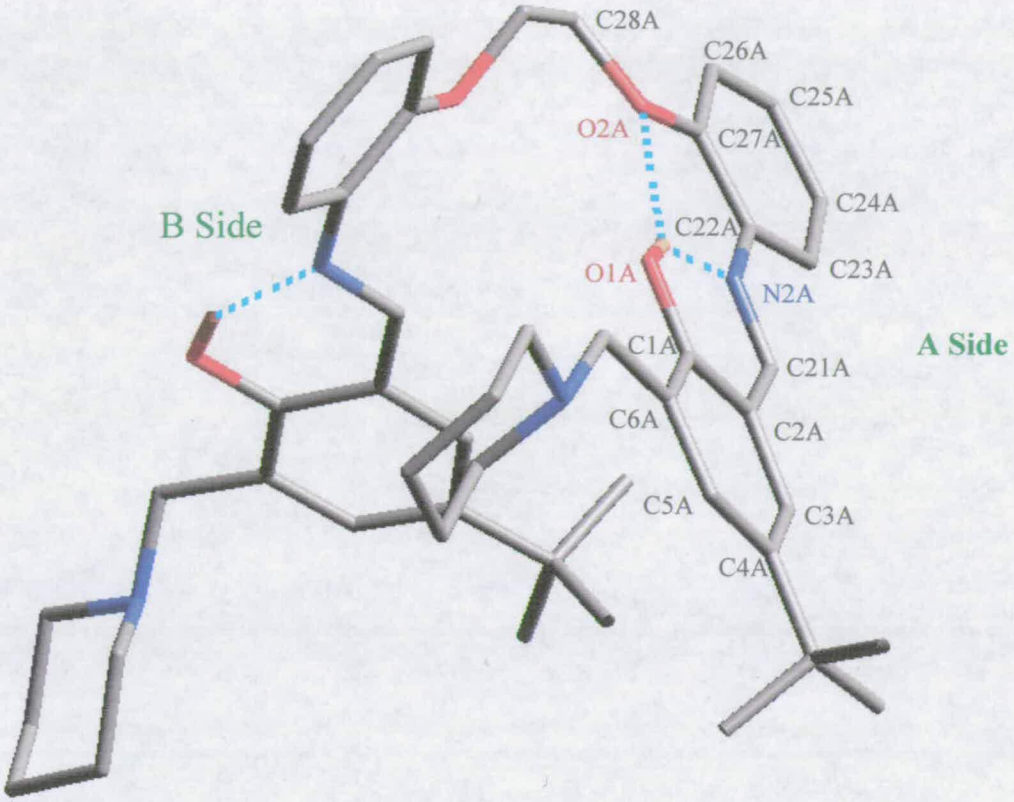

Figure 2.11 Ligand AB

The "A" side of the molecule is set up in the geometry expected for metal complex formation with a conjugated *pseudo*-planar ONO unit (Figure 2.11). The phenolic proton occupies a site close to where the metal ion will lie interacting with the lone pairs on the imino nitrogen and the phenoxyether, both of which show sp^2 hybridisation see Figure 2.12.

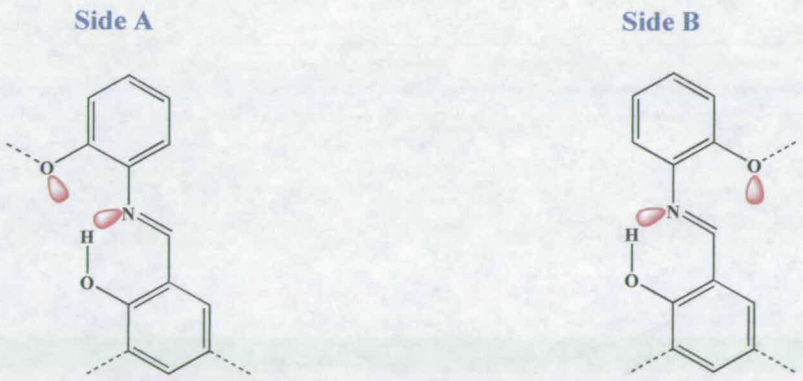

Figure 2.12 The location of the phenolic "proton" relative to the lone pairs on the NO_2^- donor set on the "A" and "B" sides of ligand **5**

The eight atoms which define the two chelate rings, O(1A), C(1A), C(2A), C(21A), N(2A), C(22A), C(27A) and O(2A), are approximately co-planar, with maximum deviation from the least squares plane defined by the above atoms being 0.04 Å and –0.04 Å for atoms O(2A) and O(1A) respectively. The average deviation from the least squares plane is 0.019 Å.

The six benzene carbon atoms from the phenol, C(1A), C(2A), C(3A), C(4A), C(5A) and C(6A), are also almost co-planar with the chelate rings, with the benzene ring being inclined by 0.9° to the mean plane through the chelating atoms.

The linking benzene ring, C(22A), C(23A), C(24A), C(25A), C(26A) and C(27A), also lies close to the chelate and phenol ring, inclined at 3.4° and 3.9° respectively.

These small displacements of the benzene rings are towards opposite sides of the overall plane see Figure 2.13.

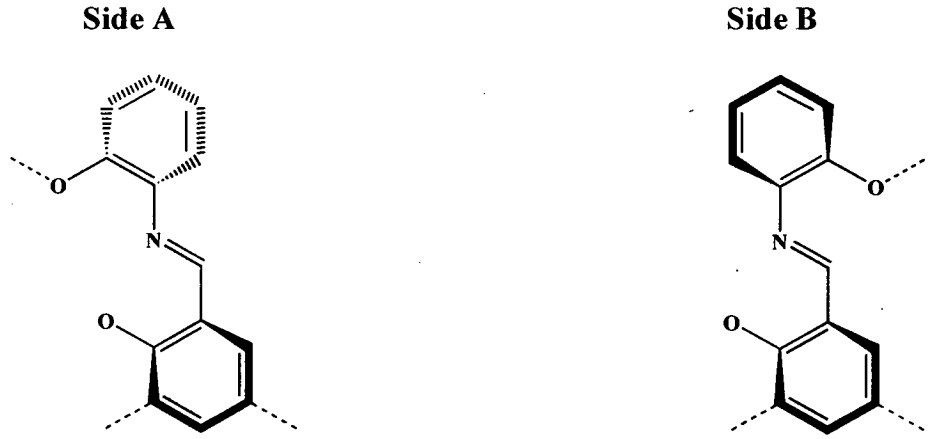

Figure 2.13 Displacement of the benzene ring relative to the mean plane through the chelating unit in sides "A" and "B" of the ligand **5**

The "B" side of the ligand is not set up to act as a tridentate ligand for a nickel ion.

The three planes as defined before are shown in Table 2.1

Table 2.1 Planes on the "B" side of Ligand AB

Atoms	Deviation from the least squares plane	
	Maximum (Å)	Mean (Å)
O(1B), C(1B), C(2B), C(21B), N(2B), C(22B), C(27B), O(2B)	0.57 C(21B) -0.84 N(2B)	0.427
C(1B), C(2B), C(3B), C(4B), C(5B), C(5B)	0.004 C(1B) -0.003 C(6B)	0.002
C(22B), C(23B), C(24B), C(25B), C(26B), C(27B)	0.02 C(22B) -0.01 C(23B)	0.009

In this arm of the ligand both phenolic and phenylene rings are bent towards the same side of the mean plane by 25.1° and 35.2° respectively.

The "A" side of the ligand is held rigidly planar by strong intramolecular hydrogen bonding between the phenolic proton and the neighbouring imino nitrogen[O(1A)-H···N(2A), 2.548 Å] and the phenolic hydrogen and the backbone oxygen [O(1A)-H···N(2A), 3.194 Å]. It is these two intra-molecular hydrogen-bonds which holds the "A" side of the ligand in the desired geometry with a conjugated *pseudo*-planar ONO unit and three donor orbitals preorganised for coordinating to the nickel cation. In comparison the "B" side of the ligand only has one intra-molecular hydrogen-bond between the phenolic hydrogen and imine nitrogen [O(1A)-H···N(2A)], 2.548 Å. However, the structure in Figure 2.14 demonstrates that it is not be possible for side "B" to also be *pseudo*-planar and in the desired geometry.

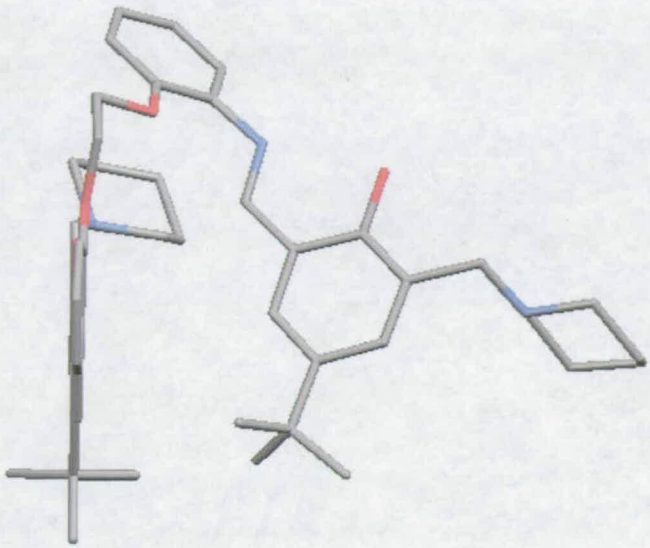

Figure 2.14 Ligand **5** with *pseudo*-planar side "A" and twisted side "B"

The bridging torsion angle [O(2A)-C(28A)-C(28B)-O(2B)] is 68.5°.

2.5 Synthesis of nickel salt complexes

The nickel salt complexes which were isolated upon complexation of the sexadentate ligands are listed in Table 2.2.

Table 2.2 Complexes of sexadentate ligands

Abbreviation	**13**	**14**	**15**	**16**
Complex	[Ni(**1**)$(C_2H_3O_2)_2$]	[Ni(**5**)(SO_4)]	[Ni(**5**)$(NO_3)_2$]	[Ni(**5**)$(Cl)_2$]
17	**18**	**19**	**20**	**21**
[Ni(**5**-2H)]	[Ni(**7**)(SO_4)]	[Ni(**7**)$(NO_3)_2$]	[Ni(**7**)$(Cl)_2$]	[Ni(**7**-2H)]
22	**23**	**24**	**25**	**26**
[Ni(**9**)(SO_4)]	[Ni(**9**)$(NO_3)_2$]	[Ni(**9**)$(Cl)_2$]	[Ni(**9**-2H)]	[Ni(**11**)(SO_4)]
27	**28**	**29**		
[Ni(**11**)$(NO_3)_2$]	[Ni(**11**)$(Cl)_2$]	[Ni(**11**-2H)]		

Metal complexes **13-29** of sexadentate ligands were synthesised by the standard one step method of one equivalent of the appropriate ligand with one equivalent of the appropriate divalent nickel salt (Equation 2.1)

Equation 2.1 $L + Ni^{2+}X^{2-} \longrightarrow LNiX$

Two different types of complexes were prepared, "metal-salt" complexes and "metal-only" complexes as shown in Scheme 2.13.

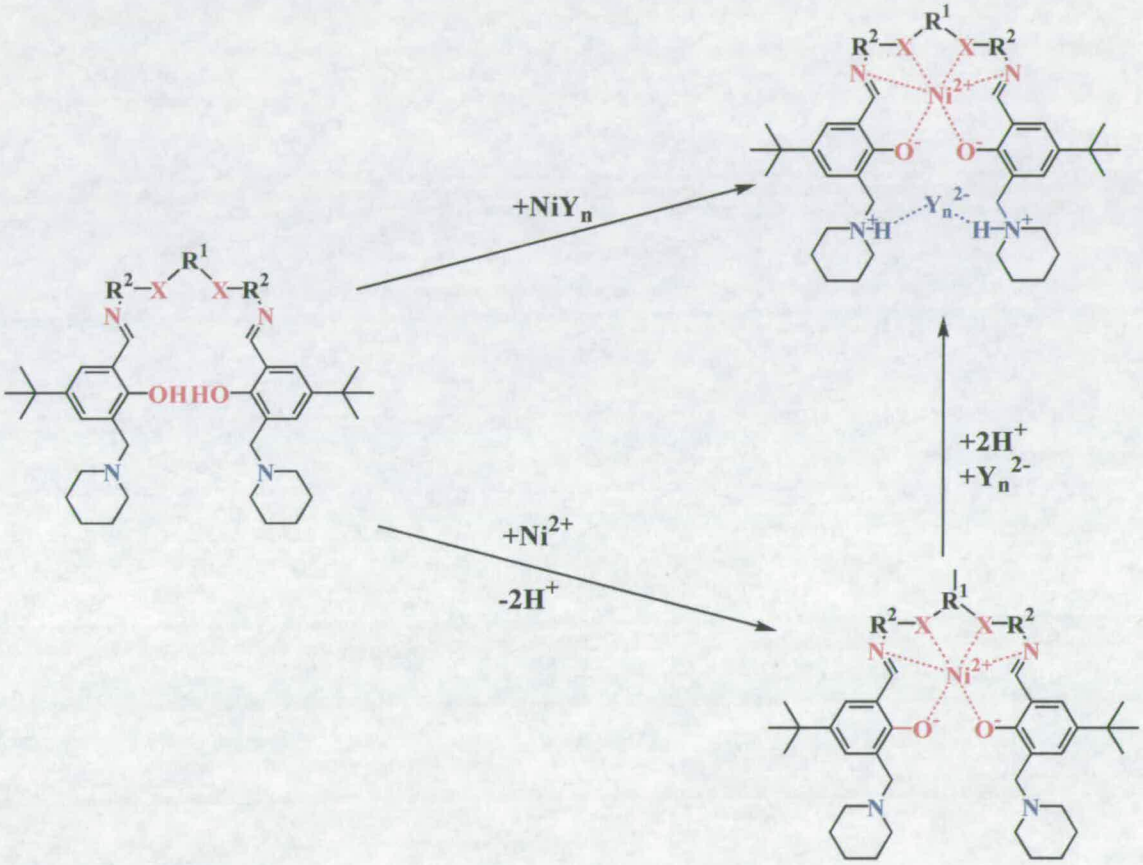

Scheme 2.13 Formation of "metal-salt" and "metal-only" complexes **13-29**

2.6 Characterisation of nickel complexes

Complexes were characterised by ^{1}H NMR, mass spectrometry, IR spectroscopy, UV-Vis spectroscopy, elemental analysis and when possible X-ray crystallography.

^{1}H NMR spectroscopy is useful since it can be used to give an insight into the geometry of the nickel. All the NMR spectra obtained showed broadening, indicating the formation of paramagnetic nickel complexes, e.g. high spin six coordinate *pseudo*-octahedral complexes.

Infrared spectroscopy can be used to confirm the presence of the attendant anions.[21] Bands for the nitrate ion are expected in the region 1380-1350 cm^{-1}, the sulfate in the 1130-1080 cm^{-1} region and the acetate in the 1610-1550 cm^{-1} region. The spectra recorded for the nitrate and sulfate complexes by solid state IR, show the appropriate peaks for their respective anions, whereas the "metal-only" complexes derived from the metal acetates displayed no peaks in the 1610-1550 cm^{-1} region confirming that acetate is not present.

The combined analytical results (mass spectrometry elemental analysis and IR spectroscopy) suggest that the ligands **5**, **7**, **9** and **11** form complexes with a ligand: nickel: anion (L:Ni:X) ratio of 1:1:1 with nickel sulfate and 1:1:2 with nickel nitrate and chloride. For the acetate complexes the results indicate a 1:1:0 (L:Ni:X) ratio. When the nickel atom is coordinated in the $X_2S_2O_2^{2-}$ donor, the two protons released by the phenol groups are captured by the acetate anions, forming acetic acid, instead of the pendant piperidine tertiary amine groups. The *p*Ka of acetic acid (4.75)[22] could be greater than that of the protonated tertiary amine group of the ditopic ligand. (This would need to be confirmed by measurement of the *p*Ka of the protonated N-substituted piperidine.) This is consistent with the previous work on the tetradentate ligands,[7] complexes and the structures obtained by X-ray crystallography, (section 2.6.1).

2.6.1 X-ray crystallography

Although the solid state structures of ligands often bear little relation to their behaviour in solution, some information on the propensity of these ligands to form the desired octahedral motif can be obtained.

Single crystals of the nickel sulfate, nitrate, chloride and "nickel-only" complexes using ligand **11** and a nickel nitrate complex with **9** were grown by diffusion method. A nickel acetate complex with **1** as grown by slow evaporation of the solvent (see section 2.9.4).

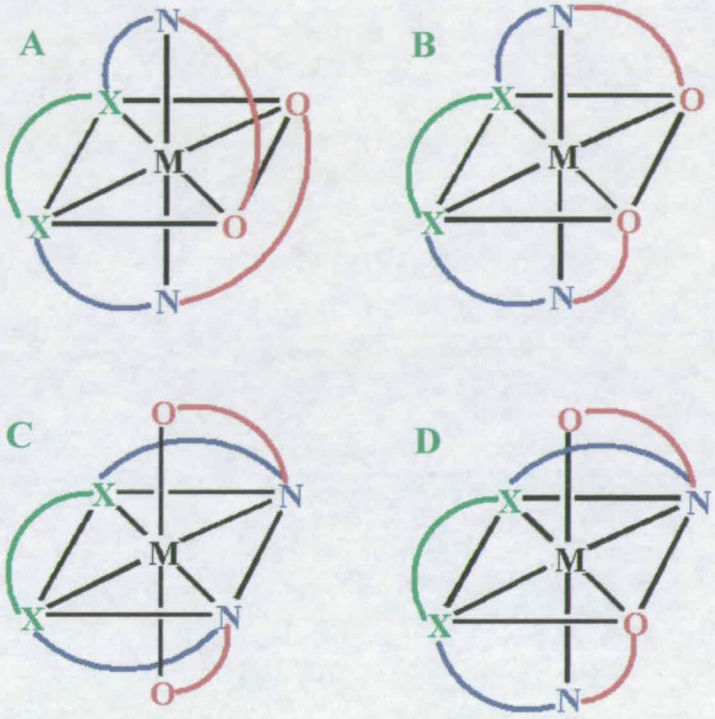

Figure 2.15 Diagram showing the four possible isomeric forms for a sexadentate ligand octahedrally coordinating to a metal cation

A schematic representation of the four possible isomeric forms of the metal coordinated to the $X_2N_2O_2$ ligands is shown in Figure 2.15. *A* and *B* present a X_2O_2 donor set in a square plane containing the MSS chelate but differ in having the XNO "arms" planar in *A* (desirable for conjugation through the imine) but bent in *B*. *C* presents a X_2N_2 donor set in a "square" plane containing MSS and has both arms bent and the terminal oxygens *trans* to each other. *D* presents a X_2NO donor set in a "square" plane containing the MSS chelate ring with both arms bent and the terminal oxygen atoms *cis* to each other.

Molecular mechanics calculations performed at The University of Edinburgh conclude that the lowest energy isomer *A* should be the most thermodynamically

stable isomer and hence the one formed. This was also suggested by Cannon, Chriswell and Venanzi who reported[23] this configuration to be the least strained.

For each isomer there are two enantiomers. Each enantiomeric pair is the mirror image of the other and are non superposable. The X-ray structures of all the complexes grown for **1**, **9** and **11** show the metal bound in an octahedral fashion in the predicted isomeric A form or as its enantomeric pair as shown in Figure 2.16.

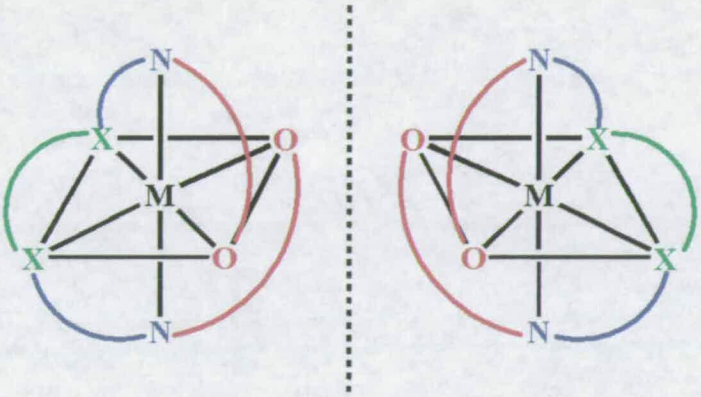

Figure 2.16 Diagram showing the enantiomeric pairs of isomer *A*

2.6.1.1 X-ray structure of [Ni(14-2H)]

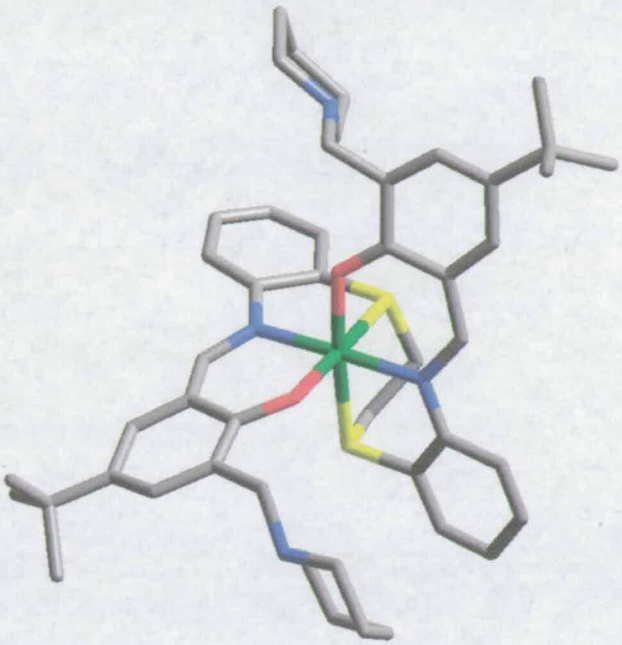

Figure 2.17 The X-ray structure of [Ni(**11**-2H)]

Single crystals of [Ni(**11**-2H)] suitable for X-ray structure determination were grown from methanol using ether as the counter solvent. There is one molecule of the complex in the asymmetric unit (Figure 2.17). The nickel is coordinated in the lowest energy isomeric form (*A*) as expected. This is seen for all the nickel complex crystal structures.

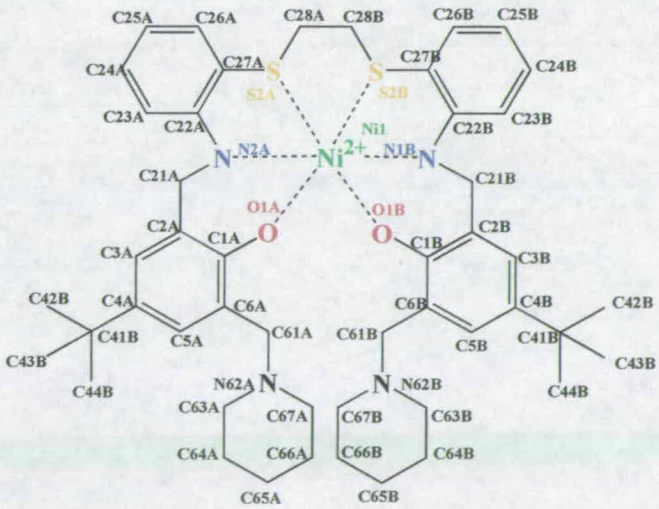

Figure 2.18 The atom labelling scheme

The crystal structures shows that by rearrangement of the piperidine rings, by rotation of the C(6)-C(61) bond, could form a cavity for a sulfate anion and the formation of a discrete 1:1:1 complex. This was seen[8] for tetradentate salen-based metal salt complexes.

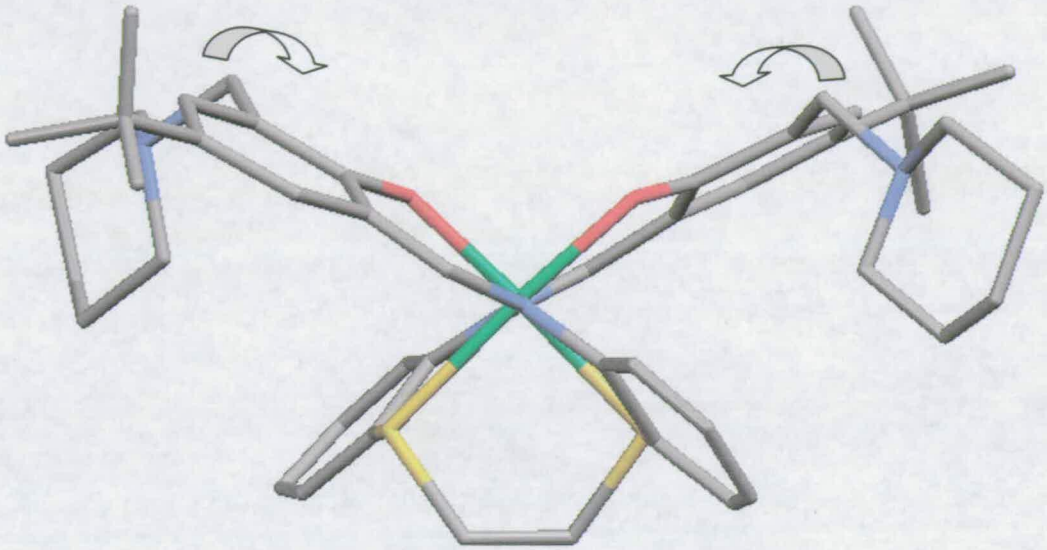

Figure 2.19 Diagram showing the rearrangement of the piperidine rings to form an anion binding cavity

The two sides of the molecule (splitting through the bridging ethane backbone) are almost identical.

In ligand **5** it was shown that the ONX plane where X=O [O(1), C(1), C(2), C(21), N(2), C(22), C(27) and O(2)] is basically flat (section 2.4.3) when we compare this to the complexes we find this is not the case. For example in the complex [Ni(**11**-2H)] the eight atoms of the ONS plane [O(1), C(1), C(2), C(21), N(2), C(22), C(27) and S(2)] have a maximum deviation from the least squares plane defined by the above atoms being 0.2055 Å [C(2A)] and -0.2650 Å [C(22A)], for side A and 0.2533 Å [C(22B)] and -0.2171 Å [C(2B)] for side B. The average deviation from the least squares plane for sides A and B are 0.1612 Å and 0.1522 Å respectively. This is also shown in Figure 2.20 below. This is the same for all the crystal structures of the sexadentate nickel complexes.

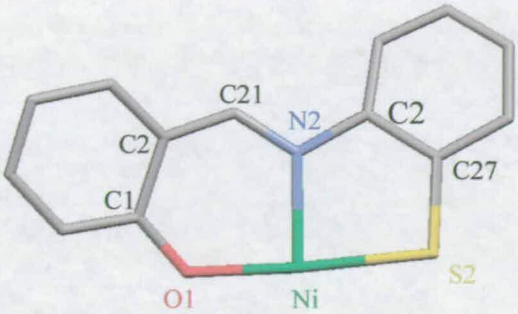

Figure 2.20 Section of [Ni(**11**-2H)] crystal structure showing the labelling scheme for the ONS plane [O(1), C(1), C(2), C(21), N(2), C(22), C(27) and S(2)]

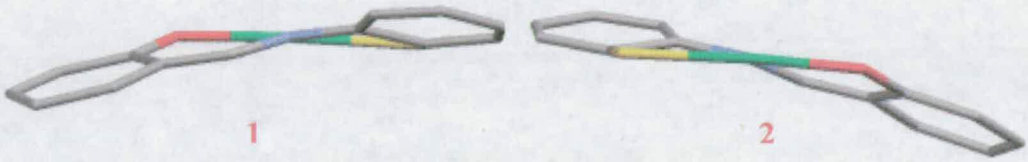

Figure 2.21 Cross sections of ONS plane, facing into the N(2)-Ni(1) bond (1) and out of the Ni(1)-N(2)bond (2)

Therefore, two planes defined for all the crystal structures are the ONXNi plane [O1, N2, X and Ni] (where X=S2 or N3) and the ObenzeneN plane [O(1), C(1), C(2), C(3), C(4), C(5), C(6), C(21), N(2)]. For complexes involving ligand **11** a third plane is also included, SbenzeneN plane [N(2), C(22), C(23), C(24), C(25), C(26), C(27) and S(2)], Figure 2.18.

The four atoms of the ONSNi plane are approximately co-planar for both the A and the B side of the complex. For side A the maximum deviation from the least squares plane defined by the above atoms is 0.0206 and –0.0362 Å for atoms O(1A) and Ni(1) respectively and for side B the maximum deviation from the least squares plane defined by the above atoms is 0.0468 and –0.0263 Å for atoms Ni(1) and O(1B) respectively. The average deviation from the least squares plane for sides A and B are 0.0187 and 0.0241 Å respectively.

The ten atoms from the ObenzeneN plane are also approximately co-planar for both the A and the B side of the complex. For side A the maximum deviation from the

least squares plane defined by the above atoms is 0.0483 Å and –0.0487 Å for atoms C(2A) and N(2A) respectively and for side B the maximum deviation from the least squares plane defined by the above atoms being 0.0752 Å and –0.0869 Å for atoms O(1B) and N(2B) respectively. The average deviation from the least squares plane for sides A and B are 0.0250 and 0.0458 Å respectively. The angle of this plane to the ONSNi plane is 19.7° and 17.6° for sides A and B respectively.

The eight atoms from the NbenzeneS plane are also approximately co-planar for both the A and the B side of the complex. For side A the maximum deviation from the least squares plane defined by the above atoms being 0.1085 Å and –0.1404 Å for atoms C(27A) and S(2A) respectively and for side B the maximum deviation from the least squares plane defined by the above atoms being 0.0711 Å and –0.0728 Å for atoms S(2B) and N(2B) respectively. The average deviation from the least squares plane for sides A and B are 0.0750 and 0.0469 Å respectively. The angle of this plane to the ONSNi plane is 7.8° and 6.3° for sides A and B respectively.

By studying the crystal structure the formation of the Ni(1), N(2), C(21), C(2), C(1) and O(1) ring causes a strain which results in the ring being puckered out of the expected conjugated ONSNi plane.

2.6.1.2 X-ray structure of [Ni(11)(SO_4)]

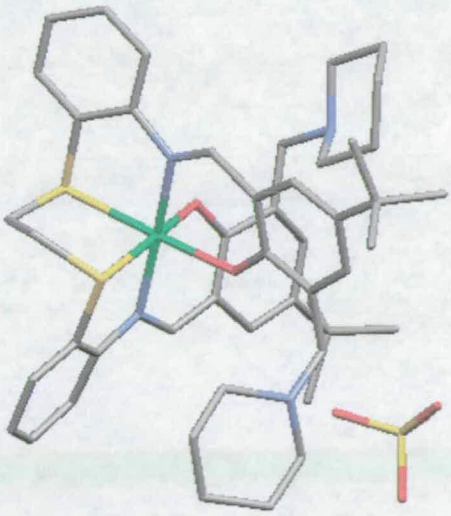

Figure 2.22 The x-ray structure of [Ni(**11**)(SO_4)]

Single crystals of [Ni(**11**)(SO_4)] suitable for X-ray structure determination were grown from dichloromethane with hexane as the counter solvent. There is one molecule of the complex in the asymmetric unit (Figure 2.22). The nickel cation is coordinated in the lowest energy isomer (A, Figure 2.15), and as the point group [P2(1)2(1)2(1)] has no inversion centre or mirror plane there is only one enatiomer of *A* found in the crystal. The piperidine arms are not arranged to form the expected anion cavity instead one of the piperidine arm (side "A"-the near side in Figure 2.23) is facing into the cavity and the other side (side "B"-the far side in Figure 2.23) out of the cavity.

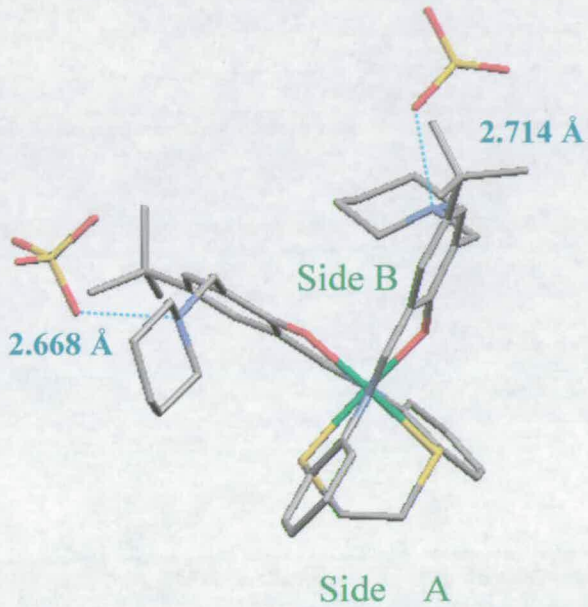

Figure 2.23 Hydrogen bond lengths measured on sides "A" and "B" of [Ni(**11**)(SO_4)]

The structure for the [Ni(**11**)(SO_4)] structure is not as expected with a discreet 1:1:1 (metal:ligand:sulfate) package containing the sulfate bound in a cavity formed by the piperidine arms. Instead, the sulfate anion acts an intermolecular crosslinker via bridging single hydrogen bonds N-H···O bonded (2.66 and 2.714 Å).

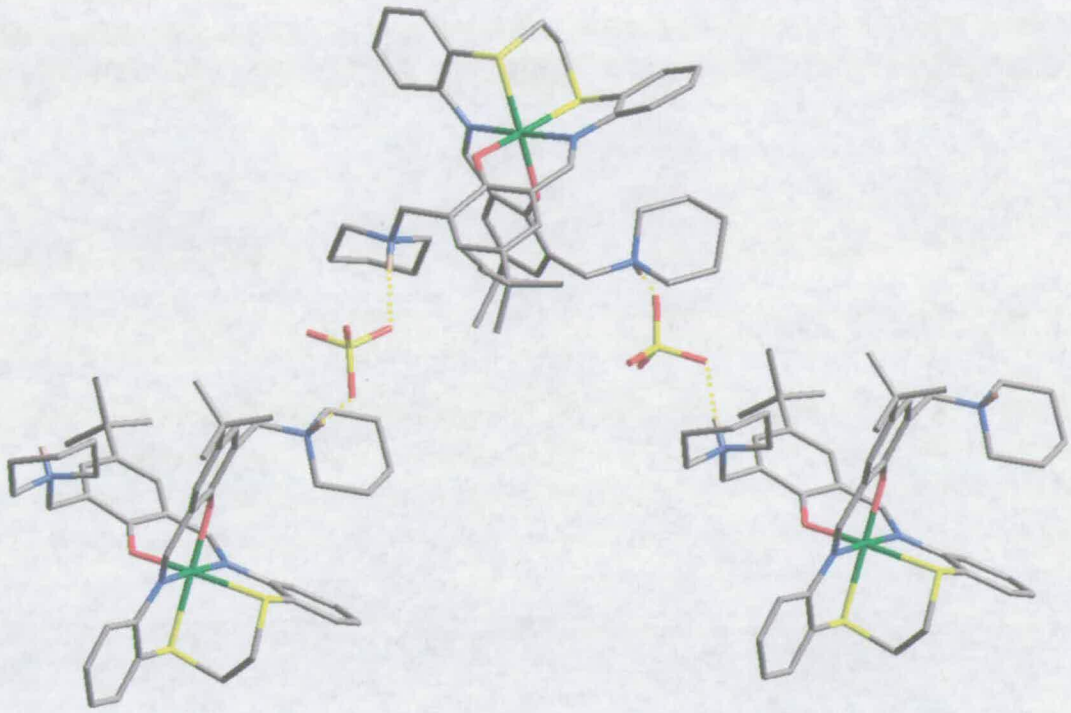

Figure 2.24 Diagram showing the sulfate anion acting as intermolecular crosslinker via single hydrogen bonds

When we compare the hydrogen-bonding to the sulfate anion with those measured in the tetradentate nickel sulfate complex shown in chapter 1 Figure 1.35[8] where the nickel sulfate is bound as a discrete 1:1:1 complex. We find that the hydrogen-bonds are longer than in the [Ni(**11**)(SO_4)] structure. In the tetradentate structure the sulfate is bound below a cavity formed by two pendant morphiline rings via two bifurcated N-H···O hydrogen bonds [2.870(4), 2.923(3), 2.993(4) and 2.915(4)].

When we compare these to other $NiSO_4$ complexes we find that they are above average.

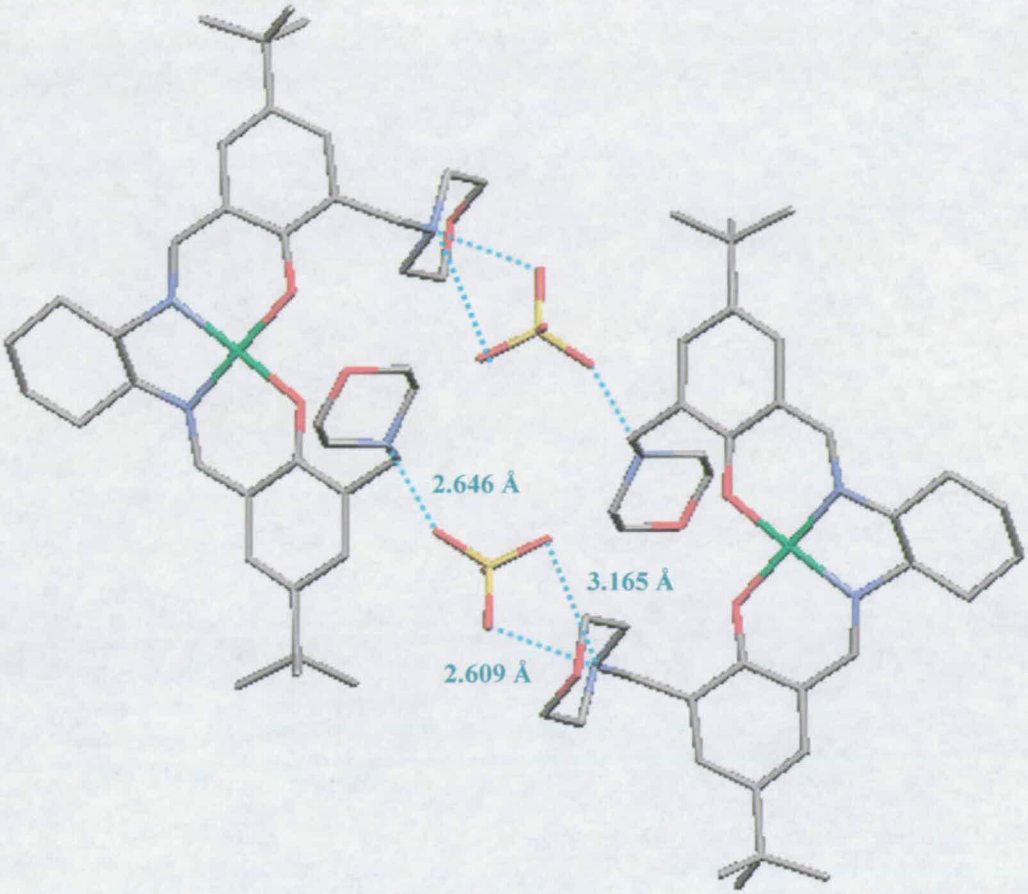

Figure 2.25 X-ray structure of a tetradentate nickel sulfate structure where two sulfates acts as intermolecular crosslinkers forming a *pseudo* macrocycle

In Figure 2.25[7] two nickel complexes of the 1,2-cyclohexane bridged tetradentate ligand are linked by two bridging sulfate anions via one single hydrogen bond (N-H···O = 2.646 Å) and a bifurcated hydrogen bond (N-H···O = 2.609 and 3.165 Å).

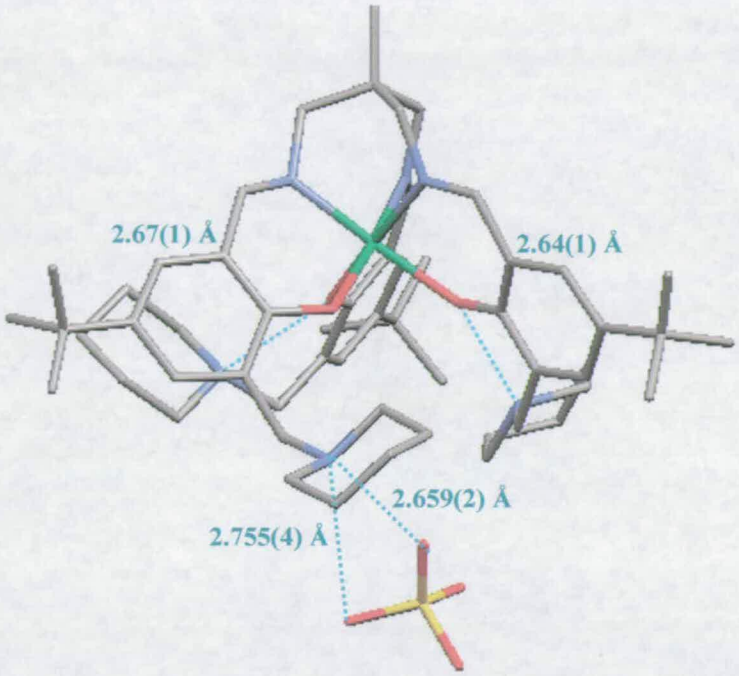

Figure 2.26 X-ray structure of a trifurcated ligand with a nickel coordinated in an octahedral geometry in a trianionic metal-binding site and a sulfate bifurcated hydrogen bound to one of the three pendant piperidine arms

Shorter hydrogen-bonds are also seen when the sulfate is hydrogen bonded to a pendant piperidine nitrogen as shown in Figure 2.26.[24] One of the piperidinium protons forms a bifurcated hydrogen bond to two oxygen atoms of the sulfate anion. The other two piperidinium protons form a hydrogen bond to the phenolate oxygen atoms on the same arm. The hydrogen bond lengths are shown in Figure 2.26.

In the 1:1:1 complex in Figure 1.34 the sulfate cannot fit into cavity formed by the morphiline rings with (N···N) separation of 5.16 Å. In [Ni(**11**)(SO_4)] and the *pseudo* macrocycle structure the sulfate is bound in its ideal cavity position between two protonated tertiary nitrogens with N···N of 6.182 and 7.088 Å respectively. Therefore ideally we want the sexadentate ligands to have a piperidine nitrogen-nitrogen distance greater than 5.16 Å e.g. around 6.182-7.088 Å to encourage extraction of nickel sulfate.

The three planes as defined in section 2.6.1.1 are shown in Table 2.3.

Table 2.3 Planes ONSNi, ObenzeneN and NbenzeneS in crystal structure of [Ni(**11**)(SO_4)]. See Figure 2.18 for numbering scheme.

Plane	**maximum deviation from the least squares plane Å**		**Average deviation from the least squares plane Å**	
	Side A	Side B	Side A	Side B
ONSNi	0.0431 Ni(1) -0.0247 O(1A)	0.0143 O(1B) -0.0256 Ni(1)	0.0225	0.0133
ObenzeneN	0.0738 N(2A) -0.0627 O(1A)	0.0383 N(2B) -0.0344 C(21B)	0.0339	0.0186
NbenzeneO	0.0215 C(22A) -0.0333 C(23A)	0.0702 (N2B) -0.0799(S2B)	0.0182	0.0463

Side B is much flatter than side A. The ObenzeneN plane is 23.4° to the ONS plane for side A and 15.5° for side B and the NbenzeneS plane is 13.7° to the ONS plane for side A and 6.9° for side B This is also seen in Figure 2.23. It seems that for side A the fact that the piperidine is facing into the cavity, pulls the phenol ring more out of the ONSNi plane and hence causes the ONS plane to be more twisted. This can be shown when comparing two planes within the ONSNi plane. The first plane is the ONNi plane [O(1), N(2), Ni(1)] and the second is the NSNi plane [N(2), S(2), Ni(1)].

Due to the ONNi and NSNi planes only incorporating three atoms they are both planar for both the A and the B sides of the complex. The NSNi plane is 3.4° to the ONNi plane for side A and 2.0° for side B hence showing side B is more planar.

2.6.1.3 X-ray structure of [Ni(11)$(NO_3)_2$]

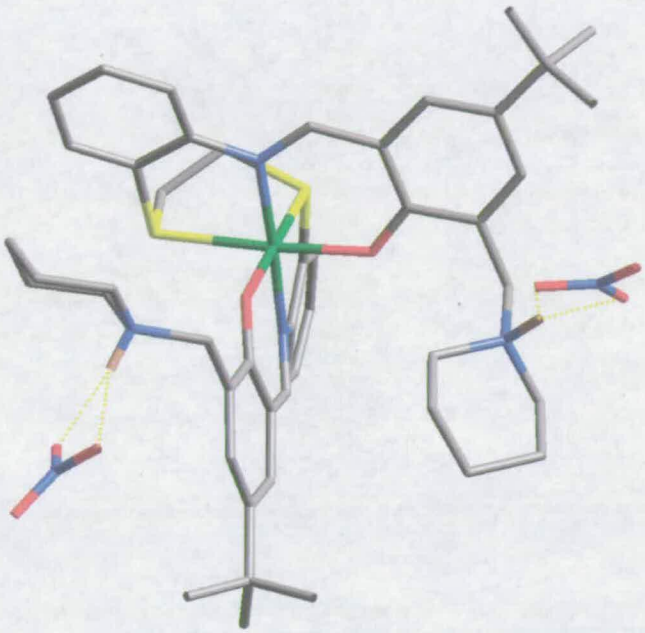

Figure 2.27 The x-ray structure of [Ni(**11**)$(NO_3)_2$]

Single crystals of [Ni(**11**)$(NO_3)_2$] suitable for X-ray structure determination were grown from dichloromethane with hexane as the counter solvent. There is one molecule of the complex in the asymmetric unit (Figure 2.27). The coordination of the nickel has liberated the phenolic protons which have been transferred to the pendant piperidine tertiary nitrogens creating separate positive sites where the nitrates are bound by a combination of electrostatic and bifurcated N-H···O hydrogen bonds to the piperidinium amine protons (Table 2.11). The nitrate anions are bound away from each other, due to the electron repulsive interactions between the nitrates and hence the quaternary protons point away from each other.

The three planes as defined before are shown in Table 2.4.

Table 2.4 Planes ONSNi, ObenzeneN and NbenzeneS in crystal structure of [Ni(**11**)$(NO_3)_2$]. See Figure 2.18 for numbering scheme.

Plane	maximum deviation from the least squares plane Å		average deviation from the least squares plane Å	
	Side A	Side B	Side A	Side B
Ni, O, N, S	0.0272 O(1A) -0.0487 Ni(1)	0.0071 Ni(1) -0.0040 O(1B)	0.0247	0.0036
ObenzeneN	0.0379 C(2A) -0.0440 C(6A)	0.0854 C(2B) -0.0978 N(2B)	0.0241	0.0456
NbenzeneO	0.0527 C(27A) -0.0688 S(2A)	0.0331 N(2B) -0.0418 S(2B)	0.0355	0.0267

By comparing the angles between the planes (Table 2.4) ONSNi to ObenzeneN and NbenzeneS it can be seen that both sides A and B are similarly twisted as shown in Figure 2.28.

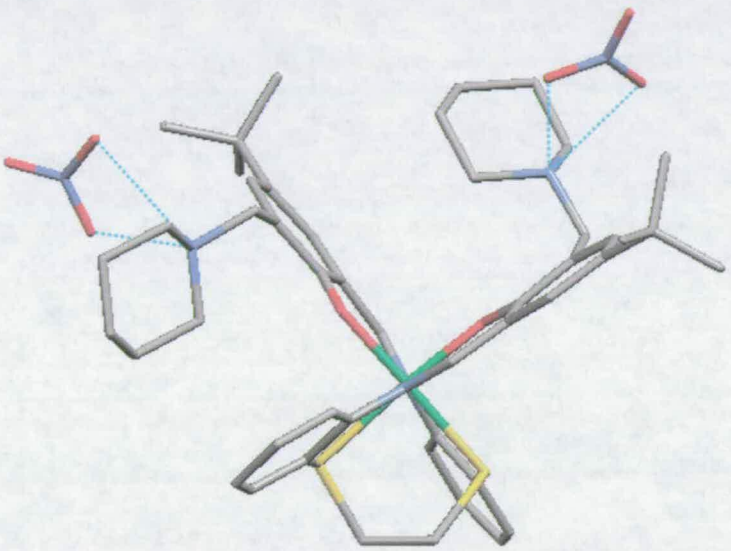

Figure 2.28 X-ray structure of [Ni(**11**)$(NO_3)_2$] showing one piperidine arm facing into the cavity and one out of the cavity

Table 2.5 Angles between the plane ONSNi and ObenzeneN and NbenzeneS (°)

Side	Angle between planes ONSNi and ObenzeneN (°)	Angle between planes ONSNi and NbenzeneS (°)
Side A	8.1	12.0
Side B	8.5	10.5

It was seen for the [Ni(**11**)(SO_4)] structure (section 2.6.1.2) the phenol ring is more out of the ONSNi plane where as for the [Ni(**11**)(NO_3)$_2$] structure the bridging benzene is further out of the plane.

A big difference is seen when we compare the two planes [ONNi plane [O(1), N(2), Ni(1)] and the second is the NSNi plane [N(2), S(2), Ni(1)]] within the ONSNi plane (Table 2.6).

Table 2.6 Angles between the planes ONNi and NSNi (°)

Side	Angle between planes ONNi and NSNi
Side A	3.9
Side B	0.6

As for structure [Ni(**11**)(SO_4)] the ONSNi plane is more planar for side B of structure [Ni(**11**)(NO_3)$_2$] where the piperidine arm is facing out of the cavity.

2.6.1.4 X-ray structure of [Ni(11)(Cl)$_2$]

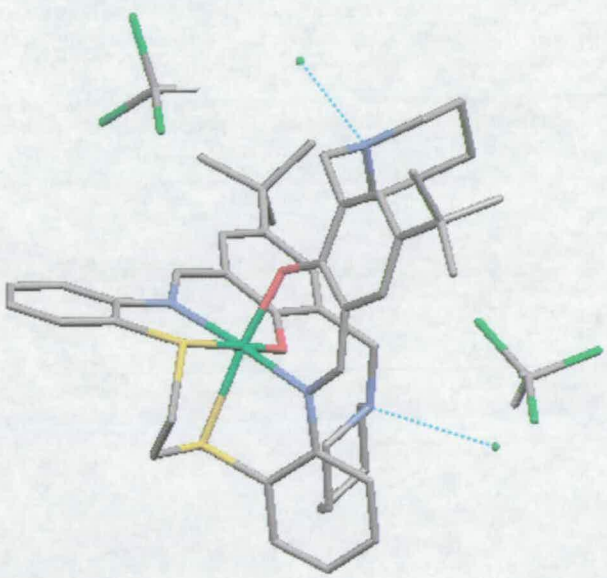

Figure 2.29 The x-ray structure of [Ni(**11**)(Cl)$_2$].2CH_2Cl_2

Single crystals of [Ni(**11**)(Cl_2)] suitable for X-ray structure determination were grown from methanol with ether as the counter solvent. There is one molecule of the

complex in the asymmetric unit. The chlorides are hydrogen bonded to the two piperidinium protons and to the lattice solvent chloroform, see Figure 2.29.

Table 2.7 Planes ONSNi, ObenzeneN and NbenzeneS in crystal structure of [Ni(**11**)(Cl_2)]. See Figure 2.18 for numbering scheme.

Plane	maximum deviation from the least squares plane Å		average deviation from the least squares plane Å	
	Side A	Side B	Side A	Side B
ONSNi	0.0044 0(1A) -0.0026 0(1A)	0.0428 Ni(A) -0.0245 O(1B)	0.0247	0.0036
ObenzeneN	0.1310 C(6A) -0.1450 0(1A)	0.0171 C(21B) -0.0191 C(2B)	0.0241	0.0456
NbenzeneO	0.0787 S(2A) -0.0525 C(27A)	0.0209 N(2B) -0.0172 C(22B)	0.0355	0.0267

By comparing the angles between the planes (Table 2.8) ONSNi to ObenzeneN and NbenzeneS it can be seen that both sides "A" and "B" are similarly twisted as in the nickel nitrate complex.

Table 2.8 Angles between the plane ONSNi and ObenzeneN and NbenzeneS (°)

Side	Angle between planes ONSNi and ObenzeneN (°)	Angle between planes ONSNi and NbenzeneS (°)
Side A	22.1	21.3
Side B	20.1	16.8

2.6.1.5 Comparison in bond lengths and angles in the coordination spheres of [Ni(11-2H)], [Ni(11)(SO_4)], [Ni(11)(NO_3)$_2$] and [Ni(11)(Cl)$_2$]

It can be seen from Table 2.9 that incorporation of either two nitrate or chloride anions or one sulfate dianion does not significantly change the nickel coordination bonds and the octahedral geometry is retained.

The incorporation of the sulfate has a smaller effect than the two nitrates. Therefore due to the minor changes in the nickel geometry between the nickel only complex and the nickel sulfate complex suggests that ligand **11** is suitable to bind a nickel dication and sulfate dianion.

Table 2.9 Bond length (Å) and angles (°) in the co-ordination spheres of the nickel complexes of ligand **11**, [Ni(**11**-2H)], [Ni(**11**)(SO_4)], [Ni(**11**)(NO_3)$_2$] and [Ni(**11**)(Cl)$_2$]. See Figure 2.18 for numbering scheme.

	[Ni(**11**-2H)]	[Ni(**11**)(SO_4)]	[Ni(**11**)(NO_3)$_2$]	[Ni(**11**)(Cl)$_2$]
Ni(1)-S(2)	2.424(3)	2.420(2)	2.408(18)	2.4498(10)
	2.418(3)	2.388(2)	2.404(15)	2.3961(10)
Ni(1)-N(2)	2.062(8)	2.047(6)	2.039(4)	2.031(3)
	2.023(10)	2.047(6)	2.049(4)	2.037(3)
Ni(1)-O(1)	1.973(7)	1.977(5)	1.969(3)	1.994(2)
	2.021(7)	2.022(5)	1.980(3)	1.972(2)
O(1A)-Ni(1)-O(1B)	94.9(9)	93.1(2)	92.78(15)	91.04(10)
O(1A)-Ni(1)-N(2B)	91.7(4)	92.0(2)	89.59(15)	92.04(10)
O(1B)-Ni(1)-N(2B)	94.3(3)	92.0(2)	92.60(14)	91.52(11)
O(1A)-Ni(1)-N(2A)	91.9(3)	91.8(2)	93.25(14)	90.33(10)
O(1B)-Ni(1)-N(2A)	90.7(3)	88.3(2)	88.14(14)	92.36(11)
N(2B)-Ni(1)-N(2A)	173.6(3)	176.2(3)	177.03(15)	175.42(12)
O(1A)-Ni(1)-S(2B)	89.5(2)	89.02(16)	87.77(11)	92.49(7)
O(1B)-Ni(1)-S(2B)	175.0(2)	175.54(16)	177.80(10)	174.05(8)
N(2B)-Ni(1)-S(2B)	82.3(3)	83.98(19)	85.27(11)	83.58(9)
N(2A)-Ni(1)-S(2B)	92.5(2)	95.59(18)	93.95(11)	92.41(9)
O(1A)-Ni(1)-S(2A)	175.8(2)	174.28(16)	175.72(11)	173.09(7)
O(1B)-Ni(1)-S(2A)	88.6(2)	90.13(14)	91.01(11)	89.59(7)
N(2B)-Ni(1)-S(2A)	91.1(3)	92.62(17)	92.23(12)	94.82(8)
N(2A)-Ni(1)-S(2A)	85.0(2)	83.6(2)	84.88(12)	82.76(8)
S(2B)-Ni(1)-S(2A)	87.78(11)	88.08(8)	88.52(5)	87.48(4)

2.6.1.6 X-ray structure of $[Ni(9)(NO_3)_2]$

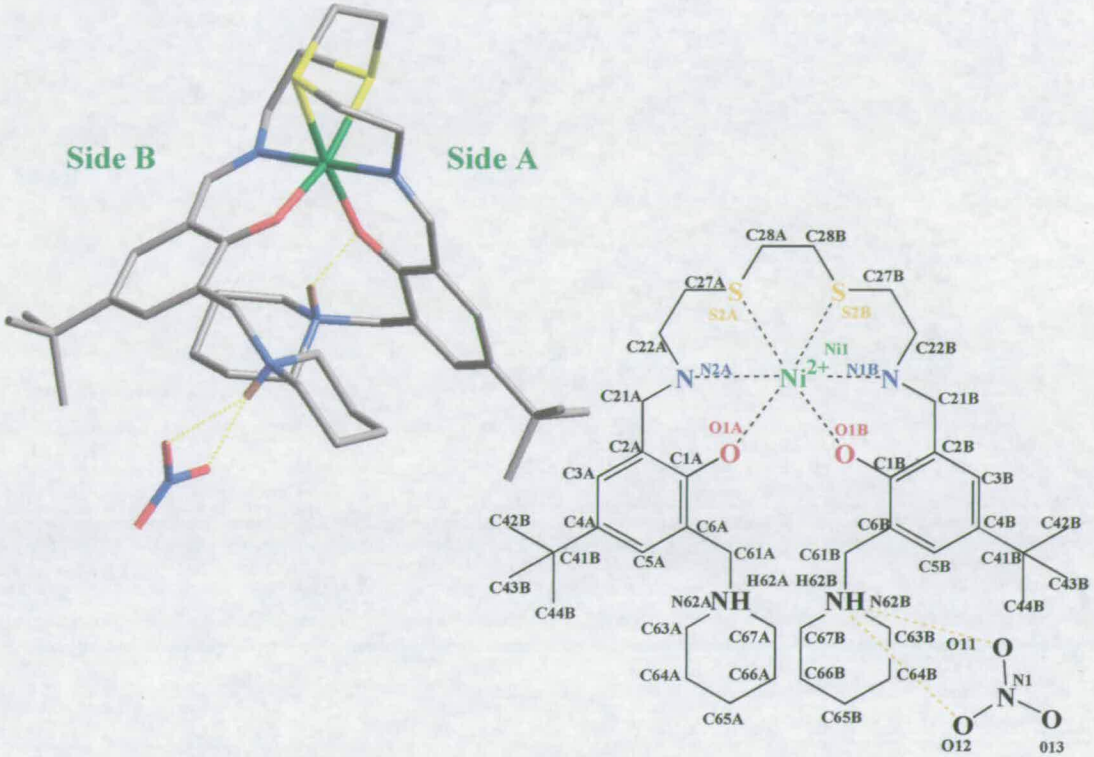

Figure 2.30 The x-ray structure of $[Ni(9)(NO_3)]^+$ and numbering scheme

Single crystals of $[Ni(9)(NO_3)_2]$ suitable for X-ray structure determination were grown from dichloromethane with hexane as the counter solvent. There is one molecule of the complex in the asymmetric unit. Both the piperidine arms face into the cavity showing that rearrangement of the piperidine rings (see section 3.5.6.1) can allow the formation of a cavity to bind sulfate in a 1:1:1 monocationic package. The structure shows only one nitrate H-bonded to the protonated piperidine nitrogen of side B (Figure 2.30). The second piperidinium proton (side A) forms a hydrogen bond to the phenolate oxygen atom on the same arm. The second nitrate is not associated with the complex.

Table 2.10 Hydrogen bond distances to the nitrate anion from the piperidinium hydrogen and the inter-hydrogen bond length to the phenolare oxygen in [Ni(**9**)$(NO_3)_2$] (Å)

	X···O (Å)
O(1)···H(62A)-N(62A)	2.677
O(11)···H(62B)-N(62B)	3.063
O(12)···H(62B)-N(62B)	2.816

Table 2.11 Hydrogen bonded distances (Å) to the nitrate anions in [Ni(**11**)$(NO_3)_2$]. See Figure 2.18 and Figure 2.30 for numbering scheme.

	N···O (Å)
O(11)···H(62A)-N(62A)	3.030
O(12)···H(62A)-N(62A)	2.887
O(21)···H(62B)-N(62B)	3.052
O(22)·· H(62B)-N(62B)	2.798

When comparing the length of the bifurcated hydrogen bond to the nitrate to those measured in the crystal structure of [Ni(**9**)$(NO_3)_2$] (Table 2.11) we find that they are very similar. This is also the case when we compare the inter-hydrogen bond between the piperidium proton and the phenolate oxygen atom in the structure and those seen in the trifurcated ligand in Figure 2.26 [N-H···O = 2.04(1) and 2.67(1) Å].

The two planes ONSNi and ObenzeneN as defined for the the complexes with ligand **11** are shown in Table 2.12. The difference between ligand **9** and **11** is the removal of the bridging benzene between the imine nitrogen and backbone sulfur. Hence removal of the NbenzeneS plane.

Table 2.12 Planes ONSNi, ObenzeneN and NbenzeneS in crystal structure of [Ni(**9**)$(NO_3)_2$]

Plane	**maximum deviation from the least squares plane Å**		**average deviation from the least squares plane Å**	
	Side A	Side B	Side A	Side B
ONSNi	0.0175 O(1A) -0.0304 Ni(1)	0.1367 Ni(1) -0.0791 O(1B)	0.0160	0.0718
ObenzeneN	O.0391 C(6A) -0.0482 O(1A)	0.0715 N(2B) -0.0477 C(2B)	0.0219	0.0297

Side "B" is a lot flatter than side "A" as shown by Table 2.12. The phenolic ring is almost in the same plane as the donor atoms and the nickel with only a 0.4° angle.

Table 2.13 Angles between the planes ONSNi and ObenzeneN (°)

Side	Angle between planes ONSNi and ObenzeneN (°)
Side A	10.1
Side B	0.4

Even though side "B" is flatter when we compare the angle between the two planes (Table 2.14) ONNi and NSNi with in the ONSNi plane we find that the coordination atoms in side "A" are flatter as required for isomer A (Figure 2.15). The H-bonding between the piperidine and the phenolic oxygen pulls the phenolic ring further out of the plane (10.1°) which causes the ONSNi plane to be flatter as shown in Table 2.14.

This is also seen in Table 2.15 where the O(1A)-Ni(1)-S(2A) angle is 174.50° compared to O(1B)-Ni(1)-S(2B) is 168.04°.

Table 2.14 Angles between the planes ONNi and NSNi (°)

Side	Angle between planes ONNi and NSNi (°)
Side A	2.3
Side B	5.2

Table 2.15 Bond length (Å) and angles (°) in the co-ordination spheres of the nickel nitrate complexes [Ni(**9**)$(NO_3)_2$] and [Ni(**11**)$(NO_3)_2$]

	[Ni(**9**)$(NO_3)_2$]	[Ni(**11**)$(NO_3)_2$]
Ni(1)-S(2)	2.4692(13)	2.408(18)
	2.4649(13)	2.404(15)
Ni(1)-N(2)	2.038(4)	2.039(4)
	2.020(4)	2.049(4)
Ni(1)-O(1)	2.029(3)	1.969(3)
	2.001(3)	1.980(3)
O(1A)-Ni(1)-O(1B)	86.28(13)	92.78(15)
O(1A)-Ni(1)-N(2B)	89.40(14)	89.59(15)
O(1B)-Ni(1)-N(2B)	90.60(14)	92.60(14)
O(1A)-Ni(1)-N(2A)	90.49(14)	93.25(14)
O(1B)-Ni(1)-N(2A)	89.46(14)	88.14(14)
N(2B)-Ni(1)-N(2A)	179.88(17)	177.03(15)
O(1A)-Ni(1)-S(2B)	94.20(10)	87.77(11)
O(1B)-Ni(1)-S(2B)	168.04(10)	177.80(10)
N(2B)-Ni(1)-S(2B)	83.73(11)	85.27(11)
N(2A)-Ni(1)-S(2B)	96.23(11)	93.95(11)
O(1A)-Ni(1)-S(2A)	174.50(11)	175.72(11)
O(1B)-Ni(1)-S(2A)	86.02(10)	91.01(11)
N(2B)-Ni(1)-S(2A)	95.58(11)	92.23(12)
N(2A)-Ni(1)-S(2A)	84.53(11)	84.88(12)
S(2B)-Ni(1)-S(2A)	84.06(4)	88.52(5)

The removal of the bridginging benzene greatly effects the coordination sphere of the nickel. The Ni-S and Ni-O bonds are longer in the [Ni(**9**)$(NO_3)_2$] complex. The removal of the benzene also causes a greater flexibility in the backbone and therefore the angle between the two sulfur atoms S(2)-Ni(1)-S(2) is smaller for the [Ni(**9**)$(NO_3)_2$] complex. This is turn cause the angle between the two phenolate oxygen atoms to be smaller in the [Ni(**9**)$(NO_3)_2$] complex (Table 2.15).

2.6.1.7 X-ray structure of $[Ni(1)(C_2H_3O_2)_2]$

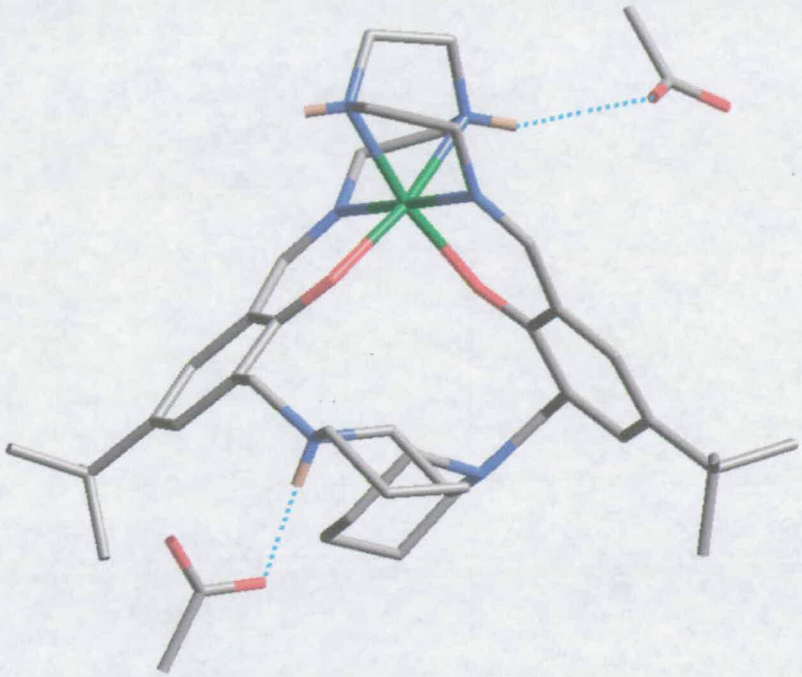

Figure 2.31 The X-ray structure of $[Ni(\mathbf{1})(C_2H_3O_2)_2]$

Single crystals of $[Ni(\mathbf{1})(C_2H_3O_2)_2]$ suitable for X-ray structure determination were grown from evaporation from hexane. There is one molecule of the complex in the asymmetric unit (Figure 2.31). This structure is unique when compared to all the other complexes formed with $Ni(C_2H_3O_2)_2$ as the acetates are hydrogen bound to the complex instead of being removed as acetic acid (see section 2.6). This is due to an alteration in the method of formation. Instead of a complexation reaction between the ligand and the nickel salt as for all the other complexes, a template reaction was used, see section 3.2.3.7. The Schiff base reaction has resulted in the complexation of the nickel to the six donor atoms (four nitrogen and two oxygen) to form the lowest energy isomer (A, Figure 2.15) as seen for all the other crystal structures.

As for the crystal structure of $[Ni(\mathbf{9})(NO_3)_2]$ both the piperidine arms are facing into the cavity. This indicates that removal of the bridging benzene in the backbone of the ligand promotes the formation of a cavity for sulfate binding. The quaternary protons are facing away from each other but rotation of the C(61)-N(62) would result in the hydrogens facing into the cavity to hydrogen bond to the sulfate. The nitrogen

separation in structures [Ni(**1**)$(C_2H_3O_2)_2$] and [Ni(**9**)$(NO_3)_2$] are 5.996 Å and 5.804 Å respectively. This is smaller than the measured N-N separation for the $NiSO_4$ complexes in section 2.6.1.2 where the sulfate acts as a crosslinker. But is greater than the tetradentate nickel sulfate structure in chapter 1 Figure 1.34 where the sulfate is bound below a cavity formed by two morphiline rings. Therefore a sulfate could be coordinated just out of a cavity with ligands **9** and **1**.

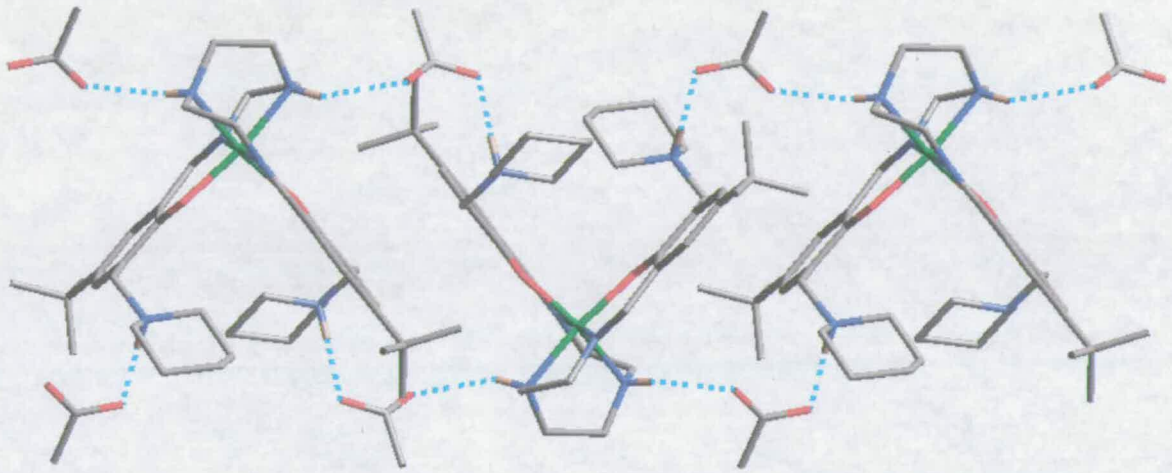

Figure 2.32 Diagram showing acetate anions acting as intermolecular crosslinkers via single hydrogen bonds

As in previous crystal structures the anion (acetate) is acting as an intermolecular crosslinker via hydrogen bonding. Each nickel complex is contacted to its two neighbouring nickel complexes via four hydrogen bonds. Between each complex there are two bridging acetates anions. Each acetate anion is hydrogen bonded between the piperidinium hydrogen of one complex and the amine hydrogen in the backbone of another complex. This forms an up-down complex chain as seen in Figure 2.32.

The two planes as defined in section 2.5.6.5 are shown in Table 2.16.

Table 2.16 Planes ONSNi and ObenzeneN in the crystal structure of [Ni(**1**)($C_2H_3O_2$)$_2$]

Plane	Maximum deviation from the least squares plane Å		Average deviation from the least squares plane Å	
	Side A	Side B	Side A	Side B
ONSNi	0.0400 O(1A) -0.0732 Ni(1)	0.0457 O(1B) -0.0836 Ni (1)	0.0394	0.0448
ObenzeneN	0.0227 C(5A) -0.0201 O(1A)	0.0115 C(3B) -0.0210 C(21B)	0.0158	0.0084

Both sides are relatively flat when compared to the previous benzene bridged complexes formed with ligand 14 (Table 2.17).

Table 2.17 Angles between the planes ONNNi and ObenzeneN (°)

Side	Angle between planes ONNNi and ObenzeneN (°)
Side A	6.6
Side B	8.6

When we compare the coordination sphere for complex [Ni(**1**)($C_2H_3O_2$)$_2$] (Table 2.18) with the previous complexes (Table 2.9 and Table 2.15) we see that as discussed in section 3.5.6.5 the removal of the bridging benzene greatly alters the coordination sphere around the nickel.

Table 2.18 Bond length (Å) and angles (°) in the co-ordination spheres of [Ni(**1**)$(C_2H_3O_2)_2$]

	[Ni(**1**)$(C_2H_3O_2)_2$]
Ni1-N3	2.122(2), 2.119(2)
Ni1-N2	2.007(2), 2.018(2)
Ni1-O1	2.0241(17), 2.0242(17)
O1A-Ni1-O1B	94.90(7)
O1A-Ni1-N2B	91.73(8)
O1B-Ni1-N2B	89.36(8)
O1A-Ni1-N2A	89.77(8)
O1B-Ni1-N2A	90.23(8)
N2B-Ni1-N2A	178.47(9)
O1A-Ni1-N3B	92.16(8)
O1B-Ni1-N3B	169.65(8)
N2B-Ni1-N3B	82.85(9)
N2A-Ni1-N3B	97.38(9)
O1A-Ni1-N3A	170.36(8)
O1B-Ni1-N3A	91.12(8)
N2B-Ni1-N3A	95.87(9)
N2A-Ni1-N3A	82.67(9)
N3B-Ni1-N3A	82.94(8)

2.7 Solvent extraction

The solvent extraction experiments carried out involved an organic solution of the ligand together with the same volume of an aqueous metal salt solution being stirred (Figure 2.33). After stirring the two phases were separated and the amount of nickel and sulfate extracted into the organic phases was measured.

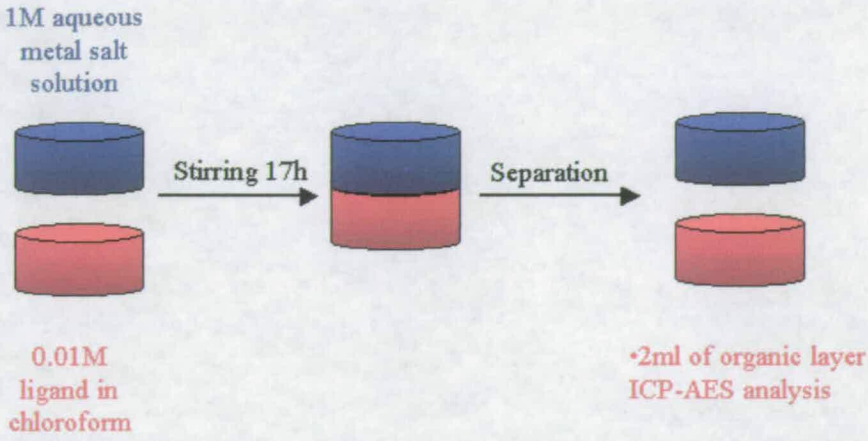

Figure 2.33 Schematic representation of the extraction

2.7.1 Metal cation analysis

The investigation into the concentration of metal extracted is not easy but there are various methods available and have been used. Until the 1940's most analysis was done classically.[25] Classic analysis is the collective term used to describe an analysis whose measurement step is a gravimetric or titrimetric step determination. Since the 1940's instrumental analysis[25] has become more important because of the increasing demands for sensitivity, speed and economy, so that today instrumental analysis has assumed the major role in the analytical laboratory. Instrumental analysis is the collective term used for an analysis whose measurement step involves an instrument.

In both classical and instrumental analysis, one or more preparatory steps almost always precede the final determination. Therefore the precision and accuracy of the analytical result are no better than the collective precision and accuracy of all the preparatory steps. Due to this all water used is of analytical quality and all the glassware is thoroughly washed to ensure no contamination.

The types of experiments that have been previously used include ion selective electrode (ISE), cation exchange column, atomic absorption (AA), inductively coupled plasma atomic emission spectroscopy (ICP-AES) or gravimetric analysis.

An ion selective electrode is not available for use with every metal studied. It also uses a PVC membrane which is not suitable for organic analysis. (See chapter 5 for a discussion on how an ion selective electrode works.)

A cation exchange column is used with aqueous media and could be used to measure the difference in the aqueous metal concentration before and after extraction. This method would involve many titrations which would be very time consuming.

Both AA and ICP directly measure the amount of metal extracted into the organic phase. For ICP the emission of light by the excited atoms or ions of the sample are measured, (see section 2.7.3 for details.) For AA the sample solution is continuously added into a flame, or a small volume of sample is placed in a graphite furnace. The solvent and volatile sample components are driven off, and the analyte is converted to gas-phase atoms. The absorption of light by these atoms in their ground state is then measured. The advantage of AA over ICP is that the AA instrumentation is relatively simple and inexpensive, but as we have an ICP machine in the department this can be over looked. Also ICP has the disadvantage of additive interferences (overlaps of emission lines of different atoms). For both techniques any solids must normally be dissolved before analysis, hence an organic solvent that dissolves the extracted complex and will also burn in the machine has to be used. The advantages of ICP over AA are that even though both can detect virtually all metals and many metalloids only ICP can detect some non-metals that emit in the vacuum-ultraviolet spectral region. But the main advantage of ICP is that it can be used for multiple element analysis with determination of over 70 elements in virtually any sample in less than two minutes.

Finally gravimetric analysis can be used to determine the mass of the metal extracted through the formation of an insoluble product (see section 5.2).

2.7.2 Anion analysis

As with cation analysis there are various methods associated with anion analysis; these include, gravimetric analysis, anion exchange column, ISE, and ICP, (see section 5.2 for a discussion of techniques).

As ICP can be used for multi elemental analysis the concentration of metal and sulfur extracted can simultaneously be measured by ICP. Therefore this technique was chosen.

2.7.3 Inductively Coupled Plasma Atomic Emission Spectroscopy

ICP-AES is a spectroscopic method for elemental analysis. It dissociates a sample into its constituent atoms and ions and causes them to emit light at a characteristic wavelength by exciting them into a higher energy level. This is accomplished by the use of an inductively coupled plasma source.

The plasma acts as a sample cell and is formed by argon gas flowing through a radio frequency where it is kept in a state of partial ionisation. When the sample flows into the plasma (in an aerosol form) the atoms present are excited from the lower energy level to a higher energy state. Each atom has a number of possible excited states. The lifetime of these excited atoms or ions is brief and when they return to the ground state they emit light (energy) of a characteristic wavelengths which corresponds to the energy difference between the excited state and ground state. The emission of radiation occurs in near ultra violet (180-300 nm) and visible (300-770 nm) regions of the electromagnetic spectrum. A monochromator can separate specific wavelength of interest and a detector is used to measure the emitted light. This information can be used to calculate the concentration of that particular element in the sample.

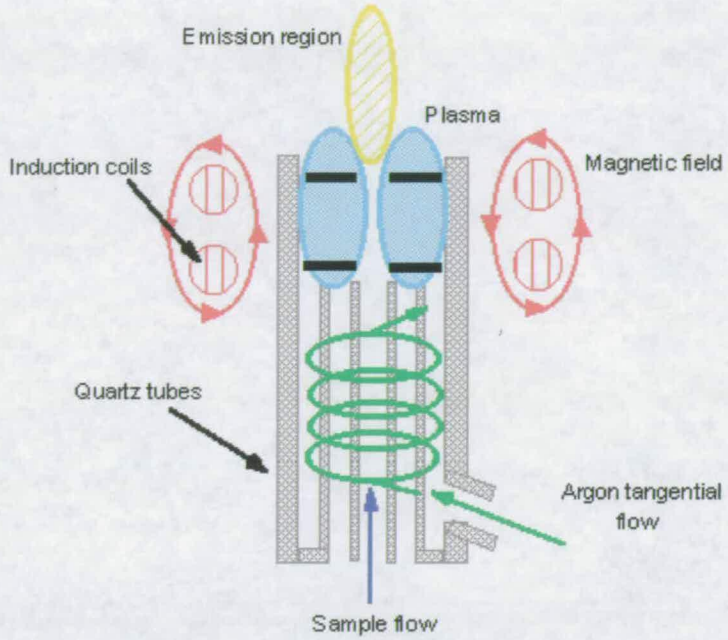

Figure 2.34 Schematic representation of an ICP torch and plasma

Before analysis the ICP-AES spectrophotometer was calibrated using freshly prepared dilute organic (butan-1-ol) nickel and sulfur standards (see Figure 2.35 for nickel calibration curve after standardisation).

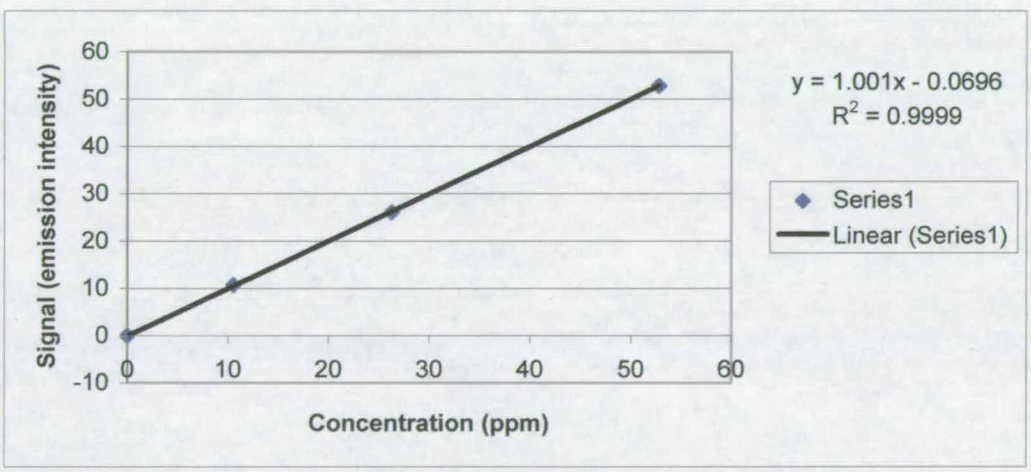

Figure 2.35 Calibration curve for nickel

All data were interpreted using thermospec/CID IRIS software. Wavelengths used to calibrate concentrations were free of spectral interferences, see Table 2.19.

Table 2.19 Wavelengths used to calibrate extraction concentrations for nickel and sulfur

Element	Sensitivity (ppb)	Emission Wavelengths/Y (nm)	Relative Intensity
Nickel	4	221.647, 231.604, 232.003*, 341.476*, 352.454*	116, 111, 112, 076, 074
Sulfur	2	180.731,* 180.731,* 180.731,* 182.034,* 182.034,* 182.034*	142, 143, 144, 141, 142, 143

The * indicates the wavelengths that were used.

2.7.4 Extraction results

No nickel or sulfur uptake was detected by ICP-AES, (see Appendix I, Figure 1) for ligands **4**, **6**, **8**, **10** and **12**. This was also confirmed by that fact that no colour changes were observed during the experiment. The results show that there are problems in transferring the nickel and sulfur in to the organic phases. This could be due to slow kinetics or unfavourable thermodynamics and hence these ligands could never be used as part of an industrial process for nickel sulfate recovery.

2.8 Conclusions

The aim of this chapter was to design ditopic sexadentate ligands for the extraction of high spin nickel and sulfate.

Five classes of ligands, one piperazine based, two bis(ether) based and two bis(thioether) based, have been successfully designed, synthesised and characterised. The ligands have been used to form a range of metal salt complexes with various nickel(II) salts (SO_4^{2-}, NO_3^- and Cl^-) and neutral "nickel-only" complexes, with nickel(II) acetate.

X-ray crystallography of the complexes show the nickel bound in the desired isomeric form and it can be envisaged that the piperidine rings could form a binding cavity thus allowing encapsulation of a sulfate anion.

Solvent extraction studies showed no nickel uptake, which could be due to constraints in the cation binding site. Therefore by "opening up" the nickel binding site may help to increase the ability of these ligands to extract high spin nickel(II).

2.9 Experimental

2.9.1 Instrumentation

Elemental analysis was performed on a Perkin Elmer 2400 elemental analyser or a Carlo Erba 1108 Elemental analyser. The infra-red spectra were obtained on a Jasco FT/IR 410 Fourier Transform IR spectrometer as potassium bromide discs. ^{1}H and ^{13}C NMR spectra were run on a Bruker AC250 spectrometers. Chemical shifts (δ) are reported in parts per million (ppm) relative to residual solvent protons as internal standards. Fast Atom Bombardment (FAB) mass spectra were obtained on a Kratos MS50TC spectrometer. Electronic absorption spectroscopy was performed on a Perkin Elmer Lambda 900 UV/VIS/NIR spectrometer. Inductively coupled plasma optical emission spectroscopy (ICP-OES) analysis was performed on a Thermo Jarrell Ash IRIS ICP-OES spectrometer.

2.9.2 Solvent and reagent pre-treatment

All reagents and solvents were commercially available (Acros or Aldrich) and were used as received. Solvents used for analytical purposes (NMR, MS, ICP) were of spectroscopic grade. ICP AES standards were purchased from Alfa Asar.

2.9.3 Ligands and their precursors

5-Alkyl-3-dialkylaminomethyl-2hydroxybenzadehydes

The 2-hydroxy-5-alkylbenzaldehydes and ethoxy-N-piperidinylmethane were prepared by the methods described by Levin *et. al.*[10] and Fenton *et. al.*[11] Ethoxy-N-dihexylaminomethane, 2-hydroxy-3-(piperidinyl-4-ylmethyl)-5-*tert*-

butylbenzaldehyde and 5-Alkyl-3-dialkylaminomethyl-2hydroxybnzadehydes were prepared by an adaptation of the method of Fenton *et. al.*[11] as follows.

Ethoxy-N-dihexylaminomethane

A suspension of paraformaldehyde (9.891 g, 0.33 mol) and K_2CO_3 (7.0 g) was cooled to 0 °C. Dihexylamine (160 ml, 0.33 mol) was added dropwise, with stirring, over 30 minutes. The suspension was then stirred for 5 days, filtered and the ethanol removed. The product was purified by distillation under reduced pressure (106 °C, 0.7 Torr) to give a colourless oil (51.94 g, 65%). (Found C, 74.8%: H, 13.6: N, 5.8. Calc. For $C_{15}H_{33}NO$: C, 74.12: H, 13.86: N, 5.83.%). ^{1}H NMR ($CDCl_3$): δ 0.79-0.84 (m, 9H, CH_3), δ 1.09-1.44 (m, 8H, CH_2), δ2.34 (t, 4H, N-CH_2), δ3.38 (d, 4H, O-CH_2), δ4.10 (s, 4H, N-CH_2-O); ^{13}C NMR ($CDCl_3$): δ 23.11-32.25 (CH_2), δ 52.42 (N-CH_2), δ 63.67 (CH_2-O), δ 85.69(N-CH_2-O). EIMS *m/z* 198 (MH^+-OEt, 100%).

2-Hydroxy-3-(piperidinyl-4-ylmethyl)-5-*tert*-butylbenzaldehyde [HPTB]

A mixture of 5-*tert*-butylbenzaldehyde (15 g, 0.1 mol) and ethoxy-*N*-piperidinylmethane (15.7 g, 0.1 mol) in acetonitrile (200 cm^3) was heated to reflux under a nitrogen atmosphere for 6 days. After cooling to room temperature the solvent was removed *in vacuo* to yield a yellow solid. The product was dissolved in CH_2Cl_2 (150 cm^3) and extracted with water (3 x 60 cm^3). The organic fraction was evaporated *in vacuo* and dried under vacuum (22.95 g, 83%). m.p. 79-82 °C. (Found C, 74.06: H, 7.51: N, 5.49. Calc. For $C_{17}H_{25}NO_2$ C, 74.14: H, 9.15: N, 5.09%). ^{1}H NMR ($CDCl_3$): δ 1.27 (s, 9H, CH_3), δ 1.39 (m, 2H, CH_2(pip)), δ 1.65 (d, 4H, CH_2(pip)), δ 2.53 (bp, 2H, CH_2(pip)), δ 3.69 (s, 2H, CH_2), δ 7.05-7.39 (m, 8H, Ar-H), δ 7.64 (s, 1H, OCH), δ 10.41 (s, 1H, OH). ^{13}C NMR ($CDCl_3$): δ 23.8 (CH_2 (pip)), δ 25.6 (CH_2(pip)), δ 31.2 (C($\underline{CH_3}$)$_3$), δ 34.0 ($\underline{C}$(CH_3)$_3$), δ 53.8 (CH_2 (pip)), δ 61.3 (NCH_2), δ 122.3 (Ar-C), δ 122.7 (Ar-C), δ 123.8 (Ar-CH), δ 132.2 (Ar-CH), δ 141.4 (Ar-C), δ 159.8 (Ar-C), δ 191.0 (C=O). MS (FAB, NOBA) *mz* 276 (95.7%).

2-Hydroxy-3-(dihexylaminomethyl)-5-*tert*-butylbenzaldehyde [HDTB]

Using the method for **HPTB,** but using 2-hydroxy-5-alkylbenzaldehyde (38.05 g, 0.21 mol), ethoxy-methyl-N-dihexyl (51.94 g, 0.21 mol) and refluxing for 10 days

produced 89 g of crude product. 9.6 g of the product was purified by a column chromatography (silica, hexane: ethyl acetate 20.1) to yield a yellow oil (6.7 g, 70 %). (Found C, 76.65: H, 10.65: N, 3.36. Calc. For $C_{24}H_{41}NO_2$ C, 76.75: H, 11.00: N, 3.73%). ^{1}H NMR ($CDCl_3$, 250 MHz): δ 0.91 (t, 6H, CH_3(hexyl)), δ 1.30 (s, 9H, $C(CH_3)_3$), δ 1.19-1.33 (m, 12H, CH_2 (hexyl)), δ 1.56 (m, 4H, $NCH_2\underline{CH_2}$ (hexyl)), δ 2.76 (t, 4H, NCH_2 (hexyl)), δ 3.80 (s, 2H, $ArCH_2N$), δ 7.12 (d, 2H, ArCH), δ 7.65 (d, H, ArCH), δ 10.46 (s, H, CHO). ^{13}C NMR ($CDCl_3$): δ 14.3 (CH_3 (hexyl)), δ 22.9 ($NCH_2CH_2CH_2CH_2\underline{CH_2}$ (hexyl)), δ 26.7 ($NCH_2CH_2CH_2\underline{CH_2}$ (hexyl)), δ 27.1 ($NCH_2CH_2\underline{CH_2}$ (hexyl)), δ 31.4 ($C(\underline{CH_3})_3$), δ 31.8 ($NCH_2\underline{CH_2}$ (hexyl)), δ 33.9 ($\underline{C}(CH_3)_3$), δ 53.9 ($N\underline{CH_2}$ (hexyl)), δ 58.8 ($ArCH_2N$), δ 122.4 (Ar-C), δ 123.9 (Ar-CH), δ 140.5 (Ar-C), δ 132.5 (Ar-CH), δ 141.7 (Ar-C), δ 160.5 (Ar-C), δ 191.7 (CHO). MS (FAB, NOBA) *mz* 376 (MH^+, 72.4%).

Attempted synthesis of ligand 1

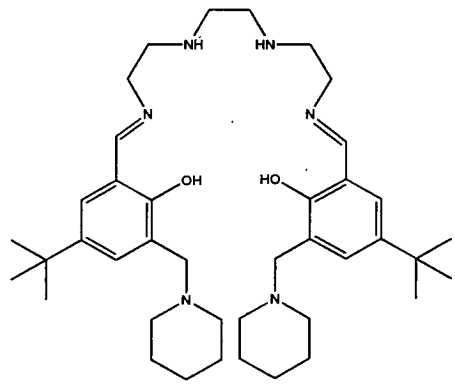

To a stirred solution of **HPTB** (2.78 g, 1.00 mmol) in diethylether (20 cm^3) was added a solution of triethylenetetramine (**triene**) (0.49 g, 0.30 mmol) in ethanol (15 cm^3). The yellow solution was stirred overnight and concentrated *in-vacuo* to yield a cream coloured solid, which was recrystallised from hexane. MS (FAB, NOBA) *m/z* 919 (MH^+, 100%). Procedure stopped as unable to purify.

Attempted synthesis of ligand 2

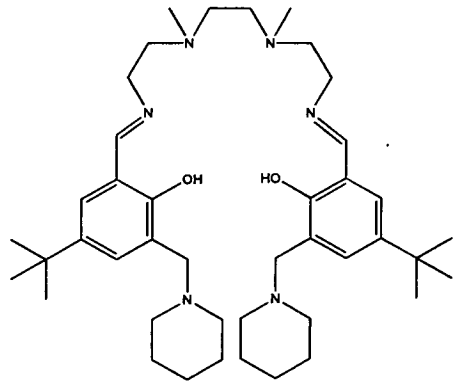

1,2-Ethanediamine,N,N'-bis(2-aminoethyl)-N,N'dimethyl, EBD

N,N'-Dimethyl-1,2,-diaminetane (8.64 g, 0.098 mol), was added dropwise to a N-(2-bromoethyl)phthalimide (50 g, 0.197 mol) whilst stirring. The solution was heated at 109 °C under nitrogen for 24 hrs to produce an orange glass. Water was added to produce a white precipitate (unreacted N-(2-bromoethyl)phthalimide) which was removed by filtration. The filtrate was concentrated in-*vacouo* and di-ethyl-ether added to yield a white hydroscopic solid (impure 4,7-dimethyl-1,4,7,10-tetra-azadeconediphthalimide) which was stored under nitrogen due to being very hydroscopic. The impure white solid (22.98 g, 0.039 mol) was suspended in an ethanol (350 cm^3) and water (150 cm^3) mixture. The suspension was heated to reflux and hydrazine monohydrate (8.0 g, 0.16 mol) was added dropwise, dissolving the white precipitate, to give a orange solution. The solution was refluxed for 20 hrs at 110 °C followed by concentration in-*vacouo*. Concentrated HCl (30 cm^3) was added to the solution which immediately produced a fine white precipitated which was removed. The yellow filtrate was concentrated *in-vacuo* to yield a dark orange solid. Procedure stopped at this point as unable to purify product.

Synthesis of BOC protected 1,2-Ethanediamine,N,N'-bis(2-aminoethyl)-N,N'dimethyl intermediate

(2-chloro-ethyl)carbamic acid *tert*-butyl ester

2-Chloroethylaminehydrochloride, (27.1 g, 0.23 mol), $(BOC)_2O$, (50.34 g, 0.23 mol), and triethylamine (37 cm^3) were heated at reflux in MeOH (413 cm^3) under nitrogen for 150 mins. The solvent was removed to give a white solid. 2 M HCl was added

and the product was extracted with (2x100 cm^3) EtOAc, washed with aq $NaHCO_3$ (2x100 cm^3) brine (2x100 cm^3) and dried over $MgSO_4$. After removal of the solvent a colourless oil was produced. The product was distilled at 66 °C, 1.5 Torr. to give a colourless oil (21.6 g, 52%). Found C, 44.76: H, 7.38: N, 7.76. Calc. for $C_7H_{14}ClNO_2$: C, 46.80: H, 7.89: N, 7.80%. ^1H NMR ($CDCl_3$, 250 MHz): δ 1.34 (s, 9H, CH_3), δ 3.29-3.56 (m, 4H, $ClCH_2CH_2NH$), δ 5.21 (bp, 4H, NCH_2). MS (FAB, NOBA) *m/z* 180 (MH^+ 6%).

BOC protected 1,2-Ethanediamine,N,N'-bis(2-aminoethyl)-N,N'dimethyl intermediate

N, N'Dimethyl-1,2-diaminoethane (3.1 g, 0.036 mol) was added to (2-chloro-ethyl)-carbamic acid tert-butylester (12.8 g, 0.071 mol) to produce a viscous yellow oil. An ethanoic solution (50 cm^3) of $NaHCO_3$ (9 g, 0.11 mol) was added slowly and then the solution was heated to reflux at 100 °C for 15 hrs. On cooling the dichloromethane was added to the oily yellow product and this was then filtered to remove a white precipitate. The solvent was removed by rotary evaporation, and the product was distilled at 100 °C 0.2 Torr to give a clear oil (0.28 g, 2%) ^1H NMR ($CDCl_3$, 250 MHz): δ 1.38 (s, 18H, $C(CH_3)$), δ 2.17 (s, 6H, NCH_3), δ 2.34 (t, 4H, NCH_2) δ 2.43 (bp, 2H, NH) δ 2.68 (t, 4H, NCH_2) δ 3.15 (t, 4H, NCH_2). MS (FAB, NOBA) *m/z* 375 (MH^+, 38.2%).

Ligand 3

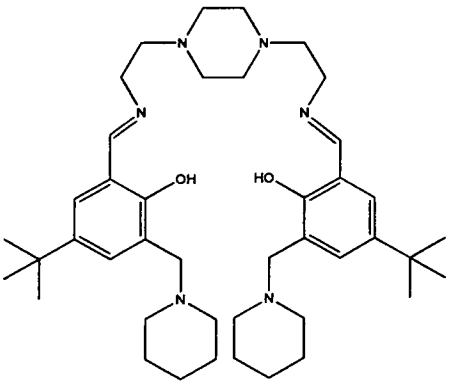

1,4-Diphthalimido-3,6-diazoctane 1,4-piperazinediethanamine, dihydrobromide

N-(2-Bromoethyl)phthalimide (63.9 g, 0.25 mol) and piperazine (10.83 g, 0125 mol) was added together and heated for 15 hrs under nitrogen at 125 °C. Once cooled the solid was ground up to a fine powder and heated to reflux in ethanol (10 ml) for 2 hrs. The solution was then hot filtered to yield a white solid (41.28 g, 56%). Found C, 47.22: H, 4.53: N, 9.41 Calc. For $C_{14}H_{12}N_2O_4$: C, 48.50: H, 4.41: N, 9.43%. ^{1}H NMR (D_2O, 250 MHz): δ 2.87 (bp, 8H, CH_2 (pipa)), δ 3.19 (t, 4H, $NCH_2\underline{CH_2}N_{pipa}$), δ 3.80 (t, 4H, $N\underline{CH_2}CH_2N_{pipa}$), δ 7.77-7.81 (m, 8H, Ar-CH). (FAB, NOBA) *m/z* 594 (MH^+-2HBr, 35.6%).

1,4-Piperazinediethanamine, dihydrochloride

1,4-Diphthalimido-3,6-diazoctane 1,4-piperazinediethanamine, dihydrobromide (37.91 g, 74.8 mmol) was suspended in an ethanol (400 cm^3) and water (200 cm^3) mixture. The suspension was heated to reflux and hydrazine monohydrate (15.4 g, 0.31 mol) was added dropwise, dissolving the white precipitate, to give a yellow solution. The solution was refluxed for 20 hrs at 100 °C. The ethanol was removed to give a yellow solution that was filtered to remove a white precipitate. Concentrated HCl (29.4 g, 0.2984 mol) was added to the yellow solution which immediately produced a fine white precipitate which was removed. The yellow filtrate was concentrated *in-vacuo* to yield a pale yellow solid. The solid was refluxed in ethanol and hot filtered to remove the hydrazine salt. The filtrate was concentrated *in-vacuo* to yield a white solid (13.32 g, 56%). Found C, 26.61: H, 5.83: N, 15.20. Calc. For $C_8H_{24}Cl_2N_4$: C, 30.20: H, 7.60: N, 17.61%. ^{1}H NMR

($CDCl_3$, 250 MHz): δ 2.36 (s, 8H, CH_2 (pipa)), δ 3.48 (s, 4H, $NCH_2\underline{CH_2}N_{pipa}$); δ 3.48 (s, 4H, $N\underline{CH_2}CH_2N_{pipa}$). (FAB, NOBA) *m/z* 318 (MH^+-2HCl, 25.8%).

Ligand 3

To a stirred solution of **[HPTB]** (0.9 g, 3.27 mmol) in diethylether (10 cm^3) was added a solution of 1,4-piperazinediethanamine, tetrahydrochloride (0.508 g, 1.6 mmol) in 0.125 M NaOH solution (30 cm^3). The phases were separated and concentrated *in-vacuo*. The starting material was recrystallised from hexane and ether to yield a yellow solid (1.83 g, 88%). Found: C, 73.43; H, 9.68; N, 12.23. Calc. for $C_{42}H_{66}N_6O_2$: C, 73.61; H, 9.88; N, 12.38%. ^1H NMR ($CDCl_3$, 250 MHz): δ 1.40 (m, 18H, CH_3 ($C(CH_3)$), δ 1.54 (bp, 4H, $NCH_2CH_2\underline{CH_2}$ (pip)), δ 1.69 (bp, 8H, $NCH_2\underline{CH_2}CH_2$ (pip)), δ 2.39 (s, 8H, CH_2 (pipa)), δ 2.56 (bp, 8H, $N\underline{CH_2}CH_2CH_2$ (pip)), δ 3.475 (s, 4H, $NCH_2\underline{CH_2}N_{pipa}$); δ 3.475 (s, 4H, $N\underline{CH_2}CH_2N_{pipa}$), δ 3.68 (s, 4H, $ArCH_2N$), δ 7.31 (s, 2H, Ar-CH), δ 7.47 (s, 2H, Ar-CH), δ 8.52 (s, 2H, N=CH). ^{13}C NMR ($CDCl_3$): δ 24.2 ($NCH_2CH_2\underline{CH_2}$ (pip)), δ 25.8 ($NCH_2\underline{CH_2}CH_2$ (pip)), δ 31.3 (($C(\underline{CH_3})_3$), δ 33.8 ($\underline{C}(CH_3)_3$), δ 54.2 ($N\underline{CH_2}CH_2CH_2$ (pip)), δ 56.2 (CH_2 (pipa)) δ 57.3 ($NCH_2\underline{CH_2}N_{pipa}$), δ 57.8 ($N\underline{CH_2}CH_2N_{pipa}$), δ 59.9 ($ArCH_2N$), δ 118.0 (Ar-C), δ 124.5 (Ar-C)), δ 125.8 (Ar-CH), δ 130.5 (Ar-CH), δ 140.3 (Ar-C), δ 157.2 (Ar-C), δ 165.0 (C=N). MS (FAB, NOBA) *m/z* 687 (MH^+, 53.2%).

Ligand 4

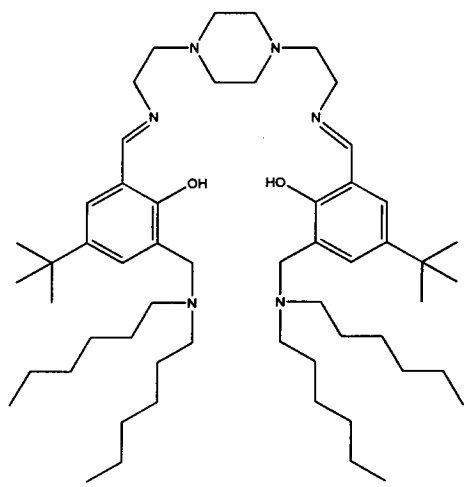

Using the method for ligand **3**, but using piperazinediethanamine dihydrochloride (0.936, 2.40 mmol) and **[HDTB]** (1.84 g, 4.90 mmol) produced a viscous orange oil

(1.90 g, 96 %). This was used without further purification. Found: C, 75.50; H, 10.48; N, 10.16. Calc. for $C_{52}H_{86}N_6O_2$: C, 75.36; H, 10.43; N, 10.28%. ^{1}H NMR ($CDCl_3$, 250 MHz): δ 0.79 (t, 12H, CH_3 (hexyl)), δ 1.23 (s, 18H, $C(CH_3)_3$), δ 1.19-1.23 (m, 24H, CH_2 (hexyl)), δ 1.44 (bp, 8H, $NCH_2\underline{CH_2}$ (hexyl)), δ 2.39 (s, 8H, CH_2 (pipa)), δ 2.41 (t, 8H, NCH_2 (hexyl)), δ 3.475 (s, 4H, $NCH_2\underline{CH_2}N_{pipa}$); δ 3.475 (s, 4H, $N\underline{CH_2}CH_2N_{pipa}$), δ 3.60 (s, 4H, $ArCH_2N$); δ 7.12 (m, 2H, ArCH), δ 7.45 (m, 2H, ArCH), δ 8.34 (s, 2H, N=CH), δ 10.35 (s, 2H, OH). ^{13}C NMR ($CDCl_3$): δ 14.0 (CH_3 (hexyl)), δ 22.6 ($NCH_2CH_2CH_2CH_2\underline{CH_2}$ (hexyl)), δ 26.7 ($NCH_2CH_2CH_2\underline{CH_2}$ (hexyl)), δ 27.1 ($NCH_2CH_2\underline{CH_2}$ (hexyl)), δ 31.3 ($C(\underline{CH_3})_3$), δ 31.7 ($NCH_2\underline{CH_2}$ (hexyl)), δ 33.8 ($\underline{C}(CH_3)$, δ 52.4 ($N\underline{CH_2}$ (hexyl)), δ 56.2 (CH_2 (pipa)) δ 57.3 ($NCH_2\underline{CH_2}N_{pipa}$), δ 57.8 ($N\underline{CH_2}CH_2N_{pipa}$), δ 60.0 ($ArCH_2N$), δ 117.9 (Ar-C), δ 124.4 (Ar-C), δ 125.4 (Ar-CH), δ 130.0 (Ar-CH), δ 140.5 (Ar-C), δ 157.0 (Ar-C), δ 165.0 (C=N). MS (FAB, NOBA) *m/z* 827 (MH^+, 68.2%).

Ligand 5

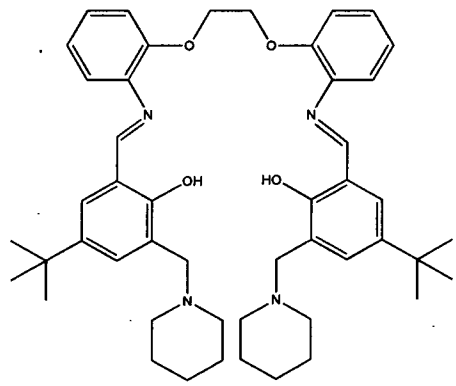

1,2-Bis(2-nitrophenyloxy)ethane

1,2-Bis(2-nitrophenyloxy)ethane was prepared by an adaptation of the method of D. K. Uppal.[12] To 2-nitrophenol (97.89 g, 0.704 mol), in hot DMF (250 cm^3) was added potassium carbonate in small portions. On gentle boiling 1,2-dibromopropethane (38 cm^3, 0.374 mol) was added over 30 minutes. The solution was gently heated to reflux for 2 hrs and the solvent was distilled from the mixture, which was then poured into de-ionised water. The yellow granular precipitate was filtered off, washed with 0.25 M sodium hydroxide (100 cm^3) and water and then dried in vacuo.

Recrystallisation from acetic acid produced a white crystalline solid (52.75 g, 46%). m.p. 106-107°C. Found C, 54.92: H, 3.98: N, 9.08 Calc. For $C_{14}H_{12}N_2O_4$: C, 55.27: H, 3.98: N, 9.25%. ^{1}H NMR ($CDCl_3$, 250 MHz): δ 4.53 (s, 4H, CH_2), δ 7.04-7.84 (m, 8H, Ar-H). ^{13}C NMR ($CDCl_3$): δ 68.5 (CH_2), δ 115.7 (Ar-CH), δ 121.3 (Ar-CH), δ 125.5 (Ar-CH), δ 134.2 (Ar-CH), δ 147.4 (Ar-C), δ 151.8 (Ar-C). EIMS *m/z* 304 (MH^+, 41.9%).

1,2-Bis(2-aminophenyloxy)ethane

1,2-Bis(2-aminophenyloxy)ethane was prepared by an adaptation of the method described by D.K.Uppal.[12] To 1,2-bis(2-nitrophenyloxy)ethane (10.17 g, 0.034 mol) was added absolute ethanol (100 cm^3) and heated to reflux under a nitrogen atmosphere. 3% palladium on activated carbon as an ethanol slurry (1 g) was added to the refluxing solution, dropwise. Hydrazine hydrate (20 cm^3) was then added to the refluxing solution dropwise. The solution was heated to reflux for 2 hrs and then an additional amount of 3% palladium on activated carbon (0.5 g) was added. The solution was then left refluxing for a further 2 hrs. The Pd/C was removed by filtration and the filtrate was evaporated to dryness yielding an oil which was recrystallised from 25% EtOH/ 75% H_2O and heated under vacuum for 4 days to form white crystals (7.01 g, 84%). m.p. 129-132°C. Found C, 67.47: H, 6.37: N, 11.23 Calc. For $C_{14}H_{16}N_2O_2$: C, 68.83: H, 6.60: N, 11.47%. ^{1}H NMR ($CDCl_3$, 250 MHz): δ 4.36 (s, 4H, CH_2), δ 3.82 (bp, 4H, NH_2), δ 6.67-6.87 (m, 8H, Ar-H). ^{13}C NMR ($CDCl_3$): δ 67.3 (CH_2), δ 112.3 (Ar-CH), δ 115.2 (Ar-CH), δ 118.3 (Ar-CH), δ 121.8 (Ar-CH), δ 136.7 (Ar-C), δ 146.1 (Ar-C). EIMS *m/z* 244 (MH^+, 55.2%).

Ligand 5

To a stirred solution of **HPTB** (2.02 g, 7.35 mmol) in diethylether (20 cm^3) was added a solution of 1,2-bis(2-aminophenyloxy)ethane (0.90 g, 3.67 mmol) in ethanol (15 cm^3). The orange solution was stirred overnight and concentrated *in-vacuo* to yield a yellow solid, which was recrystallised from hexane (1.9 g, 71%). m.p. 49-52 °C. Found: C, 74.87; H, 7.94; N, 7.22. Calc. for $C_{49}H_{64}N_4O_4$: C, 76.13; H, 8.34; N, 7.25%. ^{1}H NMR ($CDCl_3$, 250 MHz): δ 1.29 (m, 18H, CH_3), δ 1.40 (m, 4H, $NCH_2CH_2\underline{CH_2}$ (pip)), δ 1.59 (m, 8H, $NCH_2\underline{CH_2}CH_2$ (pip)), δ 2.46 (bp, 8H,

$N\underline{CH_2}CH_2CH_2$ (pip)), δ 3.59 (s, 4H, $ArCH_2N$), δ 4.36 (s, 4H, OCH_2), δ 6.61-7.40 (m, 12H, Ar-CH), δ 8.74 (s, 2H, N=CH), δ 10.41 (s, 2H, OH). ^{13}C NMR ($CDCl_3$): δ 24.1 ($NCH_2CH_2\underline{CH_2}$ (pip)), δ 25.9 ($NCH_2\underline{CH_2}CH_2$ (pip)), δ 31.3 ($C(\underline{CH_3})_3$), δ 33.8 ($\underline{C}(CH_3)_3$), δ 54.3 ($N\underline{CH_2}CH_2CH_2$ (pip)), δ 59.8 ($ArCH_2N$), δ 67.6 (OCH_2), δ 111.5 (Ar-CH), δ 115.2 (Ar-C), δ 121.8 (Ar-C), δ 121.7 (Ar-CH), δ 123.7 (Ar-CH), δ 124.8 (Ar-CH), δ 125.2 (Ar-CH), δ 127.0 (Ar-CH), δ 140.8 (Ar-C), δ 146.0 (Ar-C), δ 151.7 (Ar-C), δ 157.5 (Ar-C), δ 162.2 (C=N). MS (FAB, NOBA) *m/z 759* (MH^+, 9.4%).

Ligand 6

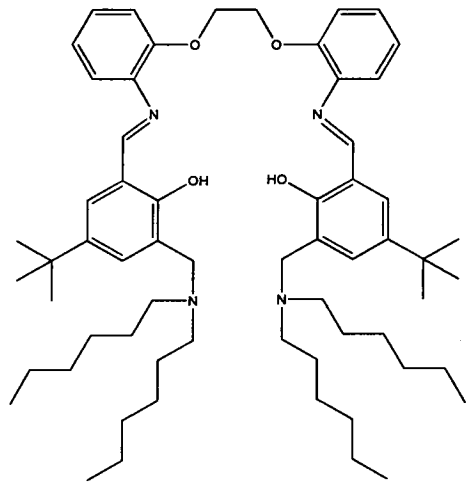

Using the method for ligand 6, but using **HDTB** (4.31 g, 12.5 mmol) and 1,2-bis(2-aminophenyloxy)ethane (4.52 g, 6.23 mmol) produced an orange solid, (4.99 g, 89%). This was used without further purification. Found: C, 77.92; H, 10.01; N, 6.06. Calc. for $C_{62}H_{94}N_4O_4$: C, 77.61; H, 9.88; N, 5.84%. ^1H NMR ($CDCl_3$, 250 MHz): δ 0.79 (m, 12H, CH_3(hexyl)), δ 1.20 (s, 18H, $C(CH_3)_3$), δ 1.12-1.25 (m, 24H, CH_2 (hexyl)), δ 1.42 (bp, 8H, $NCH_2\underline{CH_2}$ (hexyl)), δ 2.38 (t, 8H, NCH_2 (hexyl)), δ 3.58 (s, 4H, $ArCH_2N$), δ 4.35 (s, 4H, OCH_2), δ 6.56-7.57 (m, 12H, Ar-CH), 8.68 (s, 2H, N=CH), 10.35 (s, 2H, OH). ^{13}C NMR ($CDCl_3$): δ 14.2 (CH_3 (hexyl)), δ 22.8 ($NCH_2CH_2CH_2CH_2\underline{CH_2}$ (hexyl)), δ 27.2 ($NCH_2CH_2CH_2\underline{CH_2}$ (hexyl)), δ 27.4 ($NCH_2CH_2\underline{CH_2}$ (hexyl)), δ 31.6 ($C(\underline{CH_3})_3$), δ 32.0 ($NCH_2\underline{CH_2}$ (hexyl)), δ 34.1 ($\underline{C}(CH_3)_3$), δ 53.6 ($N\underline{CH_2}$ (hexyl)), δ 54.4 ($ArCH_2N$), δ 68.2 (OCH_2), δ 111.6 (Ar-CH), δ 115.1 (Ar-C), δ 118.3 (Ar-CH), δ 119.8 (Ar-CH), δ 120.8 (Ar-C), δ 125.5

(Ar-CH), δ 127.0 (Ar-CH), δ 130.4 (Ar-CH), δ 138.6 (Ar-C), δ 140.8 (Ar-C), δ 152.7 (Ar-C), δ 157.4 (Ar-C), δ 160.0 (C=N). MS (FAB, NOBA) *m/z* 959 (MH^+, 59.1%).

Ligand 7

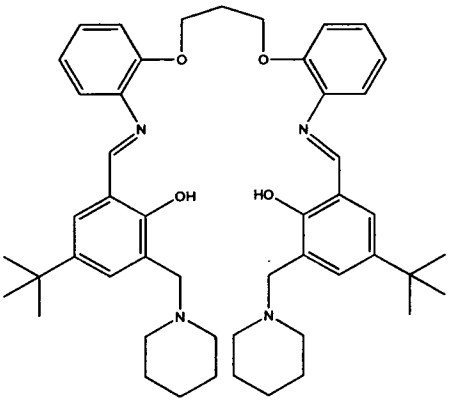

1,3-Bis(2-nitrophenyloxy)propane and 1,3-bis(2-aminophenyloxy)propane were prepared by an adaptation of the method described by D. K. Uppal.[12]

1,3-Bis(2-nitrophenyloxy)propane

Using the method for 1,2-bis(2-nitrophenyloxy)ethane, but using 2-nitrophenol (236.29 g, 1.70 mol), 1,3-dibromopropethane (91 cm^3,0.90 mol) and recrystallisation from ethanol and chloroform produced cream crystals (134.30 g, 47%). m.p. 106-107 °C. Found C, 56.65: H, 4.69: N, 8.89. Calc. For $C_{15}H_{14}N_2O_4$: C, 56.60: H, 4.40: N, 8.81%. ^1H NMR ($CDCl_3$, 250 MHz): δ 2.35 (t, 2H, CH_2), δ 4.35 (t, 4H, CH_2), δ 6.97-7.84 (m, 8H, Ar-H). ^{13}C NMR ($CDCl_3$): δ 29.0 (CH_2), δ 65.1 (O-CH_2), δ 114.4 (Ar-CH), δ 120.2 (Ar-CH), δ 125.5 (Ar-CH), δ 134.3 (Ar-CH), δ 139.5 (Ar-C), δ 152.1 (Ar-C). EIMS *m/z* 318 (MH^+, 18.3%).

1,3-Bis(2-aminophenyloxy)propane

Using the method for 1,2-bis(2-aminophenyloxy)ethane, but using 1,3-bis(2-nitrophenyloxy)propane (10.19g, 0.032 mol) produced brown crystals (5.75g, 70%). m.p. 42-46°C. Found C, 68.76: H, 6.74: N, 11.23 Calc. For $C_{15}H_{18}N_2O_2$: C, 69.74: H, 7.02: N, 10.85%. ^1H NMR ($CDCl_3$, 250 MHz): δ 2.33 (t, 2H, CH_2), δ 3.68 (bs, 4H, NH_2), δ 4.21 (t, 4H, OCH_2), δ 6.68-6.84 (m, 8H, Ar-H). ^{13}C NMR ($CDCl_3$): δ

29.3 (CH_2), δ 64.9 (OCH_2), δ 111.5 (Ar-CH), δ 115.0 (Ar-CH), δ 118.4 (Ar-CH), δ 121.2 (Ar-CH), δ 136.1 (Ar-C), δ 146.2 (Ar-C). EIMS *m/z* 258 (MH^+; 56.8%).

Ligand 7

Using the method for ligand 5, but using **HBTB** (2.02 g, 7.35 mmol) and1,3-bis(2-aminophenyloxy)propane (0.95 g, 3.67 mmol) produced an orange solid (1.9 g, 71%). m.p. 49-52 °C. Found: C, 74.87; H, 7.94; N, 7.22. Calc. for $C_{49}H_{64}N_4O_{24}$: C, 76.13; H, 8.34; N, 7.25%. ^1H NMR ($CDCl_3$, 250 MHz): δ 1.30 (m, 18H, CH_3), δ 1.37 (m, 4H, $NCH_2CH_2\underline{CH_2}$ (pip)), δ 1.61 (bp, 8H, $NCH_2\underline{CH_2}CH_2$ (pip)),δ 2.40 (m, 2H, $OCH_2\underline{CH_2}$), δ 2.49 (bp, 8H, $N\underline{CH_2}CH_2CH_2$ (pip)), δ 3.66 (s, 4H, $ArCH_2N$), δ 4.25 (m, 4H, OCH_2), δ 6.62-7.66 (m, 8H, Ar-H), δ 8.71 (s, 2H, NCH), δ 10.42 (s, 2H, OH). ^{13}C NMR ($CDCl_3$): δ 24.2 ($NCH_2CH_2\underline{CH_2}$ (pip)), δ 25.7 (CH_2), δ 25.9 ($NCH_2\underline{CH_2}CH_2$ (pip)), δ 31.3 $C(\underline{CH_3})_3$), δ 33.9 ($\underline{C}(CH_3)_3$), δ 54.2 ($N\underline{CH_2}CH_2CH_2$ (pip)), δ 59.8 ($ArCH_2N$), δ 65.0 (OCH_2), δ 111.5 (Ar-CH), δ 111.6 (Ar-C), δ 113.0 (Ar-CH), δ 114.9 (Ar-CH), δ 115.0 (Ar-C), δ 118.3 (Ar-CH), δ 118.4 (Ar-CH), δ 121.1 (Ar-CH), δ 121.2 (Ar-C), δ 127.2 (Ar-C), δ 131.1 (Ar-C),δ 157.7 (Ar-C), δ 161.6 (C=N). MS (FAB, NOBA) *m/z* 773(MH^+, 50.4%).

Ligand 8

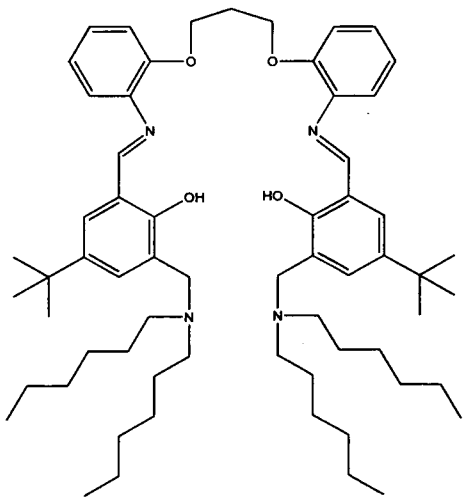

Using the method for ligand **6**, but using **HDTB** (3.38 g, 9.0 mmol) and 1,3-bis(2-aminophenyloxylpropane) (1.16 g, 4.5 mmol) produced a viscous orange oil (4.07 g, 93 %). This was used without further purification. Found: C, 78.01; H, 9.99; N,

5.86. Calc. for $C_{63}H_{96}N_4O_4$: C, 77.73; H, 9.94; N, 5.76%. ^{1}H NMR ($CDCl_3$, 250 MHz): δ 0.79 (t, 12H, CH_3(hexyl)), δ 1.23 (s, 18H, $C(CH_3)_3$), δ 1.19-1.23 (m, 24H, CH_2 (hexyl)), δ 1.44 (M, 8H, $NCH_2\underline{CH_2}$ (hexyl)), δ 2.38 (m, 2H, $OCH_2\underline{CH_2}$), δ 2.41 (t, 8H, NCH_2 (hexyl)), δ 3.64 (s, 2H, $ArCH_2N$), δ 4.26 (m, 4H, OCH_2), δ 7.12 (m, 2H, ArCH), δ 7.45 (m, 2H, ArCH), δ 8.34 (s, 2H, N=CH), δ 10.35 (s, 2H, OH). ^{13}C NMR ($CDCl_3$): δ 13.9 (CH_3 (hexyl)), δ 22.5 ($NCH_2CH_2CH_2CH_2\underline{CH_2}$ (hexyl)), δ 25.7 (CH_2), δ 26.7 ($NCH_2CH_2CH_2\underline{CH_2}$ (hexyl)), δ 27.1 ($NCH_2CH_2\underline{CH_2}$ (hexyl)), δ 31.3 ($C(\underline{CH_3})_3$), δ 31.7 ($NCH_2\underline{CH_2}$ (hexyl)), δ 31.3 $C(\underline{CH_3})_3$), δ 33.9 ($\underline{C}(CH_3)_3$), δ 52.3 ($N\underline{CH_2}$ (hexyl)), δ 59.8 ($ArCH_2N$), δ 65.0 (OCH_2), δ 111.5 (Ar-CH), δ 111.6 (Ar-C), δ 113.0 (Ar-CH), δ 114.9 (Ar-CH), δ 115.0 (Ar-C), δ 118.3 (Ar-CH), δ 118.4 (Ar-CH), δ 121.1 (Ar-CH), δ 121.2 (Ar-C), δ 127.2 (Ar-C), δ 131.1 (Ar-C),δ 157.7 (Ar-C), δ 161.6 (C=N). δ 164.9 (C=N). MS (FAB, NOBA) *m/z* 973 (MH^+, 67.5%).

Ligand 9

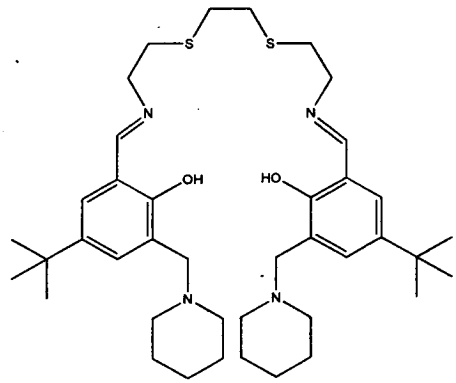

Synthesis of 2,2'-ethane-1,2-diylbissulfanyl-bis-ethylamine, (ESA) using N-2-bromoethylphthalimide protecting group.[14]

1,8-Diphthalimido-3,6-dithiaoctane

Ethanedithiol (9.3 g, 0.17 mol) was added to a solution of sodium ethoxide, sodium (12.0 g) in ethanol (70 cm^3). A solution of N-2-bromoethylphthalimide (50.8 g, 0.21 mol), in hot ethanol (100 cm^3) was then added in portions and the solution was heated to reflux for 150 mins. A cream coloured solid was formed immediately. This was collected, washed with water and ethanol, and recrystallised from boiling

acetone and glacial acetic acid to give white crystals (18.3 g, 40%). (Found C, 58.43: H, 4.69: N, 6.01. Calc. for $C_{22}H_{20}N_2O_4S_2$: C, 59.98: H, 4.58: N, 6.36%). ^{1}H NMR ($CDCl_3$, 250 MHz): δ 2.77-2.89 (m, 8H, SCH_2), δ 3.90 (t, 4H, N-CH_2), δ 7.67-7.86 (m, 8H, Ar-H). ^{13}C NMR ($CDCl_3$): δ 29.8 (SCH_2), δ 31.1 (SCH_2), δ 36.8 (N-CH), δ 123.2 (Ar-CH), δ 131.9 (Ar-C), δ 133.9 (Ar-CH), δ 168.0 (O=C), δ 152.1 (Ar-C). MS (FAB, NOBA) *m/z* 441 (MH^+, 41.5%).

ESA

A 50% solution of hydrazine hydrate (5 cm^3, excess), was added to a refluxing suspension of 1,8-diphthalimido-3,6-dithiaoctane (10.0 g, 0.023 mol). After 3 hrs the mixture was allowed to cool, concentrated HCl was added and then heated to reflux for a further hr. The solution was concentrated to a quarter of initial volume and water (100 cm^3) was added to precipitate out the phthalhydride. The solution was concentrated to half bulk and sodium hydroxide added to make alkaline. The product was extracted with ether (650 cm^3) and dried over potassium hydroxide and the ether removed to give a pale yellow oil product. Due to the amines deliquescent nature and its rapid absorption of CO_2 the amine was dissolved in ethanol (30 cm^3) and concentrated HCl was added to give the hydrochloride salt derivative-dihydrochloride, (0.72 g, 12%). (Found C, 28.15: H, 6.09: N, 10.89. Calc. for $C_6H_{18}Cl_2N_2S_2$: C 28.45: H, 7.16: N, 11.06%). ^{1}H NMR ($CDCl_3$, 250 MHz): δ 2.72 (s, 4H, SCH_2), δ 2.76 (t, 4H, SCH_2), δ 3.10 (t, 4H, NCH_2). ^{13}C NMR ($CDCl_3$): δ 29.8 (SCH_2), δ 31.1 (SCH_2), δ 36.8 (N-CH_2). EIMS *m/z* 253 (MH^+, 4%).

Synthesis of ESA using BOC protecting group

A solution of NaOEt (Na metal 2.0 g EtOH 256 ml) was added to ethanedithiol, (3.0 g, 0.034 mol), followed by the addition of KI (1.3 g) and (2-chloro-ethyl)carbamic acid tert-butyl ester (10.0 g, 0.065 mol), which was added slowly. The solution was then left refluxed for 6 hrs. The solvent was removed by rotary evaporation, water (100 ml) was added and the product was extracted with dichloromethane. The solid was dissolved in a mixture of dichloromethane (52 ml) and trifluroacetic acid (39 ml) and stirred whilst cooling in an ice-slurry for 45 mins. The solvent was removed by rotary evaporation and the residue was basified with aqueous NaOH (100 ml). The

product was extracted by dichloromethane dried over $MgSO_4$ and the solvent removed by rotary evaporation. (1.8 g, 25%). Found C, 29.68: H, 6.74: N, 9.66 Calc. for $C_6H_{18}Cl_2N_2O_2S_2$: C, 28.45: H, 7.16: N, 11.06%. ^{1}H NMR ($CDCl_3$, 250 MHz): δ 2.71 (s, 4H, SCH_2), δ 2.75 (t, 4H, SCH_2), δ 3.09 (t, 4H, NCH_2). MS (FAB, NOBA) *m/z* 253 (MH^+, 0.4%).

One step synthesis of ESA[15]

A solution of dibromomethane, (8.4 ml, 0.0968 mol), in ethanol (150 ml) distilled under nitrogen was added dropwise under nitrogen over 30 minutes to a solution of 2-aminoethanethiol hydrochloride, (20.0 g, 0.176 mol), and $NaHCO_3$, (30.0 g, 0.352 mol) in water (350 ml) distilled under nitrogen. The mixture was then heated to reflux for 17 hours. The solvent was removed in vacuo. The product and salts (NaCl and NaBr) had ether (250ml) (anhydrous degassed) added to them to dissolve the product only, but this did not work. The product was successfully dissolved in acetonitrile (degassed) with some of the salts (but this was due to some water remaining). The acetonitrile/ product/ salt solution was filtered. The solvent was then removed and heated to remove any water. The solid was redissolved in acetonitrile (degassed) and passed to a distillation vessel by cannula filtration. The solvent was removed on vacuo and the product distilled (130-132°C, 0.2mTorr), to give the product, (7.56 g, 48%). The product was stored under a nitrogen atmosphere. Found C, 29.32: H, 7.23: N, 10.98. Calc. for $C_6H_{18}Cl_2N_2S_2$: C, 28.45: H, 7.16: N, 11.06%. ^{1}H NMR ($CDCl_3$, 250 MHz): δ 2.73 (s, 4H, SCH_2), δ 2.74 (t, 4H, SCH_2), δ 3.10 (t, 4H, NCH_2). MS (FAB, NOBA) *m/z* 253 (MH^+, 60.0%).

Ligand 9

Using the method for ligand **6**, but using **HPTB** (2.21 g, 8.0 mmol) and ESA (0.99 g, 3.9 mmol) produced (1.49 g, 55%). Found C, 68.42: H, 8.76: N, 8.40. Calc. For $C_{40}H_{62}N_4O_2S_2$: C, 68.31: H, 9.09: N, 9.09%. ^{1}H NMR ($CDCl_3$, 250 MHz): δ 1.23 (s, 18H, CH_3), δ 1.36 (bp, 4H, $NCH_2CH_2\underline{CH_2}$ (pip)), δ 1.53 (bp, 8H, $NCH_2\underline{CH_2}CH_2$ (pip)), δ 2.40 (bp, 8H, $N\underline{CH_2}CH_2CH_2$ (pip)), δ 2.69 (s, 4H, SCH_2), δ 2.78 (t, 4H, $NCH_2\underline{CH_2}S$), δ 3.52 (s, 4H, $ArCH_2N$), δ 3.69 (t, 4H, $N\underline{CH_2}CH_2S$), δ 7.19 (s, 2H, Ar-H), δ 7.30 (s, 2H, Ar-H), δ 8.36 (s, 2H, N=CH), δ 10.35 (s, 2H, OH). ^{13}C NMR

($CDCl_3$): δ 24.7 ($NCH_2CH_2\underline{CH_2}$ (pip)), δ 26.4 ($NCH_2\underline{CH_2}CH_2$ (pip)), δ 31.9 ($C(\underline{CH_3})_3$), δ 34.4 ($\underline{C}(CH_3)_3$), δ 32.9 (SCH_2), δ 33.5 ($NCH_2\underline{CH_2}S$), δ 54.8 ($N\underline{CH_2}CH_2CH_2$ (pip)), δ 58.0 ($ArCH_2N$), δ 60.2 ($N\underline{CH_2}CH_2S$), δ 126.3 (Ar-CH), δ 131.1 (Ar-CH), δ 118.6 (Ar-C), δ 125.0 (Ar-C), δ 141.1 (Ar-C), δ 157.6 (Ar-C), δ 165.7 (C=N). MS (FAB, NOBA) *m/z* 695 (MH^+, 89.0%).

Ligand 10

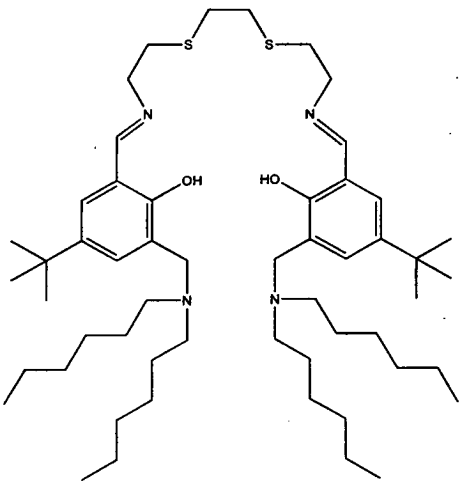

Using the method for ligand **6**, but using **HDTB** (3.20 g, 8.5 mmol) and ESA (1.06 g, 4.2 mmol) produced (3.57 g, 95%). This was used without further purification. Found C, 72.56: H, 10.68: N, 6.03. Calc. For $C_{54}H_{94}N_4O_2S_2$: C, 72.43: H, 10.58: N, 6.26%. ^1H NMR ($CDCl_3$, 250 MHz): δ 0.79 (t, 12H, CH_3 (hexyl)), δ 1.24 (s, 18H, $C(CH_3)_3$), δ 1.17-1.25 (m, 24H, CH_2 (hexyl)), δ 1.45 (m, 8H, $NCH_2\underline{CH_2}$ (hexyl)), δ 2.41 (t, 8H, $N\underline{CH_2}$ (hexyl)), δ 2.68 (s, 4H, SCH_2), δ 2.77 (t, 4H, $NCH_2\underline{CH_2}S$), δ 3.66 (s, 4H, $ArCH_2N$), δ 3.69 (t, 4H, $N\underline{CH_2}CH_2S$), δ 6.63-7.29 (m, 4H, A-CH), δ 8.29 (s, 2H, N=CH). ^{13}C NMR ($CDCl_3$): δ 13.9 (CH_3 (hexyl)), δ 22.4 ($NCH_2CH_2CH_2CH_2\underline{CH_2}$ (hexyl)), δ 26.1 ($NCH_2CH_2CH_2\underline{CH_2}$ (hexyl)), δ 26.9 ($NCH_2CH_2\underline{CH_2}$ (hexyl)), δ 31.3 ($C(\underline{CH_3})_3$), δ 31.5 ($NCH_2\underline{CH_2}$ (hexyl)), δ 32.5 (SCH_2), δ 33.0 ($NCH_2\underline{CH_2}S$), δ 33.8 ($\underline{C}(CH_3)$, δ 53.3 ($N\underline{CH_2}$ (hexyl)), δ 58.4 ($N\underline{CH_2}CH_2S$), δ 59.4 ($ArCH_2N$), δ δ 115.1 (Ar-C), δ 121.3 (Ar-C), δ 124.9 (Ar-CH), δ 129.6 (Ar-CH), δ 141.2 (Ar-C), δ 155.5 (Ar-C), δ 166.2 (C=N). MS (FAB, NOBA) *m/z* 895 (MH^+, 77.9%).

Ligand 11

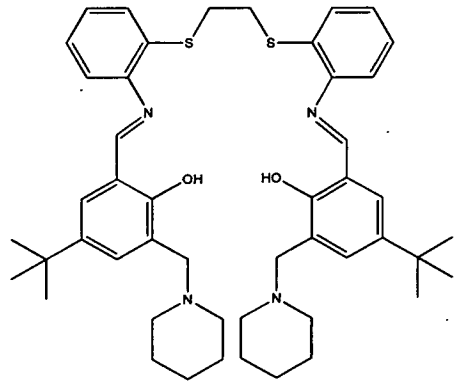

1,2-Bis(2-aminophenylthio)ethane

1,2-Bis(2-aminophenylthio)ethane was prepared by an adaptation of the method of Kumar *et. al.*[13] Sodium (6.3 g) was dissolved in MeOH (190 cm^3) and 2-aminobenzenethiol (33 g, 0.26 mol) was added. The mixture was stirred under nitrogen for 10 mins and a yellow solution was obtained. 1,2-Dibromoethane (26 g) in MeOH (50 cm^3) was then added dropwise to the solution. The mixture was stirred overnight under nitrogen then heated to reflux for 6 hrs. On cooling hydrobromic acid was added to precipitate the white dibromide salt. This was filtered, washed with cold MeOH and then recrystallised from MeOH to produce a white solid, 1,2-bis(2-aminophenylthio)ethane dibromide (23.412 g, 41%). 1,2-Bis(2-aminophenylthio)ethane dibromide (4.99g, 0.011 mol) was then suspended in a saturated aqueous solution of sodium bicarbonate (75 cm^3). CH_2Cl_2 was added and the organic phase was separated and washed with distilled water. The combined organic extracts were dried over anhydrous sodium sulfate and then evaporated to dryness under pressure. Pale yellow crystals were obtained (1.329 g, 42%). m.p. 74-76°C. Found C, 60.87: H, 5.94: N, 10.08. Calc. for $C_{49}H_{64}N_4O_4$: C, 60.83 H, 5.83: N, 10.13%. ^1H NMR ($CDCl_3$, 250 MHz): δ 3.10 (s, 4H, CH_2, δ 4.47 (bp, 4H, NH_2), δ 6.87-7.60 (m, 8H, Ar-H). ^{13}C NMR ($CDCl_3$): δ 34.3 (CH_2), δ 114.8 (Ar-CH), δ 116.6 (Ar-C), δ 118.4 (Ar-CH), δ 129.8 (Ar-CH), δ 135.9 (Ar-CH), δ 148.4 (Ar-C). MS (FAB, NOBA) *m/z* 277 (MH^+, 80.3%).

Using the method for ligand **6**, but using **HPTB** (1.99 g, 7.24 mmol) and 1,2-bis(2-aminophenylthio)ethane (1.0 g, 3.62 mmol) produced a yellow solid (1.58 g, 54.6%). m.p. 104-120 °C. Found: C, 72.05; H, 7.91; N, 6.92. Calc. for $C_{48}H_{62}N_4O_2S_2$: C,

72.87; H, 7.90; N, 7.08%. ^{1}H NMR ($CDCl_3$, 250 MHz): δ 1.32 (m, 18H, CH_3), δ 1.45 (bp, 4H, $NCH_2CH_2\underline{CH_2}$ (pip)), δ 1.61 (bp, 8H, $NCH_2\underline{CH_2}CH_2$ (pip)), δ 2.49 (bp, 8H, $N\underline{CH_2}CH_2CH_2$ (pip)), δ 3.15 (s, 4H, SCH_2), δ 3.66 (s, 4H, $ArCH_2N$), δ 7.02-7.66 (m, 12H, Ar-H), δ 8.65 (d, 2H, N=CH), δ 10.42 (s, 2H, OH). ^{13}C NMR ($CDCl_3$): δ 24.2 ($NCH_2CH_2\underline{CH_2}$ (pip)), δ 25.9 ($NCH_2\underline{CH_2}CH_2$ (pip)), δ 31.3 ($C(\underline{CH_3})_3$), δ 33.9 ($\underline{C}(CH_3)_3$), δ 54.2 ($N\underline{CH_2}CH_2CH_2$ (pip)), δ 57.7 (SCH_2), δ 61.9 ($ArCH_2N$), δ 114.8 (Ar-CH), δ 118.1 (Ar-CH), δ 118.9 (Ar-C), δ 124.7 (Ar-C), δ 126.1 (Ar-CH), δ 126.3 (Ar-CH), δ 126.7 (Ar-C), δ 128.1 (Ar-CH), δ 130.8 (Ar-C), δ 131.1 (Ar-CH), δ 141.1 (Ar-C), δ 157.2 (Ar-C), δ 191.0 (C=N). MS (FAB, NOBA) *m/z* 792 (MH^+, 62.5%).

Ligand 12

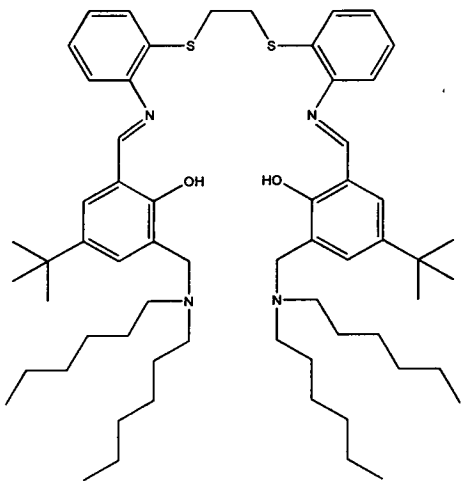

Using the method for ligand **6**, but using **HDTB** (4.13 g, 11.95 mmol) and 1,2-Bis(2-aminophenylthio)ethane (1.67 g, 5.98 mmol) produced a yellow oil, (5.8 g, 98%). This was used without further purification. Found: C, 75.40; H, 9.87; N, 5.63. Calc. for $C_{62}H_{94}N_4O_2S_2$: C, 75.10; H, 9.56; N, 5.65%. ^{1}H NMR ($CDCl_3$, 250 MHz): δ 0.79 (t, 12H, CH_3 (hexyl)), δ 1.24 (s, 18H, $C(CH_3)_3$), δ 1.17-1.25 (m, 24H, CH_2 (hexyl)), δ 1.45 (m, 8H, $NCH_2\underline{CH_2}$ (hexyl)), δ 2.41 (t, 8H, $N\underline{CH_2}$ (hexyl)), δ 3.66 (s, 2H, SCH_2), δ 8.64 (s, 4H, $ArCH_2N$), δ 6.63-7.29 (m, 4H, A-CH), δ 8.29 (s, 2H, N=CH). ^{13}C NMR ($CDCl_3$): δ 13.9 (CH_3 (hexyl)), δ 22.4 ($NCH_2CH_2CH_2CH_2\underline{CH_2}$ (hexyl)), δ 26.1 ($NCH_2CH_2CH_2\underline{CH_2}$ (hexyl)), δ 26.9 ($NCH_2CH_2\underline{CH_2}$ (hexyl)), δ 31.3 ($C(\underline{CH_3})_3$), δ 31.5 ($NCH_2\underline{CH_2}$ (hexyl)), δ 33.8 ($\underline{C}(CH_3)_3$), δ 53.3 ($N\underline{CH_2}$ (hexyl)), δ 57.22 (SCH_2), δ 61.3 ($ArCH_2N$), δ 114.82 (Ar-CH), δ 117.95 (Ar-CH), δ 118.32 (Ar-C), δ 118.61

(Ar-C), δ 126.67 (Ar-CH), δ 126.77 (Ar-CH), δ 126.96 (Ar-C), δ 130.07 (Ar-CH), δ 130.95 (Ar-C), δ 131.01 (Ar-CH), δ 136.41 (Ar-C), δ 157.10 (Ar-C), δ 192 (C=N). MS (FAB, NOBA) *m/z* 991 (MH^+, 70.5%).

2.9.4 Nickel complex synthesis

Complex 13

A 1:1 molar ratio of **Triene**: nickel acetate (0.2 moles) was stirred in methanol (20 cm^3). The solution immediately turned blue. After removal of the solvent the product was dried in *vacuo* to produce a dark blue hydroscopic oil (nickel-triene complex). MS (FAB, NOBA) *m/z* 263 (MH^+-$C_2H_3O_2$, 93.7%).

Using the method for ligand **6**, but using **HPTB** (2.21 g, 8.0 mmol) and nickel-triene (1.24 g, 3.9 mmol) produced a brown solid formulated as [Ni(**1**)$(C_2H_3O_2)_2$].CH_2Cl_2 (1.79 g, 55%). Found C, 58.23: H, 7.87: N, 9.10. Calc. For $C_{45}H_{70}Cl_2N_6NiO_6$ C, 58.71: H, 7.66: N, 9.13%. MS (FAB, NOBA) *m/z* 717 (MH^+-2($C_2H_3O_2$), 88.0%). Evaporation from hexane produced reddish brown crystals suitable for X-ray diffraction.

Complex 14

A 1:1 molar ratio of ligand: nickel salt (*c.a.* $3x10^{-4}$ moles) was stirred in methanol (20 cm^3). Colour changes were instantaneous. After removal of the solvent *in-vacuo* the products were recrystallised as indicated and dried in-*vacuo*.

[Ni(**5**)SO_4], MX_n = $NiSO_4.6H_2O$. Recrystallisation from CH_2Cl_2:$^iPr_2O$, gave a yellow crystalline material formulated as [Ni(**5**)SO_4] (0.143 g, 59%). (Found: C, 63.09; H, 7.52; N, 5.62. Calc. for $C_{48}H_{62}N_4NiO_8S$: C, 63.09; H, 6.84; N, 6.13%). ν_{max}/cm^{-1} 1115s (SO_4). MS (FAB NOBA) *m/z* 914 (MH^+, 5.9%).

Complex 15

Using the method for complex **14** [Ni(**5**)$(NO_3)_2$], MX_n = $Ni(NO_3)_2.6H_2O$. Recrystallisation from CH_2Cl_2:$^iPr_2O$, gave a yellow crystalline material formulated

as [Ni(**5**)$(NO_3)_2$].4H_2O (0.207 g, 79%). (Found: C, 56.50; H, 6.99; N, 8.49. Calc. for $C_{48}H_{70}N_6NiO_{14}$: C, 56.87; H, 6.92; N, 8.29%). ν_{max}/cm^{-1} 1385s (NO_3). MS (FAB, NOBA) *m/z* 942 (MH^+, 41.7%).

Complex 16

Using the method for complex **14** [Ni(**5**)Cl_2], MX_n = $NiCl_2.6H_2O$. A yellow solid material formulated as [Ni(**5**)Cl_2] (0.1526 g, 68%). (Found: C, 64.88; H, 7.26; N, 6.71. Calc. for $C_{48}H_{62}N_4Cl_2O_4$: C, 64.88; H, 7.03; N, 6.30%). MS (FAB, NOBA) *m/z* 889 (MH^+, 8.9%).

Complex 17

Using the method for complex **14** but after removal of the solvents the complex was washed with an aqueous solution (pH 7.5), extracted into chloroform, and dried in-*vacuo*. [Ni(**5**-2H)], MX_n = $Ni(C_2H_3O_2)_2.6H_2O$. A brown crystalline material formulated as [Ni(**5**)SO_4].4H_2O.EtOH (0.17 g, 79%). (Found: C, 64.39; H, 7.74; N, 5.91. Calc. for $C_{50}H_{74}N_4NiO_9$: C, 64.31; H, 7.99; N, 6.00%). MS (FAB, NOBA) *m/z* 816 (MH^+, 11.8%).

Complex 18

Using the method for complex **14** [Ni(**7**)SO_4], MX_n = $NiSO_4.6H_2O$. Recrystallisation from CH_2Cl_2:$^iPr_2O$, gave a yellow crystalline material formulated as [Ni(**7**)SO_4] (0.179 g, 75%). (Found: C, 63.43; H, 6.91; N, 6.16. Calc. for $C_{49}H_{64}N_4NiO_8S$: C, 63.46; H, 6.95; N, 6.04%). ν_{max}/cm^{-1} 1116s (SO_4). MS (FAB, NOBA) *m/z* 830 (MH^+-SO_4, 51.6%).

Complex 19

Using the method for complex **14** [Ni(**7**)$(NO_3)_2$], MX_n = $Ni(NO_3)_2.5H_2O$. Recrystallisation from CH_2Cl_2:$^iPr_2O$, gave a yellow crystalline material formulated as [Ni(**7**)$(NO_3)_2$].5H_2O (0.200 g, 80%). (Found: C, 56.48; H, 6.81; N, 8.25. Calc. for $C_{49}H_{74}N_6NiO_{15}$: C, 56.27; H, 7.13; N, 8.04%). ν_{max}/cm^{-1} 1384s (NO_3). MS (FAB, NBAl) *m/z* 956 (MH^+, 52.8%).

Complex 20

Using the method for complex **14** [Ni(7)Cl_2] MX_n = $NiCl_2.6H_2O$. Recrystallisation from CH_2Cl_2:$^iPr_2O$, gave a yellow crystalline material formulated as [Ni(7)Cl_2].CCl_4.CH_2Cl_2 (0.084 g, 53%). (Found: C, 54.54; H, 6.88; N, 5.83. Calc. for $C_{48}H_{62}N_4NiCl_2$: C, 54.01; H, 6.01; N, 4.84%). MS (FAB, NOBA) *m/z* 830 (MH^+,24.8%).

Complex 21

Using the method for complex **17** [Ni(7-2H)], MX_n = $Ni(C_2H_3O_2)_2.6H_2O$. A brown crystalline material formulated as [Ni(7-2H)].$3H_2O$ (0.14 g, 68%). (Found: C, 66.11; H, 7.72; N, 5.74. Calc. for $C_{49}H_{62}N_4NiO_4$: C, 65.59; H, 7.76; N, 6.34%). MS (FAB, NOBA) *m/z* 830 (MH^+, 3%).

Complex 22

Using the method for complex **14** [Ni(**9**)SO_4] MX_n = $NiSO_4.6H_2O$. Recrystallisation from CH_2Cl_2:$^iPr_2O$, gave a brown solid yellow crystalline material formulated as [Ni(**9**)SO_4].$5H_2O$ (0.043 g, 14%). (Found: C,56.87; H, 7.54; N, 6.65. Calc. for $C_{40}H_{62}N_4NiO_6S_3$: C, 56.53; H, 7.35; N, 6.59%). ν_{max}/cm^{-1} 1130s (SO_4). MS (FAB, NOBA) *m/z* 751 (MH^+-SO_4, 32.1%).

Complex 23

Using the method for complex **14** [Ni(**9**)$(NO_3)_2$] MX_n = $Ni(NO_3)_2.6H_2O$. Recrystallisation from CH_2Cl_2:$^iPr_2O$, gave a mustard yellow solid material formulated as [Ni(**9**)$(NO_3)_2$].$4H_2O$ (0.082 g, 26%). (Found C, 50.46: H, 6.87: N, 8.60. Calc. for $C_{40}H_{70}N_6NiO_{12}S_2$: C, 50.58; H, 7.43; N, 8.85%). ν_{max}/cm^{-1} 1384 s (NO_3). MS (FAB, NOBA) *m/z* 751 (MH^+-$(NO_3)_2$, 32.1%)Dissolving the material in dichloromethane and layering with hexane produced brownish green crystals suitable for X-ray diffraction.

Complex 24

Using the method for complex **14** [Ni(**9**)Cl_2] MX_n = $NiCl_2.6H_2O$. Recrystallisation from CH_2Cl_2:$^iPr_2O$, gave a yellow crystalline material formulated as [Ni(**9**)Cl_2].CH_2Cl_2 (0.084 g, 53%). (Found: C, 54.54; H, 6.88; N, 5.83. Calc. for $C_{41}H_{64}Cl_4N_4NiO_2S_2$: C, 54.14; H, 7.09; N, 6.16%). MS (FAB, NOBA) *m/z* 751 (MH^+-Cl_2, 31.3%).

Complex 25

Using the method for complex **17** [Ni(**9**-2H)] MX_n = $Ni(C_2H_3O_2)_2.6H_2O$. Recrystallisation from CH_2Cl_2:$^iPr_2O$, gave a olive yellow solid material formulated as [Ni(**9**)$(NO_3)_2$].$4H_2O$ (0.111 g, 50%). (Found C, 58.17: H, 7.84: N, 7.02% Calc. For $C_{40}H_{68}N_4NiO_6S_2$ C, 58.32: H, 8.32: N, 6.80). MS (FAB, NOBA) *m/z* 751 (MH^+, 38.1%).

Complex 26

Using the method for complex **14** [Ni(**11**)SO_4], MX_n = $NiSO_4.6H_2O$. Recrystallisation from CH_2Cl_2:$^iPr_2O$, gave a brown crystalline material formulated as [Ni(**11**)SO_4].$6H_2O$ (0.217 g, 89%). (Found: C, 54.71; H, 6.73; N, 5.08. Calc. for $C_{48}H_{74}N_4NiO_{12}S_3$: C, 54.70; H, 7.08; N, 5.32%). ν_{max}/cm^{-1} 1130s (SO_4). MS (FAB, NOBA) *m/z* 945 (MH^+, 17.2%). Dissolving the material in methanol and layering with diethylether produced dark brown crystals suitable for X-ray diffraction.

Complex 27

Using the method for complex **14** [Ni(**11**)$(NO_3)_2$], MX_n = $Ni(NO_3)_2.6H_2O$. Recrystallisation from CH_2Cl_2:$^iPr_2O$, gave a brown crystalline material formulated as [Ni(**11**)SO_4].$3½H_2O$ (0.218 g, 92%). (Found: C, 55.41; H, 6.28; N, 7.94. Calc. for $C_{48}H_{69}N_6NiO_{11.5}S_2$: C, 55.60; H, 6.71; N, 8.10%). λ_{max}/nm (CH_2Cl_2) 371, 557. λ_{max} (ε) / nm (M^{-1} cm^{-1}) 475 (23270), 315 (32495), 255 (50314). ν_{max}/cm^{-1} 1384s (NO_3). MS (FAB, NOBA) *m/z* 944 (MH^+-$2NO_3$, 62.3%). Dissolving the material in dichloromethane and layering with hexane produced dark brown crystals suitable for X-ray diffraction.

Complex 28

Using the method for complex **14** [Ni(**11**)Cl_2], MX_n = $NiCl_2.6H_2O$. Recrystallisation from CH_2Cl_2:$^iPr_2O$, gave a brown crystalline material formulated as [Ni(**11**)Cl_2].$4H_2O$ (0.262 g, 8843%). (Found: C, 58.42; H, 6.92; N, 5.54. Calc. for $C_{48}H_{70}Cl_2N_4NiO_6S_2$: C, 58.07; H, 7.11; N, 5.64%). MS (FAB) *m/z* 921 (MH^+-Cl_2, 76.7%).

Complex 29

Using the method for complex **17** [Ni(**11**-2H)], MX_n = $Ni(C_2H_3O_2)_2.5H_2O$. A dark brown crystalline material formulated as [Ni(**11**-2H)].$4H_2O$ (0.205 g, 92%). (Found: C, 62.81; H, 7.03; N, 5.90. Calc. for $C_{48}H_{68}N_4NiO_6S_2$: C, 62.67; H, 7.45; N, 6.09%). MS (FAB, NBA) *m/z* 847 (MH^+, 49.6%). Dissolving the material in dichloromethane and layering with hexane produced dark brown block crystals suitable for X-ray diffraction.

2.9.5 Solvent extraction experiments from sulfate media

10 cm^3 of 0.01 M L ((L = **4**, **6**, **8**, **10** or **12**) in chloroform was contacted with 10 cm^3 aqueous 1 M $NiSO_4$ in a tightly sealed, screw top, glass jar, equipped with a magnetic stirrer. The two-phase system was stirred at 500 r.p.m and at room temperature for 17 hrs, after which time a 2 cm^3 sample was taken from the organic phase. The samples were diluted by a factor of 1:5 with butan-1-ol and their nickel contents analysed by ICP-AES. The data collected were plotted as % uptake bar charts in Microsoft Excel.

2.9.6 X-ray crystallography

Structures **13**, **24** and **HPTB** were determined by James Davidson, **23** and **29** were determined by Dr. Andrew Parkin and **5** and **27** were determined by Dr. Simon Parsons and Dr. Robert Coxall respectively at the University of Edinburgh. In all cases data were collected at 220K on a SMART or Stoe Stadi-4 diffractometer equipped with an Oxford Cryosystems low temperature device.

Structure **26** was collected at the EPSRC National Crystallographic Service, The University of Southampton, on a Nonius Kappa-CCD diffractometer. Full listings of atomic positions and thermal parameters are provided electronically on the CD accompanying this thesis.

2.10 References

1 G. M. Ritcey, *Pub. Aust. Inst. Min. Metall.*, 1996, **6/96**, 251.

2 N. N. Greenwood and E. A. Earnshaw, 'Chemistry of the elements', ed. A. F. Trotman-Dickenson, Permangon Press, Oxford, 1984, 1328.

3 F. A. Cotton and G. Wilkinson, 'Advanced Inorganic Chemistry', John Wiley and Sons, USA, 1980, 147.

4 T. Zhu, *Miner. Process. Extr. Metall. Rev.*, 2000, **21**, 1.

5 T. Zhu, International Solvent Extraction Conference, Cape Town, South Africa, 2002, 203-207.

6 M. Laing, 'Solvent-Extraction of Metals Is Coordination Chemistry', Americal Chemical Society, Washington, 1994, 382-394.

7 H. A. Miller, N. Laing, S. Parsons, A. Parkin, P. A. Tasker and D. J. White, *J.Chem.Soc.,Dalton Trans.*, 2000, 3773.

8 D. J. White, N. Laing, H. Miller, S. Parsons, P. A. Tasker and S. Coles, *Chem.Commun.*, 1999, 2077.

9 D. F. Shriver, P. W. Atkins and C. H. Langford, 'Inrganic Chemistry', Oxford University Press, Great Britain, 1994, 213.

10 R. Aldred, R. Johnston, D. Levin and J. Neilan, *J. Chem. Soc. Perkin. Trans. I*, 1994, 1823.

11 H. Adams, N. A. Bailey, D. E. Fenton and G. Papageorgiou, *J.Chem.Soc.,Dalton Trans.*, 1995, 1883.

12 J. Uppal, 'Polytechnic of North London, PhD Thesis', 1979.

13 M. Kumar, V. Sharma nee Bhalla and P. Sharma, *Journal of Chemical Research, Synopses*, 2000, 492.

14 F. P. J. Dwyer and F. Lions, *J.Am.Chem.Soc.*, 1950, **72**, 1545.

15 Q.-Y. Zheng, C.-F. Chen and Z.-T. Huang, *J. Chem. Res., synop*, 1999, 212.

16 M. McPartlin, P. A. Tasker, N. A. Bailey, E. D. McKenzie and J. M. Worthington, *Crystal Structure Communications*, 1978, **7**, 115.

17 J. Cai, J. Myrczek, H. Chun and I. Bernal, *J.Chem.Soc.,Dalton Trans.*, 1998, 4155.

18 G. H. Searle, M. Petkovic and F. R. Keene, *Aust. J. Chem*, 1972, **25**, 2045.

19 S. G. Galbraith, P. G. Plieger and P. A. Tasker, 2002, 2662.

20 M. S. Gibson and R. W. Bradshaw, *Angew.Chem.,Int.Ed.Engl.*, 1968, **7**, 919.

21 D. H. Williams and I. Fleming, 'Spectroscopic Methods in Organic Chemistry', Mc Graw Hill Book Company, London, 1995, chapter 2, 28-62.

22 A. J. Gordon and R. A. Ford, 'The Chemist's Companion and Handbook of Practical Data, Techniques and references', John Wiley and Sons Inc., 1972, 58.

23 R. D. Cannon, B. Chiswell and L. M. Venanzi, *J. Chem. Soc. A*, 1967, 1277.

24 N. Akkus, J. C. Campbell, J. Davidson, D. K. Henderson, H. A. Miller, A. Parkin, S. Parsons, P. G. Plieger, R. M. Swart, P. A. Tasker and L. C. West, *J.Chem.Soc.,Dalton Trans.*, 2003, 1932.

25 F. A. Settle, 'Handbook of Instrumental Techniques for Analytical Chemistry', Prentice Hall, America, 1997.

Chapter Three

Tridentate ligands

Contents

3.1 Tridentate ligands for the transport of nickel(II) salts

As poor extraction of nickel(II) salts was observed for the sexadentate systems characterised in chapter 2, new ligands were considered which might also give high spin nickel(II) complexes but with less constraints on the *pseudo*-octahedral donor sets provided. Formation of complexes with nickel(II) sulfate, nickel(II) chloride and nickel(II) acetate either in solvent extraction processes or as solid state samples can be envisaged in several different ways depending on whether:

- High spin pseudo-octahedral or low spin "square" planar complexes are formed.
- Sulfate, chloride or acetate anions are present in the inner coordination sphere.
- Sulfate, chloride or acetate anions are present in the outer coordination sphere (H-bonded to protonated pendant amine groups or as separated ion pairs).
- The ligands are present in their zwitterionic or mono deprotonated forms (Figure 3.1).
- The ligands function in tridentate or bidentate modes.
- Sulfate is present as a dianion SO_4^{2-} or as the monoprotonated hydrogensulfate ion HSO_4^-.

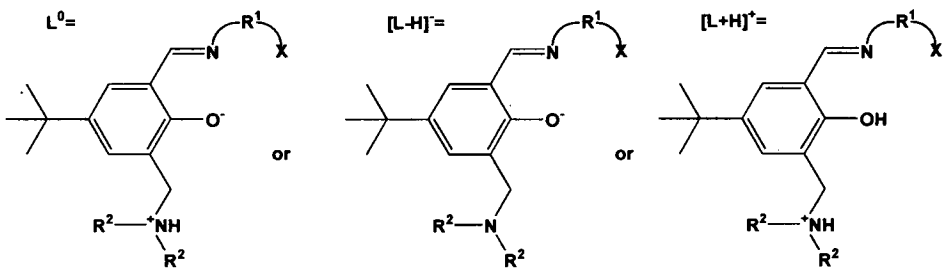

R^1 = -$(CH_2)_2$-, *o*-C_6H_4-

R^2 = *n*-C_6H_{13}, C_5H_{10} (as part of piperidine ring)

Figure 3.1 Tridentate ligands which provide octahedral XNO^- donor sets and pendant dialkylamine groups

Charge-neutral species will be more soluble in relatively non-polar water-immiscible solvents. Some of the possibilities for the formation of neutral species from two ligands in the forms L^0 or $[L\text{-}H]^-$ or $[L+H]^+$ by combination with Ni^{2+}, SO_4^{2-} or HSO_4^- are illustrated in Figure 3.2. The presence of particular combinations is expected to be dependent on the pH of the aqueous phase.

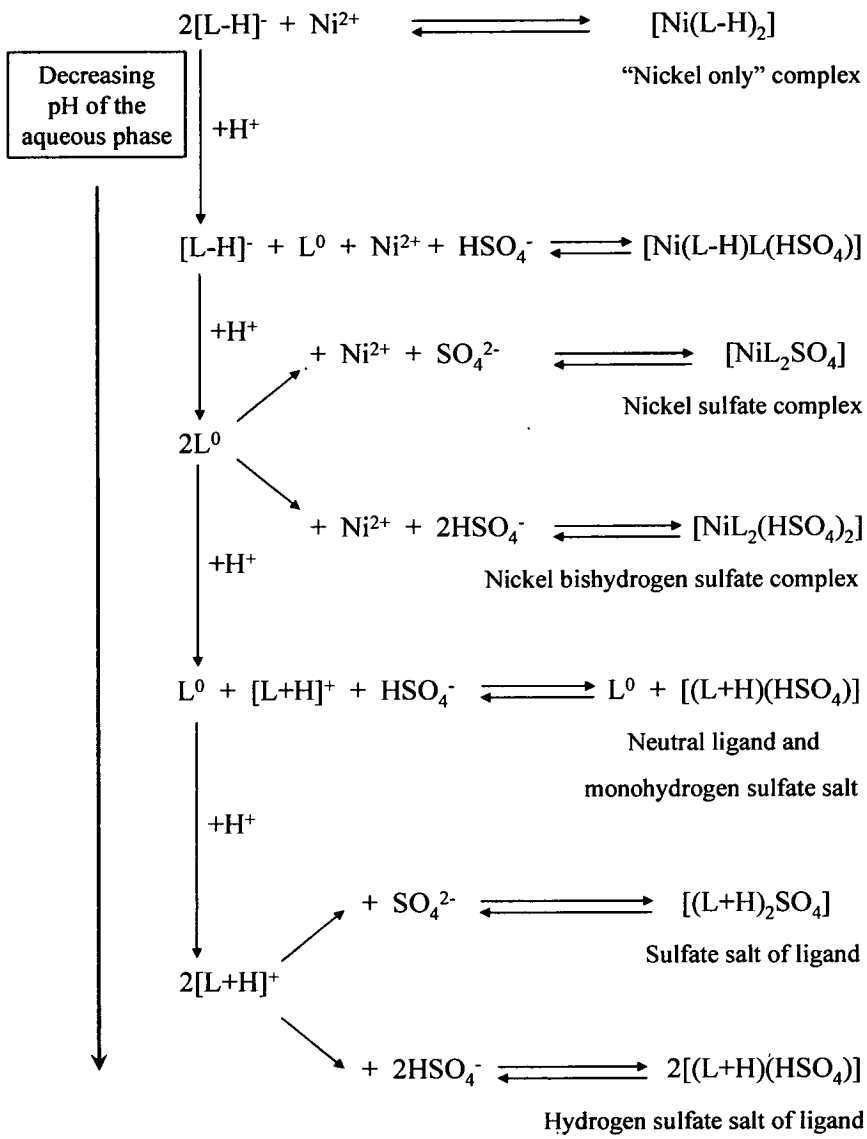

Figure 3.2 Some of the possibilities for formation of charge-neutral complexes or salts from two tridentate ligand molecules **30-37** in solvent extraction of $NiSO_4$ with variation of pH of the aqueous phase

In the 2:1 complexes $[Ni(L\text{-}H)_2]$, $[Ni(L\text{-}H)L(HSO_4)]$, $[NiL_2SO_4]$, $[NiL_2(HSO_4)_2]$, if the ligands are tridentate then the sulfate or hydrogen sulfate anions will not be present in the inner coordination sphere.

A similar sequence of species can also be envisaged for reactions with nickel(II) and one or two chloride and acetate ions.

Tridentate ligands, related to the sexadentate ligands were considered (Figure 3.3). Structurally these could either act as individual ligands with three donor atoms or form neutral multi-ligand/metal complexes. For comparisons to be made with the sexadentate ligands, the ligands are required to work as pairs and hence two tridentate ligands would behave as one sexadentate ligand producing an $X_2N_2O_2^{2-}$ donor set. This chapter deals with the preparation and characterisation of the ligands and a preliminary investigation of their coordination chemistry with nickel(II) salts.

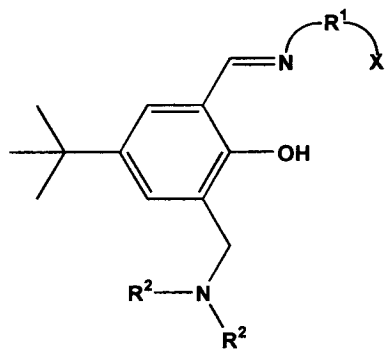

$X = OCH_3$, SCH_3, $N(CH_3)_2$

$R^1 = -(CH_2)_2-$, *o*-C_6H_4-

NR^2_2 = piperidine, $N(C_6H_{13})_2$

Figure 3.3 Tridentate ligands which provide octahedral XNO^- donor sets and pendant dialkylamine groups

There are few examples[1-6] where two tridentate ligands are coordinated to one central nickel cation. Work by Fernández *et. al.*[6] involves the use of some aromatic Schiff

base tridentate ligands which form nickel complexes with a 2:1 ligand: nickel ratio (Figure 3.4).

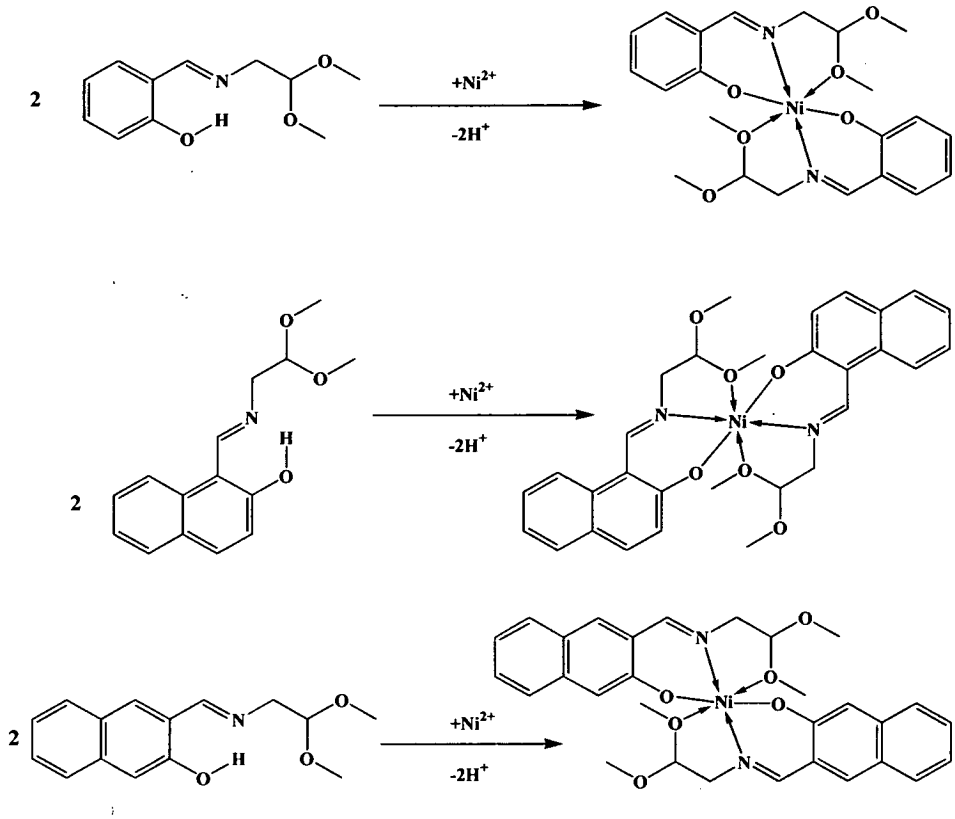

Figure 3.4 Complexation of aromatic Schiff base tridentate ligands with nickel to form 1:2 complexes[6]

This 2:1 ratio enables up to six different isomers to be formed. A schematic representation of the six possible isomers of the nickel complexes with two XNO ligands is shown in Figure 3.5. *E-H* are similar to the sexadentate isomers *A-D* shown in chapter 2 Figure 2.15. *E* and *F* present an X_2O_2 donor set in a "square" plane containing the MXX chelate but differ in having the XNO unit planar in *E* (desirable for conjugation through the imine) but bent in *F*. *G* presents an X_2N_2 donor set in a "square" plane containing MXX and has both ligands bent and the terminal oxygens *trans* to each other. *H* presents an X_2NO donor set in a "square" plane containing the MXX chelate ring with both ligands bent and the terminal oxygen atoms *cis* to each other. *I* and *J* represent the two isomers where the terminal X groups are not *cis* to each other. *I* present a *trans* isomer and *J* a *cis*.

In chapter 2 all the determined crystal structures contained the sexadentate ligands in an isomer analogous to *E*, having planar arrangement of the XNO^- units. Consequently this is expected to be the preferred isomer for complexes of tridentate analogues.

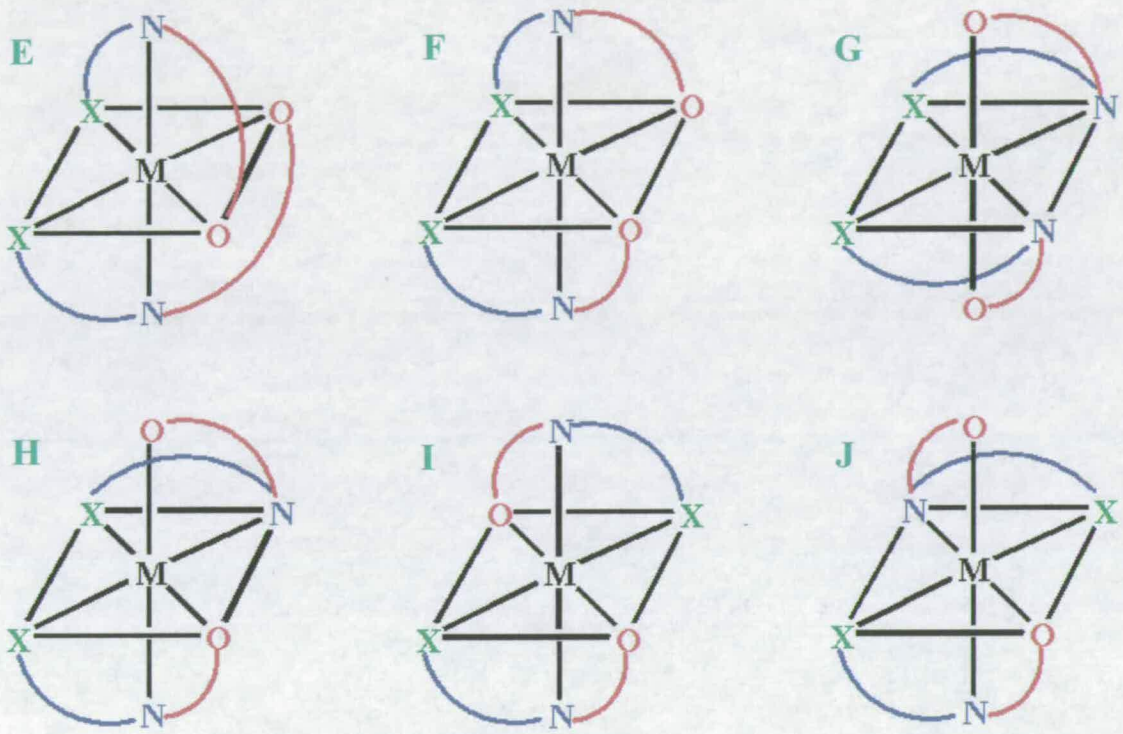

Figure 3.5 Diagram showing the six possible isomeric forms for *psueudo*-octahedral complexes containing two liner tridentate ligands with XNO donors

Various permutations to the tridentate ligand in Figure 3.1 have been synthesised.

1. The terminal X group in Figure 3.3 was varied as in chapter 2 between nitrogen (tertiary amines), oxygen (ether) and sulfur (thioether) to allow the difference between hard (oxygen) and soft (sulfur) donors on extraction to be assessed. As nickel(II) is a borderline metal[7] it should theoretically coordinate to all the above donors.

2. The R^1 group providing the link to the terminal X group (Figure 3.3) was incorporated as either one ethane linkage or an *o*-phenylene linkage for the methyl ether ligands ($X=OCH_3$). The introduction of the aromatic ring should reduce the σ-donor power of both the central imine N-donor and terminal ether group and also increase the rigidity of the donor set.

3. The R^2 group variations were made to alter the solubility of the ligand for use in extraction experiments.

3.2 Synthesis of tridentate ligands

The tridenate ligands in Figure 3.6 were prepared by adaptation of the methods described in chapter 2 (Scheme 3.1).

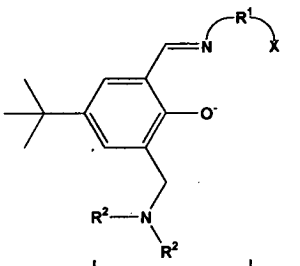

	X	R^1	NR^2_2
30	$N(CH_3)_2$	$-(CH_2)_2-$	piperidine
31	$N(CH_3)_2$	$-(CH_2)_2-$	$N(C_6H_{13})_2$
32	OCH_3	$-(CH_2)_2-$	piperidine
33	OCH_3	$-(CH_2)_2-$	$N(C_6H_{13})_2$
34	OCH_3	*o*-C_6H_4-	piperidine
35	OCH_3	*o*-C_6H_4-	$N(C_6H_{13})_2$
36	SCH_3	*o*-C_6H_4-	piperidine
37	SCH_3	*o*-C_6H_4-	$N(C_6H_{13})_2$

Figure 3.6 Tridentate ligands used in this study

The amines, all commercially available, were reacted with one equivalent of the substituted salicyaldehydes in a Schiff base condensation (Scheme 3.1). The preparation of the substituted salicyaldehydes is described in chapter 2.

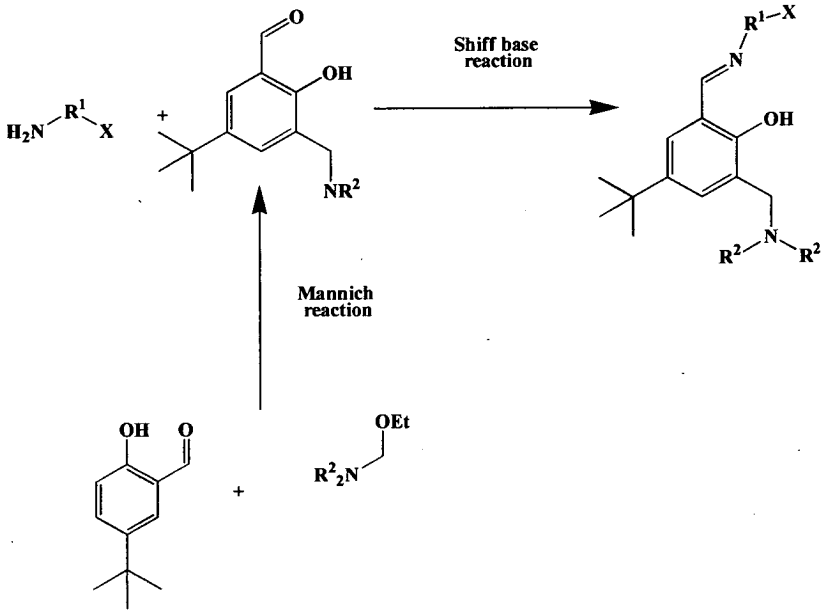

Scheme 3.1 Synthesis of ligands **30-37** (Figure 3.6) via a Mannich reaction followed by a Schiff base condensation

3.3 Characterisation of ligands

All the ligands were characterised by ^{1}H and ^{13}C NMR spectroscopy, FAB mass spectrometry, elemental analysis and for ligands **34** and **36,** by X-ray crystallography.

3.3.1 ^{1}H NMR Spectroscopy

The ^{1}H NMR spectrum (Figure 3.8) of ligand **31** is typical of the soluble di-hexyl substituted ligands. Fifteen proton resonances were observed corresponding to protons type *A-N* (Figure 3.7).

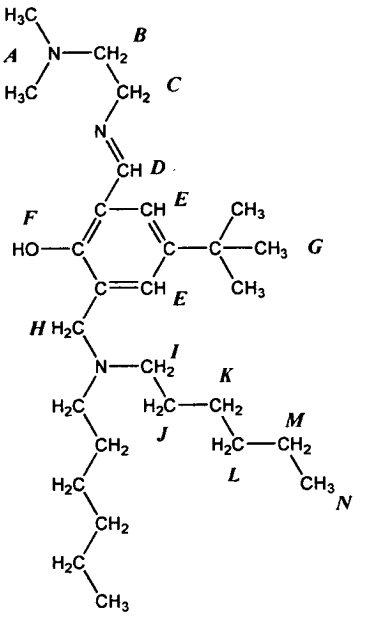

Figure 3.7 Labelling of H-atoms used for assignment of peaks in the ^{1}H spectra of ligand **31**

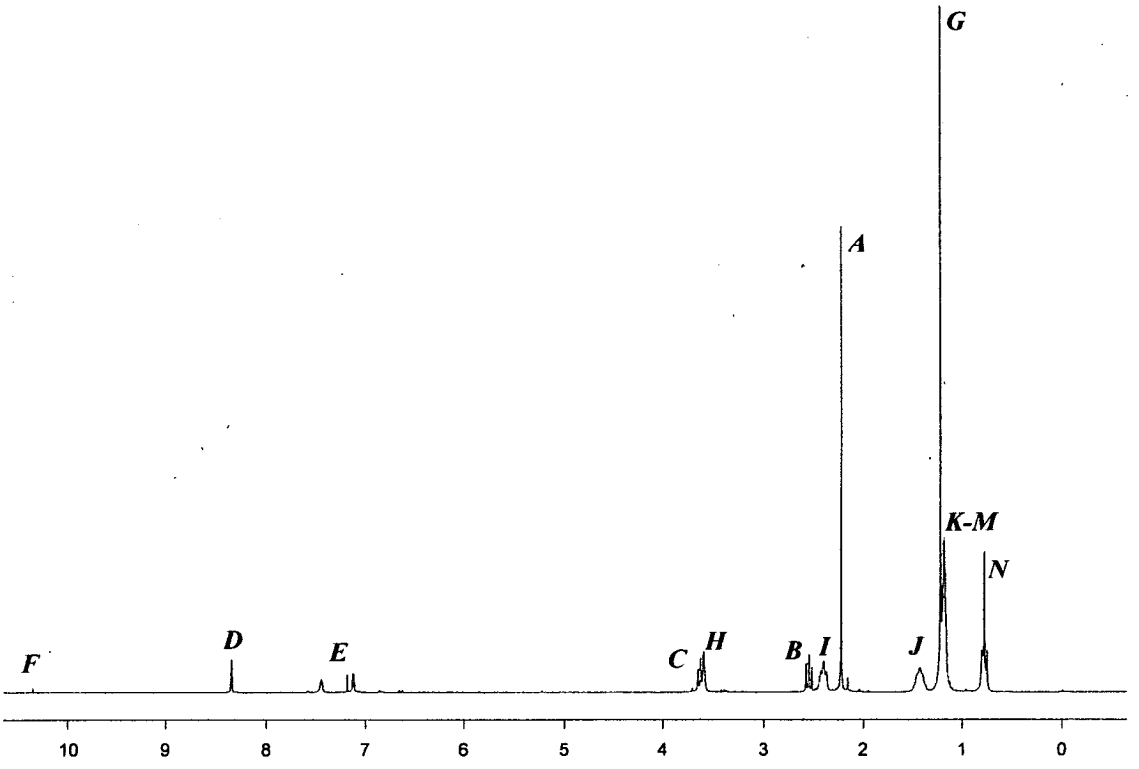

Figure 3.8 250 MHz ^{1}H Spectrum of ligand **31** in $CDCl_3$

The signals assigned to the di-hexyl chains range from 0.79-2.41 ppm with the downfield signal relating to the protons closest to the tertiary amine. The triplet at

0.79 ppm can be assigned to the six methyl protons, *N* and the mutiplet 1.19-1.23 ppm to protons *K, L* and *M*. The broad peak at 1.44 ppm is associated with *J* and the furthest downfield position to *I*. The strongest signal 1.23 ppm found underneath the 1.19-1.23 mutiplet corresponds to the nine methyl protons of the *t*-butyl groups, *G*.

The two singlets at 2.20 and 3.60 ppm represent *A* and *H* respectively. The two triplets at 2.55 and 3.64 ppm both have an integral of two protons relative to the six methyl protons of A and could be assigned to *B* or *C*. The lower field signal (3.64) which is found overlapping the singlet at 3.60 ppm (*H*) is assigned to the methylene group adjacent to the more electronegative imino nitrogen atom (*C*). The resonances from the two aromatic protons *E* appear as two singlets at 7.12 and 7.45 ppm. The remaining two singlets arise from the imine-carbon protons *D* (8.34) and the phenol protons *F* (10.35).

3.3.2 ^{13}C NMR Spectroscopy

Standard ^{13}C spectra in the range 0-220 ppm (Figure 3.10) and DEPT spectra to distinguish between the methyl, methylene, methyne and quarternary carbons were recorded for each ligand. The results for ligand **31** (Figure 3.9) are typical.

The intense resonance at 31.34 ppm was assigned to the methyl carbons *H* and the small resonance at 33.80 ppm to the fulcrum quaternary carbon *G* atoms of the *t*-butyl groups. The methylene carbons *J, K, L, M, N* of the di-hexyl chains gave the signals at 52.39, 31.70, 27.14, 26.73 and 22.55 ppm respectively. The resonance at 13.95 ppm was assigned to the methyl carbons *O* of the di-hexyl chains. The final methyl resonance at 45.71 ppm was assigned to the two methyl carbons *A*. The two signals at 54.00 and 57.99 ppm arise from the methylene groups N-CH_2-CH_2-N, carbons, the lower field resonance corresponding to *C*, adjacent to the imino nitrogen group. The resonance at 59.98 ppm corresponds to the methylene group (*I*) adjacent to the amino nitrogen group.

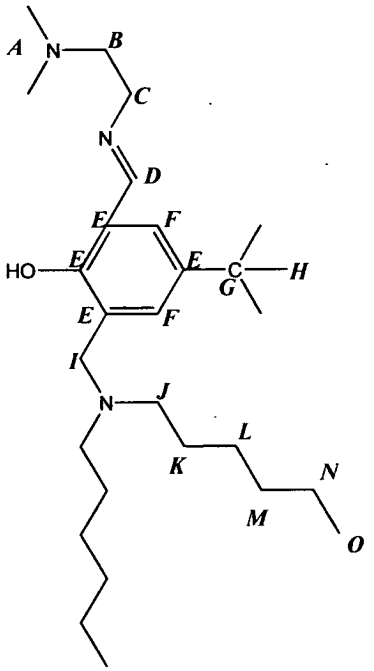

Figure 3.9 Labelling of C-atoms used for assignment of peaks in the ^{13}C spectra of ligand **31**

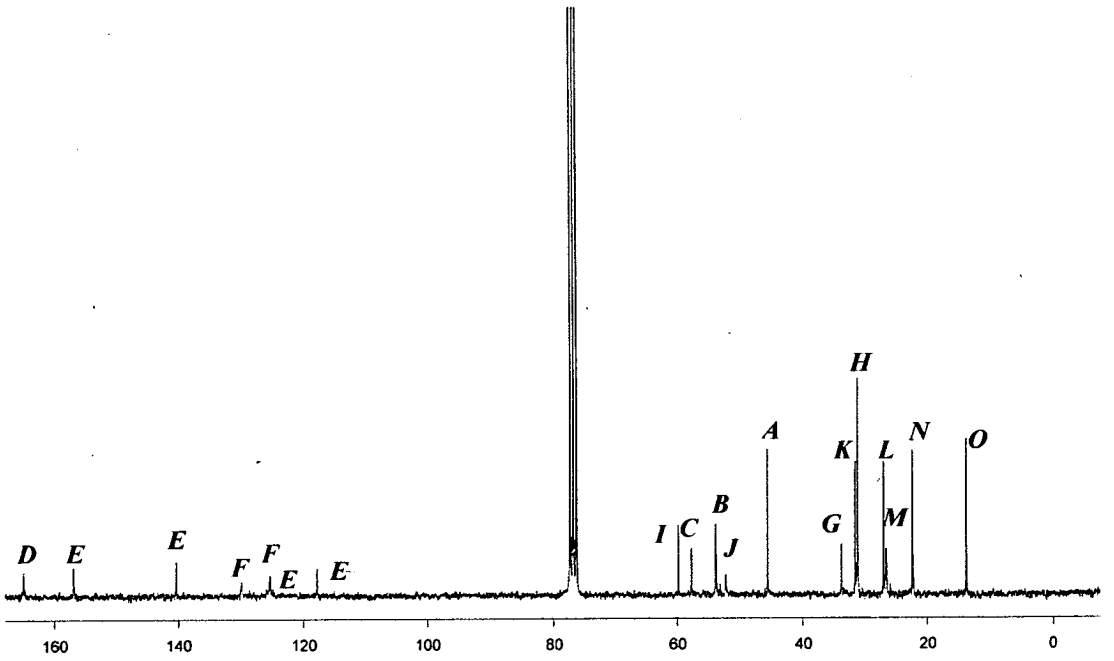

Figure 3.10 The 65 MHz ^{13}C and 65 MHz DEPT spectra of ligand **31** in $CDCl_3$

The aromatic carbons appear in the region 117.89-124.44. The resonances from methyne *F* and quarternary *E*, can be assigned using the DEPT experiment. The resonances arising from the *F* carbons occur at 125.44 and 129.99 ppm. The carbons

E give signals at 117.89, 124.44, 140.52 and 157.02 ppm. The lower field resonance at 164.97 ppm is due to the imine carbon, *D*.

3.3.3 Crystal structures of ligand 34 and 36

Single crystals of ligand **34** and **36** suitable for X-ray structure determination were grown by slow evaporation of a hexane solution. The structures are shown below in Figure 3.11.

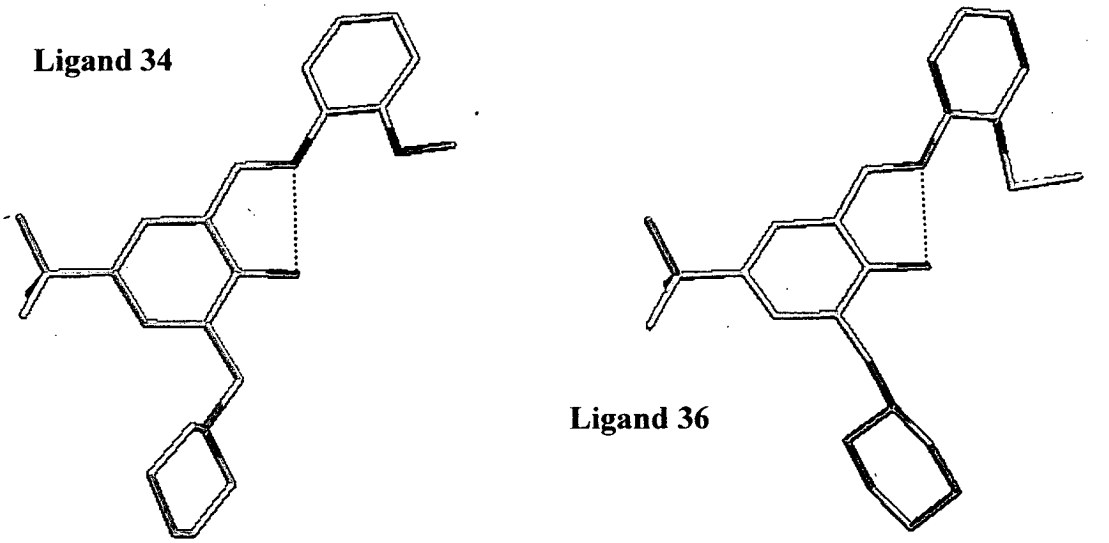

Figure 3.11 The X-ray structure of ligands **34** and **36**

Both molecules are set up in the geometry expected for nickel-complex formation. The phenolic proton in each occupies a site close to where the metal ion will lie, while the lone pairs on the imino nitrogen and the phenoxyether or phenoxythioether, point towards the metal cation binding site (see Figure 3.12). The structures also show the expected strong intramolecular hydrogen bonding between the phenolic proton and the neighbouring imino nitrogen, O(1)-H···N(2), 2.586 Å for ligand **34** and 2.610 Å for ligand **36**.

E give signals at 117.89, 124.44, 140.52 and 157.02 ppm. The lower field resonance at 164.97 ppm is due to the imine carbon, *D*.

3.3.3 Crystal structures of ligand 34 and 36

Single crystals of ligand **34** and **36** suitable for X-ray structure determination were grown by slow evaporation of a hexane solution. The structures are shown below in Figure 3.11.

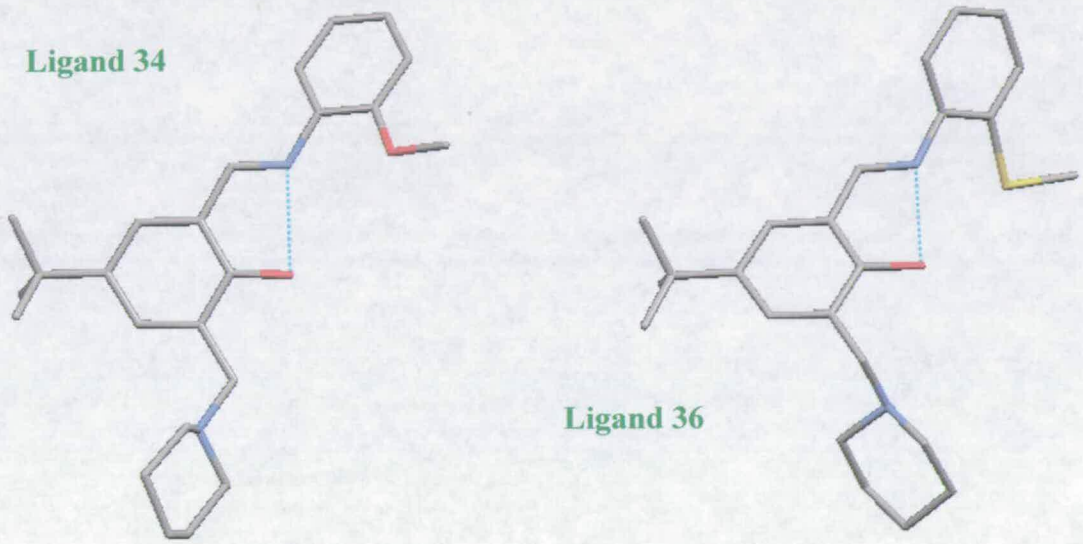

Figure 3.11 The X-ray structure of ligands **34** and **36**

Both molecules are set up in the geometry expected for nickel-complex formation. The phenolic proton in each occupies a site close to where the metal ion will lie, while the lone pairs on the imino nitrogen and the phenoxyether or phenoxythioether, point towards the metal cation binding site (see Figure 3.12). The structures also show the expected strong intramolecular hydrogen bonding between the phenolic proton and the neighbouring imino nitrogen, O(1)-H···N(2), 2.586 Å for ligand **34** and 2.610 Å for ligand **36**.

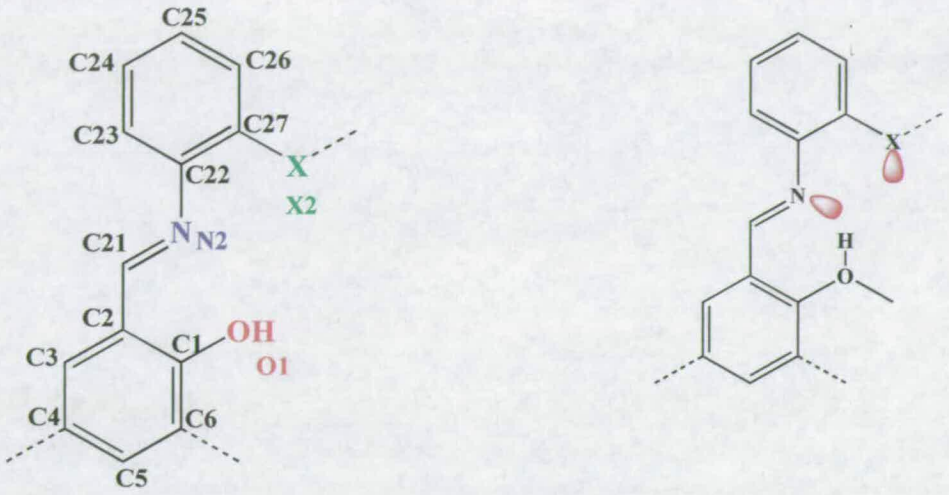

Figure 3.12 Atom labelling scheme and location of the phenolic "proton" relative to the lone pairs on the NOX^- donor set for ligand **34** (X=O) and **36** (X=S)

The sexadentate ligand **5** (side "*A*") (chapter 2) has an ONX chelating unit [O(1), C(1), C(2), C(21), N(2), C(22), C(27) and X(2)] (where X=O) that is basically flat (section 2.4.3). When we compare this to ligands **34,** which is equivalent to one side of ligand **5**, and ligand **36** we find this is not the case. The ONX planes are defined in Table 3.1 and displayed in Figure 3.13, where it can be seen that rotation along the N2-C22 bond has resulted in the phenylene rings being twisted out of the plane.

Table 3.1 ONX plane on Ligand **34** and **36**

Ligand	Atoms	Deviation from the least squares plane	
		Maximum (Å)	Mean (Å)
34	O(1), C(1), C(2), C(21), N(2), C(22), C(27), O(2)	0.2766 O(1) –0.3288 O(2)	O.2051
36	O(1), C(1), C(2), C(21), N(2), C(22), C(27), S(2)	0.6823 S(2) -0.6102 O(1)	0.3770

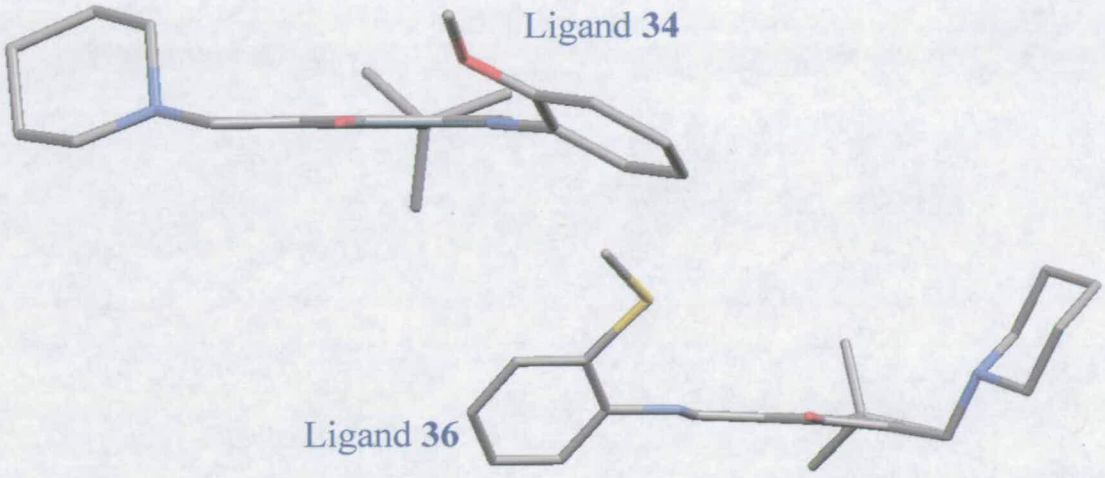

Figure 3.13 Rotation along the N(2)-C(22) bond resulting in the phenylene rings being twisted out of the ONX plane for ligand **34** and **36**

One reason why the ONX planes of ligands **34** and **36** aren't *pseudo*-planar, as in the sexadentate ligand, could be that each tridentate ligand only has one H-bond compared to the more preorganised *pseudo*-macrocyclic ligand **5.** Side "*A*" of ligand **5** is held rigidly planar by two intramolecular hydrogen-bonds (see section 2.4.3)

A second reason for the twisting of the ONX plane in ligands **34** and **36** could be the result of steric hindrance. This can be demonstrated by comparing the distance between the terminal donor atom [O(2)] and the phenolic proton of ligand **5** (2.477 Å) with the Van der Waals radii of the two atoms (1.4 and 1Å respectively) such that when in the same plane would almost touch. Consequently in the less preorganised tridentate ligands, displacement of the [X(2)] atom out of the ONO plane could be more favourable.

When we compare the distance of the terminal donor atom (O2 or S2) from the salicylaldimine plane [O(1), C(1), C(2), C(3), C(4), C(5), C(6), C(61), N(2)] in ligands **34** and **36**, we see that S(2) in ligand **36** (2.08 Å) is further from the plane than O(2) in ligand **34** (1.08 Å). This suggests the steric hindrance explanation for derivatives of the chelating sequence from plannitty as sulfur has a larger atomic radius (1.8 Å) than oxygen.

3.4 Synthesis of nickel salt complexes

Fewer neutral species can be formed when a combination of just one tridentate ligand and nickel sulfate is considered.

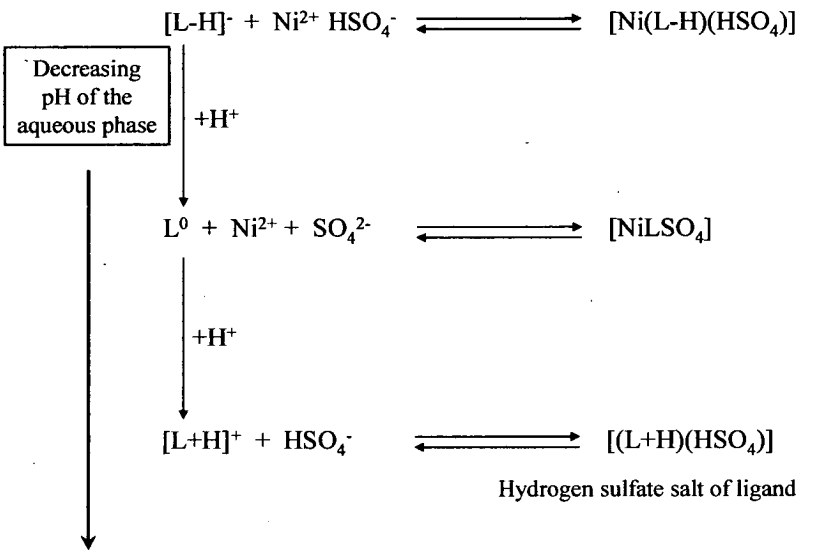

Figure 3.14 Charge neutral species which can be formed from a single molecule of the tridentate ligands **30-37** in solvent extraction of $NiSO_4$ with variation of pH of the aqueous phase

Ligands **31**, **33**, **35** and **37** (Figure 3.6) were used in extraction experiments (see section 3.5). In order to confirm that these donor sets readily form nickel(II) complexes, their piperidino analogues **30**, **32**, **34** and **36** were reacted with half mole equivalent of nickel(II) sulfate or chloride or acetate in methanol and where possible complexes were isolated and recrystallised as described in section 3.7.4. Complexes **38-49** which were readily prepared by these methods are listed in Table 3.2.

Table 3.2 Complexes of tridentate ligands

Abbreviation	**38**	**39**	**40**
Complex	$[Ni(\mathbf{30})_2(SO_4)]$	$[Ni(\mathbf{30})_2Cl_2]$	$[Ni(\mathbf{30})_2(C_2H_3O_2)_2]$

41	**42**	**43**	**44**
$[Ni(\mathbf{32})_2(SO_4)]$	$[Ni(\mathbf{32})_2Cl_2]$	$[Ni(\mathbf{32})_2(C_2H_3O_2)_2]$	$[Ni(\mathbf{34})_2(SO_4)]$

45	**46**	**47**	**48**
$[Ni(\mathbf{34})_2Cl_2]$	$[Ni(\mathbf{34})_2(C_2H_3O_2)_2]$	$[Ni(\mathbf{36})_2(SO_4)]$	$[Ni(\mathbf{36})_2Cl_2]$

49
$[Ni(\mathbf{36})_2(C_2H_3O_2)_2]$

The complexes were investigated by ^1H NMR, mass spectrometry, IR spectroscopy UV-Vis spectroscopy and elemental analysis.

3.4.1 ^1H NMR spectroscopy

^1H NMR spectroscopy is useful since it can be used to give an insight into the geometry of the nickel. The non-coordinating solvent deuterated chloroform was used to run the ^1H NMR spectra as it would not alter the coordination sphere. Complexes **41** and **44** were insoluble and **42** very quickly precipitated out as very fine needle shaped crystals. Hence NMR spectra could not be obtained for these complexes.

All the ^1H NMR spectra obtained (i.e. for **38**, **39**, **40**, **42**, **43**, **45**, **46**, **47**, **48**, **49**) were broadened, some to greater extents than others, indicating formation of paramagnetic complexes. The simplest spectrum was recorded for complex **40**. Figure 3.15 shows the free ligand (**30**) followed by the broadened nickel chloride complex (**40**). The complex spectrum is significantly spread out and broadened relative to the free ligand. The peaks relating to the protons nearest to the central metal centre are likely to be affected (shifted and broadened) the most but full assignement of the complex has not been successful.

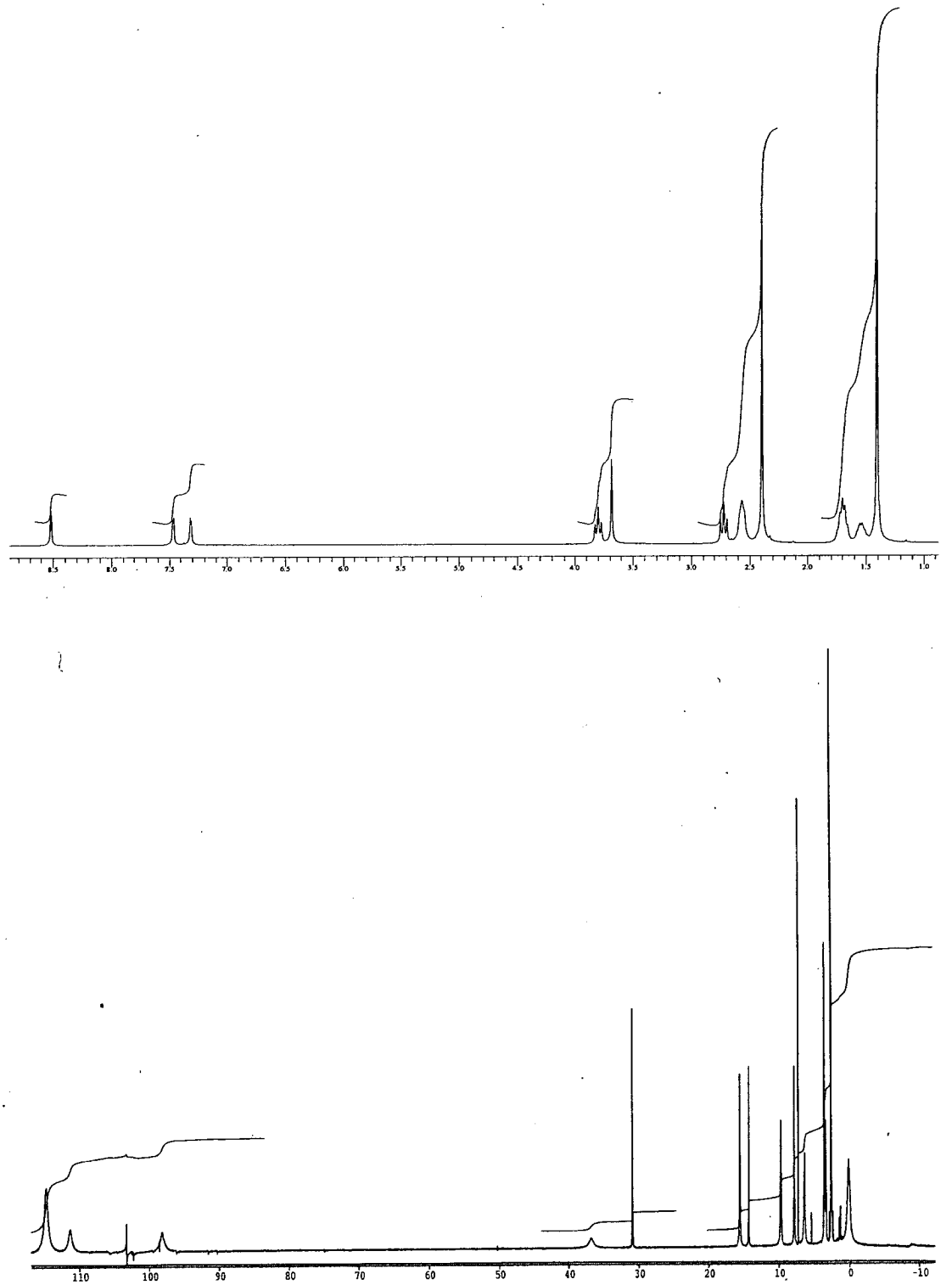

Figure 3.15 ^{1}H NMR spectrum of ligand **30** (above) and complex **40** (below)

The broadening of the NMR spectra is consistent with at least some of each complex being present as high spin six coordinate pseudo-octahedral or high spin five coordinate complexes.

3.4.2 IR Spectroscopy

IR spectroscopy was used to confirm the presence of a sulfate, or acetate anion in the complexes.

The sulfate and acetate complexes listed in Table 3.2 show bands in regions expected[8] 1130-1080 and 1610-1550 cm^{-1} respectively.

All the complexes also show a shifting in the weak band, corresponding to the C=N stretch[8] of the imine group, to a lower energy, in comparison to the free ligands.

3.4.3 Mass Spectrometry

Mass spectrometry of solid samples using Fast Atomic Bombardment (FAB) provide evidence for formation of the "nickel-only" or "nickel salt" complexes shown in Table 3.2.

All spectra of the nickel sulfate complexes in Table 3.2 show a large number of fragmentation peaks. The most intense peak always represents a $[NiLSO_4]^+$ ion, suggesting complexes with a ligand: nickel ratio of 1:1 have been formed. It must also be noted that for all spectra there are a large number of fragment peaks which have a ligand: nickel ratio of 2:1, but only complexes **41** and **47** show the desired $[NiL_2SO_4]^+$ ion peak.

As with the spectra obtained for nickel sulfate complexes, all the nickel chloride complexes have a molecular ion peak which represents a $[NiLCl]^+$ ion. For complexes **42**, **45** and **48** there were numerous fragments peaks, but for complex **40** the only fragment peaks with a higher mass/charge (m/z) ratio than $[NiLCl]^+$ are very

small (<4%). These results suggest that as above complexes formed with nickel chloride have a 1:1 (ligand: nickel) ratio.

Unlike the sexadentate systems, described in chapter 2, and the tetradentate ligands,[9] studied previously in Edinburgh, nickel complexes of **30**, **32**, **34** and **36** appear to bind acetate. All have an intense peak corresponding to a $[NiL_2(C_2H_3O_2)]^+$ ion and in some cases the molecular ion $[NiL_2(C_2H_3O_2)_2]^+$ appears as a weak peak. This is an unexpected result as complexes made from the analogous sexadentate and tetradentate ligands by reaction with nickel acetate followed by treatment with base produced "nickel-only" complexes.

The results from mass spectrometry and IR spectroscopy, suggest that nickel complexes **38**, **41**, **44** and **47** involve a sulfate anion and **40**, **43**, **46** and **49** an acetate anion(s). Mass spectrometry indicates that the nickel complexes **39**, **42**, **45** and **48** all include chloride anion(s).

3.4.4 X-Ray Crystallography

Although the solid state structures of complexes often bear little relation to their behaviour in solution, some information on the propensity of these ligands to form the desired octahedral motif can be obtained. Ideally crystal structures of the nickel bound to two ligands in an octahedral environment were required to help understand the type of coordination sphere nickel(II) can adopt in extraction.

Single crystals of nickel chloride (**39** and **48**) and nickel acetate complexes (**49**) were grown by various methods. Unfortunately, the crystals either diffracted weakly or did not produce a data set of sufficient quality to enable the structure to be determined.

A sexadentate nickel chloride complex **26** (section 2.6.1.4) shows the chlorides bound to the two pendant tertiary amines. Dr. David Henderson from The University of Edinburgh has obtained a second nickel chloride crystal using the previously made

tetradentate ligand[10] showing a five coordinate trigonal bipyramidal nickel where the fifth donor is a chloride anion (Figure 3.16).

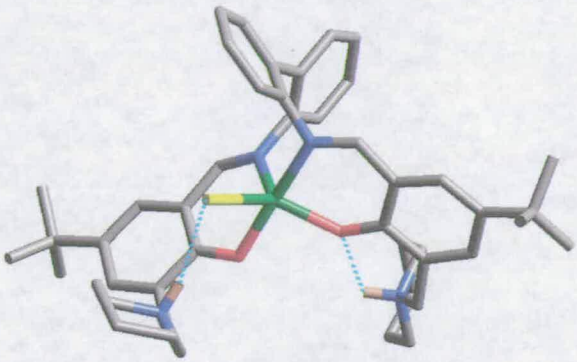

Figure 3.16 Crystal structure (N,N′-bis (5-(t-butyl)-3-(piperidinylmethyl)salicylidene)-2,2′-diphenyldiamine)-chloro-nickel(II)

As discussed earlier it is likely that either two tridentate ligands will coordinate the nickel in a 2:1 (ligand: nickel) ratio or act as independent tridentate ligands. For the nickel chloride complexes it is possible that five coordinate complexes with a nickel: ligand ratio of 1:1 have been formed, where three donor atoms are from the ligand and two chloride ions present in the inner coordination sphere (Figure 3.17).

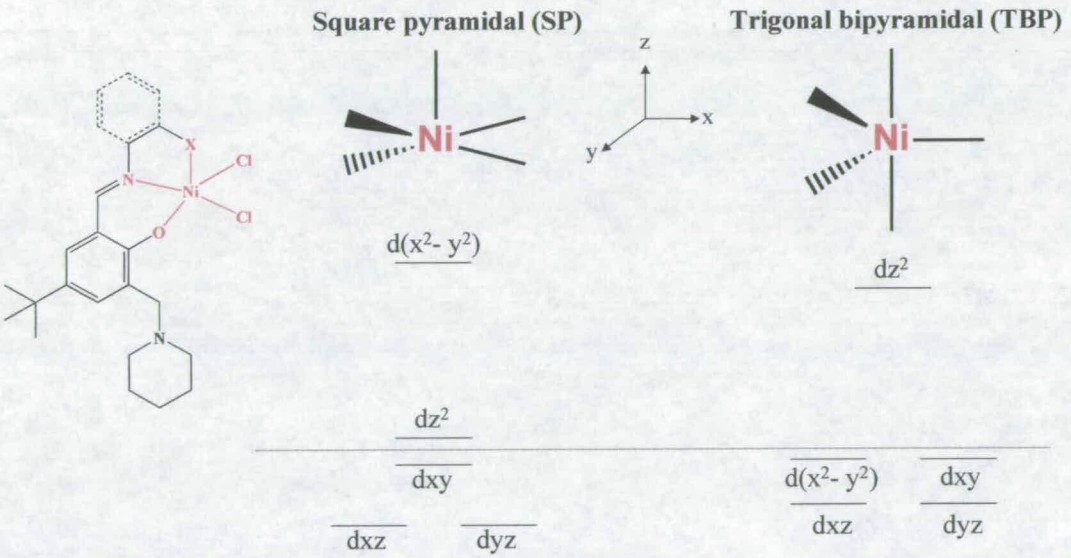

Figure 3.17 Schematic representations of five coordinate nickel chloride complexes with square based pyramidal and trigonal bipyramidal configurations[11] and orbital diagrams

A number of crystal structures of five coordinate chloro-nickel(II)complexes have been reported.[12-36] An example[36] is shown in Figure 3.18 which has an $N_3Cl_2^{2-}$ donor set in a trigonal bipyramdal configuration.

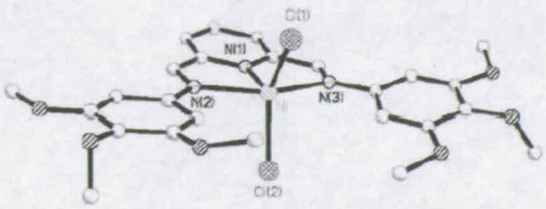

Figure 3.18 Crystal structure of dichloro-(2,6-bis((3,4,5-trimethyoxyphenyl)iminoethyl)pyridine-nickel(II)[36]

3.4.5 Electronic spectroscopy

Comparing the UV-Vis spectra of nickel, sulfate, chloride and acetate complexes formed with each ligand it should be possible to define whether the attendant anion(s) is present in the inner coordination sphere and interacting with the nickel cation. As with the NMR studies chloroform was used, as it is non-coordinating solvent.

All the complexes made with ligand **30** have a similar two band envelope at *ca.* 240 and 370 nm as do the complexes made with the other aliphatic backboned ligand **32** (Figure 3.19). Different spectra are seen for the complexes of the aromatic backboned ligands, **34** and **36** which have four and three band envelopes respectively.

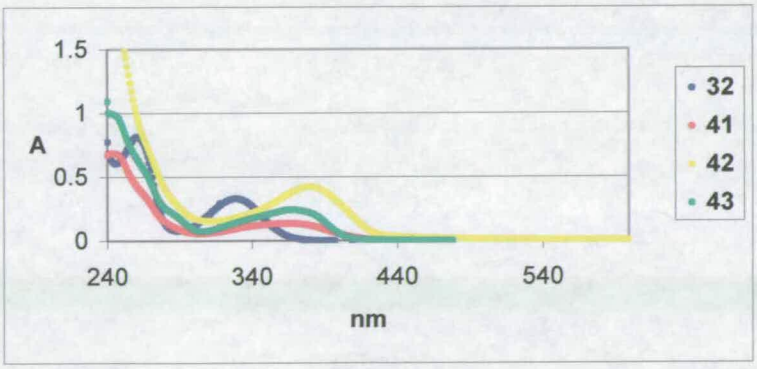

Figure 3.19 UV-Vis spectra of chloroform solutions of ligands **32** and complexes **41, 42** and **43**

3.4.6 Elemental analysis

Elemental analysis was attempted as a method to determine the composition of the complexes. As there were too many variables, for example:

- The ligand: metal: anion ratio.
- Technical difficulties within the University of Edinburgh Microanalytical service, which were unresolved at time of writing.
- The nature of the complexes, which often contain unknown quantities of the solvent of crystallisation as seen in the crystal structures of the complexes **13**, **23**, **26**, **27**, **28** and **29** (Appendix II).

The elemental analysis results therefore could not be relied upon to determine composition of the complexes.

3.5 Solvent extraction

As for the sexadentate ligands, "greasy" di-hexyl ligands (**31**, **33**, **35** and **37**) were used to measure the efficacy of the ligands to extract nickel and sulfate from an aqueous feed into an organic phase.

The procedure described in chapter 2 (section 2.7) was used where by a 0.01 M solution of ligand, in chloroform, was stirred for 17 hours with an equal volume of an aqueous 1 M nickel sulfate solution. The percentage loaded was calculated for the uptake of one nickel or sulfate by one ligand.

Unfortunately as with the sexadentate systems none of the analogous tridentate ligands exhibited significant nickel loading. For ligands **33**, **35** and **37** no uptake of nickel is observed. Ligand **31** is the "best" extractant with nickel uptake of 7%.

3.6 Conclusion

The aim of this chapter was to design and synthesis tridentate ligands for the extraction of nickel sulfate via the formation of 2:1 complexes (ligand: nickel) which would bind the nickel and sulfate in discrete sites.

Four ligands types, have been successfully designed, synthesised and characterised. The ligands have been used to form a range of nickel cation and inorganic anion(s) complexes with various nickel(II) salts (sulfate, chloride and acetate). The ^{1}H NMR spectra point to the formation of paramagnetic nickel(II) complexes. IR spectroscopy shows that sulfate or acetate anions are present in the complexes. Mass spectroscopy indicates that complexes containing at least one ligand, one nickel cation and one anion are formed. In conclusion the most likely ligand: nickel ratio is 2:1, where the nickel is found in a *pseudo*-octahedral coordination geometry with no interaction from the attendant anion(s) (sulfate, chloride and acetate). Hence complexes with the required structure have been formed and could be used in the circuit described in chapter 1 (section 1.7).

Solvent extraction studies show very low nickel uptake, probably due to the ligands being weak extractants with slow complexation kinetics. Therefore, even though solid state nickel complexes can be formed with tridentate and sexadentate ligands, their use as extractants in commercial circuits is not viable. Therefore, the ability of the ligands to complex other divalent metal salts has been studied (chapter 4).

3.7 Experimental

3.7.1 Instrumentation

Elemental analysis was performed on a Perkin Elmer 2400 elemental analyser or a Carlo Erba 1108 Elemental analyser. The infra-red spectra were obtained on a Jasco FT/IR 410 Fourier Transform IR spectrometer as potassium bromide discs. ^{1}H and ^{13}C NMR spectra were run on a Bruker AC250 spectrometers. Chemical shifts (δ)

are reported in parts per million (ppm) relative to residual solvent protons as internal standards. Fast Atom Bombardment (FAB) mass spectra were obtained on a Kratos MS50TC spectrometer. Electronic absorption spectroscopy was performed on a Perkin Elmer Lambda 900 UV/VIS/NIR spectrometer. Inductively coupled plasma atomic emission spectroscopy (ICP-AES) analysis was performed on a Thermo Jarrell Ash IRIS ICP-OES spectrometer.

3.7.2 Solvent and reagent pre-treatment

All reagents and solvents were commercially available (Acros or Aldrich) and were used as received. Solvents used for analytical purposes (NMR, MS, ICP) were of spectroscopic grade. ICP AES standards were purchased from Alfa Asar.

3.7.3 Ligands

Ligand 30

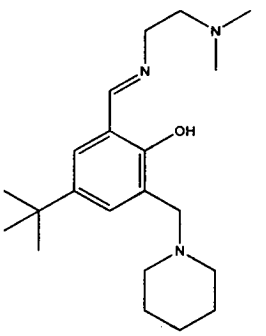

To a stirred solution of **HPTB** (2.00 g, 7.30 mmol) in diethylether (20 cm^3) was added a solution of N,N-dimethylethylenediamine (0.64 g, 7.30 mmol) in ethanol (15 cm^3). The orange solution was stirred overnight, concentrated *in-vacuo* and recrystallised from hexane to yield a yellow solid (2.12 g, 84%). Found: C, 73.14; H, 10.25; N, 12.23. Calc. for $C_{21}H_{35}N_3O$: C, 73.00; H, 10.21; N, 12.61%. ^1H NMR ($CDCl_3$, 250 MHz): δ 1.40 (m, 9H, CH_3 ($C(CH_3)$), δ 1.54 (bp, 2H, $NCH_2CH_2\underline{CH_2}$ (pip)), δ 1.69 (bp, 4H, $NCH_2\underline{CH_2}CH_2$ (pip)), δ 2.39 (s, 3H, $N(CH_3)_2$), δ 2.56 (bp, 4H, $N\underline{CH_2}CH_2CH_2$ (pip)), δ 2.71 (t, 2H, $NCH_2\underline{CH_2}N$), δ 3.68 (s, 2H, $ArCH_2N$), δ 3.80 (t, 2H, $N\underline{CH_2}CH_2N$) δ 7.31 (s, 1H, Ar-CH), δ 7.47 (s, 1H, Ar-CH), δ 8.52 (s, 1H, N=CH). ^{13}C NMR ($CDCl_3$): δ 24.2 ($NCH_2CH_2\underline{CH_2}$ (pip)), δ 25.8 ($NCH_2\underline{CH_2}CH_2$

(pip)), δ 31.3 (CH_3 ($C(CH_3)$), δ 33.8 (C ($C(CH_3)$), δ 45.6 (CH_3 ($N(CH_3)_2$), δ 54.2 ($N\underline{CH_2}CH_2CH_2$ (pip)), δ 57.3 ($NCH_2\underline{CH_2}N(CH_3)_2$), δ 57.8 ($N\underline{CH_2}CH_2N(CH_3)_2$), δ 59.9 ($ArCH_2N$), δ 118.0 (Ar-C), δ 124.4 (Ar-C)), δ 125.8 (Ar-CH), δ 130.5 (Ar-CH), δ 140.3 (Ar-C), δ 157.2 (Ar-C), δ 165.0 (C=N). ν_{max}/cm^{-1} 2953s (C-H), 1612w (C=N). λ_{max} (ε)/nm (M^{-1} cm^{-1}) ($CHCl_3$) 261 (11500), 329 (4170). MS (FAB, NOBA) *m/z* 345 (MH^+ 83.6%).

Ligand 31

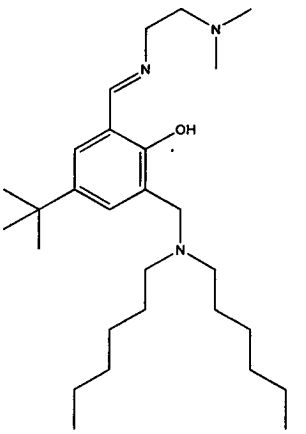

To a stirred solution of **HDTB** (2.79 g, 7.45 mmol) in diethylether (20 cm^3) was added a solution of N,N-dimethylethylenediamine (0.65 g, 7.45 mmol) in ethanol (15 cm^3). The orange solution was stirred overnight and concentrated *in-vacuo* to yield a yellow oil (3.28 g, 99%). This was used without further purification. Found: C, 74.39; H, 11.58; N, 9.39. Calc. for $C_{28}H_{51}N_3O$: C, 75.45; H, 11.53; N, 9.43%. ^1H NMR ($CDCl_3$, 250 MHz): δ 0.79 (t, 6H, CH_3(hexyl)), δ 1.23 (s, 9H, $C(CH_3)_3$), δ 1.19-1.23 (m, 12H, CH_2 (hexyl)), δ 1.44 (m, 4H, $NCH_2\underline{CH_2}$ (hexyl)), δ 2.20 (s, 6H, $N(CH_3)_2$), δ 2.41 (t, 4H, NCH_2 (hexyl)), δ 2.55 (t, 2H, $NCH_2\underline{CH_2}N(CH_3)_2$), δ 3.60 (s, 2H, $ArCH_2N$); δ 3.64 (t, 2H, $N\underline{CH_2}CH_2N(CH_3)_2$), δ 7.12 (m, H, ArCH), δ 7.45 (m, H, ArCH), δ 8.34 (s, H, N=CH), δ 10.35 (s, H, OH). ^{13}C NMR ($CDCl_3$): δ 14.0 (CH_3 (hexyl)), δ 22.6 ($NCH_2CH_2CH_2CH_2\underline{CH_2}$ (hexyl)), δ 26.7 ($NCH_2CH_2CH_2\underline{CH_2}$ (hexyl)), δ 27.1 ($NCH_2CH_2\underline{CH_2}$ (hexyl)), δ 31.3 ($C(\underline{CH_3})_3$), δ 31.7 ($NCH_2\underline{CH_2}$ (hexyl)), δ 33.8 ($\underline{C}(CH_3)$, δ 45.7 ($N(CH_3)_2$), δ 52.4 ($N\underline{CH_2}$ (hexyl)), δ 54.0 ($NCH_2\underline{CH_2}N(CH_3)_2$), δ 57.99 ($N\underline{CH_2}CH_2N(CH_3)_2$), δ 59.98 ($ArCH_2N$), δ 117.89 (Ar-

C), δ 124.4 (Ar-C), δ 125.4 (Ar-CH), δ 130.0 (Ar-CH), δ 140.5 (Ar-C), δ 157.0 (Ar-C), δ 165.0 (C=N). MS (FAB, NOBA) *m/z* 445 (MH^+ 61.4%).

Ligand 32

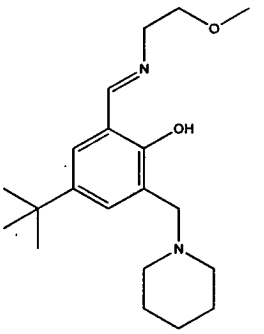

Using the method for ligand **30**, but using **HPTB** (2.00 g, 7.30 mmol) and 2-methoxyethylamine (0.55 g, 7.30 mmol) produced an orange solid (1.52 g, 63%). Found: C, 72.25; H, 10.00; N, 8.28. Calc. for $C_{20}H_{32}N_2O_2$: C, 72.25; H, 9.78; N, 8.43%. ^{1}H NMR ($CDCl_3$, 250 MHz): δ 1.22 (s, 9H, CH_3), δ 1.50 (m, 2H, $NCH_2CH_2\underline{CH_2}$ (pip)), δ 1.53 (m, 4H, $NCH_2\underline{CH_2}CH_2$ (pip)), δ 2.39 (bp, 4H, $N\underline{CH_2}CH_2CH_2$ (pip)), δ 3.28 (s, 3H, OCH_3), δ 3.55 (s, 2H, $ArCH_2N$), δ 3.57 (t, 2H, $N\underline{CH_2}CH_2O$), δ 3.66 (t, 2H, $NCH_2\underline{CH_2}O$), δ 7.15 (m, H, ArCH), δ 7.30 (m, H, ArCH), δ 8.33 (s, H, N=CH), δ 10.35 (s, H, OH). ^{13}C NMR ($CDCl_3$): δ 23.7 ($NCH_2CH_2\underline{CH_2}$ (pip)), δ 24.2 ($NCH_2\underline{CH_2}CH_2$ (pip)), δ 31.3 ($C(\underline{CH_3})_3$), δ 33.8 ($\underline{C}(CH_3)$), δ 54.3 ($N\underline{CH_2}CH_2CH_2$ (pip)), δ 57.3 ($N\underline{CH_2}CH_2O$), δ 58.8 (OCH_3), δ 59.2 ($ArCH_2N$), δ 71.8 ($NCH_2\underline{CH_2}O$), δ 118.0 (Ar-C), δ 125.0 (Ar-C), δ 125.9 (Ar-CH), δ 130.5 (Ar-CH), δ 140.3 (Ar-C), δ 157.1 (Ar-C), δ 165.7 (C=N). ν_{max}/cm^{-1} 2933s (C-H), 1581w (C=N). λ_{max} (ε)/nm (M^{-1} cm^{-1}) ($CHCl_3$) 261 (7600), 329 (3100) MS (FAB, NOBA) *m/z* 332 (MH^+ 77.2%).

Ligand 33

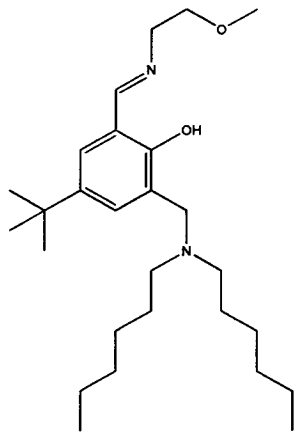

Using the method for ligand **31**, but using **HDTB** (3.01 g, 7.98 mmol) and 2-methoxyethylamine (0.60 g, 7.98 mmol) produced an orange oil (3.27 g, 95%). This was used without further purification. Found: C, 74.95; H, 11.95; N, 7.46. Calc. for $C_{27}H_{48}N_2O_2$: C, 74.95; H, 11.18; N, 6.47%. ^{1}H NMR ($CDCl_3$, 250 MHz): δ 0.79 (t, 9H, CH_3), δ 1.23 (s, 9H, $C(CH_3)_3$), δ 1.19-1.23 (bp, 12H, CH_2 (hexyl)), δ 1.43 (bp, 4H, $NCH_2\underline{CH_2}$ (hexyl)), δ 2.39 (t, 4H, NCH_2 (hexyl)), δ 3.29 (s, 2H, OCH_3), δ 3.59 (s, 2H, $ArCH_2N$), δ 3.59 (t, 2H, $N\underline{CH_2}CH_2O$), δ 3.69 (t, 2H, $NCH_2\underline{CH_2}O$), δ 7.18 (s, H, ArCH), δ 7.42 (s, H, ArCH), δ 8.32 (s, H, N=CH) δ 10.35 (s, H, OH). ^{13}C NMR ($CDCl_3$): δ 14.0 (CH_3 (hexyl)), δ 22.6 ($NCH_2CH_2CH_2CH_2\underline{CH_2}$ (hexyl)), δ 26.8 ($NCH_2CH_2CH_2\underline{CH_2}$ (hexyl)), δ 27.2 ($NCH_2CH_2\underline{CH_2}$ (hexyl)), δ 31.3 ($C(\underline{CH_3})_3$), δ 31.7 ($NCH_2\underline{CH_2}$ (hexyl)), δ 33.9 ($\underline{C}(CH_3)$, δ 52.5 ($N\underline{CH_2}$ (hexyl)), δ 54.1 ($N\underline{CH_2}CH_2O$), δ 58.9 (OCH_3), δ 59.3 ($ArCH_2N$), δ 71.9 ($N\underline{CH_2}CH_2O$), δ 117.9 (Ar-C), δ 125.5 (Ar-CH), δ 130.0 (Ar-CH), δ 132.0 (Ar-C), δ 140.5 (Ar-C), δ 156.9 (Ar-C), δ 165.8 (C=N). MS (FAB, NOBA) *m/z* 432 (MH^+ 64.3%).

Ligand 34

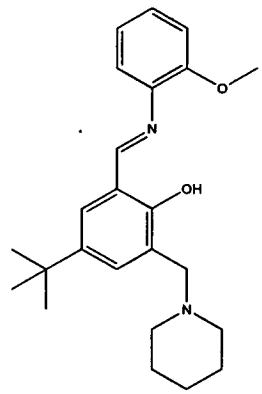

Using the method for ligand **30**, but using **HPTB** ((2.01 g, 7.30 mmol) and o-anisidine (0.90 g, 7.30 mmol) produced an orange solid (2.00 g, 72%). Found: C, 74.92; H, 8.43; N, 7.26. Calc. for $C_{24}H_{32}N_2O_2$: C, 75.75; H, 8.48; N, 7.36%. ^{1}H NMR ($CDCl_3$, 250 MHz): δ 1.60 (s, 9H, CH_3), δ 1.72 (m, 2H, $NCH_2CH_2\underline{CH_2}$ (pip)), δ 1.67 (m, 4H, $NCH_2\underline{CH_2}CH_2$ (pip)), δ 2.74 (bp, 4H, $N\underline{CH_2}CH_2CH_2$ (pip)), δ 3.90 (s, 2H, $ArCH_2N$), δ 4.09 (s, 3H, OCH_3), δ 7.25 (m, H, ArCH), δ 7.45 (m, H, ArCH), δ 8.99 (s, H, N=CH). ^{13}C NMR ($CDCl_3$): δ 24.2 ($NCH_2CH_2\underline{CH_2}$ (pip)), δ 25.9 ($NCH_2\underline{CH_2}CH_2$ (pip)), δ 31.3 ($C(\underline{CH_3})_3$), δ 33.9 ($\underline{C}(CH_3)$, δ 54.3 ($N\underline{CH_2}CH_2CH_2$ (pip)), δ 55.7 (OCH_3), δ 57.7 ($ArCH_2N$), δ 111.5 (Ar-CH), δ 119.0 (Ar-C), δ 119.9 (Ar-CH), δ 120.8 (Ar-CH), δ 124.6 (Ar-C), δ 126,0 (Ar-CH), δ 127.1 (Ar-CH), δ 130.9 (Ar-CH), δ 138.5 (Ar-C), δ 140.7 (Ar-C), δ 152.6 (Ar-C), δ 157.6 (Ar-C), δ 160.8 (C=N). ν_{max}/cm^{-1} 2933s (C-H), 1580w (C=N). λ_{max} (ε)/nm (M^{-1} cm^{-1}) ($CHCl_3$) 275 (14100), 347 (15100). MS (FAB, NOBA) *m/z* 380 (MH^+ 82.8%).

Ligand 35

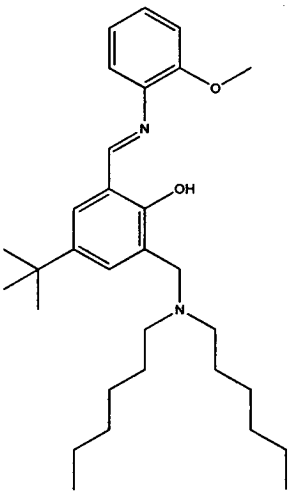

Using the method for ligand **31**, but using **HDTB** (3.20 g, 8.51 mmol) and o-anisidine (2.34 g, 8.51 mmol) produced an orange oil (3.96 g, 97%). This was used without further purification. Found: C, 77.82; H, 10.37; N, 6.02 Calc. for $C_{31}H_{48}N_2O_2$: C, 77.45; H, 10.06; N, 5.83%. ^{1}H NMR ($CDCl_3$, 250 MHz): δ 0.79 (t, 6H, CH_3 (hexyl)), δ 1.26 (s, 9H, $C(CH_3)_3$), δ 1.12-1.26 (m, 12H, CH_2 (hexyl)), δ 1.42 (m, 4H, $NCH_2\underline{CH_2}$ (hexyl)), δ 2.41 (t, 4H, NCH_2 (hexyl)), δ 3.64 (s, 2H, $ArCH_2N$), δ 3.82 (s, 3H, OCH_3), δ 6.63-7.59 (m, 6H, ArCH), δ 8.67 (s, H, N=CH), δ 10.34 (s, H, OH). ^{13}C NMR ($CDCl_3$): δ 14.0 (CH_3 (hexyl)), δ 22.5 ($NCH_2CH_2CH_2CH_2\underline{CH_2}$ (hexyl)), δ 26.9 ($NCH_2CH_2CH_2\underline{CH_2}$ (hexyl)), δ 27.1 ($NCH_2CH_2\underline{CH_2}$ (hexyl)), δ 31.2 ($C(\underline{CH_3})_3$), δ 31.7 ($NCH_2\underline{CH_2}$ (hexyl)), δ 33.9 ($\underline{C}(CH_3)$, δ 53.4 ($N\underline{CH_2}$ (hexyl)), δ 54.1 ($ArCH_2N$), δ 55.7 (OCH_3), δ 111.6 (Ar-CH), δ 118.3 (Ar-C), δ 119.8 (Ar-CH), δ 120.8 (Ar-CH), δ 125.0 (Ar-C),δ 125.5 (Ar-CH), δ 127.0 (Ar-CH), δ 130.4 (Ar-CH), δ 138,6 (Ar-C), δ 140.8 (Ar-C), δ 152.7 (Ar-C), δ 157.4 (Ar-C), δ 160.0 (C=N). MS (FAB, NOBA) *m/z* 480 (MH^+ 72.1%).

Ligand 36

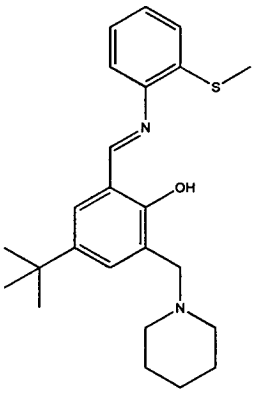

Using the method for ligand **30**, but using **HPTB** (2.00 g, 7.30 mmol) and 2-(methoxythio)aniline (1.01 g, 7.30 mmol) produced a cream solid (1.99 g, 69%). Found: C, 72.56; H, 8.01; N, 7.02. Calc. for $C_{24}H_{32}N_2OS$: C, 72.68; H, 8.13; N, 7.06%. ^{1}H NMR ($CDCl_3$, 250 MHz): δ 1.64 (s, 9H, CH_3), δ 1.77 (bp, 2H, $NCH_2CH_2\underline{CH_2}$ (pip)), δ 1.93 (bp, 4H, $NCH_2\underline{CH_2}CH_2$ (pip)), δ 2.76 (s, 3H, S-CH_3), δ 2.81 (bp, 4H, $N\underline{CH_2}CH_2CH_2$ (pip)), δ 3.98 (s, 2H, $ArCH_2N$), δ 7.41-7.77 (m, 6H, Ar-CH), δ 9.00 (s, 1H, N=CH). ^{13}C NMR ($CDCl_3$): δ 14.6 (S-CH_3), δ 24.1 ($NCH_2CH_2\underline{CH_2}$ (pip)), δ 25.8 ($NCH_2\underline{CH_2}CH_2$ (pip)), δ 31.3 (CH_3 ($C(CH_3)$), δ 33.8 (C ($C(CH_3)$), δ 54.1 ($N\underline{CH_2}CH_2CH_2$ (pip)), δ 57.5 ($ArCH_2N$)), δ 117.2 (Ar-CH), δ 118.8 (Ar-C), δ 124.5 (Ar-C), δ 124.6 (Ar-Cl)), δ 125.0 (Ar-CH), δ 126.2 (Ar-CH), δ 126.7 (Ar-CH), δ 131.2 (Ar-CH), δ 134.4 (Ar-C), δ 140.9 (Ar-C), δ 146.4 (Ar-C), δ 157.2 (Ar-C) δ 161.0 (C=N). ν_{max}/cm^{-1} 2948s (C-H), 1573w (C=N). λ_{max} (ε)/nm (M^{-1} cm^{-1}) ($CHCl_3$) 273 (33700), 362 (16400). MS (FAB, NOBA) *m/z* 396 (MH^+ 88.3%).

Ligand 37

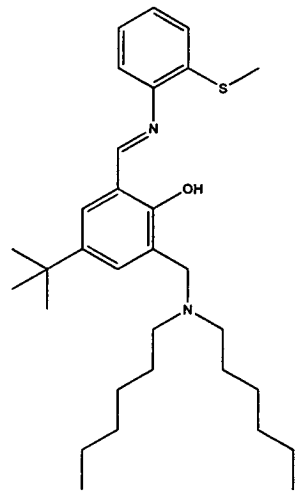

Using the method for ligand **31**, but using **HDNB** (2.91 g, 7,74 mmol) and 2-(methoxythio)aniline (2.13 g, 7.74 mmol) produced an orange oil (3.65 g, 95%). This was used without further purification. Found: C, 71.59; H, 10.10; N, 6.96. Calc. for $C_{31}H_{48}N_2OS$: C, 74.95; H, 9.74; N, 6.38%. ^{1}H NMR ($CDCl_3$, 250 MHz): δ 0.80 (d, 9H, CH_3), δ 1.2 (s, 9H, $C(CH_3)_3$), δ 1.12-1.28 (m, 12H, CH_2 (hexyl)), δ 1.45 (m, 4H, $NCH_2\underline{CH_2}$ (hexyl)), δ 2.40 (s, 3H, SCH_3), δ 2.45 (t, 4H, NCH_2 (hexyl)), δ 3.72 (s, 2H, $ArCH_2N$), δ 6.64-7.59 (m, 6H, ArCH), δ 8.63 (s, H, N=CH) δ 10.35 (s, H, OH). ^{13}C NMR ($CDCl_3$): δ 13.9 (CH_3 (hexyl)), δ 14.6 (SCH_3 (hexyl)), δ 22.5 ($NCH_2CH_2CH_2CH_2\underline{CH_2}$ (hexyl)), δ 26.1 ($NCH_2CH_2CH_2\underline{CH_2}$ (hexyl)), δ 26.9 ($NCH_2CH_2\underline{CH_2}$ (hexyl)), δ 31.2 ($C(\underline{CH_3})_3$), δ 31.5 ($NCH_2\underline{CH_2}$ (hexyl)), δ 34.0 ($\underline{C}(CH_3)_3$), δ 53.4 ($N\underline{CH_2}$ (hexyl)), δ 54.0 ($ArCH_2N$), δ 117.2 (Ar-CH), δ 118.8 (Ar-C), δ 122.3 (Ar-C), δ 123.4 (Ar-CH), δ 124.7 (Ar-CH), δ 125.1 (Ar-CH), δ 126.7 (Ar-CH), δ 129.0 (Ar-C), δ 132.0 (Ar-CH), δ 133.3 (Ar-C), δ 133.5 (Ar-C), δ 141.3 (Ar-C), δ 160.0 (C=N). MS (FAB, NOBA) *m/z* 496 (MH^+ 69.3%).

3.7.4 Nickel complexes

Complex 38

A 2:1 molar ratio of ligand: nickel salt (*c.a.* $3x10^{-4}$ moles) was stirred in methanol (20 cm^3). Colour changes were instantaneous. After removal of the solvent *in-vacuo* the products were recrystallised as indicated and dried in-*vacuo*.

[Ni(**30**)$_2$SO$_4$] MX_n = NiSO$_4$.7H$_2$O. Recrystallisation from CH$_2$Cl$_2$:^{i}Pr$_2$O, gave a green solid (0.15 g, 60%). ν_{max}/cm^{-1} 2955s (C-H), 1552s (C=N), 1117s (SO$_4$). λ_{max} (ε)/nm (M^{-1} cm^{-1}) (CHCl$_3$) 240 (23900), 371 (5000). MS (FAB, NOBA) *m/z* 500 (MH$^+$-**30**, 100%).

Complex 39

Using the method for complex **38** [Ni(**30**)$_2$Cl$_2$] MX_n = NiCl$_2$.6H$_2$O. Recrystallisation from CH$_2$Cl$_2$:^{i}Pr$_2$O, gave a green solid (0.13 g, 55%). ν_{max}/cm^{-1} 2958s (C-H), 1552w (C=N). λ_{max} (ε)/nm (M^{-1} cm^{-1}) (CHCl$_3$) 241 (23700), 371 (5800). MS (FAB, NOBA) *m/z* 438 (MH$^+$-**30**, 100%).

Complex 40

Using the method for complex **38** but after removal of the solvents the complex was washed with an aqueous solution (pH 7.5), extracted into chloroform, and dried in-*vacuo*. [Ni((**30**)$_2$(C$_2$H$_3$O$_2$)$_2$)] MX_n = Ni(C$_2$H$_3$O$_2$)$_2$.4H$_2$O. Extraction gave a dark green solid (0.13 g, 51%). ν_{max}/cm^{-1} 2953s (C-H), 1558m (acetate). λ_{max} (ε)/nm (M^{-1} cm^{-1}) (CHCl$_3$) 241 (24200), 371 (4500). MS (FAB, NOBA) *m/z* 867 (MH$^+$, 100%).

Complex 41

Using the method for complex **38** [Ni(**32**)SO$_4$] MX_n = NiSO$_4$.7H$_2$O. Recrystallisation from CH$_2$Cl$_2$:^{i}Pr$_2$O, gave a green solid (0.15 g, 63%). ν_{max}/cm^{-1} 2953s (C-H), 1544w (C=N), 1116s (SO$_4$). λ_{max} (ε)/nm (M^{-1} cm^{-1}) (CHCl$_3$) 243 (13200), 364 (2600). MS (FAB, NOBA) *m/z* 487 (MH$^+$-**32**, 100%).

Complex 42

Using the method for complex **38** [Ni(**32**)$_2$Cl$_2$] MX_n = NiCl$_2$.6H$_2$O. Recrystallisation from CH$_2$Cl$_2$:^{i}Pr$_2$O, gave a green solid (0.13 g, 60%). ν_{max}/cm^{-1} 2950s (C-H), 1541w (C=N). λ_{max} (ε)/nm (M^{-1} cm^{-1}) (CHCl$_3$) 245 (13100), 380 (3400). MS (FAB, NOBA) *m/z* 425 (MH$^+$-**32**, 100%).

Complex 43

Using the method for complex **40** [Ni((**32**)$_2$($C_2H_3O_2$)$_2$)] MX_n = Ni($C_2H_3O_2$)$_2$.4H_2O. Extraction gave a dark green solid (0.15 g, 60%). ν_{max}/cm^{-1} 2947s (C-H), 1562m (acetate). λ_{max} (ε)/nm (M^{-1} cm^{-1}) ($CHCl_3$) 240 (12600), 372 (2800). MS (FAB, NOBA) *m/z* 841 (MH^+, 73.0%).

Complex 44

Using the method for complex **38** [Ni(**34**)SO_4] MX_n = $NiSO_4$.7H_2O. Recrystallisation from CH_2Cl_2:$^iPr_2O$, gave a yellow solid (0.13 g, 52%). ν_{max}/cm^{-1} 2953s (C-H), 1541w (C=N), 1118s (SO_4). λ_{max} (ε)/nm (M^{-1} cm^{-1}) ($CHCl_3$) 243 (14600), 326 (8900), 344 (8900), 425 (5900). MS (FAB, NOBA) *m/z* 535 (MH^+-**34**, 100%).

Complex 45

Using the method for complex **38** [Ni(**34**)$_2$$Cl_2$] MX_n = $NiCl_2$.6H_2O. Recrystallisation from CH_2Cl_2:$^iPr_2O$, gave a yellow solid (0.13 g, 48%). ν_{max}/cm^{-1} 2953s (C-H), 1541w (C=N). λ_{max} (ε)/nm (M^{-1} cm^{-1}) ($CHCl_3$) 243 (14300), 326 (8500), 344 (9200), 425 (8800). MS (FAB, NOBA) *m/z* 473 (MH^+-**34**, 100%).

Complex 46

Using the method for complex **40** [Ni({**34**)$_2$($C_2H_3O_2$)$_2$)] MX_n = Ni($C_2H_3O_2$)$_2$.4H_2O. Extraction gave a brown solid (0.16 g, 57%).ν_{max}/cm^{-1} 2954s (C-H), 1560m (acetate). λ_{max} (ε)/nm (M^{-1} cm^{-1}) ($CHCl_3$) 243 (14200), 326 (8400), 344 (7200), 425 (6700). MS (FAB, NOBA) *m/z* 935 (MH^+, 50.9%).

Complex 47

Using the method for complex **38** [Ni(**36**)SO_4] MX_n = $NiSO_4$.7H_2O. Recrystallisation from CH_2Cl_2:$^iPr_2O$, gave an orange solid (0.15 g, 55%). ν_{max}/cm^{-1} 2958s (C-H), 1540w (C=N), 1115s (SO_4). λ_{max} (ε)/nm (M^{-1} cm^{-1}) ($CHCl_3$) 243 (30400), 299 (13900), 423 (5800). MS (FAB, NOBA) *m/z* 551 (MH^+-**36**, 100%).

Complex 48

Using the method for complex **38** $[Ni(\mathbf{36})_2Cl_2]$ $MX_n = NiCl_2.6H_2O$. Recrystallisation from CH_2Cl_2:$^iPr_2O$, gave an orange solid (0.19 g, 67%). ν_{max}/cm^{-1} 2952s (C-H), 1536w (C=N). λ_{max} (ε)/nm (M^{-1} cm^{-1}) ($CHCl_3$) 243 (30900), 299 (15500), 423 (9200). MS (FAB, NOBA) *m/z* 489 (MH^+-**36**, 100%).

Complex 49

Using the method for complex **40** $[Ni(\mathbf{34})_2(C_2H_3O_2)_2)]$ $MX_n = Ni(C_2H_3O_2)_2.4H_2O$. Extraction gave a brown solid (0.20 g, 72%). ν_{max}/cm^{-1} 2947s (C-H), 1560m (acetate). λ_{max} (ε)/nm (M^{-1} cm^{-1}) ($CHCl_3$) 243 (30800), 299 (13400), 423 (7800). MS (FAB, NOBA) *m/z* 697 (MH^+, 100%).

3.7.5 Solvent extraction experiments from sulfate media

10 cm^3 of 0.01M L ((L = **31**, **33**, **35** or **37**) in chloroform was contacted with 10 cm^3 aqueous 1M $NiSO_4$ in a tightly sealed, screw top, glass jar, equipped with a magnetic stirrer. The two-phase system was stirred at 500 r.p.m and at room temperature for 17 hrs, after which time a 2 cm^3 sample was taken from the organic phase. The samples were diluted by a factor of 1:5 with butan-1-ol and their nickel contents analysed by ICP-AES. The data collected were plotted as % uptake bar charts in Microsoft Excel.

3.7.6 X-ray crystallography

Structures **34** and **36** were determined by James Davidson and Patricia Lozano-Casal respectively, at the University of Edinburgh. In all cases data were collected at 220K on a SMART or Stoe Stadi-4 diffractometer equipped with an Oxford Cryosystems low temperature device.

3.8 References

1 H.-F. Klein and A. Bickelhaupt, *Inorg.Chim.Acta*, 1996, **248**, 111.

2 P.L.Orioli, M. d. Vaira and L.Sacconi, *J.Am.Chem.Soc.*, 1966, **88**, 4383.

3 D.J.Macchia, W. F. F. Junior and R.A.Lalancette, *Acta Crystallogr.,Sect.C:Cryst.Struct.Commun.*, 1993, **49**, 1706.

4 J.M.Fernandez-G., M.J.Rosales-Hoz, M.F.Rubio-Arroyo, R.Salcedo, R.A.Toscano and A.Vela, *Inorg.Chem.*, 1987, **26**, 349.

5 J.M.Fernandez-G, M.J.Rosales, R.A.Toscano and R. G. T. T, *Acta Crystallogr.,Sect.C:Cryst.Struct.Commun.*, 1986, **42**, 1313.

6 J. Fernandez, E. Cortes and J. Gomez-Lara, Proc. Int. Conf. Coord. Chem., 1974, R30, 33 pp.

7 D. F. Shriver, P. W. Atkins and C. H. Langford, 'Inrganic Chemistry', Oxford University Press, Great Britain, 1994, 213.

8 D. H. Williams and I. Fleming, 'Spectroscopic Methods in Organic Chemistry', Mc Graw Hill Book Company, London, 1995, 51.

9 H. A. Miller, N. Laing, S. Parsons, A. Parkin, P. A. Tasker and D. J. White, *J.Chem.Soc.,Dalton Trans.*, 2000, 3773.

10 R. A. Coxall, L. F. Lindoy, H. A. Miller, A. Parkin, S. Parsons, P. A. Tasker and D. J. White, *J.Chem.Soc.,Dalton Trans.*, 2003, 55.

11 E. A. K. James E. Huheey, Richard L. Keiter, 'Inorganic Chemistry: Principles of Structure and Reactivity', Harper Collins, 1993, 387.

12 A.W.Kleij, R.A.Gossage, R. J. M. K. Gebbink, N.Brinkmann, E.J.Reijerse, U.Kragl, M.Lutz, A.L.Spek and G. v. Koten, *J.Am.Chem.Soc.*, 2000, **122**, 12112.

13 R.J.Butcher and E.Sinn, *Inorg.Chem.*, 1977, **16**, 2334.

14 C.Janiak, L.Uehlin, H.-P. Wu, P.Klufers, H.Piotrowski and T.G.Scharmann, *J.Chem.Soc.,Dalton Trans.*, 1999, 3121.

15 J.C.Jansen, H. v. Koningsveld, J. A. C. v. Ooijen and J.Reedijk, *Inorg.Chem.*, 1980, **19**, 170.

16 H.S.Preston and C.H.L.Kennard, *J.Chem.Soc.A*, 1969, 2682.

17 S.Buchler, F.Meyer, A.Jacobi, P.Kircher and L.Zsolnai, *Z.Naturforsch.,B:Chem.Sci.*, 1999, **54**, 1295.

18 C. Shao, W.-H. Sun, Y. Chen, R. Wang and C. Xi, *Inorg.Chem.Commun.*, 2002, **5**, 667.

19 H.M.Powell and K.M.Chui, *J.Chem.Soc.,Dalton Trans.*, 1976, 1301.

20 T.V.Laine, M.Klinga and M.Leskela, *Eur.J.Inorg.Chem.*, 1999, 959.

21 E.Bouwman, P.Evans, H.Kooijman, J.Reedijk and A.L.Spek, *Chem.Commun.*, 1993, 1746.

22 K.Rajapandian, J.Thomas, P.Tharmaraj, V.Chandrasekhar and E.R.T.Tiekink, *J.Chem.Soc.,Dalton Trans.*, 1994, 1301.

23 W.-H. Sun, Z. Li, H. Hu, B. Wu, H. Yang, N. Zhu, X. Leng and H. Wang, *New J.Chem.*, 2002, **26**, 1474.

24 M.Konrad, F.Meyer, K.Heinze and L.Zsolnai, *J.Chem.Soc.,Dalton Trans.*, 1998, 199.

25 A.J.Pallenberg, T.M.Marschner and D.M.Barnhart, *Polyhedron*, 1997, **16**, 2711.

[26] F.Meyer, U.Ruschewitz, P.Schober, B.Antelmann and L.Zsolnai, *J.Chem.Soc.,Dalton Trans.*, 1998, 1181.
[27] G.J.Long and E.O.Schlemper, *Inorg.Chem.*, 1974, **13**, 279.
[28] L.Crociani, F.Tisato, F.Refosco, G.Bandoli and B.Corain, *Eur.J.Inorg.Chem.*, 1998, 1689.
[29] G. A. V. Albada, J.J.A.Kolnaar, W.J.J.Smeets, A.L.Spek and J.Reedijk, *Eur.J.Inorg.Chem.*, 1998, 1337.
[30] M.Koman, E.Jona and I.Kopal, *Acta Crystallogr.,Sect.C:Cryst.Struct.Commun.*, 1997, **53**, 443.
[31] Y.Yamamoto, T.Suzuki and S.Kaizaki, *J.Chem.Soc.,Dalton Trans.*, 2001, 2943.
[32] Md.A.Masood and D.J.Hodgson, *Inorg.Chem.*, 1994, **33**, 3038.
[33] E.C.Constable, D.Phillips and P.R.Raithby, *Inorg.Chem.Commun.*, 2002, **5**, 519.
[34] W.L.Driessen, R. M. d. Vos, A.Etz and J.Reedijk, *Inorg.Chim.Acta*, 1995, **235**, 127.
[35] C.R.Cheng, P.-H. Leung and K.F.Mok, *Polyhedron*, 1996, **15**, 1401.
[36] F.Morale, R.W.Date, D.Guillon, D.W.Bruce, R.L.Finn, C.Wilson, A.J.Blake, M.Schroder and B.Donnio, *Chem.-Eur.J.*, 2003, **9**, 2484.

Chapter Four

Screening study

Contents page

4.1 Introduction

As discussed in Chapter 1, a circuit that selectively extracts the metal of main commercial value, nickel, from the high pressure acid leach solution is preferred (Figure 4.1).

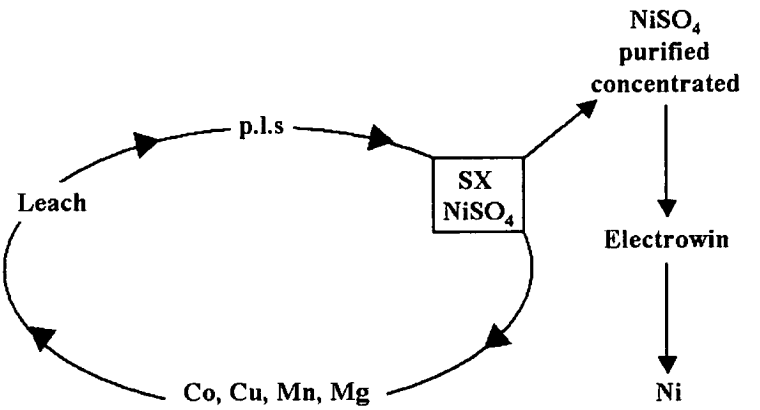

Figure 4.1 Solvent extraction circuit for the removal of nickel sulfate to generate a pure electrolyte

In an alternative strategy the nickel is not extracted but remains in the aqueous phase either until all the impurities and lower value metals have been removed by solvent extraction or other separation techniques (Figure 4.2).

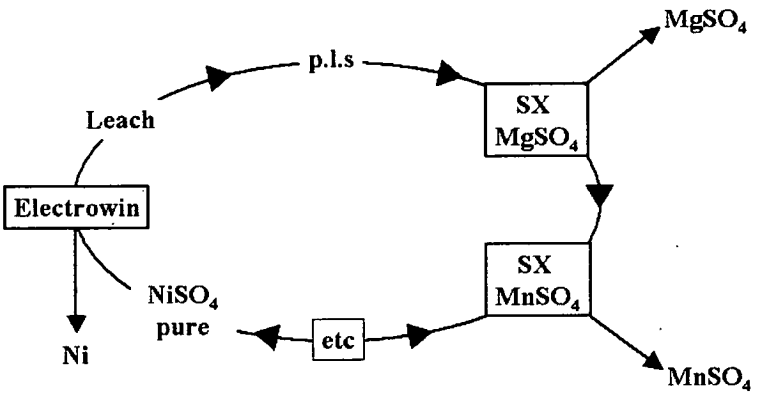

Figure 4.2 Solvent extraction circuit where all the impurities are extracted to generate a pure nickel sulfate electrolyte

The recovery of zinc from sulfidic ores[1-3] (Figure 4.3) is an example of an industrial process that is based on this type of strategy. Approximately 80% of world wide zinc production involves this roast/leach/purification/electrowin circuit.[4]

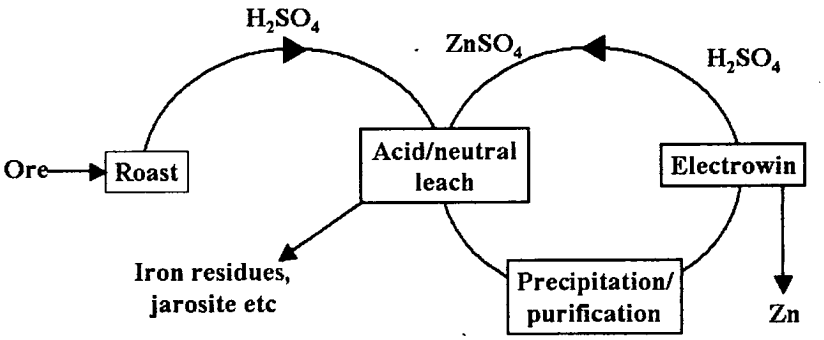

Figure 4.3 Circuit for the production of zinc from sulfidic ores by roast/leach/purification/electrowinning[4]

Initially the sulfidic ore is oxidised by roasting, to form the zinc oxide (calcined zinc oxide) (Equation 4.1).

Equation 4.1 $2ZnS + 3O_2 \rightleftharpoons 2ZnO + 2SO_2$ Roast

The zinc oxide is then dissolved in sulfuric acid (Equation 4.2) produced by recovering and oxidising the sulfur dioxide produced during roasting (Equation 4.1 and Equation 4.3).

Equation 4.2 $ZnO + H_2SO_4 \rightleftharpoons ZnSO_4 + H_2O$ Acid leach

Equation 4.3 $2SO_2 + O_2 + 2H_2O \rightleftharpoons 2H_2SO_4$ Acid production

Roasting and acid leaching also dissolves many other metals (e.g. iron, Equation 4.4 and Equation 4.5, which is the major impurity) producing a mixed metal leach solution.

Equation 4.4 $4FeS + 7O_2 \rightleftharpoons 4SO_2 + 2Fe_2O_3$ Roast

Equation 4.5 $Fe_2O_3 + 3H_2SO_4 \rightleftharpoons Fe_2(SO_4)_3 + 3H_2O$ Acid leach

As a pure zinc sulfate electrolyte is required for electrolysis,[5] the impurities formed during roasting and dissolution need to be removed. A multi-step process, each removing a specific impurity, achieves this. An example is the removal of iron via pH-adjustment and precipitation. Calcine (the mixture of zinc/iron oxides from roasting) is added to the acid leach solution, producing zinc sulfate and raising the pH. When the pH>2.5 large volumes of iron oxy-hydroxides precipitate (Equation 4.6).

Equation 4.6 $Fe_2(SO_4)_3 + H_2O + 3ZnO \rightleftharpoons 3ZnSO_4 + 2FeO(OH)\downarrow$

Neutral leach/iron precipitation

To avoid co-precipitation of arsenic, germanium and some zinc, which presents serious environmental problems in disposal, the iron is precipitated as either, jarosite,[6] $[XFe_3(SO_4)_2(OH)_6]$, geothite,[7, 8] FeO(OH) or hematite,[7] Fe_2O_3. Most commonly a jarosite (Fe(III), $X=NH_4^+$) precipitate is generated (Figure 4.3) through addition of ammonium sulfate (at 95 °C ,pH 1.5) during the neutral leach/iron precipitation step.[9]

The remaining impurities can then be removed by various techniques, namely chemical precipitation, electrolytic deposition and cementation with zinc, to give a pure zinc sulfate electrolyte.

As the sexadentate and tridentate ligands (chapters 2 and 3) have been shown to be poor extractants of nickel from a sulfate media, a screening study was devised to investigate whether they could be applied instead to extract the major metal impurities found in aqueous feed solutions from the high pressure acid leaching of nickel ores, e.g. as in the Bulong circuit.

Table 4.1 Table showing the composition of the "Bulong circuit" aqueous feed before and after extraction with Cyanex 272[10]

Metal	Before	After
Calcium	0.5 gl^{-1}	0.5 gl^{-1}
Chloride	65 gl^{-1}	65 gl^{-1}
Cobalt	235 mgl^{-1}	5.3 mgl^{-1}
Magnesium	15 gl^{-1}	14 gl^{-1}
Manganese	0.99 gl^{-1}	0.4 mgl^{-1}
Nickel	2.8 gl^{-1}	2.8 gl^{-1}
Sulfur	22 gl^{-1}	22 gl^{-1}
Zinc	29 mgl^{-1}	<0.2 mgl^{-1}

Metals commonly found in addition to nickel in such sulfate solutions are iron, (which is removed by precipitation as iron(III) oxyhydroxides after oxidation and raising the pH≥ 3.0) cobalt(II), copper(II), magnesium(II), manganese(II) and zinc(II).[11] Calcium sulfate has a low solubility and therefore usually has a low concentration in sulfate leach solutions. The high chloride content of the Bulong feed (Table 4.1) may account for its unusually high concentration.

4.1.1 Coordination chemistry of metal ions in Bulong feed streams

Nickel and cobalt are discussed in chapters 1 and 2. The coordination chemistry of the other metals commonly found in the sulfate streams from leached nickel ores, for example in Bulong, Western Australia (Table 4.1), are mentioned briefly below.

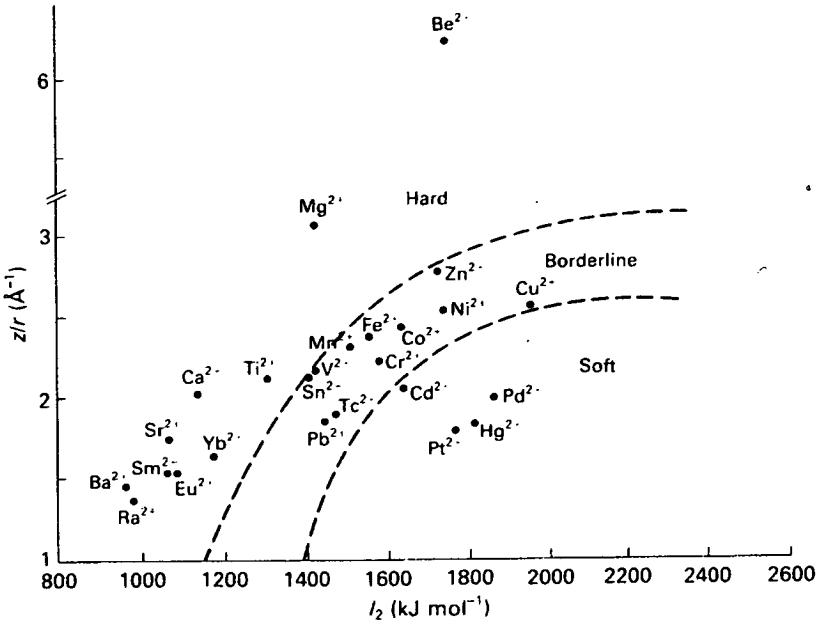

Figure 4.4 Ionic potential (z/r) against electron acceptor power for divalent ions[12]

4.1.1.1 Calcium

Calcium extraction by the ligands described in chapters 2 and 3 is not expected due to being a very hard Lewis acid (Figure 4.4) but as it is found in the Bulong feed streams it has been included in the screening experiment.

4.1.1.2 Copper

Copper is readily recovered from sulfate streams using phenolic oxime extractants (see section 1.5.1).

Complexes of copper in oxidation states I to IV are known, with copper(I) and copper(II) the most abundant.[13] Most copper(I) compounds are fairly readily oxidized to copper(II), but further oxidation to copper(III) is more difficult. The d^9 configuration makes copper(II) subject to Jahn-Teller distortion if placed in an environment of cubic symmetry. When six coordinate, the octahedron is severely distorted. The typical distortion is elongation along one four-fold axis, so that there is a planar array of four short Cu-L bonds and two *trans* long ones. Five coordinate

complexes (square pyramidal or trigonal pyramidal) are also generally distorted. For four coordinate copper(II) a regular square planar geometry may involve a slight tetrahedral distortion. Copper(II) is a borderline hard acid (Figure 4.4) and the best donor is oxygen followed by nitrogen and chloride ligands.[14] Virtually all copper complexes of simple ligands are blue or green.[15] Exceptions are generally caused by strong U.V. charge-transfer bands-tailing off into the blue end of the visible spectrum,[15] thus causing the substance to appear red or brown.

A large amount of copper is expected to be extracted due to the higher formation constants for copper(II) complexes relative to other divalent metal ions of the first row transition series (Irvine Williams order).[16]

4.1.1.3 Magnesium

As with calcium it is unlikely that magnesium will be extracted as it is hard Lewis acid and prefers to coordinate to hard donor atoms.[12, 17]

4.1.1.4 Manganese

Complexes of manganese in oxidation states III to VII with a variety of coordination geometries are known. Manganese(II) is the most stable[18] and the most common oxidation state, although it is readily oxidised in an alkaline solution. Manganese(II) has a d^5 electronic configuration, and with the exception of a few complexes,[18] the majority of manganese(II) complexes are high spin. As manganese(II) is found lower in the Irvine William series,[17] than cobalt, copper, nickel and zinc it is unlikely that as much manganese will be extracted in comparison to these metals.

4.1.1.5 Zinc

Zinc is regarded as a non-transition element as it only forms compounds where the d shell is full, as only the two 4s electrons are readily lost. However zinc(II) has some resemblance to d-group elements in its ability to form complexes, particularly with

ammonia, amines, halide ions and cyanide. A large number of zinc(II) complexes are known with oxygen, nitrogen, sulfur and to a lesser extent phosphorus ligands.[19] Coordination numbers four-six are commonly known with five being the most common. For zinc(II) complexes there is no CFSE and hence their stereochemistry is determined solely by considerations of size, electrostatic forces and covalent bonding forces. Like magnesium there is no optical transition in the electronic spectra of zinc and hence they are all colourless. Colour of salts are thus due only to colours of the anions or to lattice defects.

The majority of zinc is recovered through roasting of the sulfuric ore and dissolution in sulfuric acid (see Figure 4.3), but recently the nickel-cobalt extractant D2EHPA (section 1.5.3.2.1) has been commercially used in zinc recovery.[20] D2EHPA shows good selectivity for zinc over the most common impurities in the sulfate streams,[21, 22] namely manganese, cobalt, nickel, copper, magnesium and cadmium.

The process involves four steps:[23]

1. Zinc is extracted by D2EHPA from a mixed metal sulfate solution.
2. The organic phase is scrubbed to remove any impurities (e.g. chloride and fluoride ions) which would contaminate the electrolyte.
3. Zinc is stripped, using sulfuric acid, to produce a pure zinc sulfate solution for electrowinning.
4. Electrolysis to zinc metal

Unfortunately D2EHPA has a strong affinity for iron(III) which is not stripped with sulfuric acid and hence poisons the extractant. Therefore the commercial success of the processes depends on removal of the iron from the feed solutions, via precipitation, prior to solvent extraction. Any extracted iron can be removed by treating a bleed stream with 6 M hydrochloric acid, which regenerates D2EHPA and produces $FeCl_3$.[24]

There are several commercial processes that use D2EHPA to recover zinc.[20] The newest and largest is the Anglo American Corporation's Skorpion Mine in Namibia.[23] It was opened early 2003 and has an expected lifetime of fifteen years.[23] The deposit is an oxide ore and prior to the development of a zinc solvent extractant these minerals could not be economically processed. Initially they were producing ~50,000 Mt p.a. but once at full operation are expect to be at full capacity of 150,000 Mt p.a.[23] and will be one of the lowest cost zinc producers in the world.[23]

4.1.2 Chloride process streams

The high chloride ion constant in the Bulong streams (Table 4.1) results from a highly saline bore water used in leaching.[25] However in recent years there has also been considerable interest[26, 27] in applying chloride hydrometallurgy to extracting metals from sulfide ores as a potential low-cost, pollution free alternative to smelting.[26]

Corrosion problems connected with the corrosive nature of chloride media have been overcome[26] by the use of new polymeric construction materials and chloride hydrometallurgy can now be seen as a logical alternative for the treatment of unconventional concentrates that smelters cannot handle.

"Chloride" leach solutions can be produced in various ways, e.g. through oxidative leaching with ferric chloride and when the water supply used contains a high concentration of chloride ions.

Oxidative leaching of sulfidic ores with ferric chloride (Equation 4.7 and Equation 4.8) is favoured due to the high leaching efficiency, the rapid rate of the process and formation of elemental sulfur, thus avoiding the liberation of SO_2.[28] The elemental sulfur remains in the leach residue along with iron hydroxides and other insoluble products (e.g. silicates).

Equation 4.7 $ZnS_{(S)} + 2FeCl_3 \rightleftharpoons ZnCl_2 + 2FeCl_2 + S_{(S)}$

Equation 4.8 $Cu_2S_{(S)} + 4FeCl_3 \rightleftharpoons 2CuCl_2 + 4FeCl_2 + S_{(S)}$

The resulting mixed feed can be processed using solvent extractants. The processes often involve electrowinning of the metals from chloride solutions, thereby providing chlorine for regeneration of the ferric chloride leachant (Figure 4.5 and Figure 4.6).

$ZnS + 2FeCl_3 \rightleftharpoons ZnCl_2 + 2FeCl_2 + S$		Leach
$ZnCl_2 + \overline{L} \rightleftharpoons \overline{ZnLCl_2}$		Extract
$\overline{ZnLCl_2} \rightleftharpoons ZnCl_2 + \overline{L}$		Strip
$ZnCl_2 \rightleftharpoons Zn + Cl_2$		Electrowin
$Cl_2 + 2FeCl_2 \rightleftharpoons 2FeCl_3$		Regeneration
$ZnS \rightleftharpoons Zn + S$		Overall

Figure 4.5 The materials balance for recovery of zinc from sulfidic ores

$Cu_2S + 4FeCl_3 \rightleftharpoons 2CuCl_2 + 4FeCl_3 + S$		Leach
$2CuCl_2 + 2\overline{L} \rightleftharpoons \overline{2CuLCl_2}$		Extract
$\overline{2CuLCl_2} \rightleftharpoons 2CuCl_2 + 2\overline{L}$		Strip
$2CuCl_2 \rightleftharpoons 2Cu + 2Cl_2$		Electrowin
$2Cl_2 + 4FeCl_2 \rightleftharpoons 4FeCl_3$		Regeneration
$Cu_2S \rightleftharpoons 2Cu + S$		Overall

Figure 4.6 The materials balance for recovery of copper from sulfidic ores

When water containing a high concentration of chlorine ions in acid/oxidative leaching of nickel as in Bulong Western Australia, the resulting chloride streams could in theory be processed using a nickel chloride reagent as in Figure 4.7.

$NiCl_2 + \overline{L}$	$\rightleftharpoons \overline{NiLCl_2}$	Extract
$\overline{NiLCl_2} + 2HCl$	$\rightleftharpoons NiCl_2 + \overline{LH_2Cl_2}$	Strip
$\overline{LH_2Cl_2}$	$\rightleftharpoons \overline{L} + 2HCl$	Wash
$NiCl_2$	$\rightleftharpoons Ni + Cl_2$	Electrowin
$Cl_2 + H_2$	$\rightleftharpoons 2HCl$	Acid make up
$NiCl_2 + H_2$	$\rightleftharpoons Ni + 2HCl$	Overall

Figure 4.7 The materials balance for recovery of nickel from chloride-rich water

In this case the nickel chloride complex $\overline{NiLCl_2}$ would be stripped with hydrochloric acid (HCl), the reagent would be recovered by washing off HCl and the chlorine generated from electrowinning of nickel would be reacted with hydrogen to regenerate the HCl needed for stripping.

Because of the very high efficiency of chloride leaching systems many minor metals present in complex sulfide concentrates are also leached effectively, hence highly selective extractants are needed.

4.1.3 Alternative uses of the new sexadentate and tridentate reagents

The conclusion of the work described in chapters 2 and 3, is that the sexadentate (**4**, **6**, **8**, **10** and **12**) and tridentate ligands (**31**, **33**, **35** and **37**) are not sufficiently "strong" nickel sulfate extractants to be used commercially to process feeds such as those in the Bulong circuit. The remaining sections of this thesis consider their use in the recovery of other metal salts, particularly those formed in nickel process streams. Four tetradentate ligands **50-53** (see Table 4.2) were included in a screening programme to establish the strength and selectivity of recovery of cobalt, copper, magnesium, manganese, nickel and zinc chlorides and calcium, cobalt, copper, magnesium, manganese and zinc sulfates by the ligands **6**, **8**, **12**, **31**, **33**, **35**, **37**, **50**, **51**, **52** and **53**.

Table 4.2 Generic form of the ligands used in the screening study

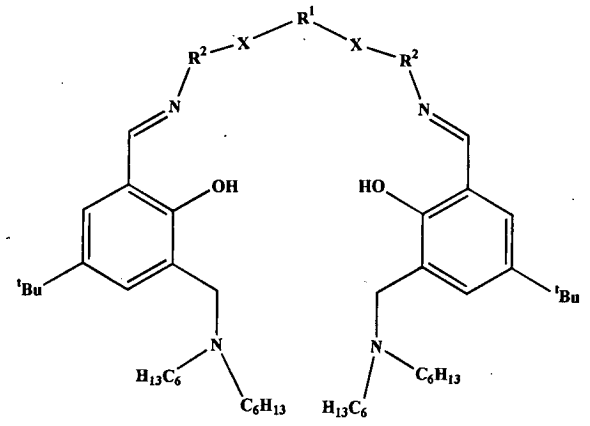				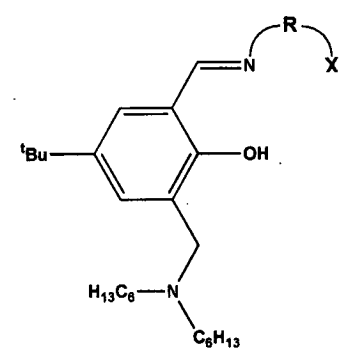			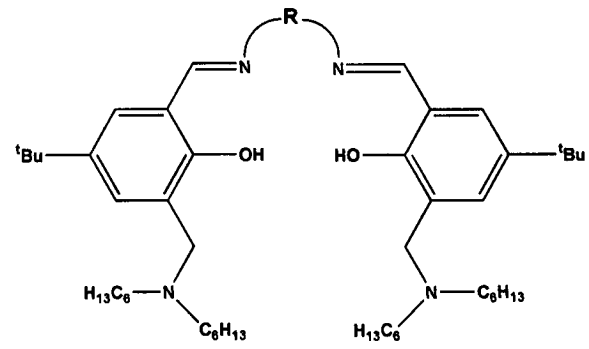	
L	**X**	**R^1**	**R^2**	**L**	**X**	**R**	**L[a]**	**R**
6	O	$-(CH_2)_2-$	*o*-C_6H_4-	**31**	$N(CH_3)_2$	$-(CH_2)_2-$	**50**	$-C_6H_{10}-$
8	O	$-(CH_2)_3-$	*o*-C_6H_4-	**33**	OCH_3	$-(CH_2)_2-$	**51**	$-C_6H_4-$
12	S	$-(CH_2)_2-$	*o*-C_6H_4-	**35**	OCH_3	*o*-C_6H_4-	**52**	-piphenyl-
				37	SCH_3	*o*-C_6H_4-	**53**	$-(CH_2)_2-$

[a] First reported by Miller *et.al.*[29]

4.1.4 Synthesis of tetradentate ligands

The tetradentate ligands **50-53** were made using a similar method to that described in chapter 2, where two equivalents of 2-hydroxy-3-(N-dihexyl-4-yl-methyl)-5-*tert*-butylbenzaldehyde were reacted with one equivalent of the appropriate di-amine. Isolation, purification and characterisation followed procedures described by Miller *et. al.*[29]

4.2 Screening experiment

A screening experiment was developed, whereby all the ligands in Table 4.2 were tested with each metal in a sulfate and chloride media. The procedure described in chapter 2 (section 2.7) was used where by a 0.01 M solution of ligand, in chloroform, was stirred for 17 hours with an equal volume of an aqueous 1 M metal salt solution. The amount of metal transferred to the water immiscible chloroform phase was measured using ICP-AES and all the data were interpreted using thermospec/CID IRIS software. The wavelengths used to calibrate concentrations, were free of spectral interferences from other elements (see appendix).

4.3 Metal loadings

The metal loadings results are present below in bar charts as percentage of the theoretical loading, assuming a 1:1 metal: ligand (M:L) ratio as either a metal salt or "metal-only" complex is formed in the organic phase.

4.3.1 Calcium and magnesium

No calcium or magnesium was extracted from either a sulfate or chloride solution by any of the ligands. This is not surprising given that calcium(II) and magnesium(II) show a strong preference for hard donors (see sections 4.1.1.1 and 4.1.1.3).

4.3.2 Manganese

No manganese extraction was measured from sulfate media but when some of the ligands (31, 50, 52) were contacted with a manganese chloride solution a larger amount of metal uptake (≤150 %) was observed, (see appendix I, Figure 2).

4.3.3 Copper results

As expected copper is loaded efficiently by all the ligands (Figure 4.8). From a sulfate media all the sexadentate and tetradentate ligands extract 100% suggesting a 1:1 (L:M) stoichiometry. The tridentate ligands only load 50% copper from a sulfate media, suggesting a 2:1 (L:M) stoichiometry.

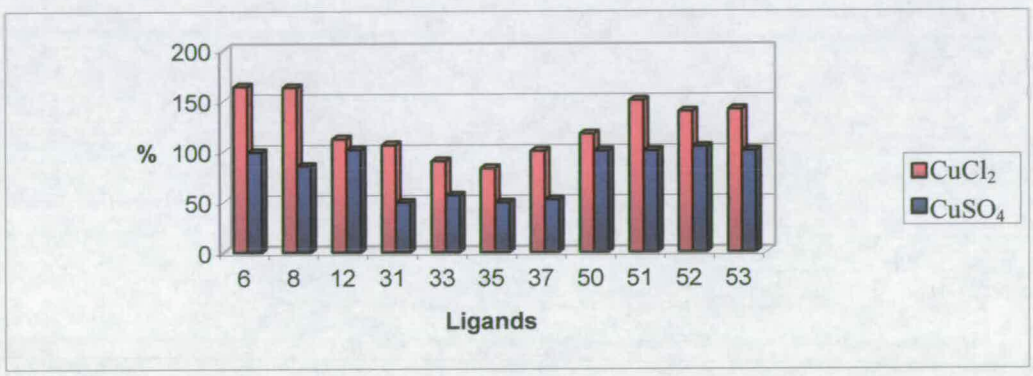

Figure 4.8 Copper extraction results (100% represents the loading of one copper cation by one ligand)

Using ICP-AES it was relatively simple to measure the amount of sulfur and hence sulfate uptake. Metal salt (sulfate) complexes were formed (not metal-only) and with in experimental error the results show (Figure 4.9) that for every mole of copper extracted one mole of sulfate is also extracted.

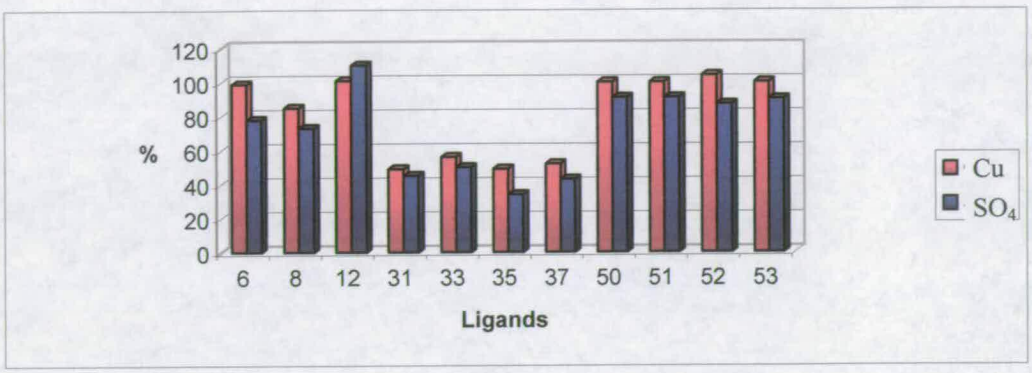

Figure 4.9 Copper and sulfur extraction results (100% represents the loading of one copper cation or one sulfate anion by one ligand)

There is a general trend showing extraction of copper from a chloride media is more efficient than for sulfate. This is expected due to the chloride ions high solubility and the "Hofmeister series".[30, 31] In some cases though we observe results higher than the theoretical 1:1 (L:M) loading. For example the results from ligand **6** imply 2:3 (L:Cu) stoichiometry. Consequently an understanding of this will require information about the chloride loading and whether the chloride is present in the inner coordination sphere of the copper or associated with the pendant amines. Some of these issues are addressed in chapter 5.

4.3.4 Nickel

The affect of the attendant anion is also seen in the nickel study (Figure 4.10).

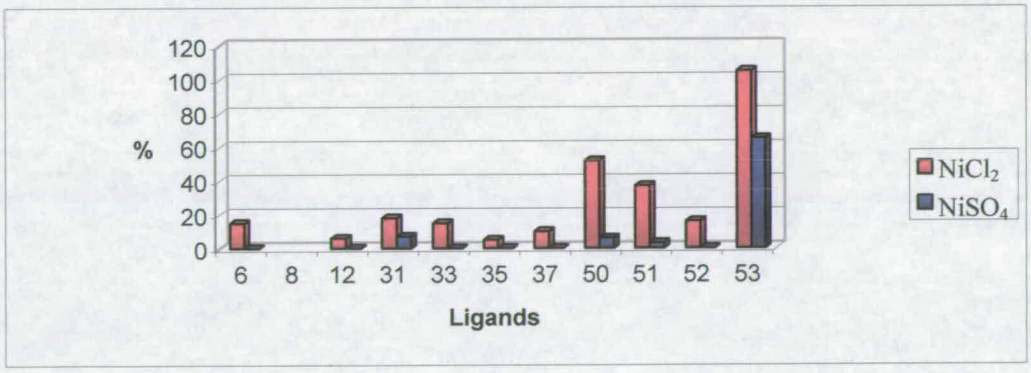

Figure 4.10 Nickel extraction results (100% represents the loading of one nickel cation by one ligand)

The results show that out of the three classes of ligands (sexadentate, tetradentate and tridentate) the tetradentates are the most efficient nickel extractants. Therefore

suggesting nickel prefers low spin tetradentate extractants in comparison to high spin sexadentate ligands.

The only ligand that shows promise as a commercial extractant is the least rigid ethane bridged ligand **53**, which fully loads nickel from a chloride media.

4.3.5 Cobalt results

The most noticeable result is the large increase in the percentage uptake of cobalt when the attendant anion(s) are exchanged from a sulfate to a chloride (Figure 4.11).

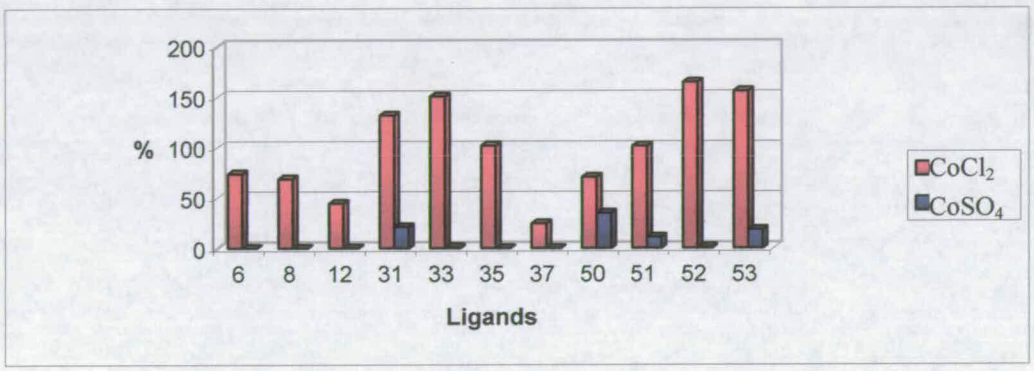

Figure 4.11 Cobalt extraction results (100% represents the loading of one cobalt cation by one ligand)

The only ligands that extract $CoSO_4$ are the tetradentate ligands and the tridentate ligand **31** with the N_2O^- donor set. This suggests that the cobalt prefers stabilising donors with strong ligand field contributions namely nitrogen. This suggests that the cobalt is oxidised to cobalt(III), see chapter 5 (section 5.3.4).

4.3.6 Zinc results

For zinc the anion has an even greater affect on metal uptake. The amount of zinc extracted from a sulfate media is negligible but when a chloride media is used the results show up to 1:3 (L:Zn) stoichiometry for the sexadentate and tetradentate ligands and 2:3 for the tridentates (Figure 4.12).

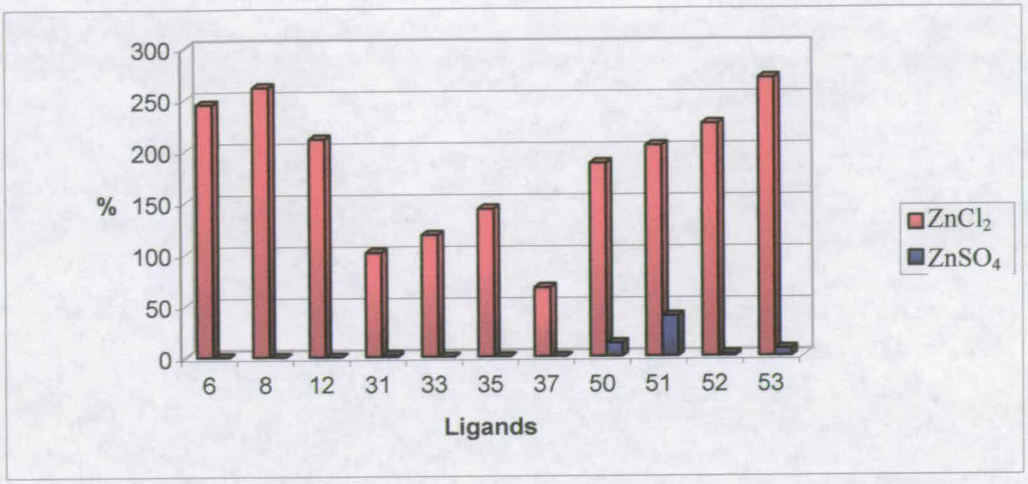

Figure 4.12 Zinc extraction results (100% represents the loading of one cation by one ligand)

Even though the tetradentate ligands have less donors, they appear to be equally capable of extracting three zinc cations. A theory as to the complexes formed is discussed in chapter 5.

4.4 Conclusions

The major result obtained from the screening experiment is the affect the attendant anion has on the amount of metal extracted. Apart from copper there is no notable extraction from sulfate solutions. When a chloride media is used the amount of metal extracted greatly increases. The most interesting result is seen for zinc extraction from chloride media, where for each mole of ligand up to three moles of zinc are extracted. This result is significant as the commercial success of an extractant depends on high mass transport, as this is improves the efficiency and economics of an industrial plant.

For calcium and magnesium no extraction is recorded when either media is used, but this was expected.

The amount of chloride extracted and experiments to help determine the connectivity of the complexes (cobalt, copper, nickel and zinc) formed through extraction are discussed in chapter 5.

4.5 Experimental

4.5.1 Instrumentation

Elemental analysis was performed on a Perkin Elmer 2400 elemental analyser or a Carlo Erba 1108 Elemental analyser. ^{1}H and ^{13}C NMR spectra were run on a Bruker AC250 spectrometers. Chemical shifts (δ) are reported in parts per million (ppm) relative to residual solvent protons as internal standards. Fast Atom Bombardment (FAB) mass spectra were obtained on a Kratos MS50TC spectrometer. Inductively coupled plasma optical emission spectroscopy (ICP-OES) analysis was performed on a Thermo Jarrell Ash IRIS ICP-OES spectrometer.

4.5.2 Solvent and reagent pre-treatment

All reagents and solvents were commercially available (Acros or Aldrich) and were used as received. Solvents used for analytical purposes (NMR, MS, ICP) were of spectroscopic grade. ICP AES standards were purchased from Alfa Asar.

4.5.3 Ligands

Ligand 50

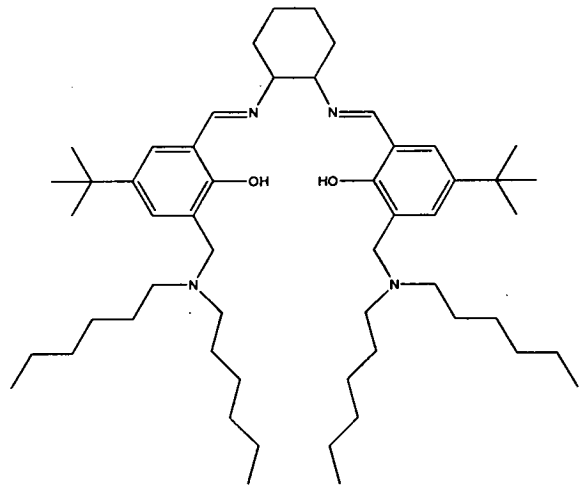

To a stirred solution of **HDTB** (1.58 g, 4.2 mmol) in diethylether (20 cm^3) was added a solution of (±)trans-cyclohexane-1,2-diamine(0.24 g, 2.1 mmol) in ethanol (15

cm^3). The orange solution was stirred overnight and concentrated *in-vacuo* to yield a orange oil (1.65 g, 95%). This was used without further purification. Found: C, 78.32; H, 11.20; N, 6.65. Calc. for $C_{54}H_{92}N_4O_2$: C, 78.20; H, 11.18; N, 6.76%. ^1H NMR ($CDCl_3$, 250 MHz): δ 0.78 (t, 12H, CH_3 (hexyl)), δ 1.17 (s, 18H, $C(CH_3)_2$), δ 0.08-1.27 (m, 24H, CH_2 (hexyl)), δ 1.40 (m, 8H, $NCH_2\underline{CH_2}$ (hexyl)), δ 1.84 (bp, 4H, CH_2 (cyclic)), δ 2.38 (t, 4H, NCH_2 (hexyl)), δ 3.22 (bp, 4H, CH_2 (cyclic)), δ 3.45 (s, 2H, CH (cyclic)), δ 3.56 (s, 4H, $ArCH_2N$); δ 6.97 (s, 2H, ArCH), δ 7.42 (s, 2H, ArCH), δ 8.22 (s, 2H, N=CH). ^{13}C NMR ($CDCl_3$): δ 14.0 (CH_3 (hexyl)), δ 22.6 ($\underline{CH_2}CH_3$(hexyl)), δ 24.1 (CH_2 (cyclic)), δ 26.9 ($\underline{CH_2}CH_2CH_3$ (hexyl)), δ 27.2 ($\underline{CH_2}CH_2CH_2CH_3$ (hexyl)), δ 31.3 ($C(\underline{CH_3})_3$), δ 31.8 ($NCH_2\underline{CH_2}$ (hexyl)), δ 33.2 (CH_2 (cyclic)), δ 33.8 ($\underline{C}(CH_3)_3$), δ 52.0 ($N\underline{CH_2}$ (hexyl)), δ 54.2 ($ArCH_2N$), δ 72.6 (CH_2 (cyclic)), δ 117.4 (Ar-C), δ 125.7 (Ar-CH), δ 126.7 (Ar-C), δ 129.7 (Ar-CH), δ 140.4 (Ar-C), δ 156.8 (Ar-C), δ 164.7 (C=N). MS (FAB, NOBA) *m/z* 829 (MH^+, 66.5%).

Ligand 51

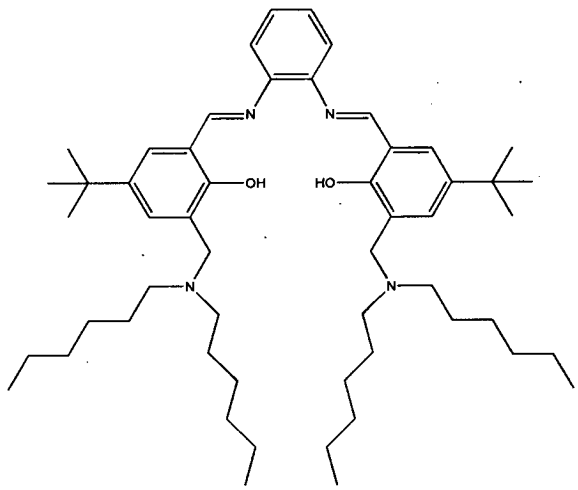

Using the method for ligand **50**, but using **HDTB** (1.73 g 4.6 mmol) and benzene-1,2-diamine (0.25 g, 2.3 mmol) produced an orange oil (1.67 g, 89%). This was used without further purification. Found: C, 78.30; H, 10.54; N, 6.92. Calc. for $C_{54}H_{86}N_4O_2$: C, 78.78; H, 10.53; N, 6.81%. ^1H NMR ($CDCl_3$, 250 MHz): δ 0.89 (t, 12H, CH_3 (hexyl)), δ 1.33 (s, 18H, $C(CH_3)_2$), δ 0.10-1.34(m, 24H, CH_2 (hexyl)), δ 1.53 (bp, 8H, $NCH_2\underline{CH_2}$ (hexyl)), δ 2.54 (t, 8H, NCH_2 (hexyl)), δ 3.73 (s, 4H,

$ArCH_2N$), δ 6.78 (m, 2H, Ar-CH), δ 7.08 (m, 2H, Ar-CH), δ 7.46 (m, 2H, Ar-CH), δ 7.64 (d, 2H, Ar-CH), δ 8.83 (s, 2H, N=CH). ^{13}C NMR ($CDCl_3$): δ 14.4 (CH_3 (hexyl)), δ 22.9 ($\underline{CH_2}CH_3$(hexyl)), δ 26.6 ($\underline{CH_2}CH_2CH_3$ (hexyl)), δ 27.1 ($\underline{CH_2}CH_2CH_2CH_3$ (hexyl)), δ 31.9 ($C(\underline{CH_3})_3$), δ 32.2 ($NCH_2\underline{CH_2}$ (hexyl)), δ 34.4 ($\underline{C}(CH_3)_3$), δ 53.9 ($N\underline{CH_2}$ (hexyl)), δ 54.4 ($ArCH_2N$), δ 115.8 (Ar-C), δ 118.4 (Ar-C), δ 119.8 (Ar-CH), δ 125.4 (Ar-CH), δ 127.1 (Ar-CH), δ 130.3 (Ar-CH), δ 141.4 (Ar-C), δ 141.7 (Ar-C), δ 161.1 (C=N). MS (FAB, NOBA) *m/z* 824 (MH^+, 36.0%).

Ligand 52

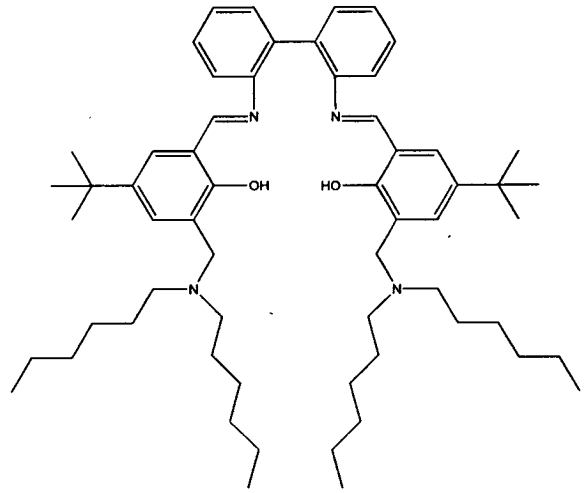

Using the method for ligand **50**, but using **HDTB** (1.11 g, 3.0 mmol) and 2,2′-diaminobiphenyl (0.27 g, 1.5 mmol) produced an orange oil (1.21 g, 90%). This was used without further purification. Found: C, 80.85; H, 10.09; N, 6.21. Calc. for $C_{60}H_{90}N_4O_2$: C, 80.13; H, 10.09; N, 6.23%. ^1H NMR ($CDCl_3$, 250 MHz): δ 0.79 (t, 12H, CH_3 (hexyl)), δ 1.17 (s, 18H, $C(CH_3)_2$), δ 1.07-1.25 (m, 24H, CH_2 (hexyl)) δ 1.39 (m, 8H, $NCH_2\underline{CH_2}$ (hexyl)), δ 3.28 (d, 8H, NCH_2 (hexyl)), δ 3.48 (s, 4H, $ArCH_2N$), δ 7.04-7.59 (s, 12H, Ar-CH), δ 8.44 (s, 2H, N=CH). ^{13}C NMR ($CDCl_3$): δ 14.0 (CH_3 (hexyl)), δ 22.6 ($\underline{CH_2}CH_3$(hexyl)), δ 27.1 ($\underline{CH_2}CH_2CH_3$ (hexyl)), δ 27.2 ($\underline{CH_2}CH_2CH_2CH_3$ (hexyl)), δ 31.3 ($C(\underline{CH_3})_3$), δ 31.8 ($NCH_2\underline{CH_2}$ (hexyl)), δ 33.8 ($\underline{C}(CH_3)_3$), δ 52.2 ($N\underline{CH_2}$ (hexyl)), δ 54.1 (Ar-CH_2-N), δ 118.2 (Ar-CH), δ 118.4 (Ar-C), δ 126.0 (Ar-CH), δ 126.5 (Ar-C), δ 128.6 (Ar-CH), δ 130.4 (Ar-CH), δ 130.7 (Ar-CH), δ 132.0 (Ar-CH), δ 134.5 (Ar-C), δ 140.5 (Ar-C), δ 147.9 (Ar-C); δ 156.8 (Ar-C), δ 162.4 (C=N). MS (FAB, NOBA) *m/z 899* (MH^+, 64.4%).

Ligand 53

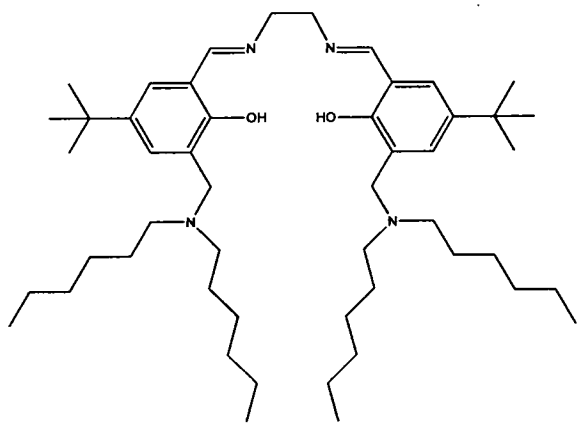

Using the method for ligand **50**, but using **HDTB** (1.27 g, 3.4 mmol) and ethane-1,2-diamine (0.10 g, 1.7 mmol) produced an orange oil (1.15 g, 87%). This was used without further purification. Found: C, 78.06; H, 12.02; N, 7.23. Calc. for $C_{50}H_{86}N_4O_2$: C, 77.46; H, 11.18; N, 7.23%. ^{1}H NMR ($CDCl_3$, 250 MHz): δ 0.79 (t, 12H, CH_3 (hexyl)), δ 1.21 (s, 12H, $C(CH_3)_2$), δ 0.10-1.23 (m, 24H, CH_2 (hexyl)), δ 1.41 (m, 8H, $NCH_2\underline{CH_2}$ (hexyl)), δ 2.37 (t, 4H, NCH_2 (hexyl)), δ 3.56 (s, 4H, $ArCH_2N$), δ 3.83 (s, 4H, CH_2 (N-en-N)), δ 7.11 (s, 2H, ArCH), δ 7.41 (s, 2H, ArCH); δ 8.34 (s, 2H, N=CH). ^{13}C NMR ($CDCl_3$): δ 14.0 (CH_3 (hexyl)), δ 22.6 ($\underline{CH_2}CH_3$ (hexyl)), δ 26.9 ($\underline{CH_2}CH_2CH_3$ (hexyl)), δ 27.2 ($\underline{CH_2}CH_2CH_2CH_3$ (hexyl)), δ 31.3 ($C(\underline{CH_3})_3$), δ 31.7 ($NCH_2\underline{CH_2}$ (hexyl)), δ 33.9 ($\underline{C}(CH_3)_3$), δ 52.6 ($N\underline{CH_2}$ (hexyl)), δ 54.1 ($ArCH_2N$), δ 60.1 (N-en-N), δ 117.82 (Ar-C), δ 125.4 (Ar-CH), δ 126.4 (Ar-C), δ 129.9 (Ar-CH), δ 140.5 (Ar-C), δ 156.8 (Ar-C), δ 165.8 (C=N). MS (FAB, NOBA) *m/z* 775 (MH^+, 14.8%).

4.5.4 Screening experiments from sulfate media

10 cm^3 of 0.01 M L ((L = **6**, **8**, **12**, **31**, **33**, **35**, **37**, **50**, **51**, **52 or 53**) in chloroform was contacted with 10 cm^3 aqueous 1 M MSO_4 in a tightly sealed, screw top, glass jar, equipped with a magnetic stirrer. The two-phase system was stirred at 500 r.p.m and at room temperature for 17 hrs, after which time a 2 cm^3 sample was taken from the organic phase. The samples were diluted by a factor of 1:5 with butan-1-ol and

their nickel contents analysed by ICP-AES. The data collected were plotted as % uptake bar charts in Microsoft Excel.

4.5.5 Screening experiments from chloride media

Using the method from the "screening experiments from sulfate media" (section 4.5.4) but with 1 M MCl_2.

4.6 References

1 J. G. Peacey and P. J. Hancock, Proceedings of the International symposium on Iron Control in Hydrometallurgy, 2nd, Ottawa, 1996, 17-35.

2 S. Chen, X. Li and H. Huang, Hydrometallurgy, Kunming, China, 1998, 509-512.

3 L. I. Rosato and M. J. Agnew, Iron Control and Disposal, Proceedings of the International Symposium on Iron Control in Hydrometallurgy, 2nd, Ottawa, 1996, 77-89.

4 I. Palencia Perez and J. E. Dutrizac, *Hydrometallurgy*, 1991, **26**, 211.

5 G. M. Ritcey and A. W. Ashbrook, 'Process Metallurgy, Vol. 1: Solvent Extraction: Principles and Applications to Process Metallurgy, Pt. 2', 1979, 737.

6 R. V. Pammenter and C. J. Haigh, *Extr. Metall. '81, Pap. Symp.*, 1981, 379.

7 J. M. Cigan, T. S. Mackey, T. J. O'Keefe and Editors, Proceedings of a World Symposium on Metallurgy and Environmental Control, Las Vegas, Nevada, 1979, 1045.

8 P. T. Davey and T. R. Scott, *Hydrometallurgy*, 1976, **2**, 25.

9 Kirk-Othlmer, 'Encyclopaedia of Inorganic Chemistry', Wiley, New York, 1980, 739-767.

10 K. Soldenhoff, N. Hayward and D. Wilkins, EPD Congress 1998, Proceedings of Sessions and Symposia held at the TMS Annual Meeting, San Antonio, 1998, 153-165.

11 D. B. Harris, 'Personal Communication', 2002

12 J. J. R. Frausto-da-Silva and R. J. P. Williams, in 'The Biological Chemistry of the Elements The Inorganic Chemistry of Life', Oxford, 1991, 35.

13 N. N. Greenwood and E. A. Earnshaw, 'Chemistry of the Elements', Permangon Press, Oxford, 1984, 1364.

14 B. J. Hathaway, 'Comprehensive Coordination Chemistry, Late Transition Elements', ed. S. G. Williamson, R. D. Gillard, and J. A. Mccleverty, Permangon Press, Oxford, 1987, 533.

15 F. A. Cotton and G. Wilkinson, 'Advanced Inorganic Chemistry', John Wiley and Sons, USA, 1980, 768.

16 D. F. Shriver, P. W. Atkins and C. H. Langford, 'Inorganic Chemistry', Oxford University Press, Oxford, 1994, 213.

17 D. F. Shriver, P. W. Atkins and C. H. Langford, 'Inorganic Chemistry', Oxford University Press, Oxford, 1994, 229.

18 F. A. Cotton and G. Wilkinson, 'Advanced Inorganic Chemistry', John Wiley and Sons, USA, 1980, 697.

19 R. H. Prince, in 'Late Transition Metal Elements', ed. S. G. Wilkinson, R. D. Gillard, and J. A. McCleverty, Oxford, 1987, 925.

20 J. Sewart, "Personal Communication", 2003

21 M. J. Nicol, C. A. Fleming and J. S. Preston, 'Application to Extractive Metallurgy', ed. S. G. Wilkinson, Pergamon Press, Oxford, 1987, 779-842.

22 K. C. Sole and P. M. Cole, 2002, **15**, 143.

23 Metalline Mining Company, Skorpion Mine, www.metalin.com, 2003

24 K. C. Sole and P. M. Cole, International Solvent Extraction Conference, Cape Town, South Africa, 2002, 863-870.

[25] C. Y. Cheng, M. Urbani and M. Houchin, Hydrometallurgy 2003-Fifth International Conference in Honor of Professor Ian Ritchie, South Africa, 2003, 787.

[26] A. Jakubiak, J. Szymanowski and G. Cote, Value Adding through Solvent Extraction, ISEC'96, Melbourne, 1996, 517-522.

[27] K. Sarangi, B. R. Reddy and R. P. Das, *Hydrometallurgy*, 1999, **52**, 253.

[28] A. W. Fletcher, R. B. Sudderth and S. M. Olafson, *JOM-J. Miner. Met. Mater. Soc.*, 1991, **43**, 56.

[29] H. A. Miller, N. Laing, S. Parsons, A. Parkin, P. A. Tasker and D. J. White, *J.Chem.Soc.,Dalton Trans.*, 2000, 3773.

[30] S. Lewith, *Naunyn-Schmeidebergs Arch. Exp. Pathol. Pharmakol.*, 1888, **23**, 1.

[31] F. Hofmeister, *Naunyn-Schmeidebergs Arch. Exp. Pathol. Pharmakol.*, 1888, **23**, 247.

Chapter Five

Preliminary investigations into the complexes formed through extraction

Contents page

5.1 Introduction

The screening study produced some interesting results, most significantly the high metal loading for cobalt, copper and zinc when chloride solutions were used.

While chapters two and three have discussed the number of complexes that can be formed between a sexadentate or tridentate ligand and metal sulfate, it is apparent that for metal chloride complexes the number of permutations greatly increases. This could be due to the formation of metal chlorometallates, e.g. MCl_4^{2-}, which can act as an attendant dianion. Chlorometallates have a tetrahedral geometry.[1] Cobalt(II),[2] copper(II)[3] and zinc(II) readily form tetrahedral complexes[4] where as nickel(II) prefers a square planar geometry.[5] Figure 5.1 and Figure 5.2 list some of the types of neutral complexes formed in a water immiscible solvent by extraction from a metal chloride solution.

Formation of complexes with metal sulfate or chloride in the screening programme can be envisaged in several ways depending on:

- The anions are present in the inner coordination sphere (i.e. directly bound to the metal).
- The anions are present in the outer coordination sphere (H-bonded to protonated pendant amine groups or as separate ion pairs).
- The ligands are present in their zwitterionic, mono-deprotonated or di-deprotonated forms.
- The metal is present as a chlorometallate (MCl_4^{2-})
- The number of the ligand donor atoms involved in coordination e.g. the ligands function in bidentate, tridentate, tetradentate, pentadentate or sexadentate modes.
- The metal extracted is in a divalent form.

Some of the possibilities for the formation of neutral species with one sexadentate, tetradentate or two tridentates ligands in the forms L^0, $[L\text{-}H]^-$ or $[L+H]^+$ by combination with M^{2+}, Cl^- or MCl_4^{2-} are illustrated in Figure 5.1.

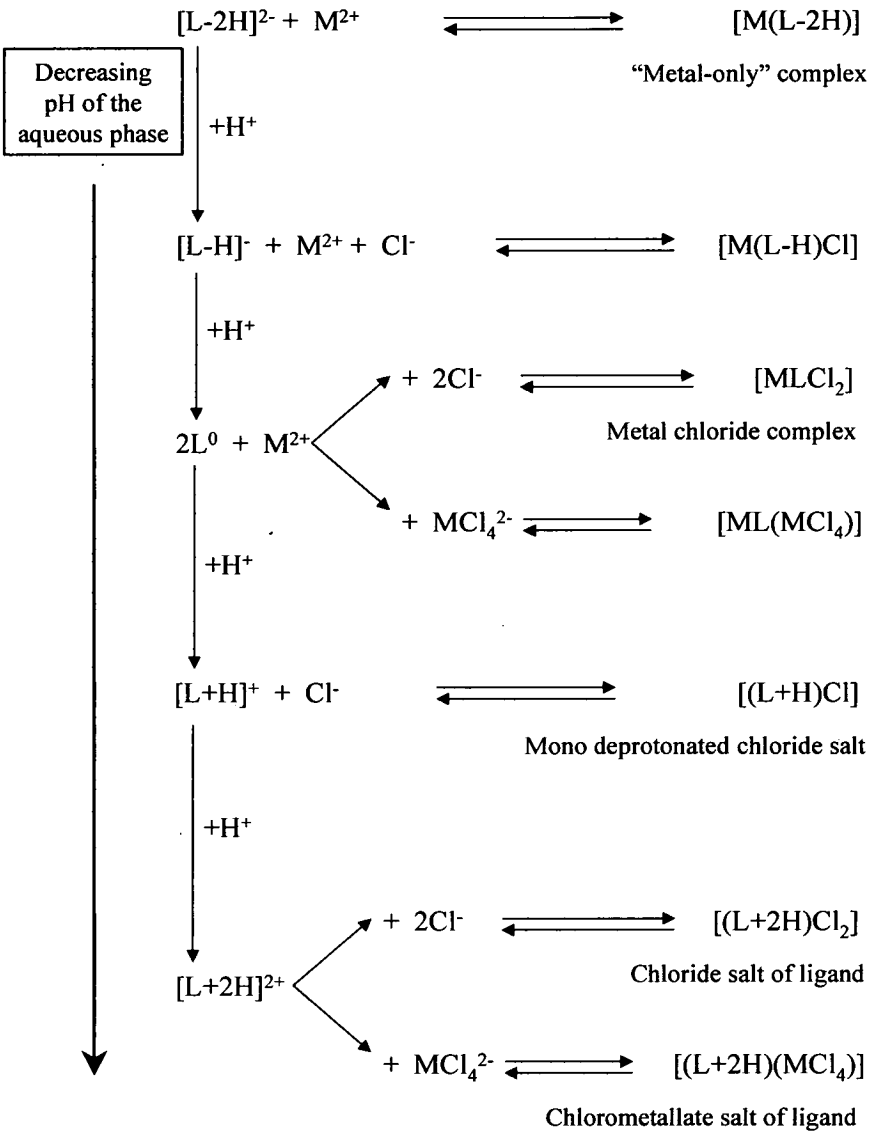

L^0 = sexadentate or pair of tridentate neutral ligands

Figure 5.1 Some of the possibilities for formation of charge neutral complexes or salts from sexadentate, tetradentate or pair of tridentate neutral ligands

Fewer neutral species can be formed when a combination of just one tridentate ligand and metal(II) chloride is considered (Figure 5.2).

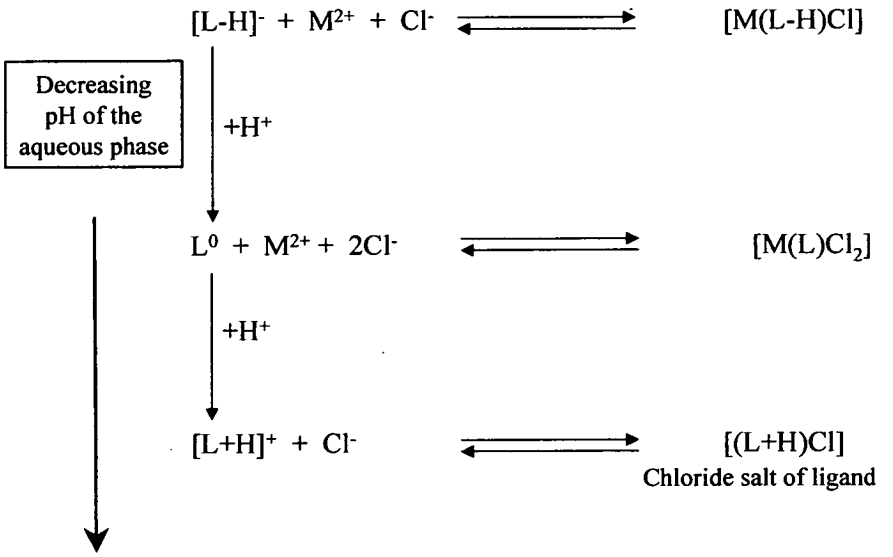

Figure 5.2 Charge neutral species which can be formed from a single molecule of the tridentate ligands **30-37** in solvent extraction of MCl_2 with variation of pH of the aqueous phase

Due to the large number of possible permutations, the amount of chloride extracted needs to be measured and the different modes of binding investigated. Therefore this chapter initially examines the amount of chloride extracted when the ligand is contacted with a metal chloride solution and compares the results with the metal loadings percentages obtained in chapter 4. It also investigates the various modes of binding in respect to copper, cobalt and zinc. Primarily this will involve analysis of the loaded organic phase from the screening studies and the formation of various solid state structures.

5.2 Chloride Analysis

There are a number of methods available for anion measurement[6]; these include, gravimetric analysis, anion exchange column, ISE, and ICP. The applicability of these for our systems will be addressed in turn.

Gravimetric and titrimetry are based solely on atomic weights (relative atomic masses), experimentally measured masses and atomic weight ratios obtained from well characterised chemical reactions involving the element/species to produce an

insoluble precipitate. Usually the precipitate is formed from an aqueous solution. For chloride analysis the complex could be reacted with silver nitrate, which would form the insoluble silver chloride. This method may not give accurate results as chlorides coordinated to a metal or H-bonded to the pendant amines may not react with silver nitrate.

Titrimetry is the determination of an element or species through the measurement of the mass of a chemical necessary to complete a definite chemical reaction in a solution containing that element or species. The mass of the element is obtained indirectly by measuring the volume of a standard solution of that chemical. Where a greater degree of accuracy is required, a mass titration must be used. Titrimetric methods can be based on acid-base, precipitation, complexation and on oxidation and reduction reactions. For chloride analysis a similar procedure, as for metal analysis, could be carried out using an anion exchange column instead of a cation exchange column (see chapter 2). Once again this method would involve many titrations which would be very time consuming and hence not suitable for a large number of samples.

The errors associated with classic analysis are widely known. For gravimetric analysis all precipitates contain small amounts of co-precipitation and occluded substances while all filtrates from precipitates contain small amounts of the dissolved precipitate. In addition to these problems, titrimetric errors occurring as a result of interference from competing side reactions have to be accounted for. Further errors may be caused when the indicator does not truly reflect the true end-point.

As ICP can be used for multi elemental analysis, ideally the concentration of chloride extracted would be simultaneously measured as for sulfur. Unfortunately, due to the low intensity of chloride emissions, attempts to analyse the chloride contents in the organic layer by ICP-AES were disappointing. Consequently an alternative method for chloride analysis was required. Although there are many methods available, a technique using an ion selective electrode was selected.

5.2.1 Chloride Selective electrode

A chloride selective electrode produces a potential that is proportional to the concentration of an analyte, hence measuring with a chloride selective electrode is a form of potentiometry.

Potentiometry is the field of electro analytical chemistry in which potential is measured under the conditions of no current flow. The measured potentials may then be used to determine the concentration of free chloride ions. The potential that develops in the electrochemical cell is the result of the free energy change that would occur if equilibrium had been reached.

Equation 5. 1 $\Delta G_{rxn} = -nFE_{rxn}$

Where ΔG_{rxn} is the free energy, n is the number of electrons transferred, F is the Faraday's constant and E_{rxn} is the potential.

The chloride electrode used consists of a sensing element bonded into an epoxy body. When the sensing element is contacted with a solution containing chloride ions, an electrode potential develops across the sensing element. The potential, which depends on the level of free chloride ions in solution, is measured against a constant reference potential with a digital pH/mV meter. The measured potential corresponding to the level of chloride ion in solution is described by the Nernst equation (Equation 5.2).

Equation 5.2 $$E = E_o - \frac{RT}{nF}\ln[A]$$

Where E is the measured electrode potential, E_o is the reference potential (a constant), R is the ideal gas constant, T is the temperature and A is the chloride ion activity level in solution. This can be abbreviated to:

Equation 5.3 $E = E_o + S \ln[A]$

Where S = constant to account for all the other potentials.

The chloride ion activity, A, is related to the free chloride ion concentration, Cl^-, by the activity coefficient, γ.

Equation 5.4 $A = \gamma[Cl^-]$

If the background ionic strength, γ, is high and constant relative to the sensed ion concentration, the activity coefficient is constant and activity is directly proportional to concentration. For example if $\gamma=1$, $A=[Cl^-]$.

Ideally we would like to directly measure the chloride extracted into the organic phase. However due to the limitations of the electrode, it cannot be used in organic solvents due to degradation of the electrode. This is unfortunate as our complexes are designed to be soluble in organic solvents. Therefore various chloride analysis experiments have been attempted, for example using nitric acid to destroy the complex and so release the free chloride into an aqueous phase for analysis. Sections 5.2.2 and 5.2.3 report on the two most useful techniques.

5.2.2 Chloride uptake in the organic phase-analysis by difference in the aqueous phase: - technique one

The first technique involved analysis of the aqueous phase before and after extraction. To measure the change in chloride concentration an extraction experiment with a ligand: metal ratio of 1:2 was carried out. The percentage uptake of metal by the extractants was measured by ICP and compared to the amount of chloride extracted. The chloride concentrations were determined via direct analysis of the aqueous phase before and after extraction after standardisation of the electrode.

To standardise the electrode a known concentration of a chloride ion solution was titrated whilst measuring the electrode response. The E and ln[A] values were recorded and a graph E against ln[A] was plotted. As the electrode potential is directly proportional to the log of the free chloride ion activity level in solution (Nernst equation), a straight line was obtained and E_o and constant were determined (Figure 5.3).

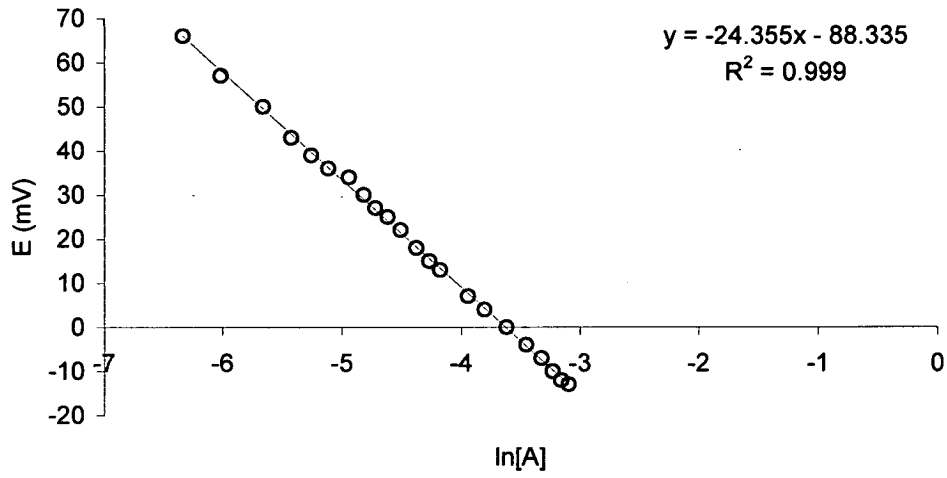

Figure 5.3 Calibration of the chloride selective electrode with a 0.1 M NaCl, 0.1 M $NaNO_3$ solution into 10 ml of a 0.2 M $NaNO_3$ solution. The straight line is the best fit of data to Nernst equation

The results obtained using technique one, (from ICP and chloride analysis), with ligands **6**, **12**, **31**, **33**, **35**, **37**, **50**, **51**, **52** and **53**, showed minimal metal and chloride uptake for cobalt and nickel. Where as for copper and zinc the percentage uptake of metal was greater as was the amount of chloride extracted hence the amount of metal extracted could be compared to the chloride results, see Table 5.1.

Table 5.1 Chloride to metal molar ratio in uptake by $CHCl_3$ solutions of various ligands (10 cm^3, 0.01 M) from $CuCl_2$ or $ZnCl_2$ aqueous solutions (10 cm^3, 0.02 M)

Ligand	Cl/M molar ratios	
	M=Copper	M=Zinc
6	2.0	2.1
12	1.8	1.9
31	1.6	1.7
33	1.5	2.0
35	2.5	2.2
37	2.3	***a***
50	1.7	2.0
51	1.6	1.8
52	1.7	1.7
53	2.1	1.8

a This showed negligible extraction of Zn

The observed copper: chloride (Cu:Cl) ratios fell in the range 1.5-2.5 and the zinc: chloride (Zn:Cl) ratios in the 1.7-2.2 range.

5.2.3 Chloride uptake in the organic phase-analysis by back extraction into an aqueous phase: - technique two

This approach was based on a method developed by Stuart Galbraith[7] at the University of Edinburgh, which involves displacement of the chloride anions by nitrate anions. The Hofmeister series[8, 9] states that a nitrate anion is less strongly hydrated than a chloride anion and therefore when possible a complex will bind nitrate over chloride. Hence contacting the loaded organic phase with an aqueous phase containing a high nitrate concentration will theoretically lead to exchange of the chloride and nitrate anions, giving an aqueous solution containing the concentration of chloride loaded by the ligands.

The technique has been used to produce a set of results,[7] plotting the percentage uptake of chloride in to a "metal-only" complex at various pHs. As a result the complexes in the organic phase only ever had a ligand: metal ratio of 1:1.

The method was based on the original extraction experiment (chapter 2) where a 0.01 M solution was contacted with a 1 M solution. The chloride was stripped back into

the aqueous phase, by contacting the loaded organic solution (1 cm^3) with a 0.1 M $NaNO_3$ (10 cm^3) solution. The concentration of chloride anions in the aqueous phase is then measured using the chloride electrode. Before analysis the ionic strength and pH of the aqueous phase was adjusted to ensure it was in the probe's pH range.

The chloride electrode was standardised as described in section 5.2.2 but using a 0.01 M NaCl, 0.01 M $NaNO_3$ solution and a 10 cm^3, 0.02 M $NaNO_3$ due to the lower concentration of chloride being measured.

Using this technique produced erroneous results for the copper and zinc extractions as while carrying out the experiment it was noted that a precipitate was often formed when the metal chloride complex was contacted with $NaNO_3$ and in some cases a coloured aqueous solution was formed.

The "nitrate method" assumes that all chloro complexes and salts in the organic phase are converted to nitrate salts and that free chloride is transferred to the aqueous phase. This will not necessarily be the case if $ZnCl_4^{2-}$ or $CuCl_4^{2-}$ is present in the organic phase. Consequently the displacement of chlorometallates, by the nitrate anions, could also explain the unusual results.

Metals salt complexes where the attendant anion is a chlorometallate have been produced. For example previous work by Schrőder *et.al.*[10] has shown that by linking an azathioether macrocycles to a urea groups produces a receptor for transition metal salts. Figure 5.4 shows the of crystal structure of a copper complex, $(LCuCl)_2CuCl_4$, with a single hydrogen bond from the receptor to a bridging tetrachlorocopperate ($CuCl_4^{2-}$) anion.

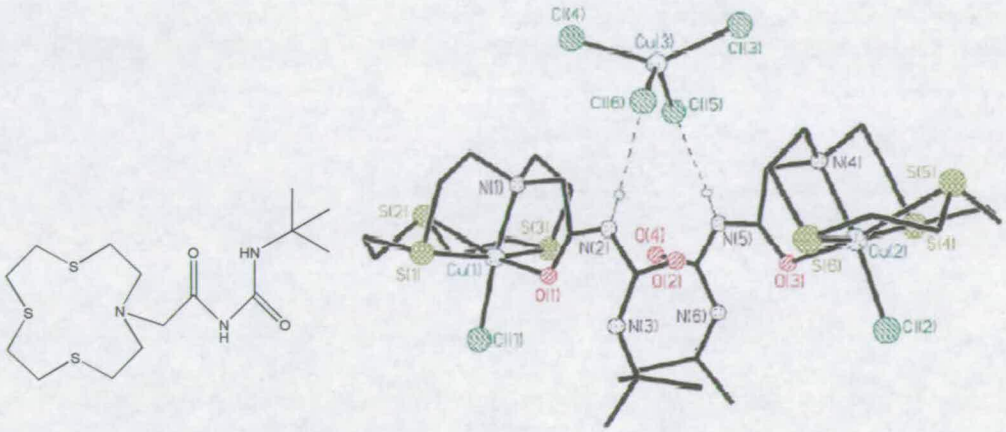

Figure 5.4 Diagram showing the ligand, L, (azathioether macrocycles linked to a urea groups) and the crystal structure of the complex $(LCuCl)_2CuCl_4$[10]

The results obtained from the nickel chloride extractions using the tetradentate ligands are more consistent with a nickel: chloride (Ni:Cl) ratios in the range 1.8-2.3 (Table 5.2).

Table 5.2 Chloride to metal molar ratio in uptake by $CHCl_3$ solutions of ligands (**50-53**) (10 cm^3, 0.01 M) from $NiCl_2$ aqueous solutions (10 cm^3, 0.02 M)

Ligand	Ni:Cl molar ratios
50	1:2.0
51	1:1.9
52	1:2.3
53	1:1.8

5.2.4 Conclusions

There are numerous combinations that could give a M:Cl ratio of complexes of 2:1. Equally, there are a range of complexes that would give M:Cl <1:2 and >1:2. see Figure 5.1 for examples of how the M:L:Cl ratio can vary.

5.3 Formulation of the extracted complexes

The high metal chloride to ligand ratios observed in extraction could underpin efficient recovery processes but any rational development of such reagents should be based on an understanding of the speciation in the organic phase. Some of the possibilities have been discussed in section 5.1. In the remaining sections of this chapter UV-Vis spectroscopy, ^{1}H NMR spectroscopy, IR and mass spectra of selected complexes are discussed and in combination with the metal: ligand: chloride ratios are used to assign possible structures for complexes formed in the chloroform solution.

Examples of possible structural formulations are shown in Figure 5.5. For all the complexes the coordination number of the metal is always ≤ 6, the overall charge of the complex =0 and the oxidation state is two.

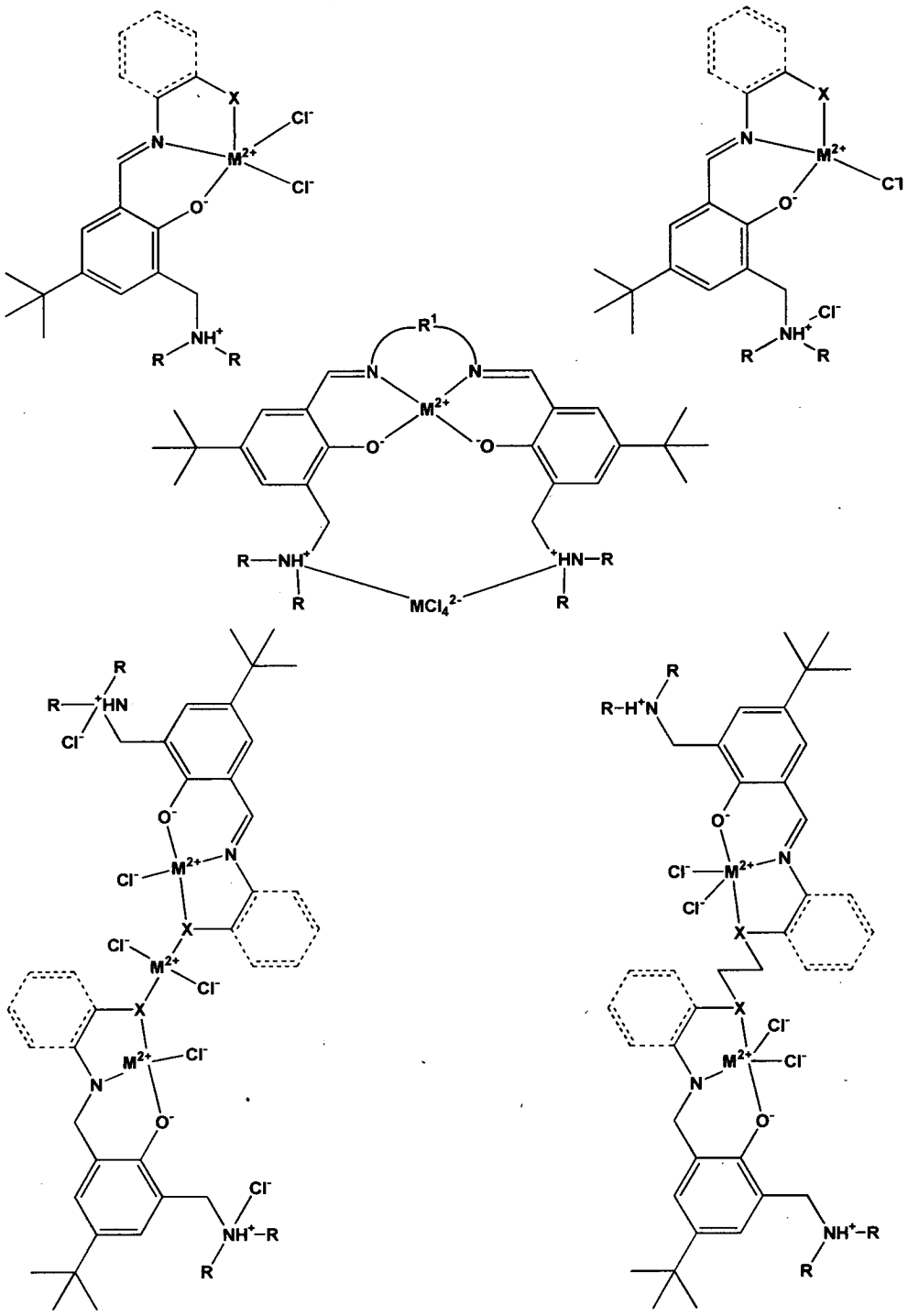

Figure 5.5 Possible structural formulations for the extracted metal chloride complexes.

5.3.1 Copper analysis

The copper and chloride loadings (sections 4.3.3 and 5.2.2) suggest the formation of species with a Cu:L:Cl ratio of 2:1:4 (for the sexadentate and tetradentate ligands)

and 2:2:4 (for the tridentate ligands). The results and observations from section 5.2.3 indicate the presence of $CuCl_4^{2-}$ as the attendant anion. Two possible structures are shown below (Figure 5.6).

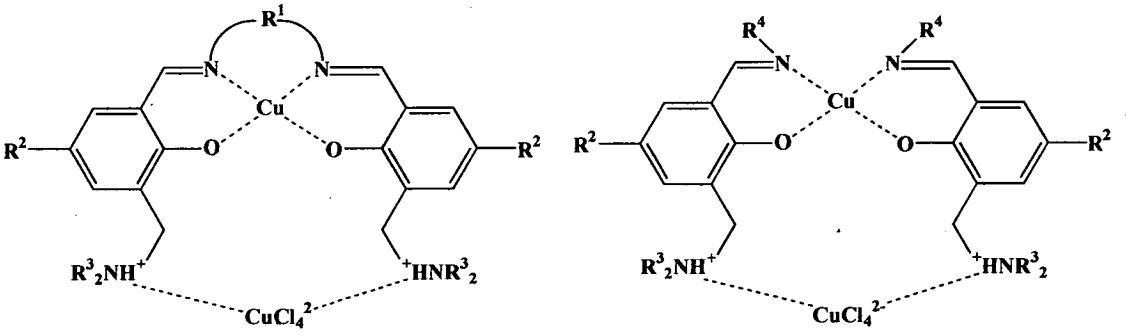

Figure 5.6 Schematic diagram for the proposed copper chloride complexes formed through extraction

Fast Atom Bombardment (FAB) mass spectra were obtained for all the extracted complexes, as for the nickel complexes in chapters 2 and 3. All of the complexes formed with the sexadentate (**6**), tridentate (**31, 33, 35** and **37**) and tetradentate ligands, show fragment peaks arising from at least one ligand and one copper being present. The complexes formed with the tridentate and tetradentate ligands (**50-51**) show fragment peaks involving one or more chlorides.

Samples of the loaded organic layer were removed for UV-Vis spectroscopy. As the concentration of the complex was unknown only the peak positions were recorded.

A crystal structure of a copper complex of the sexadentate ligand **5** is discussed in section 5.4.1. It shows the copper bound to four of the available donors (phenolate oxygen and imine nitrogen atoms) in a distorted square planar geometry. Therefore, it was hypothesised that in both cases one copper is coordinated to four donors in the cation binding site using very similar $N_2O_2^{2-}$ donor sets.

The UV-Vis spectra of $CuCl_4^{2-}$ has four peaks, resulting from d-d transitions, at 240, 265-270 370-380 nm[11] and 960 nm. In the spectra of the extracted complexes, if the $CuCl_4^{2-}$ species is present as the attendant anion, then the first peaks (at lower wave length) would be obscured by the more intense charge transfer peaks but the peak at 960 nm should be visible. On analysing the spectra of ligands **6, 33, 35** and **37** after

extraction from a 1M $CuCl_2$ solution, no such peaks were detected. Therefore, it may be concluded that copper is not extracted in the proposed tetrachlorocopperate form as shown in Figure 5.6. Further work into the speciation of the copper chloride complexes needs to be completed.

5.3.2 Zinc chloride analysis

As with copper, the results from sections 5.2.2 show that for every zinc cation extracted, two chloride anions are extracted. Given the high L:Zn loading levels it was again presumed that the attendant anion is tetrachlorozincate $ZnCl_4^{2-}$.

Again, Fast Atom Bombardment (FAB) mass spectra were obtained showing various fragment peaks suggesting the formation of zinc chloride complexes. All the complexes have fragment peaks involving at least one ligand, one zinc and one chloride. The complexes formed with the sexadentate ligands (**6** and **12**) show a fragment peak (LZn_2Cl_2) suggesting the attendant anion $ZnCl_4^{2-}$ has been lost. The complexes formed with the tridentate ligands (**31, 33** and **35**) show fragment peaks (LZnCl) suggested fragmentation of the complexes whereas the complexes formed with ligand **37** has a fragment peak ($L_2Zn_2Cl_2$) suggesting a complex with a similar structure as to those formed with ligands **6**and **12** where the attendant anion ($ZnCl_4^{2-}$) has been lost. The complexes formed with the tetradentate ligands (**50, 52** and **53**) have fragment peaks involving one ligand, two zincs and two or three chlorides, whereas the complex formed with ligand **51** has been fragmented to give a peak relating to LZnCl.

Unfortunately the presence of the tetrachlorozincate species cannot be confirmed by UV-Vis analysis as was used with tetrachlorocopperate. However, even though it has been concluded that the copper is not extracted in the tetrachlorometalate form it is still worth considering this proposed theory for zinc as the formation of tetrachlorozincate is more favourable than the formation of tetrachlorocopperates.[1]

Zinc complexes are always diagmagnetic and therefore NMR analysis can be used to look for any signs of symmetry within the complex and look for shifts in the peaks from the free ligand spectra which would highlight those atoms involved in complexation and anion binding. As in chapter three all the NMR spectra were run on complexes dissolved in the non-coordinating solvent chloroform (deuterated).

Each spectra obtained for the zinc chloride complexes demonstrate shifting in all the peaks as seen with other zinc complexes. All the peaks are slightly broadened but there is no peak splitting indicating the formation of symmetrical complexes as expected for the schematic structures in Figure 5.7.

The ICP combined with the chloride analysis, mass spectrometry and NMR, indicates that each zinc chloride complex has a L:Zn ratio of 2:3 for the tridentate ligands and a L:Zn ratio of 1:3 for the sexadentate and tetradentate ligands. Proposed structures are shown in Figure 5.7 and involve two zincs and two chlorides coordinated in the cation binding site and a tetrachlorozincate dianion hydrogen bonded to the pendant amines.

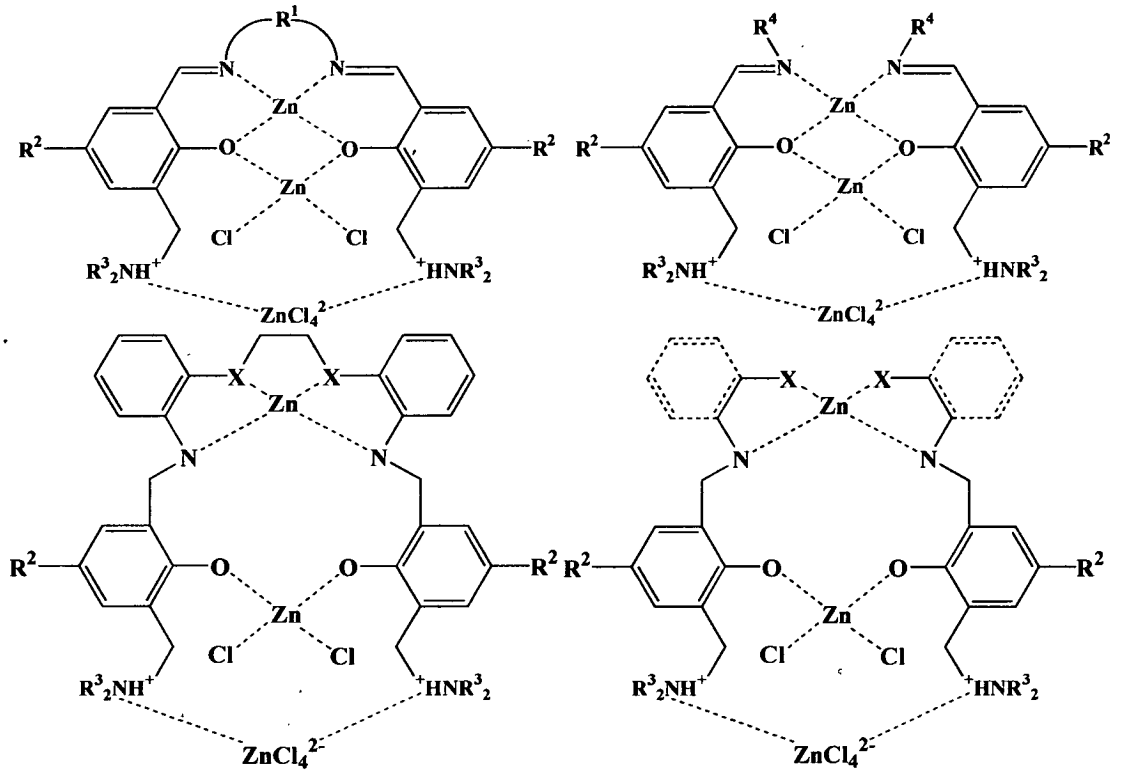

Figure 5.7 Suggested zinc chloride complexes

There are numerous crystal structures displaying two zinc cations coordinated within a single cavity.[12-31] An example,[28] shown in Figure 5.8 has one zinc cation coordinated in a square bipyramidal geometry to two phenolic oxygens, two imine nitrogens and a methanolic oxygen. The second zinc is also coordinated to the two phenolic oxygens and two chloride anions in a tetrahedral geometry.

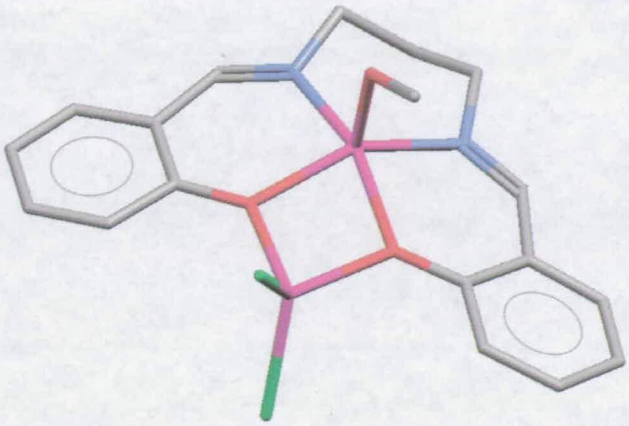

Figure 5.8 Crystal structure of μ-N,N′-bis(salicylidene)-1,-propanediaminato-dichloro-methanol-di-zinc(II)methanol solvate

Due to the size of a tetrachlorozincate anion it is unlikely that it could fit into a cavity formed by the pendant tertiary amines. Instead, a more likely structure would involve the tetrachlorozincate anion acting as an intermolecular crosslinker via hydrogen bonds. This ability of an attendant anion to act as intermolecular crosslinker is seen in the nickel sulfate crystal structure of complex **26** (Figure 5.9), (See chapter 2 for discussion of structure.)

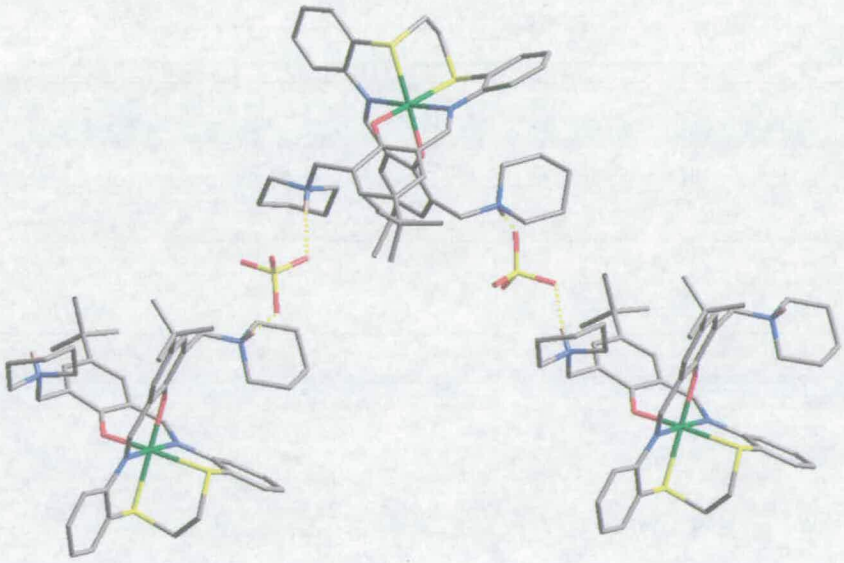

Figure 5.9 Diagram showing the sulfate anion acting as intermolecular crosslinker via single hydrogen bonds

5.3.3 Nickel chloride analysis

The results from the screening study show that nickel loadings never exceeded the expected 1:1 (L:Ni) complex formation with the sexadentate and tetradentate ligands or 2:1 complex formation with the tridentate ligands. This also helps to explain why the chloride contents could only be measured for the nickel extractions when using technique two (section 5.2.3).

Two solid state nickel chloride complexes (Figure 5.10) show the nickel cation bound in the expected cation binding site with either two chloride anions H-bonded to the pendant piperidines, (complex **28,** chapter 2) or with one chloride coordinated to the nickel and the second one free in the crystal lattice, (N,N′-bis (5-(t-butyl)-3-(piperidinylmethyl)salicylidene)-2,2′-diphenyldiamine)-chloro-nickel(II), chapter 3).

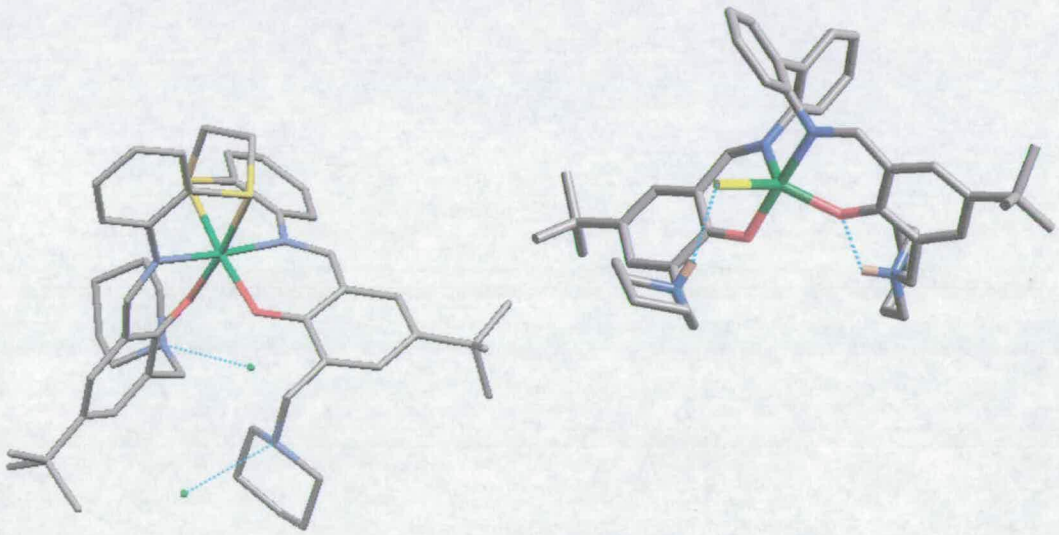

Figure 5.10 Crystal structures of complex **28** and (N,N′-bis (5-(t-butyl)-3-(piperidinylmethyl)salicylidene)-2,2′-diphenyldiamine)-chloro-nickel(II)

UV-Vis spectra of the free ligands and loaded organic phase are similar in nearly every case, due to the low levels of nickel extracted. An exception to this is observed in the spectra (Figure 5.11) obtained for the nickel sulfate and chloride complexes of the tetradentate ligand **53** which are very similar. Therefore, it is probable that in both cases that the nickel is bound in the same coordination sphere

and hence the attendant anion(s) are not associated with the nickel inner coordination sphere.

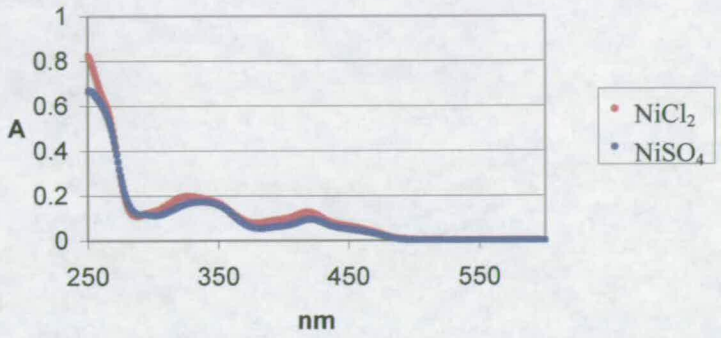

Figure 5.11 UV-Vis spectra of chloroform solutions of ligands **53** after extraction from a 1 M $NiCl_2$ and 1 M $NiSO_4$ solution

5.3.4 Cobalt analysis

Initially it was thought that the high cobalt: ligand results were due to the formation of tetrachlorocobaltate. On comparison between the UV-Vis spectra of the extracted complexes and a prepared $CoCl_4^{2-}$ sample ($CoCl_2$ dissolved in concentrated hydrochloric acid) it was seen that this was not the case. The spectra of the $CoCl_4^{2-}$ sample (Figure 5.12) displays peaks in the 570-720 nm region, which could be detected if the $CoCl_4^{2-}$ dianion was present in the complexes. On analysing the complexes formed with the ligands (**6**, **12**, **31**, **33**, **35**, **37**, **50**, **51**, **52** and **53**) no such peaks were detected and therefore it can be concluded that cobalt is not extracted in the tetrachlorometalate form.

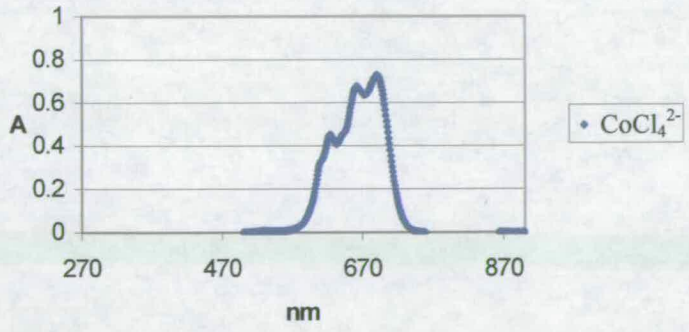

Figure 5.12 UV-Vis spectra of $CoCl_4^{2-}$ sample

The fact that tetrachlorocobaltates are not present questions the formation of the tetrachlorozincate dianions in section 5.3.2. However, unlike zinc, cobalt(II) can be oxidised, during extraction, to cobalt(III).[32] For this group of salen based ligands it is highly likely that oxidation of cobalt is occurring as the ligands all contain stabilising donors with strong ligand field contributions,[33] e.g. nitrogen, which are known to readily oxidise cobalt(II).

Proposed structures of neutral cobalt complexes, where the oxidation state of cobalt is three are shown below in Figure 5.13.

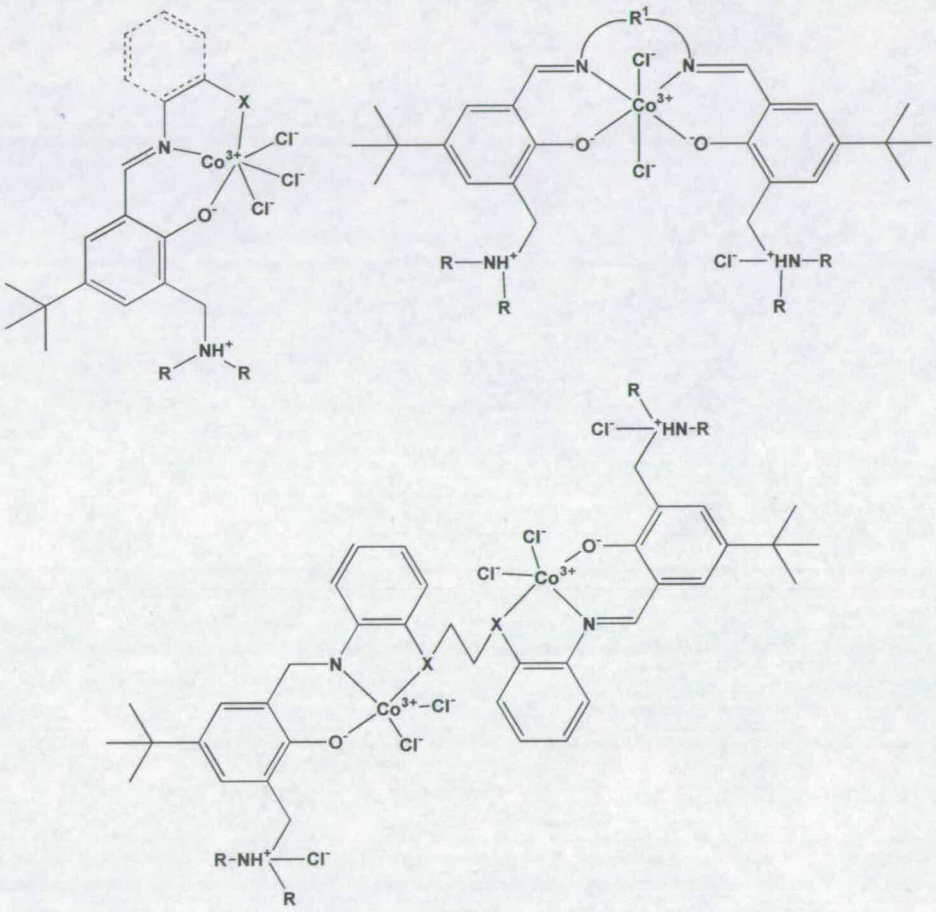

Figure 5.13 Proposed cobalt(III) structures

This may also explain why the cobalt extraction results (chapter 4) were lower than those for zinc.

5.3.5 Infra red spectroscopy

IR spectroscopy was attempted to confirm the presence of the anion in the complexes involving ligand **6**.

As stated in chapter three, sulfate ions are expected to show a band[34] in the region 1130-1080 cm^{-1}. For the chlorometallate anion there are four normal modes of vibration (Figure 5.14). All four vibrations are Raman active, whereas only ν_3 and ν_4 are infrared active.[35]

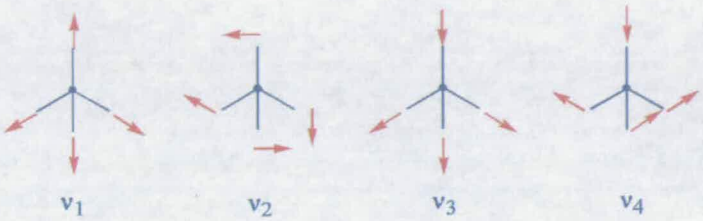

Figure 5.14 Normal modes of vibration of tetrahedral $[MCl_4]^{2-}$

From the extraction studies with ligand **6**, all the loaded organic phases were analysed. The extractions from a sulfate media all show a peak between 1117-1119 cm^{-1} confirming the presence of a sulfate anion. Due to the low wavelengths of the chlorometallate vibrations/bands (Table 5.3) these could not definitely be identified.

Table 5.3 The ν_3 and ν_4 vibrations (cm^{-1}) for the metal tetrachlorides cobalt, copper, nickel and zinc[35]

	ν_3	ν_4
$CoCl_4^{2-}$	311, 291	135
$CuCl_4^{2-}$	267, 248	136, 118
$NiCl_4^{2-}$	294, 280	119
$ZnCl_4^{2-}$	277	126

5.4 Solid state structures

To help investigate the types of complexes formed through extraction, solid state analogues were synthesised by a one step process. Ligands **5**, **11**, **30**, **32**, **34** and **36**

were dissolved in methanol and added to a methanolic solution of the required metal salt. The metal salts used were copper, cobalt and zinc (sulfate, chloride and acetate). The reaction mixtures were all stirred for 24 hours before work-up. The metal complexes were isolated and all analysed by mass spectrometry to confirm complexation had occurred. Complexes formed were used in various crystal growing experiments.

5.4.1 Crystal structure of complex 54

Single crystals of [Cu(**5**-H)($C_2H_3O_2$)]] suitable for X-ray structure determination were grown from methanol using di-ethyl-ether as the counter solvent. There is one molecule of the complex in the asymmetric unit (Figure 5.15) and one of the *t*-butyl groups is disordered. The copper is coordinated in a distorted square planar geometry by the two phenolic oxygen and the two imine nitrogen donors.

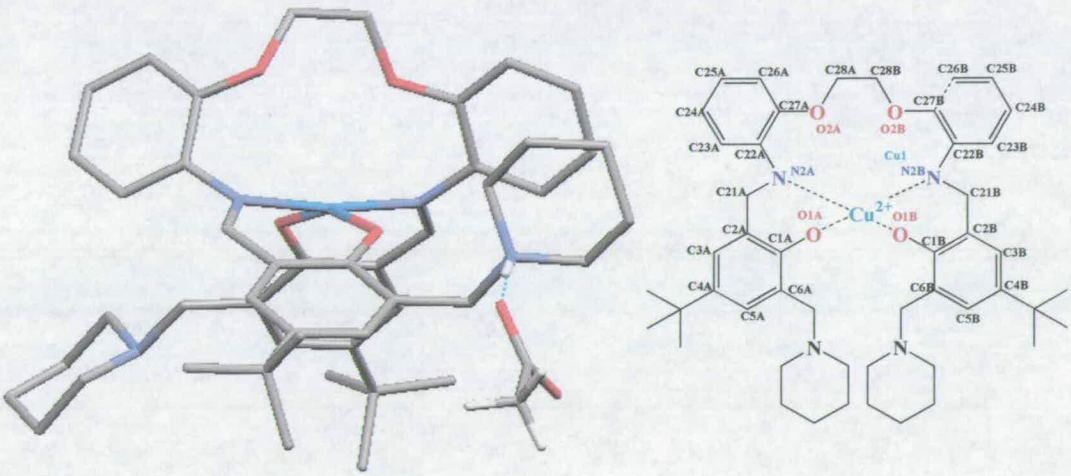

Figure 5.15 The X-ray structure of [Cu(**5**-H)($C_2H_3O_2$)] (protons and ^{t}Bu groups have been removed for clarity) with atom labelling scheme

The coordination plane [O(1A), N(2A), Cu(1), N(2B), O(1B)] is slightly puckered with the imine nitrogen donors being above the plane and the phenolic oxygen donors below the plane. As seen in Table 5.4 the maximum deviation from the least squares plane defined by the above atoms is 0.2804 Å and –0.2323 Å for atoms O(1B) and N(2A) respectively. The average deviation from the least squares plane is

0.2206 Å. The angles around in the coordination sphere are around 90°, as expected (Table 5.4).

Table 5.4 Deviations from the coordination plane

	Deviation Å
O(1A)	0.2711
N(2A)	-0.2323
Cu(1)	-0.0920
N(2B)	-0.2272
O(1B)	0.2804

Table 5.5 Angles around the copper

	Angle (°)
O1A-Cu1-N2A	89.32(8)
O1A-Cu1-N2B	91.38(8)
O2A-Cu1-N2B	91.64(8)
O2A-Cu1-N2A	91.74(8)

The X-ray structure shows an unexpected result in which one of the pendant piperidine nitrogen has been protonated while the second has not. This results in one acetate anion being H-bonded to the protonated piperidine nitrogen of side "A" (Figure 5.15). The second acetate is not associated with the complex but has been removed as acetic acid. The attendant acetate anion is H-bonded outside the cavity as both the pendant arms are facing outside the cavity but Figure 5.16 shows that rearrangement of the piperidine rings by rotation of the C(6)-C(61) (see Figure 5.15 for labelling scheme) bond could form of a cavity to bind sulfate in a 1:1:1 monocationic package.

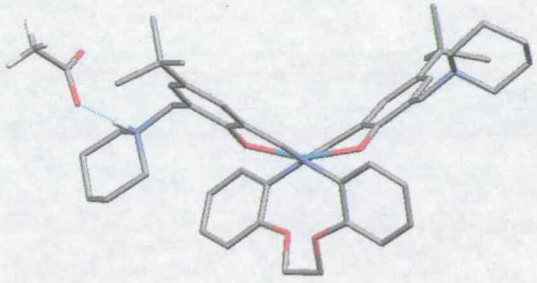

Figure 5.16 Diagram showing the rearrangement of the piperidine rings to form an anion binding cavity

In chapter 2 it was shown that in the related free ligand **5,** the conjugated *pseudo*-planar ONO plane [O(1), C(1), C(2), C(21), N(2), C(22), C(27) and O(2)] is basically flat (section 2.3.3). When compared to the copper complex it is found that the plane has been puckered (Figure 5.17).

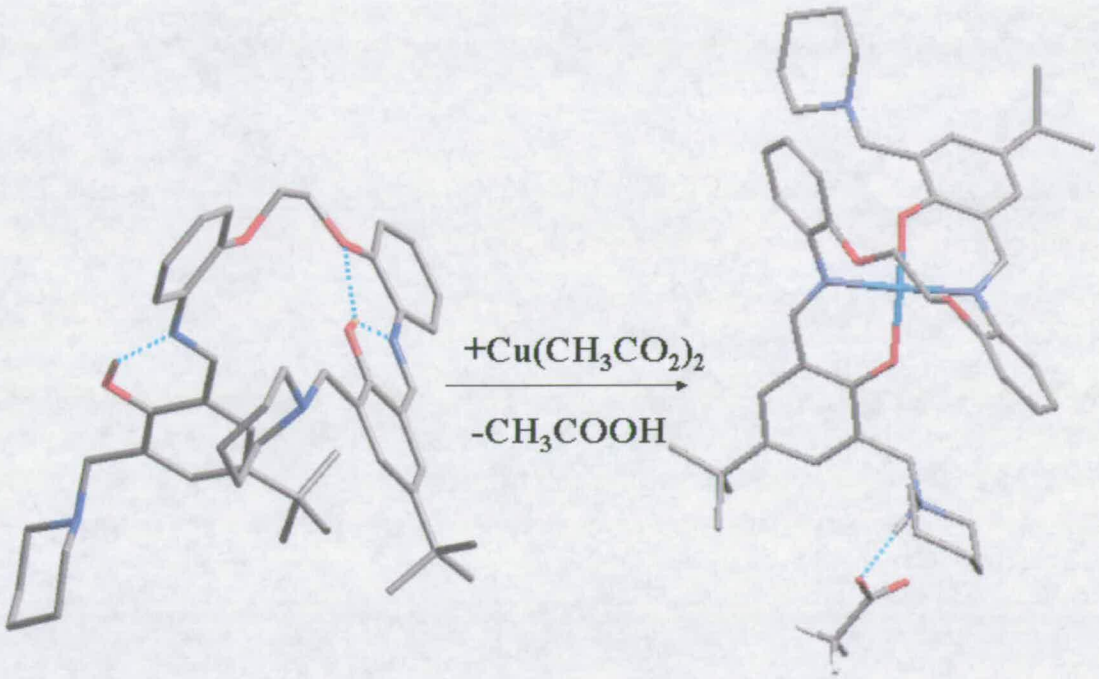

Figure 5.17 Complexation of ligand **5** with $Cu(CCH_3O_2)_2$ to form complex **54**

In the copper complex **54** the eight atoms of the ONO plane [O(1), C(1), C(2), C(21), N(2), C(22), C(27) and O(2)] (Figure 5.15) have a maximum deviation from the least squares plane defined by the above atoms being 0.4469 Å [O1A)] and –0.5724 Å [O2A)] for side A and 0.3948 Å [O(2B))] and –0.3543 Å [N(2B)] for side B. The average deviation from the least squares plane for sides A and B are 0.3235 Å and 0.2793 Å respectively. This is the largest average deviation for any of the ligands or complexes that have formed crystals.

This puckering is shown in Figure 5.18 below. By studying the crystal structure it can be seen that the complexation of the copper has resulted in the formation of a trans square planar coordination site. This has caused the di-ether bridge to twist across the coordination site and hence results in the benzene ring [C(22), C(23), C(24), C(25), C(26), C(27), C(28)] being puckered out of the expected conjugated *pseudo*-planar ONO.

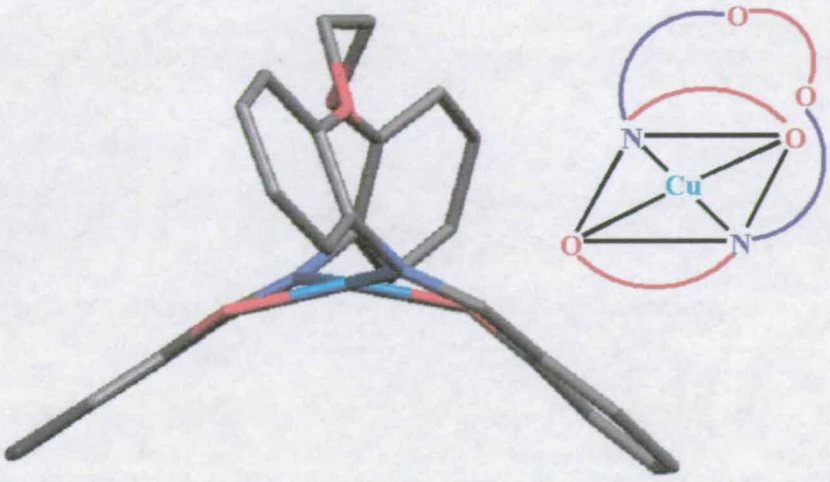

Figure 5.18 Twisting of bridge across coordination site causinf trans coordination geometry

When we observe the CuphenolN plane [Cu1, O(1), C(1), C(2), C(3), C(4), C(5), C(6), C(21), N(2)] the ten atoms are not planar as would be expected if they were fully conjugated. For side "A" the maximum deviation from the least squares plane defined by the above atoms is 0.3191 Å and –0.2081 Å for atoms Cu(1) and O(1A) respectively. For side "B", the maximum deviation from the least squares plane defined by the above atoms is 0.3307 Å and –0.4226 Å for atoms O(1B) and Cu(1) respectively. The average deviation from the least squares plane for sides "A" and "B" are 0.1056 and 0.1466 Å respectively.

A crystal structure of a copper sulfate complex formed with the ethane bridged tetradentate ligand (Figure 5.19), displays the copper coordinated to the same four donors atoms as in complex **54** (O_2N_2). However in complex **54** the di-ether containing bridge increases the rigidity of the ligand and therefore a *trans* square planar copper complex is formed whereas for the tetradentate copper complex a *cis* copper complex is formed.

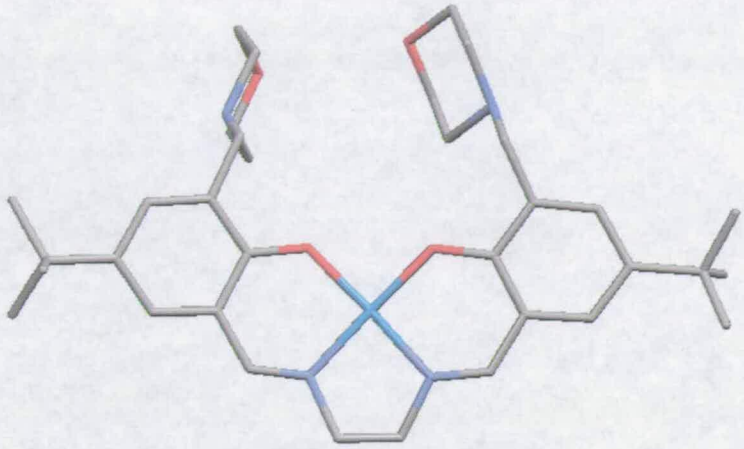

Figure 5.19 X-ray structure of a tetradentate copper structure where the copper is coordinated in a square planar environment and the pendant piperindine arms are preorganised to form an anion binding cavity. (The attendant anion has been removed)

When comparing the bond distances around the copper centre in the two structures it is found that are very similar (Table 5.6).

Table 5.6 Distances from copper to donor atoms for complex **54** and tetradentate complex

	Complex 54 Å	**Tetradentate complex Å**
Cu1-O1A	1.9054 (18)	1.8913 (0.0020)
Cu1-O1B	1.8921 (18)	1.8987 (0.0020)
Cu1-N2A	1.982 (2)	1.9385 (0.0025)
Cu1-N2B	1.9905 (19)	1.9314 (0.0023)

5.5 Conclusions

While there is the potential for a significant number of species to be formed during metal chloride extraction. The analysis appears to indicate that only one complex is formed with a M:Cl ratio of 1:2 for all the metals, however the L:M ratios vary.

The initially proposed structure for the copper chloride complexes involving one copper(II) cation coordinated to four donor atoms (two phenolic oxygen and two imine nitrogen atoms) in a distorted square planar arrangement and a second existing as a tetrachlorocopperate dianion H-bonded to the pendant tertiary amines has been

proved incorrect by electronic spectroscopy. More work/analysis needs to be carried out in order to determine the correct structural arrangement of these complexes.

It is probable that each nickel complexes contains one nickel(II) dication coordinated in the expected dibasic cavity with either two chlorides or one sulfate anion H-bonded to the pendant tertiary amines.

The zinc chloride complexes probably have a structure involving two zinc(II) cations coordinated to donor atoms of the dibasic binding cavity site and to two chloride donor atoms, and with tetrachlorozincate as the attendant anion. However, no evidence for this has been established.

It has been shown by electronic spectroscopy that cobalt is not extracted as a tetrachlorometalate dianion. However, it is likely that the cobalt (II) has been oxidised to cobalt(III) and has adopted a different configuration in comparison to the copper and zinc chloride complexes.

5.6 Experimental

5.6.1 Instrumentation

Elemental analysis was performed on a Perkin Elmer 2400 elemental analyser or a Carlo Erba 1108 Elemental analyser. The infra-red spectra were obtained on a Perkin Elmer Paragon 1000 FT-IR spectrometer as potassium bromide discs. ^{1}H and ^{13}C NMR spectra were run on a Bruker AC250 spectrometers. Chemical shifts (δ) are reported in parts per million (ppm) relative to residual solvent protons as internal standards. Fast Atom Bombardment (FAB) mass spectra were obtained on a Kratos MS50TC spectrometer. Electronic absorption spectroscopy was performed on a Unicam UV2 spectrometer. Inductively coupled plasma optical emission spectroscopy (ICP-OES) analysis was performed on a Thermo Jarrell Ash IRIS ICP-OES spectrometer. Chloride measurements were performed using a Thermo Orion Chloride/chloride combination electrode and a Fisher Scientific Dual Channel

pH/Ion/Conductivity meter. The chloride probe was calibrated using a freshly prepared $NaCl/NaNO_3$ solution and a $NaNO_3$ prepared from ultra pure water.

5.6.2 Solvent and reagent pre-treatment

All reagents and solvents were commercially available (Acros or Aldrich) and were used as received. Solvents used for analytical purposes (NMR, MS, ICP) were of spectroscopic grade.

5.6.3 Chloride analysis experiments

Chloride analysis: -technique one

The chloride contents of aqueous MX (0.02 M) (MX=$CoSO_4$, $CoCl_2$, $CuSO_4$, $CuCl_2$, $NiSO_4$, $NiCl_2$, $ZnSO_4$, $ZnCl_2$) solutions were analysed using the chloride probe. 10 cm^3 of the 0.02 M MX solutions were then contacted with 10 cm^3 of 0.01 M L in chloroform in a tightly sealed, screw top, glass jar, equipped with a magnetic stirrer. The two-phase system was stirred at 500 r.p.m at room temperature for 17 hrs, after which time a 2 cm^3 sample was taken from the organic phase for metal analysis. The 2 cm^3 samples were diluted by a factor of 1:5 with butan-1-ol and their metal contents analysed by ICP-AES. The chloride contents of aqueous phase was re-measured using the chloride probe. The data collected were calculated to give the extracted metal: chloride ratios in Microsoft Excel.

Chloride analysis: -technique two

10 cm^3 of 0.01 M L in chloroform was contacted with 10 cm^3 aqueous 0.1 M MX (MX=$CoSO_4$, $CoCl_2$, $CuSO_4$, $CuCl_2$, $NiSO_4$, $NiCl_2$, $ZnSO_4$, $ZnCl_2$) in a tightly sealed, screw top, glass jar, equipped with a magnetic stirrer. The two-phase system was stirred at 500 r.p.m at room temperature for 17 hrs, after which time a 2 cm^3 sample was taken from the organic phase for metal analysis and 1 cm^3 was taken for chloride analysis. The 2 cm^3 samples were diluted by a factor of 1:5 with butan-1-ol

and their metal contents analysed by ICP-AES. The 1 cm^3 sample was stirred at room temperature for 17 hrs with a $NaNO_3$ (0.1M) solution. The two phases were separated and 3 cm^3 of the aqueous was removed, added to 3 cm^3 NaOH (0.1M) to raise the pH to the working range of the probe (pH 2-12) and the chloride contents analysed using the chloride probe. The data collected were calculated to give the extracted metal: chloride ratios in Microsoft Excel.

5.6.4 Extraction complexes

1 cm^3 of the loaded organic phase was diluted with chloroform to an appropriate concentration for UV-Vis spectroscopy.

5.6.4.1 Cobalt complexes

Ligand L	**Mass Spectrometry** *m/z*	**UV-Vis spectroscopy** λ_{max} nm
6	1018 (LCo, 38.1%)	293, 418
12	1049 (LCo, 48.9%)	276, 449
31	954 (L_2Co, 12.4%)	368
33	923 (L_2Co, 11.2%)	328, 358
35	1019 (L_2Co, 29.3%)	339, 349, 379, 407
37	590 (LCoCl, 64.9%)	345
50	887 (LCo, 31.2%)	405
51	1048 (LCo_2Cl_3, 48.9%)	276, 334
52	956 (LCo, 85.2%)	384

5.6.4.2 Copper chloride complexes

Ligand L	Mass Spectrometry *m/z*	UV-Vis spectroscopy λ_{max} nm
6	1023 (LCu, 22.0%)	265, 272, 402, (591)
12	992 (L, 39.0%)	272, 297, 405,
31	54.3 (LCuCl, 68.8%)	374
33	530 (LCuCl, 68.0%)	369, (798)
35	1094 ($L_2Cu_2Cl_2$ 16.7%)	273, 391, (692)
37	594 (LCuCl 48.9%)	292, 302, 399, (674)
50	1027 (LCu_2Cl_2, 8.3%)	249, 373
51	824 (LCu_2Cl_2, 5.5%)	259, 290, 297, 352
52	960 (LCu, 53.4%)	285, 399

() represent d-d transitions

5.6.5 Copper sulfate complexes

Ligand L	Mass Spectrometry *m/z*	UV-Vis spectroscopy λ_{max} nm
6	1122 ($LCuSO_4$, 49.2%)	274, 292, 400
12	1055 (LCu, 15.1%)	274, 291, 394
31	607 ($LCuSO_4$, 97.6%)	388
33	626 (LCu, 62.6%)	374
35	1025 (L_2Cu, 67.8%)	273, 327, 428
37	1057 (L_2Cu, 36.0%)	269, 391
50	991 ($LCuSO_4$, 29.9%)	277, 378
51	826 (L, 13.0%)	277, 320, 436
52	961 (LCu, 74.7%)	241,254,263,286,406

5.6.5.1 Nickel chloride complexes

Ligand L	Mass Spectrometry *m/z*	UV-Vis spectroscopy λ_{max} nm
6	1017 (LNi, 10.6%)	276, 294, 339
12	1047 (LNi, 32.4%)	360
31	597 ($LNiCl_2$, 8.4%)	320, 346
33	923 (L_2Ni, 2.0%)	330
35	481 (L, 67.9%)	339
37	501 (L, 13.7%)	341
50	886 (LNi, 34.9%)	328
51	824 (L, 18.5%)	295, 325
52	955 (LNi, 33.7%)	341
53	831 (LNi, 26.8%)	330, 419

5.6.6 Nickel sulfate complexes

Ligand L	Mass Spectrometry *m/z*	UV-Vis spectroscopy λ_{max} nm
53	832 (LNi, 5.0%)	337, 421

5.6.6.1 Zinc complexes

Ligand L	Mass Spectrometry *m/z*	UV-Vis spectroscopy λ_{max} nm
6	1161 (LZn_2Cl_2, 9.1%)	295, 331, 349, 409
12	1191 (LZn_2Cl_2, 48.3%)	270, 383
31	544 (LZnCl, 59.4%)	269, 371
33	531 (LZnCl, 50.6%)	269, 276, 365
35	579 (LZnCl, 61.7%)	254, 334, 349, 410
37	1193 ($L_2Zn_2Cl_2$, 14.0%)	271, 360
50	1065 (LZn_2Cl_3, 9.8%)	245, 273, 368
51	924 (LZnCl, 5.6%)	-
52	1099 (LZn_2Cl_2, 10.0%)	270, 309, 376
53	1011 (LZn_2Cl_3, 8.9%)	278, 365

NMR Spectroscopy-zinc chloride complexes

Ligand 6

^{1}H NMR ($CDCl_3$, 250 MHz): δ 0.79 (t, 12H, CH_3(hexyl)), δ 1.18 (s, 18H, $C(CH_3)_3$), δ 1.14-1.26 (m, 24H, CH_2 (hexyl)), δ 1.59 (bp, 8H, $NCH_2\underline{CH_2}$ (hexyl)), δ 3.16 (t, 8H, NCH_2 (hexyl)), δ 4.30 (s, 4H, $ArCH_2N$), δ 4.35 (s, 4H, OCH_2), δ 6.60-7.80 (m, 12H, Ar-CH), 7.95 (s, 2H, NCH).

Ligand 31

^{1}H NMR ($CDCl_3$, 250 MHz): δ 0.79 (t, 12H, CH_3(hexyl)), δ 1.20 (s, 18H, $C(CH_3)_3$), δ 1.18-1.23 (m, 24H, CH_2 (hexyl)), δ 1.79 (m, 8H, $NCH_2\underline{CH_2}$ (hexyl)), δ 2.48 (s, 12H, $N(CH_3)_2$), δ 2.78 (t, 8H, NCH_2 (hexyl)), δ 2.97 (m, 4H, $NCH_2\underline{CH_2}N(CH_3)_2$), δ 3.67 (t, 4H, $N\underline{CH_2}CH_2N(CH_3)_2$), δ 4.04 (bs, 4H, $ArCH_2N$), δ 6.97 (bs, 2H, ArCH), δ 7.06 (m, 2H, ArCH), δ 8.25 (s, 2H, N=CH).

Ligand 33

^{1}H NMR ($CDCl_3$, 250 MHz): δ 0.80 (m, 12H, CH_3), δ 1.19 (s, 18H, $C(CH_3)_3$), δ 1.19-1.30 (m, 24H, CH_2 (hexyl)), δ 1.80 (bp, 8H, $NCH_2\underline{CH_2}$ (hexyl)), δ 3.04 (bp, 8H, NCH_2 (hexyl)), δ 3.44 (s, 4H, OCH_3), δ 3.69 (bp, 4H, $N\underline{CH_2}CH_2O$), δ 3.75 (bp, 4H, $NCH_2\underline{CH_2}O$), δ 4,27 (bp, 4H, $ArCH_2N$), δ 7.18 (m, 2H, ArCH), δ 7.19 (m, 2H, ArCH), δ 8.18 (s, 2H, N=CH).

Ligand 35

^{1}H NMR ($CDCl_3$, 250 MHz): δ 0.79 (t, 12H, CH_3 (hexyl)), δ 1.23 (s, 18H, $C(CH_3)_3$), δ 1.20-1.34 (m, 24H, CH_2 (hexyl)), δ 1.74 (bp, 8H, $NCH_2\underline{CH_2}$ (hexyl)), δ 2.95 (bp, 8H, NCH_2 (hexyl)), δ 4.01 (s, 6H, OCH_3), δ 4.14 (s, 4H, $ArCH_2N$), δ 6.67-7.23 (m, 12H, ArCH), δ 7.95 (s, 2H, N=CH).

Ligand 37

^{1}H NMR ($CDCl_3$, 250 MHz): δ 0.82 (d, 12H, CH_3), δ 1.14 (s, 18H, $C(CH_3)_3$), δ 1.09-1.28 (m, 24H, CH_2 (hexyl)), δ 1.52 (bp, 8H, $NCH_2\underline{CH_2}$ (hexyl)), δ 2.53 (s, 6H, SCH_3), δ 3.01 (t, 8H, NCH_2 (hexyl)), δ 4.15 (bp, 4H, $ArCH_2N$), δ 7.14-7.54 (m, 12H, ArCH), δ 7.94 (s, 2H, N=CH).

Ligand 50

^{1}H NMR ($CDCl_3$, 250 MHz): δ 0.79 (t, 12H, CH_3 (hexyl)), δ 1.12 (s, 18H, $C(CH_3)_2$), δ 1.17-1.27 (m, 24H, CH_2 (hexyl)), δ 1.69 (bp, 8H, $NCH_2\underline{CH_2}$ (hexyl)), δ 2.21 (bp, 4H, CH_2 (cyclic)), δ 2.93 (bp, 4H, NCH_2 (hexyl)), δ 3.22 (bp, 4H, CH_2 (cyclic)), δ 3.85 (bp, 2H, CH (cyclic)), δ 4.11 (s, 4H, $ArCH_2N$); δ 6.93-7.27 (m, 4H, ArCH), δ 8.68 (s, 2H, N=CH).

Ligand 52

^{1}H NMR ($CDCl_3$, 250 MHz): δ 0.77 (bp, 12H, CH_3 (hexyl)), δ 1.13-129 (m, 18H, $C(CH_3)_2$), δ 1.13-1.29 (m, 24H, CH_2 (hexyl)) δ 1.48 (bp, 8H, $NCH_2\underline{CH_2}$ (hexyl)), δ 3.42 (bp, 8H, NCH_2 (hexyl)), δ 4.76 (m, 4H, $ArCH_2N$), δ 7.00-7.76 (m, 12H, Ar-CH), δ 8.82 (s, 2H, N=CH).

Ligand 53

^{1}H NMR ($CDCl_3$, 250 MHz): δ 0.80 (d, 12H, CH_3 (hexyl)), δ 1.15 (s, 12H, $C(CH_3)_2$), δ1.16-1.25 (m, 24H, CH_2 (hexyl)), δ 1.71 (bp, 8H, $NCH_2\underline{CH_2}$ (hexyl)), δ 2.90 (t, 4H, NCH_2 (hexyl)), δ 4.04 (s, 4H, CH_2 (N-en-N)), δ 4.29 (s, 4H, NCH_2), δ 6.98 (s, 2H, ArCH), δ 7.30 (s, 2H, ArCH); δ 8.60 (s, 2H, N=CH)

5.6.7 Solid state complex synthesis

Sulfate and acetate complexes

A 1:1 ratio (sexadentate ligands) and 2:1 ratio (tridentate ligands) of ligand: metal salt was stirred, (*c.a.* $3x10^{-4}$ moles) of ligand in methanol (10 cm^3) with the equivalent solution of the appropriate metal salt in methanol (10 cm^3), overnight. Colour changes due to complex formation were instantaneous. After removal of the solvent *in-vacuo* the sulfate products were extracted into CH_2Cl_2 filtered and recrystallised with $^iPr_2O$. The acetate complexes were washed with an aqueous solution (pH 7.5), extracted into chloroform, and dried in-*vacuo*. MS (FAB, NBA) all the spectra confirmed the presence of the specific metal with in the complex.

Cobalt and copper chloride complexes

A 1:2 ratio (sexadentate ligands) and 1:1 ratio (tridentate ligands) of ligand: metal salt was stirred, (*c.a.* $3x10^{-4}$ moles) of ligand in methanol (10 cm^3) with the equivalent solution of the appropriate metal salt in methanol (10 cm^3), overnight. Colour changes due to complex formation were instantaneous. After removal of the solvent *in-vacuo* products were extracted into CH_2Cl_2 filtered and recrystallised with $^iPr_2O$. MS (FAB, NOBA) all the spectra confirmed the presence of the specific metal with in the complex.

Zinc chloride complexes

A 1:3 ratio (sexadentate ligands) and 2:3. ratio (tridentate ligands) of ligand: metal salt was stirred, (*c.a.* $3x10^{-4}$ moles) of ligand in methanol (10 cm^3) with the equivalent solution of the appropriate metal salt in methanol (10 cm^3), overnight. Colour changes due to complex formation were instantaneous. After removal of the solvent *in-vacuo* products were extracted into CH_2Cl_2 filtered and recrystallised with $^iPr_2O$. MS (FAB, NOBA) all the spectra confirmed the presence of the specific metal with in the complex.

5.6.8 X-ray crystallography

Structure **81** was determined by James Davidson at the University of Edinburgh. Data was collected at 220K on a SMART diffractometer equipped with an Oxford Cryosystems low temperature device.

5.7 References

1 D. F. Shriver, P. W. Atkins and C. H. Langford, 'Inorganic Chemistry', Oxford University Press, Oxford, 1994, 229.

2 F. A. Cotton and G. Wilkinson, 'Advanced Inorganic Chemistry', John Wiley and Sons, USA, 1980, 727.

3 F. A. Cotton and G. Wilkinson, 'Advanced Inorganic Chemistry', John Wiley and Sons, USA, 1980, 767.

4 D. F. Shriver, P. W. Atkins and C. H. Langford, 'Inorganic Chemistry', Oxford University Press, Oxford, 1994, chapter 7, 274-312.

5 F. A. Cotton and G. Wilkinson, 'Advanced Inorganic Chemistry', John Wiley and Sons, USA, 1980, 747.

6 F. A. Settle, 'Handbook of Instrumental Techniques for Analytical Chemistry', Prentice Hall, America, 1997.

7 S. Galbraith, The University of Edinburgh, Edinburgh, Awaiting publication.

8 S. Lewith, *Naunyn-Schmeidebergs Arch. Exp. Pathol. Pharmakol.*, 1888, **23**, 1.

9 F. Hofmeister, *Naunyn-Schmeidebergs Arch. Exp. Pathol. Pharmakol.*, 1888, **23**, 247.

10 J. B. Love, J. M. Vere, M. W. Glenny, A. J. Blake and M. Schroeder, *Chem.Commun.*, 2001, 2678.

11 M. Elleb, J. Meullemeestro, M.J.. Schwing-Weill and V. F, *Inorg. Chem.*, 1980, **19**, 2699.

12 A. Erxleben, *Inorg.Chem.*, 2001, **40**, 208.

13 A. I. Gusev, E. B. Chuklanova, B. Murzubraimov and A. Toktomamatov, *Koord.Khim.(Russ.)(Coord.Chem.)*, 1985, **11**, 1154.

14 A. J. Atkins, D. Black, R. L. Finn, A. Marin-Becerra, A. J. Blake, L. Ruiz-Ramirez, W.-S. Li and M. Schroder, *J.Chem.Soc.,Dalton Trans.*, 2003, 1730.

15 B.DasGupta, R.Haidar, W.-Y. Hsieh and L.J.Zompa, *Inorg.Chim.Acta*, 2000, **306**, 78.

16 C.K.Williams, N.R.Brooks, M.A.Hillmyer and W.B.Tolman, *Chem.Commun.*, 2002, 2132.

17 E.Berti, A.Caneschi, C.Daiguebonne, P.Dapporto, M.Formica, V.Fusi, L.Giorgi, A.Guerri, M.Micheloni, P.Paoli, R.Pontellini and P.Rossi, *Inorg.Chem.*, 2003, **42**, 348.

18 H.Adams, L.R.Cummings, D.E.Fenton and P.E.McHugh, *Inorg.Chem.Commun.*, 2003, **6**, 19.

19 H.Adams, D.Bradshaw and D.E.Fenton, *Eur.J.Inorg.Chem.*, 2001, 859.

20 W. Huang, S. Gou, H. Qian, D. Hu, S.Chantrapromma, H.-K. Fun and Q. Meng, *Eur.J.Inorg.Chem.*, 2003, 947.

21 J.D.Ranford, J.J.Vittal and D. Wu, *Angew.Chem.,Int.Ed.Engl.*, 1998, **37**, 1114.

22 J.J.Vittal and X. Yang, *Cryst.Growth Des.*, 2002, **2**, 259.

23 L.Tatar, O.Atakol and D.Ulku, *Acta Crystallogr.,Sect.E*, 2002, **58**, 83.

24 L.-S. Long, K.-Y. Ding, X.-M. Chen and L.-N. Ji, *Inorg.Chem.Commun.*, 2000, **3**, 65.

[25] M.B.Ferrari, G.G.Fava, C.Pelizzi and P.Tarasconi, *J.Chem.Soc.,Dalton Trans.*, 1992, 2153.
[26] M.Doring, M.Ciesielski, O.Walter and H.Gorls, *Eur.J.Inorg.Chem.*, 2002, 1615.
[27] N.Mangayarkarasi, M.Prabhakar and P.S.Zacharias, *Polyhedron*, 2002, **21**, 925.
[28] O.Atakol, L.Tatar, M.A.Akay and D.Ulku, *Anal.Sci.*, 1999, **15**, 199.
[29] S.Brooker, P.D.Croucher and F.M.Roxburgh, 1996, 3031.
[30] S.R.Korupoju, N.Mangayarkarasi, S.Ameerunisha, E.J.Valente and P.S.Zacharias, *J.Chem.Soc.,Dalton Trans.*, 2000, 2845.
[31] J. Wang, D. Kong, A. E. Martell, R. J. Motekatis and J. H. Reibenspies, *Inorg.Chim.Acta*, 2001, **324**, 194.
[32] I. Mihaylov, E. Krause, D. F. Colton, Y. Okita, J. P. Duterque and J. L. Perraud, *CIM Bull.*, 2000, **93**, 124.
[33] N. N. Greenwood and E. A. Earnshaw, 'Chemistry of the Elements', Permangon Press, Oxford, 1984, 1290.
[34] D. H. Williams and I. Fleming, 'Sectroscopic Methods in organic Chemistry', McGraw-Hill, London, 1995, chapter 2, 28-62.
[35] K. Nakamoto, 'Infrared and Raman Spectra of Inorganic and Coordination compounds', John Wiley and sons, New York, 1986, 133.

Chapter six

Conclusions and Future work

6.1 Conclusions

The main objectives of the work presented in this thesis were to:

1. Design and synthesise new classes of ligands that would co-extract high spin nickel(II) and sulfate from an aqueous solution into an organic phase. The new extractants were designed to present *pseudo*-octahedral $X_2N_2O_2^{2-}$ donor sets to a nickel(II) dication by extending the ligand back bone of tetradentate saliclaldiminato $N_2O_2^{2-}$ systems studied previously.[1-3]
2. Screen the "nickel-salt" extractants to examine their potential for recovery of other divalent metals salts commonly found in nickel feed streams.

Synthesis of the sexadentate ligands, with $X_2N_2O^{2-}$ donor sets where X=O and S, was relatively straight forward, whereas where X=N, proved to be more problematic. 1:1 ligand: nickel complexes were formed exclusively and X-ray crystal structures of the complexes displayed nickel coordinated in *pseudo*-octahedral arrangement in the most thermodynamically stable isomer. When the attendant anion was sulfate, chloride and nitrate, metal salt complexes were formed whereas acetate was used to produce "nickel-only" complexes.

Analogous tridentate ligands with XNO^- donor sets proved to be simple to make. Although no X-ray structures were obtained, results indicate that it is likely that 2:1 ligand: nickel complexes were formed. In all cases complexes were formed with the attendant anion present (sulfate, chloride and acetate).

It was hoped that changing the backbone of the ligands from the previously studied planar four coordinate systems to six coordinate octahedral system would lead to an increase in the selectivity and "strength" of nickel sulfate extraction. In practice both the new sexadentate and new tridentate ligands proved to be weaker extractants than the previously studied tetradentate ligands.

The screening programme showed that the new sexadentate and tridentate ligands are efficient reagents for recovery of copper from both sulfate and chloride media but do not show any particular benefit over the previously studied tetradentate analogues. All the ligands show greater efficiency of recovery of base metals (cobalt, copper, nickel and zinc) from chloride than sulfate media, consistent with the higher lipophility of chloride ions (Hofmeister series[4, 5]).

Very high transport efficiencies of zinc chloride were observed in some cases with *ca* 250% zinc loading being recorded. Approximately 150% loading efficiencies were also detected for $CoCl_2$ and $CuCl_2$.

A development programme, which would involve further investigations into the ligands, is needed if these systems are to be utilised as commercial extractants. This would require a greater understanding of the solution species present through extraction (and if possible some X-ray crystal structures). The ligand structures may need to be fine-tuned for selectivity and solubility. Enhancements in the selectivity for metal transport, such as zinc(II) and copper(II) and also the anion transport (chloride over sulfate) may need to be made and their solubility in hydrocarbons e.g. kerosene may need to be increased. Good extraction kinetics should not be a problem with zinc(II) or copper(II) but this would still need investigation. For the system to be a commercial success the process would also require good phase separation, high stripping efficiency and regeneration of the ligand without decomposition e.g. through hydrogenation or oxidation.

1 D. J. White, N. Laing, H. Miller, S. Parsons, S. Coles and P. A. Tasker, *Chem. Commun.*, 1999, 2077.

2 H. A. Miller, N. Laing, S. Parsons, A. Parkin, P. A. Tasker and D. J. White, *J. Chem. Soc.-Dalton Trans.*, 2000, 3773.

3 R. A. Coxall, L. F. Lindoy, H. A. Miller, A. Parkin, S. Parsons, P. A. Tasker and D. J. White, *J. Chem. Soc.-Dalton Trans.*, 2003, 55.

4 S. Lewith, *Naunyn-Schmeidebergs Arch. Exp. Pathol. Pharmakol.*, 1888, **23**, 1.

5 F. Hofmeister, *Naunyn-Schmeidebergs Arch. Exp. Pathol. Pharmakol.*, 1888, **23**, 247.

Appendix I

Table 1 Wavelengths used to calibrate extraction concentrations

Element	Sensitivity (ppb)	Emission Wavelengths/Y (nm)	Relative Intensity
Cobalt	2	228.616*, 228.616*, 237.862*, 238.892*, 238.892*	113, 114, 109, 108, 109
Copper	0.9	224.700, 324.754*, 327.396*	115, 080, 079
Manganese	0.4	257.610, 257.610*, 260.569, 293.306	100, 101, 100, 089
Zinc	1	202.548, 206.200, 213.856, 213.856, 334.502, 334.502*, 481.053*	128, 126, 121, 122, 077, 078, 054

The * indicates the wavelengths that were used.

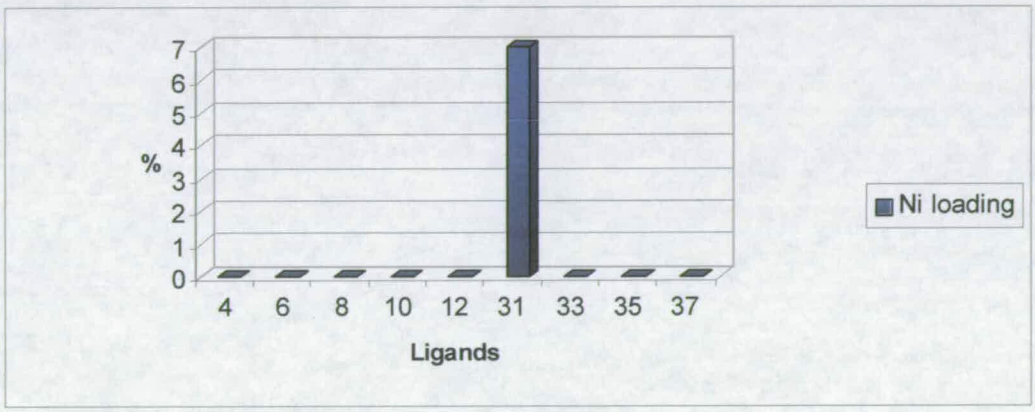

Figure 1 Nickel extraction results (100% represents the loading of one copper cation by one ligand)

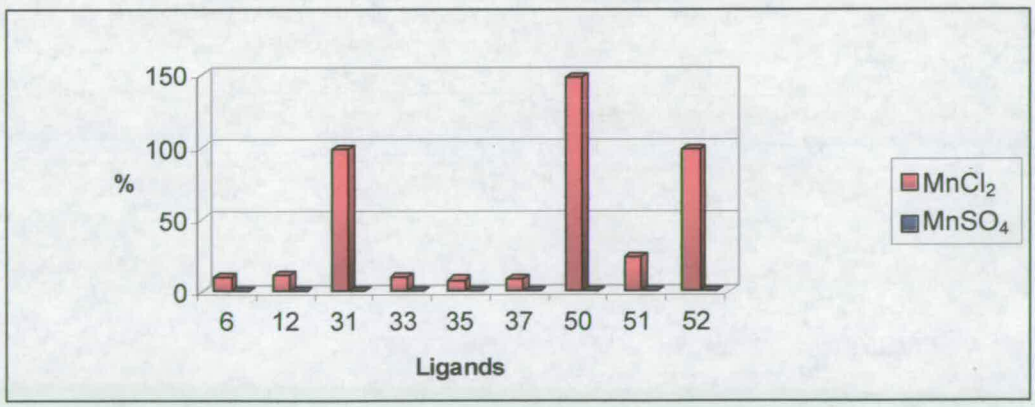

Figure 2 Manganese extraction results (100% represents the loading of one copper cation by one ligand)